

# **Improved Calculation of Scour Potential in Cohesive Soils and Scour-susceptible Rock**

**Final Report**

**Report Number: OR19-132**

Michigan Department of Transportation  
Office of Research Administration  
8885 Ricks Road  
Lansing, MI 48909

By

Zhen (Leo) Liu, Darud E Sheefa, Stanley Vitton, and Brian Barkdoll

Michigan Technological University  
1400 Townsend Drive  
Houghton, MI 49931

**December 2020**

## Technical Report Documentation Page

<b>1. Report No.</b> SPR-1688	<b>2. Government Accession No.</b> N/A	<b>3. MDOT Project Manager</b> Rebecca Curtis	
<b>4. Title and Subtitle</b> Improved Calculation of Scour Potential in Cohesive Soils and Scour-susceptible Rock		<b>5. Report Date</b> February 2020	
		<b>6. Performing Organization Code</b> N/A	
<b>7. Author(s)</b> Zhen (Leo) Liu, Darud E Sheefa, Stanley Vitton, and Brian Barkdoll		<b>8. Performing Org. Report No.</b> N/A	
<b>9. Performing Organization Name and Address</b> Michigan Technological University 1400 Townsend Drive Houghton, MI 49931		<b>10. Work Unit No. (TRAIS)</b> N/A	
		<b>11. Contract No.</b> 2016-0067	
		<b>11(a). Authorization No.</b> Z9	
<b>12. Sponsoring Agency Name and Address</b> Michigan Department of Transportation Research Administration 8885 Ricks Rd. P.O. Box 30049 Lansing, MI 48909		<b>13. Type of Report &amp; Period Covered</b> Final Report 5/01/2017 - 12/31/2020	
		<b>14. Sponsoring Agency Code</b> N/A	
<b>15. Supplementary Notes</b>			
<b>16. Abstract</b> This report summarizes the work on the improved calculation of scour potential in cohesive soils and scour-susceptible rock. A state of the practice survey was first conducted to gather information about the scour evaluation in cohesive soils and scour-susceptible rock. This includes a literature review covering the concepts and understanding of scour susceptibility, material sampling, and erodibility testing techniques, bridge scour calculation methods and other factors that can affect the scour analysis in cohesive soils and scour-susceptible rock, and a summary of the information gathered in communications with engineers from MDOT and other state DOTs. Based on the survey, three scour analysis methods, i.e., SRICOS-EFA, EIM, and GSN were selected. Detailed theories, implementation, needed input, and expected output as well as relevant testing were investigated to prepare the knowledge and guidelines that MDOT engineers will need for using these methods. Case studies of two clay-bedded bridge sites and two rock-bedded bridge sites were performed with typical information such as plans and geotechnical reports. Based on the survey, theoretical analysis, and case studies, detailed guidelines for applying the methods, including sampling, testing, and calculation, were presented in the form of flowcharts. Next, the surface geology of Michigan was discussed to help engineers gain a general understanding of the rock in Michigan for bridge scour considerations, and a rock classification was provided to assist more specific assessments. Typical issues for the application of the selected methods, i.e., at sites without stream gages and sites with layered earth strata, were discussed together with their solutions.			
<b>17. Key Words</b> Bridge Scour, Cohesive Soils, Scour-susceptible Rock, Scour Analysis		<b>18. Distribution Statement</b> No restrictions. This document is available to the public through the Michigan Department of Transportation.	
<b>19. Security Classification - report</b> Unclassified	<b>20. Security Classification - page</b> Unclassified	<b>21. No. of Pages</b> 228	<b>22. Price</b> \$90417.82

## **Acknowledgment**

The authors would like to thank the Michigan Department of Transportation (MDOT) for the financial support and the MDOT staff, especially the research advisory panel consisting of Michael Townley, Rebecca Curtis, Erik Carlson, Andrew Zwolinski, Ryan Snook, Harold Zweng, Elizabeth McCann, Steve Katenhus, Bradley Wagner, Paul Schiefer, Christopher Johnecheck, and Chad Skrocki, for their cooperation and for providing suggestions, data, access to databases, and feedback on preliminary results. The authors want to extend their appreciation to all the state Departments of Transportation that participated in the state of the practice survey including but not limited to Florida, Kansas, Pennsylvania, South Carolina, Nebraska, Montana, Missouri, Ohio, Arkansas, Minnesota, Oklahoma, Alabama, Iowa, Louisiana, New Jersey, Oregon, Texas, Wisconsin, Idaho, and Missouri.

## **Research Report Disclaimer**

“This publication is disseminated in the interest of information exchange. The Michigan Department of Transportation (hereinafter referred to as MDOT) expressly disclaims any liability, of any kind, or for any reason, that might otherwise arise out of any use of this publication or the information or data provided in the publication. MDOT further disclaims any responsibility for typographical errors or accuracy of the information provided or contained within this information. MDOT makes no warranties or representations whatsoever regarding the quality, content, completeness, suitability, adequacy, sequence, accuracy, or timeliness of the information and data provided, or that the contents represent standards, specifications, or regulations.”

## Executive Summary

It has been widely recognized that the use of the scour prediction equations developed based on tests with cohesionless soils, such as the HEC-18 cohesionless bed equation currently used by MDOT, can possibly significantly overestimate the scour depth in cohesive soils and scour-susceptible rock. This project was conducted to search for calculation methods that can better predict the scour in cohesive soils and scour-susceptible rock in Michigan. Considering the available time and resources, this project was focused on methods that have been tested or extensively discussed. Based on a thorough literature review and communications with other state DOTs, it was concluded that scour analysis in cohesive soils and scour-susceptible rock is still under development, though several methods have been proposed and tested in research projects.

Based on the literature review, three methods, together with sampling and testing methods needed for their implementation, were selected and investigated in this project. These methods were implemented at four bridge sites, i.e., two on clay and the other two on rock, to test the needed input, procedure, typical results, and possible issues for their applications in Michigan. Among them, the SRICOS-EFA method was recommended for clay. EFA tests, which are currently absent in most geotechnical reports, are highly desired for accurate predictions, while for rough estimates, predictions can also be made with assumptions via simple relationships between conventional soil properties and the erosion characteristics of soil in the place of an EFA test.

For scour in rock, only the quarrying and plucking mode and the abrasion mode are believed to be concerns in Michigan. The EIM method is recommended to calculate the quarrying and plucking mode of scour, which is primarily for highly fractured or/and highly weathered rocks. However, such rocks may not be common in Michigan due to the history of glaciation, in which such rocks were primarily removed by the glaciers. Therefore, the EIM method can be adopted only when heavily fractured or heavily weathered rock in its natural state (before any sampling, testing, or construction) is observed in the field. While the igneous and metamorphic rocks in Upper Michigan are usually strong and intact, the EIM may primarily apply to sedimentary rocks in the Michigan basin in Lower Michigan. When applying the EIM to bridge sites on such rocks with severe fracturing or/and weathering, sampling needs to be done with appropriate coring techniques and care to ensure the sampled cores have engineering properties that are not significantly different from natural rock. The GSN method is recommended for predicting the

abrasion mode of scour, which occurs in sedimentary rocks especially those with a high content of clay-like minerals such as some types of soft shale. The modified slake durability test, which is absent in current geotechnical reports, is needed for the accurate prediction of this type of scour. It is noted that we implemented the GSN with modified slake durability test results for rocks similar to the rock types studied in this study and found that scour depth from this type of scour is negligible in the cases that have been analyzed. Therefore, the analysis of the abrasion mode of scour may only be needed in a few types of sedimentary rocks.

For scour prediction method implementation, MDOT engineers, primarily hydraulic engineers who conduct scour analysis, can check the flowcharts presented in Chapter 6 for quick reference. In short, one can go to the flowcharts for the SRICOS-EFA method for clay, refer to the flowcharts for the EIM for highly fractured/weathered rock, and check the flowcharts for the GSN for sedimentary rocks with high clay-like minerals. The geological information and rock classification for scour considerations in Chapter 5 can be used to obtain a rough estimate of rock conditions, possible scour mode(s), and needs for further testing. The flowcharts for individual methods present a step-by-step procedure for method application. Once a method is selected, further information regarding the method, such as theories and equations, can be found in Chapter 3 to guide the application of such methods. When more guidance is needed for the implementation of each method, one can check the case studies in Chapter 4, which provide examples for applying these methods at typical bridge sites in Michigan. If information is needed to understand the geology of Michigan, one can refer to Chapter 5. Chapter 5 also includes information regarding issues that one may expect for applying these methods: analysis at sites without USGS gage data, analysis in layered soil strata, and needed testing methods.

Results from this project also shed light on the collaboration between geotechnical engineers and hydraulics engineers. This is significant because geotechnical engineers usually provide input, especially material properties and geological conditions, for hydraulic engineers to run the scour calculation. However, there may be a lack of communication between these two groups in the research team's communications with many state DOTs. This project emphasizes the input for the scour calculation methods as well as sampling and testing that are needed for obtaining such input. It is recommended that future geotechnical reports for MDOT include the following extra information for scour considerations. For clay, the EFA test is desired for the use of the SRICOS-

EFA method. When the EFA test is not available, RETA and JET can also be considered. For highly fractured or weathered rock, calculation with the EIM will need the UCS and RQD (part of the RMR) as well as other geological characteristics of the rock, including the number of joint sets, joint roughness, joint alteration, and block dimensions (ratio between length and thickness). In addition, for soft rocks (e.g., sedimentary rocks in the Lower Michigan), it is extremely important to ensure that drilling and coring will not significantly affect the mechanical properties of the collected sample, while for hard rocks (e.g., igneous and metamorphic rocks in the Upper Michigan), scour may not be a concern unless heavy weathering and/or fractures are identified. For sedimentary rocks with a high content of clay-like minerals, the application of the GSN method will require the modified slake durability test. Alternatively, the EFA and modified slake durability tests can be excluded from the geotechnical reports and conducted by hydraulics engineers in later stages when these tests are deemed as needed in the geotechnical report.

# Table of Contents

<b>Technical Report Documentation Page</b> .....	<b>ii</b>
<b>Acknowledgment</b> .....	<b>iii</b>
<b>Research Report Disclaimer</b> .....	<b>iii</b>
<b>Executive Summary</b> .....	<b>iv</b>
<b>List of Tables</b> .....	<b>xv</b>
<b>Chapter 1 Introduction</b> .....	<b>19</b>
1.1 Statement of the Problem.....	19
1.2 Objectives of the Study .....	21
1.3 Overview of Research Tasks .....	21
1.4 Organization of This Report .....	23
<b>Chapter 2 Literature Review</b> .....	<b>26</b>
2.1 Bridge Scour Susceptibility .....	26
2.1.1 Scour Susceptibility of Bridges on Cohesive Soil .....	26
2.1.2 Scour Susceptibility of Bridges on Rock .....	27
2.2 Sampling and Erodibility Testing .....	28
2.2.1 Sampling .....	28
2.2.2 Erodibility Testing .....	34
2.3 Scour Analysis Approaches for Erodible Rock and Cohesive Soil .....	39
2.3.1 Scour in Cohesive Soil.....	39
2.3.2 Scour on Erodible Rock .....	45
2.4 Survey of the State DOT Practices .....	47
2.4.1 Overview .....	47
2.4.2 Summary of Practices Related to HEC-18.....	48
2.4.3 Scour Evaluation Methods Practiced by Other States .....	52
<b>Chapter 3 Scour Analysis Methods for Erodible Rock and Cohesive Soil</b> .....	<b>53</b>
3.1 Background .....	53
3.1.1 Types of Bridge Scour .....	53
3.1.2 Bed Shear Strength and Stress .....	54
3.1.3 Stream Power .....	54

3.1.4	Mode of Scour.....	55
3.2	Scour Analysis Methods for Erodible Rock and Cohesive Soil .....	56
3.2.1	SRICOS-EFA.....	56
3.2.2	EIM .....	58
3.2.3	GSN.....	64
<b>Chapter 4</b>	<b>Implementation of Selected Methods for Bridge Scour Analysis at Four Michigan Sites.....</b>	<b>66</b>
4.1	Overview.....	66
4.2	M-43 EB Over the Grand River.....	69
4.2.1	General Information.....	69
4.2.2	Scour Analysis Using SRICOS-EFA.....	72
4.2.3	Scour Analysis Using EIM .....	79
4.2.4	Scour Analysis Using GSN.....	84
4.2.5	Comparison of Results.....	85
4.3	US-2 and US-41 over the Escanaba River.....	89
4.3.1	General Information.....	89
4.3.2	Scour Analysis Using SRICOS-EFA.....	92
4.3.3	Scour Analysis Using EIM .....	95
4.3.4	Scour Analysis Using GSN.....	99
4.3.5	Comparison of Results.....	100
4.4	M-20 over the Tittabawassee River .....	101
4.4.1	General Information.....	101
4.4.2	Scour Analysis Using SRICOS-EFA.....	106
4.4.3	Scour Analysis Using EIM .....	113
4.4.4	Comparison of Results.....	119
4.5	M-64 over the Ontonagon River.....	122
4.5.1	General Information.....	122
4.5.2	Scour Analysis Using SRICOS-EFA.....	126
4.5.3	Scour Analysis Using EIM .....	132
4.5.4	Comparison of Results.....	136
4.6	Summary of the Implementation .....	139

<b>Chapter 5</b>	<b>Michigan-Specific Considerations for Scour Analysis in Erodible Rock and Cohesive Soil</b> .....	<b>141</b>
5.1	Surface Geology of Michigan.....	141
5.1.1	Bedrock Geology of the Lower Peninsula.....	143
5.1.2	Bedrock Geology of the Eastern Upper Peninsula.....	144
5.1.3	Bedrock Geology of the Western Upper Peninsula.....	146
5.2	Material (Rock) Classification for Scour Considerations.....	148
5.3	Scour Analysis without Gage Data.....	158
5.3.1	Use of SRICOS-EFA at Ungaged Sites.....	158
5.3.2	Use of GSN at Ungaged Sites.....	161
5.4	Scour Analysis in Layered Earth Strata.....	163
5.5	Material Testing Methods.....	166
5.5.1	SRICOS-EFA.....	166
5.5.2	EIM.....	168
5.5.3	GSN.....	169
5.6	Comparison of Scour Analysis Methods.....	170
5.6.1	SRICOS-EFA and HEC-18 Sand Equation.....	170
5.6.2	GSN and HEC-18 Sand Equation.....	173
<b>Chapter 6</b>	<b>Recommended Procedure for Bridge Scour Analysis in Erodible Rock and Cohesive Soil in Michigan</b> .....	<b>174</b>
6.1	Overview.....	174
6.2	Selection of New Methods.....	174
6.3	SRICOS-EFA.....	176
6.4	EIM.....	181
6.5	GSN.....	184
<b>Chapter 7</b>	<b>Conclusions</b> .....	<b>185</b>
7.1	Summary of Major Findings.....	185
7.2	Recommendations for Future Work.....	189
<b>Appendix</b>	.....	<b>192</b>
	<b>Illinois</b> .....	192
	<b>Indiana</b> .....	193

<b>Iowa</b> .....	195
<b>Kansas</b> .....	196
<b>Kentucky</b> .....	197
<b>Maryland</b> .....	198
<b>Minnesota</b> .....	199
<b>Missouri</b> .....	200
<b>Nebraska</b> .....	201
<b>New Jersey</b> .....	202
<b>New York</b> .....	203
<b>Ohio</b> .....	204
<b>Pennsylvania</b> .....	205
<b>Virginia</b> .....	208
<b>West Virginia</b> .....	209
<b>Wisconsin</b> .....	210
<b>Others</b> .....	211
<b>References</b> .....	<b>212</b>

## List of Figures

Figure 2.1 Different types of drilling apparatus: (a) hand auger, (b) simple auger, (c) rotary bucket, (d) continuous flight auger, (e) core drill with valve, (f) spoon core drill, (g) example of a clamshell grab (Monnet 2015). .....	33
Figure 2.2 Schematic diagram of common erosion rate test devices: piston type (left), rotating type (middle), and jet type (right) (Arneson 2012).....	35
Figure 2.3 Schematic of maximum scour depth and equilibrium scour depth based on Arneson (2012).....	42
Figure 2.4 Critical shear stress vs particle grain size (Briaud et al. 2011) .....	50
Figure 2.5 Erosion rate vs. velocity for a wide range of geomaterials (Briaud et al. 2011) .....	50
Figure 3.1 Erosion category curves for different earth materials (Retrieved from Briaud (2008), Briaud et al. (2019)).....	57
Figure 4.1 Location of M-43 EB over the Grand River (The image has been retrieved from Google Earth 2018 (Google)) .....	70
Figure 4.2 Earth cross-section at M-43 EB over the Grand River.....	71
Figure 4.3 Assumed/interpreted erosion curves on Briaud’s erosion category plot (Briaud 2008; Briaud et al. 2019) for the earth layers at Pier #1 of M-43 EB over the Grand River .....	73
Figure 4.4 Assumed/interpreted erosion curves on Briaud’s erosion category plot (Briaud 2008; Briaud et al. 2019) for the earth layers at Pier #2 of M-43 EB over the Grand River .....	74
Figure 4.5 Scour depth at Pier #1 of M-43 EB when Layer # 2 has critical shear of 2 Pa .....	78
Figure 4.6 Scour depth at Pier #1 of M-43 EB when Layer # 2 has critical shear of 9.5 Pa or 43 Pa or 80 Pa .....	78
Figure 4.7 Scour depth at Pier #2 of M-43 EB when Layer # 2 has critical shear of 9.5 Pa & Layer #3 has 43 Pa or when Layer # 2 has critical shear of 5 Pa & Layer #3 has 9.5 Pa.....	79

Figure 4.8 Cumulative scour depth of sandstone bedrock of Grand River at M-43 EB (a) using GSN as $4.54 \times 10^{-6} \text{ ft}[\text{ft} - \text{lbsft}^2]^{-1}$ and (b) using GSN as $2.53 \times 10^{-5} \text{ ft}[\text{ft} - \text{lbsft}^2]^{-1}$ .....	85
Figure 4.9 Location of US-2 and US-41 over the Escanaba River (The image has been retrieved from Google Earth, 2018 (Google)).....	90
Figure 4.10 Assumed/interpreted erosion curves on Briaud’s erosion category plot (Briaud 2008; Briaud et al. 2019) for the earth layers at Pier #1 of US-2 and US-41over the Escanaba River ..	92
Figure 4.11 Assumed/interpreted erosion curves on Briaud’s erosion category plot (Briaud 2008; Briaud et al. 2019) for the earth layers at Pier #2 of US-2 and US-41over the Escanaba River ..	93
Figure 4.12 Scour depth at Pier #1 of US-2 and US-41 over the Escanaba River.....	95
Figure 4.13 Scour depth at Pier #2 of US-2 and US-41 over the Escanaba River.....	95
Figure 4.14 Cumulative scour depth of Limestone bedrock of Escanaba River at US-2 and US-41 .....	100
Figure 4.15 Location of M-20 over the Tittabawassee River (The image has been retrieved from Google Earth, 2018 (Google)) .....	103
Figure 4.16 Assumed/interpreted erosion curves on Briaud’s erosion category plot (Briaud 2008; Briaud et al. 2019) for the earth layers at Pier #1 of M-20 over the Tittabawassee River .....	106
Figure 4.17 Assumed/interpreted erosion curves on Briaud’s erosion category plot (Briaud 2008; Briaud et al. 2019) for the earth layers at Pier #2 of M-20 over the Tittabawassee River .....	107
Figure 4.18 Assumed/interpreted erosion curves on Briaud’s erosion category plot (Briaud 2008; Briaud et al. 2019) for the earth layers at Pier #3 of M-20 over the Tittabawassee River .....	108
Figure 4.19 Scour depth of Pier #1 of M-20 over the Tittabawassee River .....	112
Figure 4.20 Scour depth of Pier #2 of M-20 over the Tittabawassee River .....	112
Figure 4.21 Scour depth at Pier #3 of M-20 over the Tittabawassee River.....	113

Figure 4.22 Location of M-64 over the Ontonagon River (The image has been retrieved from Google Earth, 2018 (Google)) .....	122
Figure 4.23 Assumed erosion curves on Briaud’s erosion category plot (Briaud 2008; Briaud et al. 2019) for the earth layers at Pier #7 of M-64 over the Ontonagon River .....	126
Figure 4.24 Assumed erosion curves on Briaud’s erosion category plot (Briaud 2008; Briaud et al. 2019) for the earth layers at Pier #8 of M-64 over the Ontonagon River .....	127
Figure 4.25 Assumed erosion curves on Briaud’s erosion category plot (Briaud 2008; Briaud et al. 2019) for the earth layers at Pier #9 of M-64 over the Ontonagon River .....	128
Figure 4.26 Assumed erosion curves on Briaud’s erosion category plot (Briaud 2008; Briaud et al. 2019) for the earth layers at Pier #10 of M-64 over the Ontonagon River .....	129
Figure 4.27 Scour depth at Pier #7 of M-64 over the Ontonagon River.....	131
Figure 4.28 Scour depth at Pier #8 of M-64 over the Ontonagon River.....	131
Figure 4.29 Scour depth at Pier #9 of M-64 over the Ontonagon River.....	132
Figure 4.30 Scour depth at Pier #10 of M-64 over the Ontonagon River.....	132
Figure 5.1 Generalized bedrock geology of Michigan (DEQ 2020) .....	142
Figure 5.2 Bedrock geology of Michigan in detail (DEQ 2020) .....	148
Figure 5.3 Interpreted erosion categories – unit stream power dissipation vs eGSI (datapoints in brackets have high uncertainty in one or more parameters, and are not contoured) (based on Pells (2016)).....	150
Figure 5.4 Effects of different pier parameters [based on Briaud et al. (2011)].....	161
Figure 5.5 Cumulative Scour depth of US-2 and US-41 over the Escanaba River assuming a constant flow for 75 years.....	163
Figure 5.6 SRICOS-EFA Software Soil Input Window .....	164
Figure 5.7 An example of SRICOS-EFA software output for scour depth over time .....	165

Figure 5.8 Cumulative scour depth at Pier #2 of M-20 over the Tittabawassee River using SRICOS-EFA software.....	172
Figure 6.1 Flow-chart showing the steps for selecting scour analysis method.....	175
Figure 6.2 Flow-chart showing the steps for obtaining the soil input categories for SRICOS-EFA .....	178
Figure 6.3 Flow-chart showing the steps for obtaining the geometry inputs for SRICOS-EFA.....	179
Figure 6.4 Steps for obtaining the water input categories for SRICOS-EFA.....	180
Figure 6.5 Conceptual flow chart of SRICOS-EFA .....	181
Figure 6.6 Flow-chart showing the steps for scour analysis using the EIM for rock .....	183
Figure 6.7 Flow-chart showing the steps for scour analysis using the EIM for cohesive soil layers .....	183
Figure 6.8 Flow-chart showing the steps for scour analysis using the GSN method .....	184

## List of Tables

Table 1.1 Relationship between research tasks, chapters, and research products .....	24
Table 2.1 Sampling techniques for different conditions of cohesive soil.....	29
Table 2.2 Field identification and unconfined compressive strength for rock .....	31
Table 2.3 Rock joint and gouge categorization .....	31
Table 2.4 Recommended rock sampling technique .....	34
Table 2.5 Relevant information from HEC-18 .....	48
Table 3.1 Mass strength number for rock ( $M_s$ ) based on Kirsten (1982) and Annandale (1995)	59
Table 3.2 Joint set number ( $J_n$ ) for rock based on Kirsten (1982) and Annandale (1995) .....	59
Table 3.3 Joint roughness number ( $J_r$ ) for rock based on Kirsten (1982) and Annandale (1995)	59
Table 3.4 Joint alteration number ( $J_a$ ) for rock based on Kirsten (1982) and Annandale (1995)	60
Table 3.5 Relative ground structure number ( $J_r$ ) for rock based on Kirsten (1982) and Annandale (1995).....	60
Table 3.6 Mass strength number for granular soil ( $M_s$ ) based on Kirsten (1982) and Annandale (1995).....	62
Table 3.7 Mass strength number for granular soil ( $M_s$ ) based on Kirsten (1982) and Annandale (1995).....	62
Table 4.1 Table for assigning RMR to rocks after AASHTO (2010).....	68
Table 4.2 Summary of drilled shaft foundation of M-43 over the Grand River.....	70
Table 4.3 Attributes of the earth layers at M-43 EB over the Grand River.....	72
Table 4.4 RMR of the 3 <sup>rd</sup> layer at Pier #1 and the 4 <sup>th</sup> layer at Pier #2 of M-43 EB over the Grand River.....	75

Table 4.5 Range of joint spacing for the 3 <sup>rd</sup> layer at Pier #1 and the 4 <sup>th</sup> layer at Pier #2 of M-43 EB over the Grand River.....	75
Table 4.6 Critical shear stress of each earth layer at M-43 EB over the Grand River based on the erosion category curves.....	76
Table 4.7 Scour determination at Pier #1 of M-43 over the Grand River using EIM .....	82
Table 4.8 Scour determination at Pier #2 of M-43 over the Grand River using EIM .....	82
Table 4.9 Sensitivity study of selected parameters on erodibility index and scour depth for rock layer at Pier #1 of M-43 over the Grand River .....	84
Table 4.10 Comparison of scour analysis results of M-43 over the Grand River .....	88
Table 4.11 Summary of foundation system of US-2 and US-41 over the Escanaba River .....	90
Table 4.12 Attributes of the earth layers at US-2 and US-41 over the Escanaba River .....	91
Table 4.13 Joint spacing and critical shear stress of each earth layer at US-2 and US-41 over the Escanaba River.....	93
Table 4.14 Scour determination at Pier #1 of US-2 and US-41 over the Escanaba River using EIM .....	98
Table 4.15 Scour determination at Pier #2 of US-2 and US-41 over the Escanaba River using EIM .....	98
Table 4.16 Comparison of scour analysis results at the bedrock of US-2 and US-41 over the Escanaba River.....	100
Table 4.17 Summary of drilled shaft foundation of M-20 over the Tittabawassee River .....	103
Table 4.18 Attributes of the earth layers at M-20 over the Tittabawassee River .....	104
Table 4.19 Attributes of earth layers at Pier #1 of M-20 over the Tittabawassee River .....	109
Table 4.20 Attributes of earth layers at Pier #2 of M-20 over the Tittabawassee River .....	110

Table 4.21 Attributes of earth layers at Pier #3 of M-20 over the Tittabawassee River .....	110
Table 4.22 Scour determination at Pier #1 of M-20 over the Tittabawassee River using EIM..	116
Table 4.23 Scour determination at Pier #2 of M-20 over the Tittabawassee River using EIM..	116
Table 4.24 Scour determination at Pier #3 of M-20 over the Tittabawassee River using EIM..	117
Table 4.25 Comparison of scour analysis results at M-20 over the Tittabawassee River .....	120
Table 4.26 Attributes of the earth layers at M-64 over the Ontonagon River .....	124
Table 4.27 Critical Shear Stress [lb/ft <sup>2</sup> (Pa)] of different earth layers at the Piers #7 through #10 of M-64 over the Ontonagon River .....	129
Table 4.28 Scour determination at Pier #7 of M-64 over the Ontonagon River using EIM.....	134
Table 4.29 Scour determination at Pier #8 of M-64 over the Ontonagon River using EIM.....	134
Table 4.30 Scour determination at Pier #9 of M-64 over the Ontonagon River using EIM.....	135
Table 4.31 Scour determination at Pier #10 of M-64 over the Ontonagon River using EIM.....	135
Table 4.32 Comparison of scour analysis results at M-64 over the Ontonagon River .....	137
Table 5.1 Classification of Michigan Bedrock for Scour Considerations .....	152
Table 5.2 Correction factor, <i>K</i> <sub>1</sub> for pier nose shape (Richardson et al. 2001) .....	160
Table 5.3 Scour depth at Pier #2 of M-20 over the Tittabawassee River over the for different discharges.....	161
Table 5.4 Scour depth of US-2 and US-41 over the Escanaba River for different discharges...	162
Table 5.5 Calculations of available and required stream power for scour depth determination at M-43 EB Pier #1 .....	165
Table 5.6 Table for scour depth in the event of 50-year flow equivalent to 32,678 cfs at Pier #2 of M-20 over the Tittabawassee River .....	171

Table 5.7 Table for comparing HEC-18 sand method and SRICOS-EFA for different flow duration  
at Pier #2 of M-20 over the Tittabawassee River ..... 171

# Chapter 1 Introduction

## 1.1 Statement of the Problem

Catastrophic bridge failures due to scour can result in a direct economic loss of millions of U.S. dollars and the indirect costs can be five times higher (Lagasse 2007; Lagasse and Richardson 2001; Liang et al. 2009) in addition to the loss of human lives (Jones and Richardson 2004; Little 2003). Approximately 60 percent of highway bridge failures in the U.S. resulted from scour (Lagasse 2007; Lagasse and Richardson 2001). During the 1985 flood season, for example, 73 bridge failures occurred in Virginia, West Virginia, and Pennsylvania. In 1987, 17 bridges sustained damage in New England and New York, and in 1994, 23 bridge failures occurred in the upper Mississippi basin and 500 bridges in Georgia were affected (Arneson 2012). In 1993, more than 2500 bridges were significantly affected by scour caused by severe flooding in the midwestern states (Mueller and Wagner 2005).

The failure of the Interstate Highway (I-90) Bridge over Schoharie Creek in New York during a flood in 1987 resulted in the Federal Highway Administration (FHWA) developing policies directed to the evaluation of all highway bridges with scour-critical conditions (Keaton et al. 2012). These policies have been implemented within the United States and direct either research or the direct measurement of bridge foundation scour susceptibility, the estimation of scour depth, and a general determination of scour susceptibilities for bridges in the United States (Moore 2012).

A comprehensive analysis of scour is published by the FHWA in three Hydraulic Engineering Circulars: “HEC-20 Stream Stability at Highway Structures” (Lagasse et al. 2012), “HEC-18 Evaluating Scour at Bridges” (Arneson 2012), and “HEC-23 Bridge Scour and Stream Instability Countermeasures” (Lagasse et al. 2009). The HEC-18 report is the primary guidance document for bridge scour analysis methodologies and is based generally on geomaterials and conditions in which scour can develop. Most of the U.S. Departments of Transportation (DOTs) have adopted the FHWA HEC-18 procedures although in some cases with modification for the state’s specific conditions (Benedict and Caldwell 2016; Carpenter and Miller 2011; Schuring et al. 2010; TxDOT 2018). HEC-18 equations for non-cohesive materials (addressed as HEC-18 sand throughout this report), which have been in practice since the late 1980s, are well established (Benedict 2014).

A major concern, however, is that the HEC equations over-predict the scour depth for certain geologic and hydraulic conditions. One major reason for the over-prediction is the unreasonable scaling and/or unrealistic representation of field conditions, especially because of the wide diversity of hydrologic, hydraulic, and geotechnical conditions that exist across the nation. Consequently, it is of interest to many road agencies to modify and/or calibrate the equations for more accurate scour depth calculations for Michigan-specific conditions. For example, MDOT launched a research project in 2007 to revise the HEC scour-prediction procedures to allow MDOT engineers to more accurately predict bridge scour and subsequently more efficiently and confidently design new bridge crossings and/or modify existing bridges (MDOT RC-1547).

The second concern, and the primary emphasis of this study, is the inadequate consideration of cohesive soils and scour-susceptible rock in the scour prediction equations. Scour in cohesive soils and scour-susceptible rock has been a challenge for engineers in designing safe and cost-effective bridges with these site characteristics. Cohesive soils and rocks different exhibit scour processes from cohesionless soils. The most obvious difference is that materials scour at different rates. Loose granular soils are rapidly eroded by flowing water, while cohesive or cemented soils are more scour resistant. Under constant flow conditions, scour will reach the maximum depth in the sand and gravel-bed material in hours; cohesive material beds possibly in days; glacial till, sandstones, and shale in months; limestone in years, and dense granite in centuries (Arneson 2012; Gazi et al. 2019). Under normal flow conditions typical of actual bridge crossings, several floods may be needed to attain the maximum scour. A considerable amount of research has been conducted to understand the uniqueness of cohesive soils, and a couple of studies are available for scour in erodible rock. Although there have been some studies conducted to assess or support the performance of HEC-18 Edition 5, minimal information or direction has been provided on abutment scour for cohesive soils and erodible rock (Arneson 2012). These limitations necessitate a study of the existing procedures and their performance in the field of scour analysis in cohesive soils and erodible rock considering the geological and hydrological conditions of Michigan.

## **1.2 Objectives of the Study**

The overall goal of the study is to establish the necessary information for developing improved calculations for scour potential in cohesive soils and scour-susceptible rock. This overall goal is achieved through the accomplishment of a series of objectives by leveraging existing research, technology, and MDOT resources. The detailed study objectives are as follows.

1. Summarize the state of the art in evaluating scour potential in cohesive soils and scour-susceptible rock and classify various types of rocks as foundationally stable.
2. Identify any unique characteristics of Michigan hydrology or geology that is not currently covered in existing research, testing, or literature.
3. Recommend any areas that would require investigations to aid MDOT in fully implementing advanced testing and analysis of cohesive soil and scour-susceptible rock.

## **1.3 Overview of Research Tasks**

The above three objectives were achieved via the following five tasks. This section outlines the research tasks and the major research and action items for each task.

### **Task 1 State of the Practice Survey for Scour Analysis in Cohesive Soil and Scour-susceptible Rock**

Task 1 gathered necessary background knowledge for bridge scour evaluations for cohesive soils and scour-susceptible rock via:

- ❖ Reviewing existing literature and state of the practice regarding the application of sampling, scour calculations, and erodibility determinations for typical cohesive soil and rock types in Michigan,
- ❖ Surveying MDOT engineers to identify current practices for sampling, scour calculations, and scour susceptibility determinations of cohesive soil and rock, and
- ❖ Interviewing other state DOTs to understand the state of practice for scour analysis in cohesive soils and scour-susceptible rock.

### **Task 2 Survey of Sampling and Testing Techniques for Cohesive Soil and Scour-susceptible Rock**

Task 2 was conducted to synthesize the existing information on the following topics and their scour applicability in the Michigan geologic and hydraulic environment:

- ❖ Cohesive soil sampling techniques and testing devices that are related to scour analysis and
- ❖ Rock sampling techniques and testing devices that are related to scour analysis.

### **Task 3 Evaluation of Scour Analysis Methods**

Task 3 was devoted to the selection, implementation, and evaluation of scour analysis methods for non-cohesive soils and scour-susceptible rock and the associated testing and input data via the following research activities:

- ❖ The most suitable methods were selected and applied to selected bridge sites in Michigan to test the applicability, needed data, and possible issues.
- ❖ Sensitivity analysis was carried out to test the effect of different parameters on the analysis results to draw conclusions that can guide future applications of these methods. Comments were made to summarize the factors relevant to the problems.
- ❖ Based on the analysis, workflows in the form of flowcharts were developed to show the procedure for implementing the selected methods in Michigan, including sampling and testing in Task 2, input for the selected methods, steps for implementing the methods, and anticipated analysis results as the output.

### **Task 4 Investigation of Factors and Issues Affecting Scour Evaluations in Michigan's Cohesive Soil and Scour-susceptible Rock**

Task 4 was proposed to investigate the factors that can affect the application of the above bridge sampling, testing, and scour analysis methods. Such factors were identified in the state of the practice survey, the survey on the sampling and testing methods, and the implementation of the selected bridge scour analysis methods at the selected bridge sites. Specifically, the following three aspects are covered in detail.

- ❖ The surface geology of Michigan was discussed for bridge scour. This provides Michigan engineers with a geology background in the preliminary assessment of bridge scour.
- ❖ A material classification was presented to estimate the scour susceptibility of typical rocks in Michigan.

- ❖ Issues identified in the application of the selected bridge scour analysis methods are discussed and their solutions are detailed.

## **Task 5 Development of Final Report**

This task summarizes the findings and recommendations for drafting the final report.

### **1.4 Organization of This Report**

This report was organized into seven chapters and an appendix. The contents of each chapter can be seen in the Table of Contents. The titles of the chapters are listed in the following:

Chapter 1 Introduction

Chapter 2 Literature Review

Chapter 3 Scour Analysis Methods for Erodible Rock and Cohesive Soil

Chapter 4 Implementation of Selected Methods for Bridge Scour Analysis at Four Michigan Sites

Chapter 5 Michigan-Specific Considerations for Scour Analysis in Erodible Rock and Cohesive Soil

Chapter 6 Recommended Procedure for Bridge Scour Analysis in Erodible Rock and Cohesive Soil in Michigan

Chapter 7 Conclusions

The major objective of the project is to accomplish the scour analysis methods for bridges founded on cohesive soils and scour-susceptible rock in Michigan. To meet this objective, Chapter 1 first presents a statement of the problem, the objective of this study, and the organization of this report. Next, Chapter 2 shares the knowledge gained in the literature review and communications with engineers from MDOT and other state DOTs. This knowledge covers the essential aspects of bridge scour in cohesive soils and scour-susceptible rock, including scour susceptibility concepts, sampling, erodibility testing, and scour analysis methods. Chapter 3 introduces the theories underlying three methods that are selected for the scour analysis for cohesive soils and scour-

susceptible rock in this project. Then, in Chapter 4, the implementation of these three methods for analyzing the bridge scour at four bridge sites are introduced: two for clay and the other two for rock. In Chapter 5, Michigan’s geologic information, mainly the surface bedrock and cohesive soil and their scour susceptibility, a rock classification for scour considerations, and other issues in the application of the selected bridge scour analysis methods are documented. Chapter 6 provides flowcharts and their descriptions to illustrate how to apply these three scour analysis methods, from sampling, testing, to detailed steps of bridge scour analysis.

There are clear relationships between the research tasks, chapters, and major research products as shown in Table 1.1. Chapter 1 offers an overview of the whole project, laying down a statement of the problem, objectives of the study, research plan with detailed research tasks, and the organization of the report. This will set up a solid basis for conducting the five research tasks. The effort made in Task 1 is detailed in Chapter 2, leading to a literature review on relevant sampling, testing, and bridge scour analysis, and a summary of the other state DOT’s practices in scour analysis for cohesive soil and erodible rock. The work in Task 3, including three selected scour analysis methods and their implementation are organized into theories in Chapter 3 and case studies of four bridge sites in Michigan in Chapter 4. Geology information for bridge scour considerations in Michigan, rock classification for scour in Michigan, and issues and solutions for scour analysis in Michigan are documented in Chapter 5. To facilitate application, flowcharts are given in Chapter 5 to guide the evaluation of bridge scour in cohesive soils and scour-susceptible rock, with the selected methods and their associated sampling and testing techniques. Task 7 summarizes all the accomplished work to generate this report.

Table 1.1 Relationship between research tasks, chapters, and research products

Task	Chapter	Major Products
Task 1	Chapter 2	State of the practice review
Task 2	Chapters 2 & 3	Scour analysis methods for cohesive soil and erodible rock
Task 3	Chapters 3 & 4	Implementation of the three selected methods; Case studies of the bridge scour at four clay/rock sites

Task 4	Chapters 5 & 6	Geology information for bridge scour considerations in Michigan; rock classification for scour in Michigan; issues and solutions for scour analysis in Michigan
Task 5	Chapters 1-7	This report.

---

## **Chapter 2 Literature Review**

This chapter provides a literature review study that summarizes knowledge about the state of practice for analyzing bridge scour in cohesive soils and scour-susceptible rock from both the literature and communication with other road agencies. The definition, mechanisms, and factors of bridge scour will be introduced first. Next, relevant sampling and erodibility testing techniques will be summarized. Then, existing analysis approaches will be discussed for cohesive soil and scour-susceptible rock. Finally, information gained from communications with other road agencies regarding their bridge scour considerations in these two materials will be presented.

### **2.1 Bridge Scour Susceptibility**

Soil erosion involves complex mechanisms, which become more complex in the presence of water. The erosion process in a channel bed depends on the cohesion of the bed material. While a typical non-cohesive bed erodes particle by particle, a cohesive or sand-clay mixture bed erodes chunk by chunk, particle by particle, and/or aggregate by aggregate (Chaudhuri and Debnath 2013; Kothyari et al. 2014). Even the same type of soil that originated at different locations can have different erodibility (Song et al. 2005). Under a normal flow condition, a cohesive river bed may erode over several days; by contrast, a sandy or fine gravel bed may erode within hours. Rocks are generally more scour resistant – sandstone, glacial till, and shales need months to erode, limestones require years, and granites remain coherent over centuries (Arneson 2012; Gazi et al. 2019). Factors and mechanisms that can affect the scour susceptibility of bridges founded on erodible rock and cohesive soil will be introduced in the following sub-sections.

#### **2.1.1 Scour Susceptibility of Bridges on Cohesive Soil**

Cohesive soil's erodibility increases with the increase of the void ratio, soil swell, sodium absorption ratio, soil temperature, and water temperature. However, an increase in the soil unit weight, undrained shear strength, plasticity index, or amount of clay content can strengthen the cohesive soil against scour (Arneson 2012). The erodibility of cohesive soil can be assessed in

terms of the bed strength, e.g., the Unconfined Compressive Strength (UCS) and vane shear strength (Harris and Whitehouse 2017). While the UCS is suitable for clay-sand-gravel mixed beds (Kamphuis and Hall 1983; Kothyari and Jain 2008; Kothyari and Jain 2010; Kothyari et al. 2014; Robinson and Hanson 1995), the vane shear strength is good for soft clayey channel beds (Debnath and Chaudhuri 2010; Kothyari et al. 2014). The bed strength parameter is related to the critical shear stress - a very significant parameter for assessing scour susceptibility of cohesive beds (Wei et al. 1997). Below this shear stress value, cohesive soil shows no or little trace of erosion; but when this value is exceeded, remarkable erosion takes place (Teisson et al. 1993). Studies found that the critical shear stress of cohesive soil is directly proportional to the UCS, vane shear strength, unit weight, and consolidation stress but inversely proportional to the water content and void ratio (Harris and Whitehouse 2017; Rahimnejad and Ooi 2016). As a preliminary step, erodibility, or in other words, scour susceptibility of a cohesive stream bed can be determined from the erosion rate vs. shear stress curve provided by Briaud (2008) (Arneson 2012; Briaud et al. 2011).

### **2.1.2 Scour Susceptibility of Bridges on Rock**

For bridges founded on rock, the scour mode is an essential term in scour susceptibility testing. Rock erosion can take place in four different modes in natural channels – Dissolution, Cavitation, Quarrying and Plucking, and Abrasion (Arneson 2012; Hancock et al. 1998; Whipple et al. 2000). Dissolution is the scour mode applicable for soluble rock. Only strong soluble mineral types such as limestone and dolostone are used for bridge foundations, and they do not have any evidence of scour within the life span of the founded structures (Keaton et al. 2010). Besides, mineral types with noticeable dissolution in engineering timescales, e.g., halite, sylvite, anhydrite, are usually identified in site investigations before construction, and as a result, structures would not be founded on these rock types considering their general poor mechanical properties (Titi et al. 2017). Cavitation is a very common phenomenon in pipe and tunnel design (Keaton et al. 2010). Though cavitation sometimes can also take place in natural streams, it is not common at the bridge sites (Arneson 2012; Keaton et al. 2012). The quarrying and plucking mode of scour usually occurs in rocks with fractures and/or joints. This process involves block removal and is governed by the block size and geometry, stream velocity, and turbulence intensity (Keaton et al. 2010). Abrasion

is the gradual and progressive mode of scour for degradable rocks that takes place due to hydraulic loading over time. Scour of degradable rocks depends not only on their geological properties but also on the flow condition of the channels (Keaton et al. 2012). Apart from these scour modes, physical and chemical weathering, wetting and drying, heating and cooling, and freezing and thawing can also lead to rock degradation (Arneson 2012; Keaton et al. 2009).

The NCHRP-717 report titled ‘Scour at Bridge Foundations on Rock’ presents a flow chart for identifying possible bridge scour modes in erodible rock (Keaton et al. 2010; Keaton et al. 2012). Niemann et al. (2017) worked with West Virginia DOT and proposed a risk-based screening approach for bridge foundations in erodible rock. In this approach, a bridge site can be scored based on the geologic province, rock type, weathering effect, longitudinal flow profile, presence of joints, condition of the scour surface, sample field test, and lab test results. Based on that, any bridge founded on rock can be labeled as one of three tiers: Tier I is for bridges which are safe from future scour, Tier II is for bridges exposed to the abrasion mode of scour, and Tier III is for bridge sites having the quarrying mode of scour (Niemann et al. 2017; Zatar et al. 2013).

## **2.2 Sampling and Erodibility Testing**

### **2.2.1 Sampling**

Core samples representative of undisturbed soil layers are desired for obtaining material properties needed for bridge scour analysis of cohesive soil. Various sampling techniques are available for cohesive soils depending on the properties/category of the soil. Table 2.1 shows several sampling techniques and their use for different conditions of cohesive soil.

If the site has very soft to soft, fine soil, then a stationary piston core drill can be used by continuously sinking it under force. Thin-walled core drill with casing can also be used in a similar manner, however, in the presence of slurry. An auger and rotary bucket with a rotation mode can also be used for collecting undisturbed core from a very soft to soft, fine soil site.

For firm, fine soil, a stationary piston core drill and thin-walled core drill with/without casing can be used in a similar way as soft fine soil, and can also be used by hammering. A triple corer with

overturning case, triple corer, or double corer can also be used for collecting firm fine soil samples by rotation in the presence of water/slurry. An auger and rotary bucket, which works by rotation, can also be used at such sites, in addition to collecting samples by hand, mechanical shovel, or box.

For sampling stiff to very stiff, fine soil, a thin-walled or thick-walled corer can be used by hammering or continuously sinking it under force. A triple corer with overturning case, triple corer, or double corer can be used by rotation in the presence of water/slurry. A simple corer or an auger and a rotary bucket can be used by rotation. Collecting sample by hand, mechanical shovel or box will also work.

For a hard, fine soil site, sampling can be done either by triple corer with overturning case, triple corer, double corer, simple corer, auger, and rotary bucket in rotation, or by collecting a sample by hand, mechanical shovel, or box. Whatever the sampling technique is in the case of hard fine soil, the presence of water is always necessary.

Table 2.1 Sampling techniques for different conditions of cohesive soil

<b>Cohesive Material Category</b>	<b>Sampling Tool</b>	<b>Tool Use</b>	<b>Fluid</b>
Very soft to soft fine soil	Stationary piston core drill	Continuous sinking under force	N/A
	Thin-walled core drill with casing	Continuous sinking under force	Slurry
	Auger and rotary bucket	Rotation	N/A
Firm, fine soil	Stationary piston core drill	Continuous sinking under force	N/A
	Thin-walled core drilling with or without casing	Continuous sinking under force	Slurry
		Hammering	N/A
	Triple corer with overturning case	Rotation	Water or slurry
	Triple corer	Rotation	Water or slurry
	Double corer	Rotation	Water or slurry
Auger and rotary bucket	Rotation	N/A	

	Sampling blocks by hand	By hand	N/A
	Sampling blocks by box	By hand or sinking under force	N/A
	Loose	Mechanical shovel	N/A
Stiff to very stiff fine soil	Thin-walled corer	Continuous sinking under force Hammering	N/A
	Thick-walled corer	Continuous sinking under force Hammering	N/A
	Triple corer with overturning case	Rotation	Water or slurry
	Triple corer	Rotation	Water or slurry
	Double corer	Rotation	Water or slurry
	Simple corer	Rotation	N/A
	Auger and rotary bucket	Rotation	N/A
	Sampling blocks by hand	manual	N/A
	Sampling blocks by box	By hand or by forced sinking	N/A
	Loose	Mechanical shovel	N/A
Hard, fine soil	Triple corer with overturning case	Rotation	Water
	Triple corer	Rotation	Water
	Double corer	Rotation	Water
	Simple corer	Rotation	Water
	Auger and rotary bucket	Rotation	Water
	Sampling blocks by hand	manual	Water
	Sampling blocks by box	By hand or by forced sinking	Water
	Loose	Mechanical shovel	Water

For rock scour evaluations, samples need to be collected with the consideration of possible scour modes and other geologic characteristics. Conventional sampling procedures for site characterization (e.g., for foundation design) can be used for considering scour in the dissolution or cavitation mode. The quarrying and plucking modes need field observations, measurements, and lab tests, such as the Unconfined Compressive Strength (UCS), Rock Quality Designation (RQD), number of rock joints/fissures, joint condition, description of gouge, joint spacing, dip angle, dip direction, and rock length and width ratio (Arneson 2012; Keaton et al. 2012). Table 2.2 and Table 2.3 show examples of field observations and measurements summarized in Kirsten (1982), Annandale (1995), Keaton et al. (2012), and the HEC-18 Edition 5 (Arneson 2012).

Table 2.2 Field identification and unconfined compressive strength for rock

<b>Field Identification</b>	<b>Hardness</b>	<b>UCS (MPa)</b>
Material crumbles under firm (moderate) blows with the sharp end of the geological pick and can be peeled off with a knife; is too hard to cut triaxial sample by hand.	Very soft rock	< 3.3
Material can just be scraped and peeled with a knife; indentations 1 mm to 3-mm show in the specimen with firm (moderate) blows of the pick point.	Soft rock	3.3-13.2
Material cannot be scraped or peeled with a knife; hand-held specimen can be broken with hammer end of geological pick with a single firm (moderate) blow.	Hard rock	13.2-26.4
Hand-held specimen breaks with hammer end of pick under more than one blow.	Very hard rock	26.4 -106.0
Specimen requires many blows with geological pick to break through intact material.	Extremely hard rock	> 212

Table 2.3 Rock joint and gouge categorization

Number of rock joint/fissure category	Intact, no or few joints/fissures
	One joint/fissure set
	One joint/fissure set plus random
	Two joint/fissure sets
	Two joint/fissure sets plus random
	Three joint/fissure sets
	Three joint/fissure sets
	Four joint/fissure sets
	Multiple joint/fissure sets
Condition of Joint category	Stepped joints/fissures
	Rough or irregular, undulating
	Smooth undulating
	Slickensided undulating
	Rough or irregular, planar
	Smooth planar
	Slickensided planar
Joints/fissures either open or containing relatively soft gouge of sufficient thickness to prevent joint/fissure wall contact upon excavation	

Shattered or micro-shattered clays	
Description of Gouge	Tightly healed, hard, non-softening impermeable filling
	Unaltered joint walls, surface staining only
	Slightly altered, non-softening, non-cohesive rock mineral or crushed rock filling
	Non-softening, slightly clayey non-cohesive filling
	Non-softening, strongly over-consolidated clay mineral filling, with or without crushed rock
Softening or low friction clay mineral coatings and small quantities of swelling clays	
Softening moderately over-consolidated clay mineral filling, with or without crushed rock	
Shattered or micro-shattered (swelling) clay gouge, with or without crushed rock	

For the abrasion mode of scour in rock, both manually collected samples and core samples are important (Keaton et al. 2012). Where coring is not possible, hand samples can be an alternative (Titi et al. 2017). Hand samples can be collected using the following procedure. These steps can also be followed for cohesive soil hand sampling when necessary (Monnet 2015):

- ❖ Clean the ground surface,
- ❖ Identify the sample to collect,
- ❖ Carefully, begin to dig around,
- ❖ Continue to dig around the sample and trim the sides,
- ❖ Cut the sample from its substratum,
- ❖ If the sample is fragile, put it in a box before cutting away,
- ❖ Use removable plastic film- paraffin wax along all the sides of the sample,
- ❖ Fill the space between the box and the paraffined sample with damp sand or sawdust.

Core samples of rock can be collected by core drilling, semi-destructive drilling, or destructive drilling. Typical core drilling techniques include punch core drilling and rotary core drilling. Punch core drilling involves beating, jacking, or vibro sinking. A rotary corer can be a simple corer, double corer, or triple corer. Semi destructive drilling extracts soil samples in a continuous manner in an amended form using hand augers, simple augers, rotary buckets, drilling with continuous flight auger, valve drilling, or clamshell grab and spoon sampler (Figure 2.1). Destructive drilling

includes hammering, rotation, or vibro sinking of the drill bit in the presence of drilling fluids, water, slurry, or air.

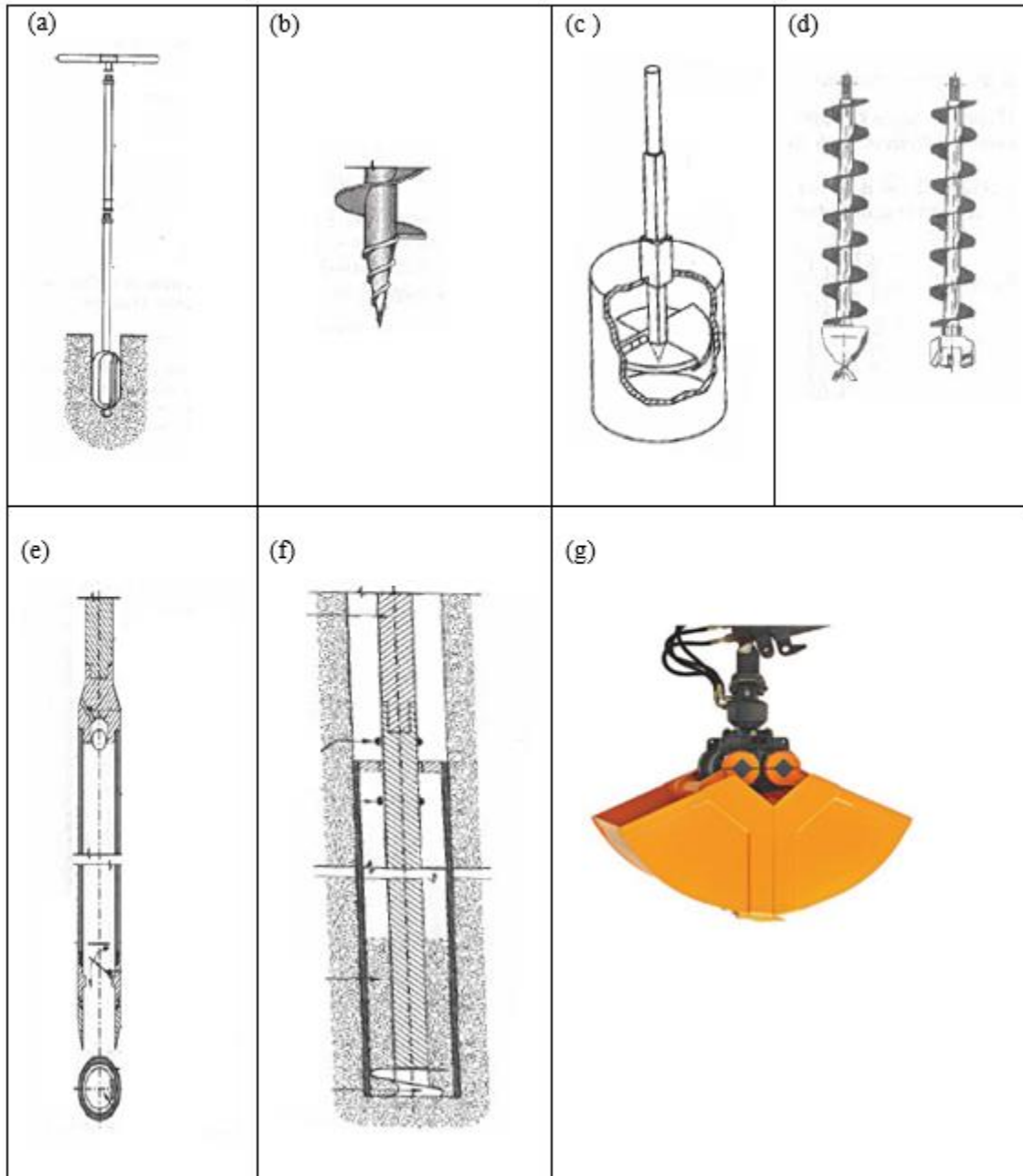


Figure 2.1 Different types of drilling apparatus: (a) hand auger, (b) simple auger, (c) rotary bucket, (d) continuous flight auger, (e) core drill with valve, (f) spoon core drill, (g) example of a clamshell grab (Monnet 2015).

Table 2.4 shows the rock sampling techniques recommended by Monnet (2015). A simple corer, double corer, or triple corer can be used by rotation, and a disintegrator can be used by rotation or roto-percussion. The core drill can be cooled by water or water and slurry. Generally, a simple corer is recommended for sound rock, whereas, a double corer is good for loose ground, soft rock, and altered rock.

Table 2.4 Recommended rock sampling technique

Sampling Tool	Tool Use	Fluid
Simple corer	Rotation	
Double corer	Rotation	Water or
Triple corer	Rotation	Water + Slurry additive
Disintegrator	Rotation or roto-percussion	

### 2.2.2 Erodibility Testing

Erodibility of rock and cohesive beds in streams involves both the hydraulic action of water and the erosion resistivity of the geomaterials. As a result, the relationship between the erodibility rate and shear stress of the stream bed is important in the scour depth calculation for these two types of strata. Three common types of devices are available for erodibility testing of soil or rock – piston, rotating, and submerged jet type devices (Figure 2.2). Piston and rotating type devices are laboratory devices, but a submerged jet type device can be used both in the field and laboratory. Data taken from all these test devices can be used to develop a relationship between the erodibility rate and shear stress of the sample (Arneson 2012).

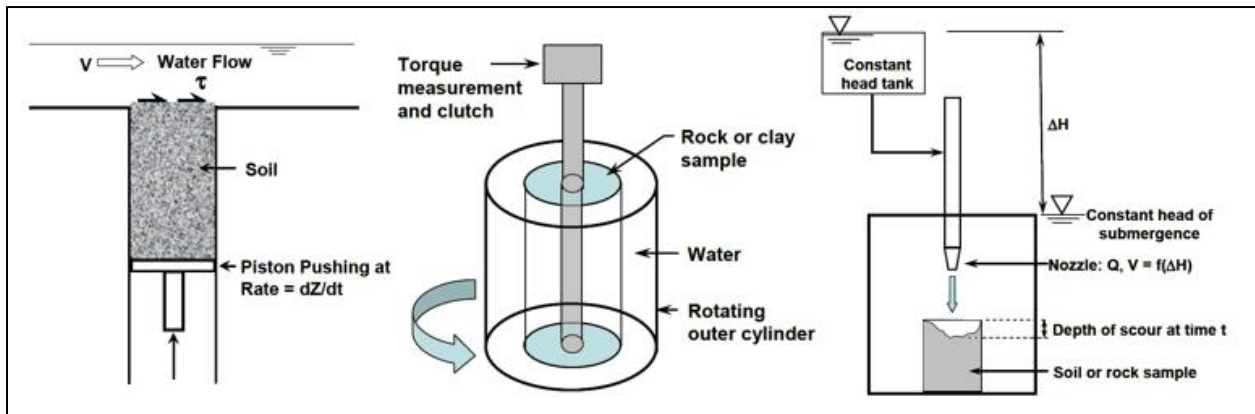


Figure 2.2 Schematic diagram of common erosion rate test devices: piston type (left), rotating type (middle), and jet type (right) (Arneson 2012).

In the following, erodibility testing for cohesive soils and erodible rock will be discussed first. Then, more information will be provided for popular erodibility testing techniques.

### **Erodibility Testing for Cohesive Soil**

Briaud et al. (2001a) developed a piston-type device called the Erosion Function Apparatus (EFA) (Figure 2.2), mainly for cohesive soils, which allows minimal sample disturbance and is suitable for site-specific scour studies. This apparatus develops a relationship between erosion rate and shear stress. EFA is an expensive laboratory device and primarily available in research institutes (Rahimnejad and Ooi 2017). A pocket erodometer can be a quick and simple option for determining the preliminary strength of the in-situ soil (Briaud et al. 2012; Briaud and Oh 2010). The Jet Erosion Test (JET) is a submerged jet type device suitable for both in situ and laboratory testing (Hanson 1990b; Hanson and Cook 1997; Hanson and Simon 2001) and is considered to be the standard for determining the erodibility of cohesive soil (Daly et al. 2013). Another in-situ erodibility testing method of cohesive soils entitled 'Borehole Erosion Test' (BET) has been proposed, which requires further testing on its functionality (Briaud et al. 2017). Rotating Erosion Testing Apparatus (RETA) is a rotating type device (Figure 2.2) which was developed at the University of Florida to determine the relationship between the shear stress and erosion rate of rock and stiff clays (Bloomquist and Sheppard 2010; Henderson 1999; Kerr 2001; Sheppard and Bloomquist 2005). RETA is also used for the erodibility testing of cohesive soil by some DOTs like FDOT (FDOT 2019). The integration of computerized Sediment Erosion Rate Flume (SERF) with EFA or RETA can provide a time rate of erosion (Crowley et al. 2012), which is the primary factor for scour in cohesive soil.

## **Erodibility Testing for Rock**

Preliminary assessment of the scour susceptibility of rock can be conducted with visual inspection for weak zones in the rock bed and other field test results. To characterize the scour resistivity of a rock sample, core recovery techniques can be used (KYTC 2019). For estimating the rock quality, the Rock Quality Designation (RQD) (Deere et al. 1966) is also widely adopted in practice (Arneson 2012; Deere 1988). For example, shale and limestone with an RQD of less than 20% can have lead up to 6 inches of scour depth below the foundation level (Hopkins and Beckham 1999). However, this parameter might not always lead to the right direction, especially, for quarrying and plucking mode of scour. For example, a rock with a low RQD value might not be susceptible to scour in all flow conditions (Keaton et al. 2012; Niemann et al. 2017; Palmstrom 2005). The Modified RQD test, Slake Durability Index test (SDI), Jar Slake Test, and Cone Penetration Test (CPT) are also frequently used in practice (KYTC 2019; NRCS 2001; TxDOT 2018).

Florida DOT has saved a significant amount of money by using RETA results, which eliminated the need for scour protection of several bridge sites (Bloomquist et al. 2012). The disadvantages of RETA are that the sample must have some minimum durability (Keaton 2013; Keaton et al. 2012) and the test results do not measure the horizontal surface erosion rate (Bloomquist et al. 2012). Annandale (1995) suggested a method called the erodibility index method, which incorporates both hydraulics and engineering geology to determine the critical erosion threshold for any earth material including cohesive soil and rock. The erodibility index is similar to the headcut erodibility index (Moore 1997; Moore et al. 1994; NRCS 2001). It measures the resistance of any earth material to erosion based on Kirsten's rippability index (Kirsten 1982) and is a function of the material's mass strength, particle/block size, discontinuity/inter-particle bond shear strength, and relative ground structure (Annandale 1995). All these geological parameters can be obtained by some field tests by using the standard tables provided by Kirsten (1982). Field tests include the Standard Penetration Test (SPT), Unconfined Compressive Strength (UCS), RQD, and visual inspection for the number of joints, dip angle and direction, joint roughness, and joint alteration (Annandale 1995; Kirsten 1982). Unfortunately, this erodibility index method did not account for protruding rocks (Coleman et al. 2003; Coleman et al. 2005) and the continuous movement of water and bedload over the rock-bed channel (Dickenson and Bailie 1999). Bollaert (2010) proposed a set of threshold velocities for rock plucking where the rock protrusion was

addressed. Dickenson and Bailie (1999) worked with the Oregon DOT and modified the standard slake durability (ASTM 2016) test for continuous abrasion testing and suggested the abrasion number for quantifying rock's response under submerged tumbling action. Keaton and Mishra (2010) further modified this test and termed it a "modified slake durability test" to determine geotechnical scour number, which can be a potential parameter in rock scour depth calculation (Keaton et al. 2012).

### **In-situ Erosion Tests**

- ❖ Field Jet Erosion Test (JET): JET (Hanson 1990a; Hanson 1990b) was developed at the U.S. Department of Agriculture, Agricultural Research Service in 1990, and is considered to be the standard for determining the erodibility of cohesive soil (Daly et al. 2013). In this test procedure, water is allowed to flow through a submerged, vertical jet at various velocities perpendicularly to the soil surface and the depth of the hole made by the jet at every sequence is recorded as a function of time.
- ❖ In Situ Erosion Evaluation Probe (ISEEP): ISEEP (Gabr et al. 2013) is a vertical jet type device developed at North Carolina State University, and is suitable for the erodibility of any soil at any depth. The methodology of the test includes penetration of the jet probe at various velocities and the outcome is the rate of advancement of the jet probe versus the stream power achieved by the soil due to the jet velocity.
- ❖ Borehole Erosion Test (BET): BET (Briaud et al. 2017) is suitable for any soil or rock which can be drilled. This test provides erodibility as a function of depth. This test method requires a hole to be drilled at the desired depth, where water is circulated at various velocities to record the erosion rate. Also, the erosion rate versus shear stress can be obtained from this test.
- ❖ Pocket Erodrometer Test (PET): Pocket erodometer (Briaud et al. 2012; Briaud and Oh 2010) is a mini jet-type device developed at Texas A&M University. It is used to record the erosion depth created at the sample surface due to 20 impulses of water at a velocity of 8.0 m/s. The erosion depth can be plugged into the erosion category curve (Briaud et al. 2012) to obtain the erodibility state and the erosion rate of the sample.

- ❖ In Situ Scour Testing Device (ISTD): The cylindrical-shaped in-situ scour testing device (ISTD) (Zinner et al. 2016) is capable of estimating the erodibility of soil at any depth. It can fit both in the boring test rig and steel casing of a hollow stem auger. The development of the device supported by FHWA is still in progress. Its function is limited to upper soil layers, the soil below the groundwater table, and soil having N-value less than 30.
- ❖ Field flume tests: Sediment Erosion at Depth Flume has a portable version that can be carried to the site to measure the erodibility of the soil sample. The advantage of this test is that it has field representation as the field water can be used, but the major drawback is that this test can only be used for disturbed samples.

### **Laboratory Erosion Tests**

- ❖ Lab Jet Erosion Test (JET): A lab version of JET was developed by Hanson and Hunt (2007). This test apparatus has a circular jet submergence tank where the compacted soil sample is placed and water is allowed to flow through the jet at a given velocity perpendicular to the soil surface. The depth of the hole made due to water flow is recorded as a function of time.
- ❖ Rotating Cylinder Test (RCT) and improved versions: Moore and Masch Jr (1962) developed RCT for cohesive soil to record the critical shear stress under rotating flow around the side of the cylindrical sample. Later, this test was modified by Chapuis and Gatién (1986) to record the erosion rate of cohesive soil for various shear stress.
- ❖ Rotating Erosion Testing Apparatus (RETA): RETA is a rotating-type device that was developed at the University of Florida to determine the relationship between the shear stress and erosion rate of stiff clays and hard rock such as limestone and sandstone (Bloomquist and Sheppard 2010; Henderson 1999; Kerr 2001; Sheppard and Bloomquist 2005). The disadvantages of RETA are that the sample must have some minimum durability (Briaud et al. 2019; Keaton 2013; Keaton et al. 2012) and the test results lack the horizontal surface erosion rate (Bloomquist et al. 2012).
- ❖ Erosion Function Apparatus (EFA) and similar versions: Briaud et al. (2001a) developed EFA, a piston-type device (Figure 2.2) for a wide range of cohesive soil, non-cohesive soil, and soft rock (Briaud et al. 2019), which allows minimal sample disturbance and is suitable

for site-specific scour studies. This apparatus can be used to measure the relationship between the erosion rate and velocity/shear stress. The Sediment Erosion Rate Flume (SERF), Sediment Erosion at Depth Flume (SEDflume), and Ex Situ Scour Testing Device (ESTD) work similarly. SERF is no longer used in practice due to the user inconvenience and costly setup. Neither SEDflume nor ESTD can measure the field erodibility conditions well since they are only suitable for disturbed or handmade samples.

## **2.3 Scour Analysis Approaches for Erodible Rock and Cohesive Soil**

Most of the scour analysis studies before the late 1990s were for non-cohesive soil and the method followed was HEC-18 (Richardson and Davis 2001), which was developed based on FHWA's previous versions of the report on evaluating bridge scour (Chaulagai et al. 2016). Recently, several researchers including some DOTs have studied the HEC-18 sand equation for cohesive soils and/or erodible rocks and found that HEC-18 overpredicts in both cases and consequently leads to costly design (Annandale and Smith 2001; Calappi et al. 2010; Ettema et al. 2011; Kassem et al. 2003; Lee and Hedgecock 2008; Williams-Sether 1999; Zhang et al. 2013). Some studies contain site- and/or soil-specific equations or curves (Benedict and Caldwell 2016; Benedict et al. 2016; Lee and Hedgecock 2008; Rahimnejad and Ooi 2016; Rahimnejad and Ooi 2017), but universal approaches in this arena still need more research.

### **2.3.1 Scour in Cohesive Soil**

Hosny (1996) was the first to conduct a systematic investigation of bridge scour in a cohesive soil and the mixture of cohesive and non-cohesive channel beds. From this research, an equation for bridge pier scour in cohesive soil was proposed based on several flume experiments, but the results were not verified in either the laboratory or the field. Gudavalli (1998) proposed another equation containing pier and flow properties based on laboratory flume tests but did not include soil properties. Scour depth as a function of the pier and flow conditions, ignoring soil properties, implied that piers having the same properties and same flow conditions had the same scour depth, irrespective of the types of underlying erodible soils (Devi and Barbhuiya 2017; Salaheldin et al. 2003). One way to consider all field variabilities is by mimicking the field conditions in a small-

scale lab model for scour monitoring and scaling up the recorded erosion rate and depth to obtain relationships that can be used in the field (Kassem et al. 2003; Salaheldin et al. 2003), which is, however, not always feasible. Ansari et al. (2002) developed a mathematical algorithm based on soil properties for pier scour. Several flume tests were conducted at Texas A & M University and maximum pier, contraction, and abutment scour depth equations (Eq. 2.1 to Eq. 2.4) incorporating bed critical velocity were proposed after various analyses (Briaud et al. 2011; Li 2003; Oh 2009). Briaud (2015) recommended multiplying 1.5 as a factor of safety when calculating the maximum scour depth using these equations.

The maximum pier scour depth can be calculated as (Briaud et al. 2011; Oh 2009)

$$\frac{y_{s(pier)}}{\alpha'} = 2.2 \cdot K_w \cdot K_1 \cdot K_L \cdot K_{sp} \cdot (2.6 \cdot Fr_{(pier)} - Fr_{c(pier)})^{0.7} \quad \text{Eq. 2.1}$$

where  $y_{s(pier)}$  is the maximum complex pier scour depth,  $\alpha'$  is the projected pier width,  $K_w$  is the water depth correction factor,  $K_1$  is the pier nose correction factor,  $K_L$  is the aspect ratio correction factor for a rectangular pier,  $K_{sp}$  is the pier spacing correction factor,  $Fr_{(pier)}$  is the Froude number based on approaching velocity, and  $Fr_{c(pier)}$  is the Froude number based on critical velocity. The projected pier width is based on the pier length, pier width, and attack angle of water flow and the correction factors, and can be obtained from several equations provided by Briaud et al. (2011).

The maximum contraction scour depth can be calculated as (Briaud et al. 2011; Li 2003; Oh 2009)

$$\frac{y_{s(contraction)}}{y_{m1}} = 1.27(1.83Fr_{m2} - Fr_{mc}) \text{ in the transition zone (Briaud 2004)} \quad \text{Eq. 2.2}$$

$$\frac{y_{s(contraction)}}{y_{m1}} = 0.94(1.83Fr_{m2} - Fr_{mc}) \text{ far from the transition zone (Briaud 2004)} \quad \text{Eq. 2.3}$$

where,  $y_{s(contraction)}$  is the maximum contraction scour depth in the transition zone or far from the transition zone,  $y_{m1}$  is the main channel depth in the approaching section,  $Fr_{m2}$  is the Froude number in the main channel at the bridge section, and  $Fr_{mc}$  is the critical Froude number in the main channel of the bridge section.

The maximum abutment scour depth can be calculated as (Briaud et al. 2011; Briaud et al. 2009)

$$\frac{y_s(abutment)}{y_{f1}} = K_1 K_2 K_L K_G K_p 243 Re_{f2}^{-0.28} (1.65 Fr_{f2} - Fr_{fc}) \quad \text{Eq. 2.4}$$

where  $y_s(abutment)$  is the maximum abutment scour depth,  $K_1$  is the abutment shape correction factor,  $K_2$  is the abutment skew correction factor,  $K_L$  is the abutment location correction factor,  $K_G$  is the channel geometry correction factor,  $K_p$  is the pressure-flow correction factor,  $Re_{f2}$  is the Reynolds number at the tow of the abutment,  $Fr_{f2}$  is the Froude number around the toe of the abutment, and  $Fr_{fc}$  is the critical Froude number around the toe of the abutment. All these correction factors are obtainable from Briaud et al. (2011).

The equilibrium scour depth, which is assumed to be 10% less than the maximum scour depth (Arneson 2012), has also attracted many researchers' attention (Figure 2.3). Kho et al. (2004) proposed an equation for the equilibrium pier scour depth in cohesive/non-cohesive soil mixtures in terms of Reynold's number and clay content from their flume test results and also concluded that the proposed equation underestimated the scour depth at higher flow velocities. Debnath and Chaudhuri (2010) proposed equations (Eq. 2.5 to Eq. 2.9) for the maximum equilibrium scour depth for cylindrical piers embedded in clay-sand mixtures in terms of Froude's number, clay content, and water content. These equations' performance was later verified by Najafzadeh and Barani (2014).

$$y_s = 2.05 F_{rp}^{1.72} C^{-1.29} \tau_s^{-0.37} \text{ for } W_c = 20 - 23.22\% \text{ \& } 20\% \leq C_p \leq 85\% \quad \text{Eq. 2.5}$$

$$y_s = 3.64 F_{rp}^{0.22} C^{-1.01} \tau_s^{-0.69} \text{ for } W_c = 27.95 - 33.55\% \text{ \& } 20\% \leq C_p \leq 50\% \quad \text{Eq. 2.6}$$

$$y_s = 20.52 F_{rp}^{1.28} C^{0.19} \tau_s^{-0.89} \text{ for } W_c = 27.95 - 33.55\% \text{ \& } 50\% \leq C_p \leq 100\% \quad \text{Eq. 2.7}$$

$$y_s = 3.32 F_{rp}^{0.72} C^{-0.62} W_c^{0.36} \tau_s^{-0.29} \text{ for } W_c = 33.60 - 45.92\% \text{ \& } 20\% \leq C_p \leq 70\% \quad \text{Eq. 2.8}$$

$$y_s = 8 F_{rp}^{0.61} C^{0.58} W_c^{1.24} \tau_s^{-0.19} \text{ for } W_c = 33.60 - 45.92\% \text{ \& } 70\% \leq C_p \leq 100\% \text{ W} \quad \text{Eq. 2.9}$$

where,  $y_s$  is the non-dimensional equilibrium scour depth,  $F_{rp}$  is the pier Froude number,  $C$  is the clay fraction,  $C_p$  is the clay percentage,  $\tau_s$  is the bed shear strength, and  $W_c$  is the water content.

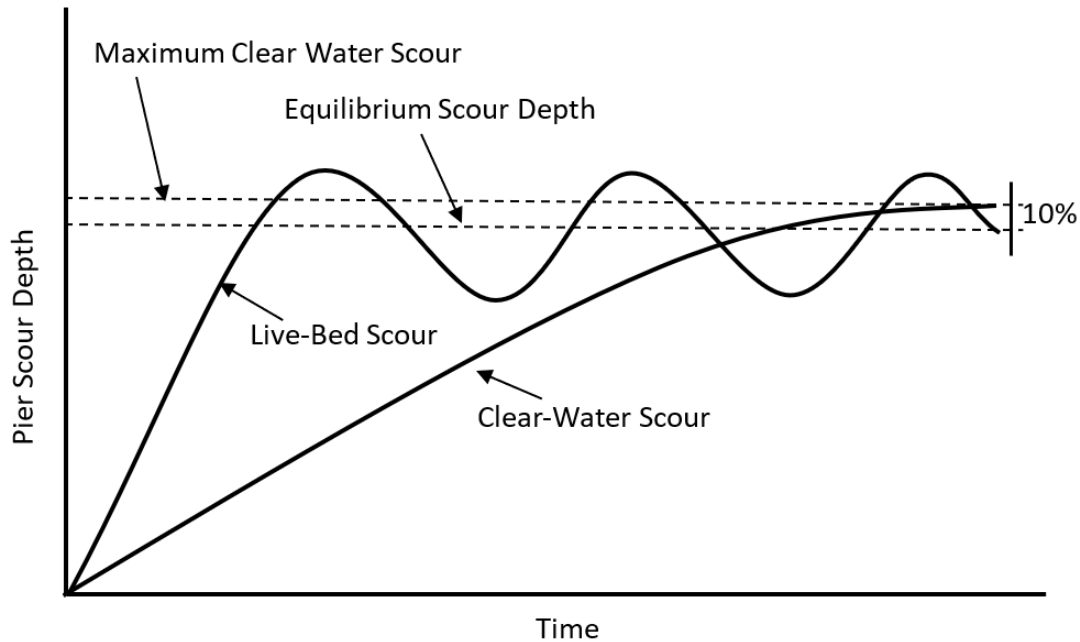


Figure 2.3 Schematic of maximum scour depth and equilibrium scour depth based on Arneson (2012)

Abou-Seida et al. (2012) proposed an equation for the equilibrium vertical wall abutment scour depth in cohesive bed as a function of the clay content, soil compaction, and liquidity index, and Debnath et al. (2014) proposed the same for both vertical wall and wing wall abutments in terms of the clay content, water content, Froude number, and shear stress. Danish (2014) applied gene expression programming for the data set used by Debnath et al. (2014) and proposed a single equation for the abutment scour depth in cohesive soil. Chaudhuri et al. (2019) proposed an equation for contraction scour in cohesive beds as a function of the contraction ratio, clay fraction, flow depth, shear stress, and water content, which is applicable only for the contraction of natural stream in the presence of man-made rigid guide bank. However, these equations were not verified against other data set.

The time rate of scour is an important factor for cohesive soil. The maximum scour depth, which is reached within a short time in non-cohesive soils, might not be reached for the structures founded on cohesive soils within single events (Chaulagai et al. 2016). Briaud et al. (1999) for the first time talked about the importance of the time rate of scour for cohesive soils. They proposed a method

named SRICOS (Scour Rate in Cohesive Soil) and proposed a hyperbolic function for cohesive soil erodibility. Ting et al. (2001) concluded from their flume test results that, ignoring the time rate of scour for bridges in cohesive soils might result in over predictions of scour depths. Later Rambabu et al. (2003) verified the hyperbolic functionality of the erodibility of cohesive soil. For measuring the erodibility rate of cohesive soil, Briaud et al. (2001a) proposed the Erosion Function Apparatus (EFA). These two methods can be combined, called the SRICOS-EFA method, to find the scour depth over time for a cylindrical pier founded on cohesive soils (Briaud et al. 2001b). The SRICOS-EFA was further developed for contraction scour, complex pier scour, abutment scour, varying velocity, and multilayered soil (Briaud et al. 2004; Briaud et al. 2005; Briaud and Oh 2010; Briaud et al. 2011; Briaud et al. 2009; Briaud et al. 2001b; Li 2003; Oh 2009). Once the maximum scour depth at a pier, a contracted section, or an abutment is known, the design scour depth can be calculated with the following equation (Eq. 2.10) (Briaud et al. 1999).

$$y_s(t) = \frac{t}{\frac{1}{z_i} + \frac{t}{y_s(max)}} \quad \text{Eq. 2.10}$$

where  $y_s(t)$  is the scour depth after a storm of duration  $t$ ,  $z_i$  is the initial rate of scour, and  $t$  is the duration of flow.

The development of a computer program, i.e., E-SRICOS (Briaud et al. 2001b), made it easier to consider all the factors associated with bridge scour. Many researchers have used the SRICOS-EFA for bridge scour in cohesive soils and found this method can predict a reasonable ‘localized scour depth’ (Benedict 2014; Briaud 2008; Ghelardi 2004; Güven et al. 2005; Kwak et al. 2004). Incorporating a probabilistic model in this scour prediction model could further improve the results (Bolduc et al. 2008). The SRICOS-EFA needs daily flow data forming a hydrograph to develop a series of hyperbolic functions to represent a continuous scour history and yields the final scour depth at the end of the hydrograph (Ting et al. 2011). In future scour depth predictions, a synthetic hydrograph can be developed from a log-normal distribution (Briaud 2015). In the absence of daily flow data, peak discharge, rainfall distribution, and drainage-area characteristics can be used (Ting et al. 2011). Stochastic flow analysis coupled with a scour model could provide synthetic stream flow along with the scour depth at any time within the life span of the bridge (Brandimarte et al. 2006; Sidorchuk 2005; Utley and Wynn 2008). Najafzadeh et al. (2013) applied the Group Method of Data Handling with Back Propagation algorithm (GMDH-BP) as a soft computing technique to

predict the scour depth around bridge piers embedded in a cohesive bed and showed its better performance compared with many traditional equations including Rambabu et al. (2003), Molinas and Hosny (1999), Najafzadeh (2009), Debnath and Chaudhuri (2010).

Some DOTs like the Texas DOT use Annandale's EIM (Annandale 1999; Annandale and Smith 2001; Annandale and Smith 1998; Annandale and Smith 1999) for pier and contraction scour in cohesive soil along with the SRICOS and HEC-18 sand equation limiting  $D_{50}$  to 0.2mm (TxDOT 2018). The Florida DOT has developed its own methodology for pier scour calculation, applicable for both clear water scour and live bed scour, where they have considered a median particle size of bed material ( $D_{50}$ ) along with pier properties and flow condition (FDOT 2005; FDOT 2019). The HEC-18 Edition 5 has also included the FDOT methodology as an alternative to the HEC-18 sand equation, especially for wide piers founded on cohesive beds with a shallow water depth (Arneson 2012).

FDOT equations (Eq. 2.11 to 2.16) are given below:

$$\frac{y_s}{a^*} = 2.5f_1f_2f_3 \text{ for } 0.4 \leq \frac{V_1}{V_c} < 1.0 \quad \text{Eq. 2.11}$$

$$\frac{y_s}{a^*} = f_1 \left[ 2.2 \left\{ \frac{\frac{V_1}{V_c} - 1}{\frac{V_{lp}}{V_c} - 1} \right\} \right] + 2.5f_3 \left\{ \frac{\frac{V_{lp}}{V_c} - \frac{V_1}{V_c}}{\frac{V_{lp}}{V_c} - 1} \right\} \text{ for } 1.0 \leq \frac{V_1}{V_c} \leq \frac{V_{lp}}{V_c} \quad \text{Eq. 2.12}$$

$$\frac{y_s}{a^*} = 2.2f_1 \text{ for } \frac{V_1}{V_c} > \frac{V_{lp}}{V_c} \quad \text{Eq. 2.13}$$

$$f_1 = \tanh \left[ \left( \frac{y_1}{a^*} \right)^{0.4} \right] \quad \text{Eq. 2.14}$$

$$f_2 = \left[ 1 - 1.2 \left\{ \ln \left( \frac{V_1}{V_c} \right) \right\}^2 \right] \quad \text{Eq. 2.15}$$

$$f_3 = \left[ \frac{\left( \frac{a^*}{D_{50}} \right)^{1.13}}{10.6 + 0.4 \left( \frac{a^*}{D_{50}} \right)^{1.33}} \right] \quad \text{Eq. 2.16}$$

where  $y_s$  stands for the depth of the scour hole,  $a^*$  is the effective pier width in feet,  $V_1$  is the mean velocity of the flow direction upstream of the pier in ft/s,  $V_c$  is the critical velocity for movement of the median grain size of  $D_{50}$ , and  $V_{lp}$  is the velocity of the live-bed peak scour.

### 2.3.2 Scour on Erodible Rock

Erosion of rock in the presence of water depends on both the flow conditions and rock properties (Annandale 2000; Bollaert and Schleiss 2002). The erosion capability of flowing water is termed the erosive power, which quantifies the stream power for scour. Erosion occurs when this erosive power exceeds the relative scour resistivity of the earth material (Annandale 2000). To characterize the ability of rocks to resist erosion, a geomechanical classification system along with erosion threshold, i.e., the erodibility index, was proposed by Annandale (1995). The erodibility index is the function of the rock mass strength and shear strength, block size, joint orientation, and shape. Based on that, the erosion threshold was proposed to indicate the stream power required for initiating the erosion of the bed material with a certain erodibility. Later, this Erodibility Index Method (EIM) was used in clear water scour predictions for bridge piers founded on rock (Annandale 1999; Annandale and Smith 2001; Annandale and Smith 1998; Annandale and Smith 1999). The erodibility index of any earth material, including rock, can be calculated from the following equation (Eq. 2.17) and all the parameters of the equation can be determined from the standard tables provided by Kirsten (1982) (Annandale 1995; Arneson 2012):

$$K = M_s \cdot K_b \cdot K_d \cdot J_s \quad \text{Eq. 2.17}$$

where  $K$  is the erodibility index,  $M_s$  is the intact rock mass strength parameter based on the UCS,  $K_b$  is the block size parameter based on RQD and joint separation,  $K_d$  is the shear strength parameter based on the condition of joint and joint separation, and  $J_s$  is the relative orientation parameter based on the dip angle, dip direction, and joint spacing.

When the stream power at the bottom of the scour hole reaches the critical stream power of the channel bed, erosion begins. Annandale (2006) proposed the following two equations (Eq. 2.18, Eq. 2.19) for determining the scour depth.

$$P_c = K^{0.75} \quad \text{Eq. 2.18}$$

$$\frac{P}{P_a} = 8.42e^{-0.712\left(\frac{y_s}{b}\right)} \quad \text{Eq. 2.19}$$

where  $P_c$  is the critical stream power,  $P$  is the stream power at the bottom of the scour hole,  $P_a$  is the stream power of the approaching flow,  $y_s$  is the depth of the scour hole, and  $b$  is the pier width perpendicular to the flow direction.

Numerical modeling of threshold flow velocities was developed by Bollaert (2010) using the Comprehensive Scour Model (CSM) (Bollaert 2004; Bollaert and Schleiss 2002; Bollaert and Schleiss 2005) for predicting the scour depth with regard to the pier diameter. Both the EIM and the method developed by Bollaert (2010) were capable of determining the equilibrium or maximum scour depth especially for the quarrying and plucking mode of scour (Annandale 2009; Keaton et al. 2010). However, the structures founded on degradable rocks might experience a different scour mode, e.g., abrasion, and might not reach the maximum scour depth within their life span. So, the time rate of scour is an important parameter for the abrasion mode of rock scour. A modification of the EIM was proposed by Huang et al. (2013) for soft bedrock erosion. The rate of submerged rock erosion was claimed to depend on the 1. lithology, 2. frequency, character, and orientation of the rock discontinuities, 3. degree of weathering and induration of sedimentary rock, 4. rock density, strength, abrasion resistance, and slake durability, 5. channel geometry, 6. year-round flow characteristics such as intensity and duration of flood events, and 7. energy gradient and bedload characteristics (Arneson 2012). Keaton et al. (2009); (2010) suggested a probability-weighted approach to represent the channel annual average scour condition and hydraulic loading for predicting rock scour. Hydraulic loading represents the accumulated stream power over the life cycle of a bridge structure, where instantaneous stream power is the function of shear stress and stream velocity and also representative of the rate of energy dissipation per unit width of flow (Annandale and Kirsten 1994; Bagnold 1966; Mishra et al. 2010; Smith 1994). The relationship between the observed scour depth over a certain period and the stream power accumulated over the same time can provide an important index of relative erodibility called the ‘Scour Number’ (Mishra et al. 2010). This index can also be used to estimate future scour depth using Eq. 2.20 if future hydraulic loading is known for the same channel section (Keaton et al. 2012).

$$y_s = K_s \Omega_{future} \quad \text{Eq. 2.20}$$

where  $y_s$  is the scour depth,  $K_s$  is the scour number, and  $\Omega_{future}$  is the future cumulative hydraulic loading. The Scour Number can also be used for other structures founded on similar rock formation and similar flow properties (Titi et al. 2017). In the absence of historical data of hydraulic loading and/or scour depth, the modified slake durability test (Keaton 2011; Keaton and Mishra 2010) results can be used to derive Geotechnical Scour Number (GSN) as an alternative to empirical Scour Number (Keaton 2015; Keaton et al. 2010; Keaton et al. 2012; Mishra et al. 2010).

Calibration of the GSN method was conducted for two samples of siltstones from the Sacramento River at Redding, California (Keaton et al. 2010). Equivalent Scour Depth (ESD) and Equivalent Stream Power (ESP) are terms derived from the modified slake durability test. The following equations (Eq. 2.21 to Eq. 2.24) can be used to predict the scour depth due to the design storm for the abrasion mode of scour (Keaton and Mishra 2010; Keaton et al. 2010; Keaton et al. 2012).

$$ESD = \frac{\Delta W}{\gamma} \cdot \frac{1}{A_{unit}} \quad \text{Eq. 2.21}$$

$$ESP = W_{avg} \cdot \frac{d_{eq}}{\Delta t} \cdot \frac{1}{8} A_{test\ drum} \quad \text{Eq. 2.22}$$

$$GSN = \frac{ESD}{ESP} \quad \text{Eq. 2.23}$$

$$y_s = GSN \cdot \Omega \quad \text{Eq. 2.24}$$

where  $\Delta W$  is the weight loss of the sample during the test increment,  $\gamma$  is the unit weight of the sample,  $A_{unit}$  is the unit area,  $W_{avg}$  is the average weight of the sample,  $d_{eq}$  equivalent distance traveled during the test increment,  $\Delta t$  is the cycle duration,  $A_{test\ drum}$  is the area of the test drum,  $GSN$  stands for Geotechnical Scour Number, and  $\Omega$  is the cumulative stream power over a certain period.

This method has been published in NCHRP 717 (Keaton et al. 2012) as well as HEC-18 Edition 5 (Arneson 2012). The validity of the method for the prediction of the abrasion mode of scour has been tested in the bedrock of West Virginia (Zatar et al. 2013) and Wisconsin (Titi et al. 2017). Niemann et al. (2017) concluded from their research that this method is a good predictor of scour depth for the abrasion mode of rock scour but not suitable for quarrying and plucking mode.

## 2.4 Survey of the State DOT Practices

### 2.4.1 Overview

Twenty eight state DOTs were contacted to investigate the procedures they use for assessing the erodibility of rock. Most DOTs follow the guidance provided in either the 4<sup>th</sup> or 5<sup>th</sup> edition of the HEC-18 manual. Each state, however, adapts the guidance to fit their specific geologic and hydrologic conditions of the state. In general, however, most states do not have significant rock

scour problems. The states that do, have conducted research to address rock scour to some degree. Ohio, for example, does not allow spread footings to be placed on unconsolidated soils and requires that, if spread footings are used, they should be placed on non-erodible rock. Thus, Ohio has developed guidance based on the 5<sup>th</sup> Edition of the HEC-18 manual. No other state surveyed has set limits for the rock parameters introduced into the 5<sup>th</sup> Edition. On the other hand, while the South Dakota DOT follows the general bridge scour guidance in the 4<sup>th</sup> Edition it does not address rock scour. Instead, South Dakota has identified one geological formation in the state that is prone to have rock scour and does not allow spread footings to be constructed on this formation.

Considering that HEC-18 is the key reference in most state DOTs’ practices, the essential technical information of the 4<sup>th</sup> or 5<sup>th</sup> editions of the HEC-18 manual will be summarized in the following sub-section first. Based on this information and that collected from the interviews/questionnaires with the other state DOTs, discussions on the state DOTs’ practices on the scour analysis in cohesive soil and scour susceptible rock will be performed.

#### 2.4.2 Summary of Practices Related to HEC-18

Both the 4<sup>th</sup> and 5<sup>th</sup> Edition of the HEC-18 manual provide guidance on rock erodibility. The information provided in the 4<sup>th</sup> Edition (2001) is summarized in Table 2.5. In general, most State DOT’s follow at some level follow this guidance. The 5<sup>th</sup> Edition of HEC-18 (2012), which was published in 2012, provided additional guidance but did not include the information provided in Table 2.5.

Table 2.5 Relevant information from HEC-18

<b>Method</b>	<b>Rock Scourability</b>
Subsurface investigation	Determine rock type Frequency of discontinuities Minimum one boring per foundation Minimum depth below footing 10 feet Use NX double or triple core barrels
Geologic Formation/Discontinuities	Difficult to determine from vertical bore holes One fracture per foot – good rock quality Five or six fractures per rock quality
Rock Quality Designation (RQD)	RQD < 50 rock is scourable

Unconfined Compressive Strength (UCS) (ASTM D29361)	UCS < 250 psi is considered soil
Slake Durability Index (SDI)	SDI < 90 considered poor rock quality
Soundness (AASHTO T104)	Threshold of 12 (sodium) - rock scourable Threshold of 18 (Magnesium) – rock scourable
Abrasion (Los Angeles Abrasion test)	Loss percentages greater than 40 should be considered scourable.

HEC-18 Edition 5 provided the following technical information:

- ❖ Improved section on rock mass description and characteristics based on information of the Society for Rock Mechanics (ISRM 1981) and Geotechnical Engineering Circular No. 5 (FHWA 2002).
- ❖ A short discussion on shear stress that included critical shear stress vs. particle grain size is shown in Figure 2.4 by Briaud et al. (2011). While this figure was provided no discussion was provided for scourable rock.
- ❖ Figure 2.5 of the 5<sup>th</sup> Edition included the Briaud et al. (2011) erosion rate vs. velocity for a wide range of geomaterials. This chart includes rock in categories III through VI. Again, the 5<sup>th</sup> edition did not provide any guidance on its use.
- ❖ The Rock Mass Rating System (RMR), developed by Bieniawski (1988) was included. The RMR system is now a standard rock mass classification system used in most civil and mining engineering fields. Again, only limit discussion was provided in the 5<sup>th</sup> Edition.
- ❖ The Erodibility Index Method developed by Annandale (1995) is the method present to estimate rock scourability. This method is adapted from Kirsten (1982) and has been used by the USDA in their National Engineering Manual since 1995. An example problem is provided later in the 5<sup>th</sup> Edition to provide guidance on its use.

The rock scour information is summarized in Table 2.5, however, is not directly included although some of the parameters are used in the RMR. It is unclear as to why this information was not discussed in the 5<sup>th</sup> Edition.

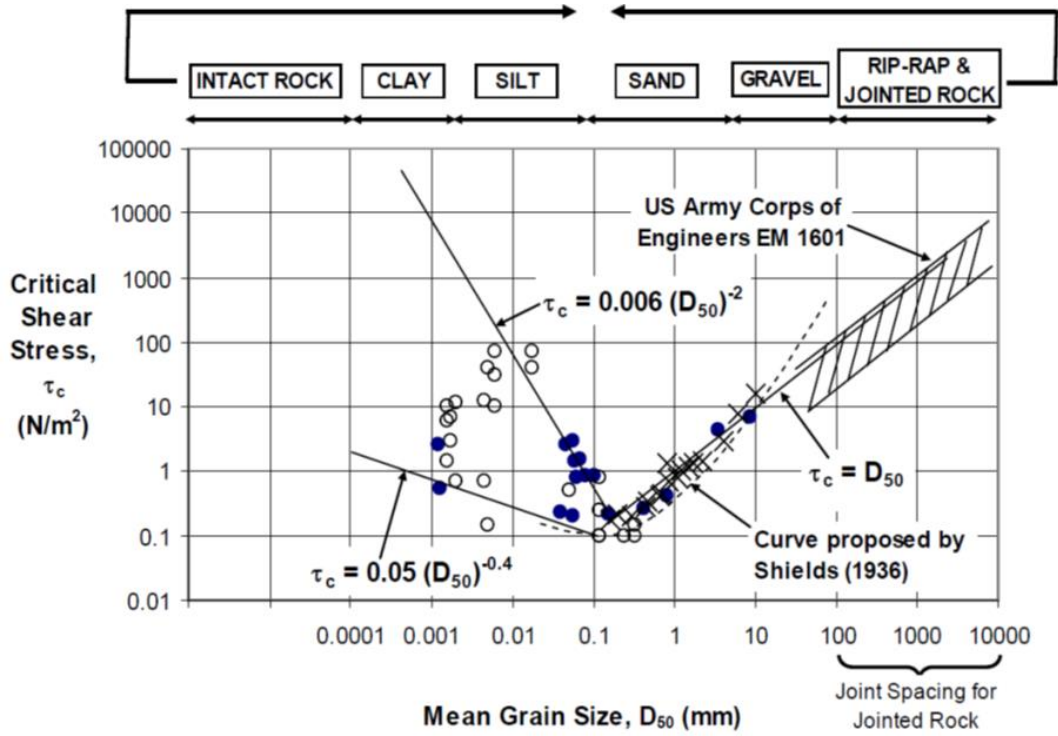


Figure 2.4 Critical shear stress vs particle grain size (Briaud et al. 2011)

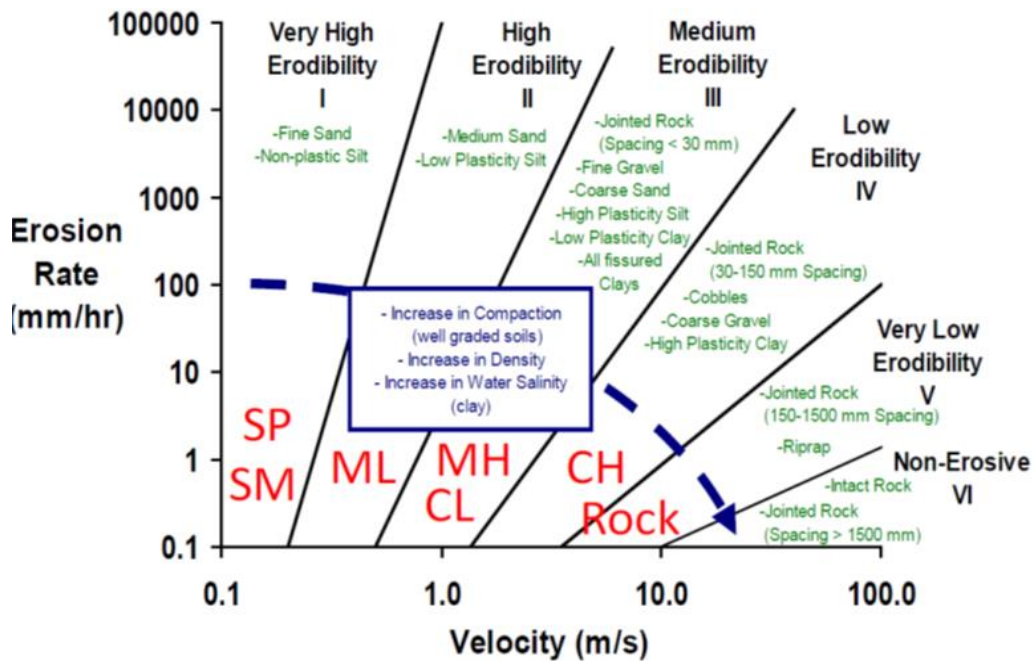


Figure 2.5 Erosion rate vs. velocity for a wide range of geomaterials (Briaud et al. 2011)

With respect to scour in general, there are issues between the 4<sup>th</sup> and 5<sup>th</sup> editions. The Virginia DOT Bridge Drainage Design Memorandum (DDM) addresses this issue with the following discussion points:

- ❖ The methods provided in HEC-18, 5th edition, were largely developed in isolation from one another and there are significant gaps between the theory as presented, and the hydraulic and geotechnical conditions found in the field.
- ❖ The processes and procedures within HEC-18, 5<sup>th</sup> edition, do not describe how to incorporate the computational process when the geotechnical report returns results that provide an increasing  $D_{50}$  with depth.
- ❖ The processes and procedures within HEC-18, 5<sup>th</sup> edition, do not include discussion or practices to evaluate the scour potential in materials that can be cored, but is fractured and does not meet an RQD of 50%.
- ❖ In general, the procedures in HEC-18, 5<sup>th</sup> edition, treat live-bed scour and clear-water scour as a binary choice determined based on the flood condition. However, the live-bed scour equations alone are not capable of incorporating the effects of a coarser material overlain by a finer material. This procedure will also look at both conditions to evaluate which condition controls.
- ❖ This DDM establishes an expanded procedure for the estimation of bridge scour using the existing equations available within HEC-18, 5th edition. In the event that supplemental guidance is issued by the FHWA, these processes will need to be reevaluated for applicability.

In 2012, the same year that the 5<sup>th</sup> Edition was published, the NCHRP Project 24-29 - Scour at Bridge Foundations on Rock, now listed as NCHRP Report 717. This report provided significantly more technical information and analysis on rock scour than did HEC-18 4<sup>th</sup> or 5<sup>th</sup> Editions. While Report 717 uses the RMR method and the Erodibility Index Method developed by Annandale (1995) and Kirsten (1982), they have added the Geologic Strength Index (GSI) and other recently develop rock engineering method to assist in assessing rock scourability.

### **2.4.3 Scour Evaluation Methods Practiced by Other States**

Twenty-eight state DOTs were interviewed for this report. The interview method utilized the report format used in MDOT RC-1547, “A Critical Evaluation of Bridge Scour for Michigan Specific Conditions” by Carpenter and Miller (2011). RC-1547 interviewed 16 state DOTs. This report included these 16 states and updated the information. The information that we received is summarized in the following, while the detailed feedback is compiled in the Appendix.

Almost all stated that use HEC-18. When asked if they use the 4<sup>th</sup> or 5<sup>th</sup> edition most assumed they were using the 5<sup>th</sup> edition. When asked about how they determined the RMR for a specific rock formation they were not sure and would get back with us. It appears that many of the geotechnical engineers the research team spoke with were not familiar, with the RMR system nor the GSI system used in NCHRP Report 717. All of the geotechnical Engineers, however, were very familiar with rock drilling and the standard methods of determining and using the Rock Quality Designation (RQD) or core recovery data, indicating that they have been using the guidance in the HEC-18 4<sup>th</sup> Edition.

It has only been recently, within the last ten years or so, that geotechnical engineering textbooks have started to include aspects of rock engineering. In general, rock engineering has been taught mostly in mining and geological engineering programs. Most of the methods that are currently being used today were developed by Evert Hoek in the 1980s and 1990s. Thus, it is not uncommon for geotechnical engineers to have used these systems and therefore are somewhat reluctant to use them.

A more important factor, however, is that even if knowledgeable about rock engineering techniques, it is not easy to determine the Rock Mass Rating (RMR) or GSI from vertical boreholes. These systems were developed based on mining and tunneling projects, where extensive drilling programs and geologic analysis are conducted on a routine basis by trained engineers. Additional schooling and experience are needed to be able to adapt geotechnical engineers to be able to effectively utilize the guidance in NCHRP Report 717.

## **Chapter 3 Scour Analysis Methods for Erodible Rock and Cohesive Soil**

This chapter introduces three methods selected for analyzing bridge scour in cohesive soils and scour-susceptible rock, based on the state-of-the-practice survey in Chapter 2. For piers founded on bedrock, scour depth can be calculated using the SRICOS-EFA, EIM, or GSN. For piers on cohesive soils, scour depth can be calculated using either the SRICOS-EFA or EIM. All these three methods can calculate the scour depth for design discharge (flow events). The SRICOS-EFA and GSN methods are well recognized for calculating the variation of the cumulative scour depth over time. Since structures founded on cohesive soil or rock may not experience the maximum scour depth within events or even their service lives, scour depth over time may be more important for these soil strata (Chaulagai et al. 2016; Keaton et al. 2012). This chapter first presents some basic knowledge for discussing bridge scour analysis: types of bridge scour, shear stress and scour threshold, stream power, and mode of scour. Based on the knowledge, details about the three selected methods will be offered.

### **3.1 Background**

#### **3.1.1 Types of Bridge Scour**

Soil removal from a stream channel (including riverbed and river banks) due to flowing water is called river scour. General scour is a natural phenomenon, which takes place irrespective of the existence of any structure. The presence of a bridge in a river or a stream cross-section can cause soil erosion primarily during floods. Scour occurring around a bridge foundation such as a pier and an abutment is called local scour. The existence of a bridge can also initiate scour called ‘contraction or constriction scour’ at the constricted section of the channel. Local scour and contraction scour together are called localized scour. Localized scour can occur as ‘clear water scour’ or ‘live bed scour’. Scour is called clear water scour if the scour hole remains pristine after the flood, and is called live bed scour if the scour hole gets sediment deposition from the upstream (Gazi et al. 2019; Liang et al. 2009; Melville and Coleman 2000).

### 3.1.2 Bed Shear Strength and Stress

Shear strength is a term used in soil mechanics to describe the magnitude of the shear stress that a soil can sustain. The shear resistance of a saturated soil is a result of friction and interlocking of particles, and possibly cementation or bonding at particle contacts. Due to interlocking, particulate materials may attempt to expand or contract in volume when it is subject to shear strains. If soil expands, the density of particles decreases and the strength decreases. In this case, the peak strength would be followed by a reduction of shear stress. The stress-strain relationship levels off when the material stops expanding or contracting, and when interparticle bonds are broken. The theoretical state in which the shear stress and density remain constant while the shear strain increases is often referred to as the residual strength. However, soils with a high clay content will continue to lose strength with even larger strains because of the clay particles, which can easily become aligned with one another to form shear surfaces due to their platy shape.

While the shear strength is a material property, the bed shear stress describes a state or an action caused by the flow. The bed shear stress ( $\tau$ ) is expressed as the following equation (Eq. 3.1):

$$\tau = \gamma y S_f \quad \text{Eq. 3.1}$$

where  $\gamma$  is the unit weight of water ( $9800 \text{ N/m}^3$ ),  $y$  is the depth of the approaching flow (m), and  $S_f$  is the slope of the energy grade line. Once the shear stress for flow in a system is known, then it is possible to compare it with the critical shear stress of the material (an indicator of shear strength) to determine the erodibility of the material. This is a method that can be used for both cohesive and non-cohesive materials.

### 3.1.3 Stream Power

The stream power describes the rate of energy dissipation in flowing water. By making use of this variable it is possible to quantify the relative magnitude of pressure fluctuations which play an important role in initiating sediment motion and maintaining sediment transport. To support the hypothesis that the rate of energy dissipation can be used to represent the relative magnitude of pressure fluctuations, Annandale (1995) analyzed observations by Fiorotto and Rinaldo (1992), who measured pressure fluctuations under hydraulic jumps. The results of the analysis indicated

that the standard deviation of six pressure fluctuations is directly proportional to the rate of energy dissipation. This finding supports the use of stream power to quantify the relative magnitude of the erosive power of water. Increases in stream power are related to increases in the fluctuating pressures, which form the basis of the conceptual model of the erosion process. The following equation (Eq. 3.2) represents stream power ( $P$ ).

$$P = \tau v \quad \text{Eq. 3.2}$$

where  $\tau$  is the local shear stress at the pier (lb/ft<sup>2</sup> or N/m<sup>2</sup>) and can be obtained from Eq. 3.3 and  $v$  is the velocity of the approaching flow (ft/s or m/s).

$$\tau = \left( \frac{nK_p V}{1.486} \right)^2 \left( \frac{\gamma}{y_0^3} \right) \quad \text{Eq. 3.3}$$

In Eq. 3.3,  $n$  is the Manning's roughness coefficient,  $K_p$  is the turbulence-related velocity enhancement factor (1.0 for approaching flow, 1.5 for round-nosed piers, 1.7 for square-nosed piers), 1.486 is the factor for U.S. customary units (1.0 for metric units),  $\gamma$  is the unit weight of freshwater (62.4 lb/ft<sup>3</sup> or 9,802 N/m<sup>3</sup>), and  $y_0$  is the depth of the approaching flow (ft or, m)

### 3.1.4 Mode of Scour

For bridges founded on rocks, scour mode is an essential term in scour susceptibility testing. As introduced in Chapter 2, rock erosion can take place in four different modes in natural channels – Dissolution, Cavitation, Quarrying and Plucking, and Abrasion (Arneson 2012; Hancock et al. 1998; Whipple et al. 2000). Dissolution is the scour mode applicable for soluble rock. Among soluble rocks, only limestone and dolostone are used for bridge foundations, but they do not have any evidence of scour within the life span of the founded structures (Keaton et al. 2010). Cavitation is a very common phenomenon in pipe and tunnel applications (Keaton et al. 2010). Although cavitation sometimes can also take place in natural streams, it is not common at the bridge sites considering the available erosive forces (Arneson 2012; Keaton et al. 2012). The quarrying and plucking mode of scour usually occurs in rocks with fractures and/or joints. The process takes place in terms of block removals and is governed by the block size and geometry, stream velocity, and turbulence intensity (Keaton et al. 2010). Abrasion is the gradual and progressive mode of

scour that usually takes place in degradable rocks due to hydraulic loading over time. Scour in degradable rocks depend not only on their geological properties but also on the flow conditions of the channels (Keaton et al. 2012). Apart from these scour modes, physical and chemical weathering, wetting and drying, heating and cooling, and freezing and thawing can also lead to rock degradation (Arneson 2012; Keaton et al. 2009). The mode of scour has no impact on cohesive soil scour. Therefore, the quarrying and plucking mode and the abrasion model of scour will be the two considered in this study.

## **3.2 Scour Analysis Methods for Erodible Rock and Cohesive Soil**

### **3.2.1 SRICOS-EFA**

Briaud et al. (2004) developed a computer program for applying the SRICOS-EFA for scour analysis of most earth materials, though its application in cohesive soils has been more widely accepted. The software is available online at <https://ceprofs.civil.tamu.edu/briaud/sricos-efa.htm> and free to use. The input data needed for using this method are listed as follows:

- ❖ **Soil/Material Properties:** Number of soil layers, thickness, and critical shear stress of each layer, and erosion rate vs. shear stress curve are the input data needed for describing the earth strata. The shear stress and erosion rate data can be acquired by performing a lab test. Briaud et al. (2001a) recommended the EFA lab test for this purpose, however, RETA and JET can also produce similar data with some limitations. RETA can be used for stiff clay and erodible rock such as limestone, sandstone (Bloomquist et al. 2012); by contrast, JET is good for any type of soil. If none of these lab apparatuses are available, erosion category curves proposed by Briaud (2008) can be used for preliminary analysis (Oh 2009). Figure 3.1 is the improved version of Briaud's erosion category plot, where USCS soil classification has been included by Briaud et al. (2019) to make the plot more user-friendly.

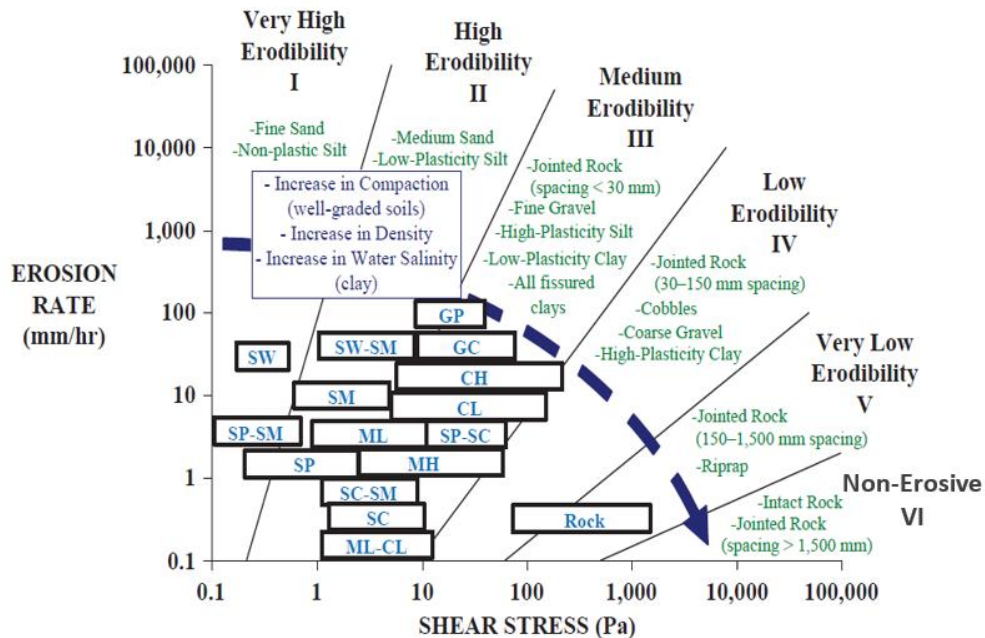


Figure 3.1 Erosion category curves for different earth materials (Retrieved from Briaud (2008), Briaud et al. (2019))

- ❖ Water/Hydraulic Parameter: Manning’s coefficient, daily discharge – in other words daily hydrograph from the nearest USGS gaging station, and HEC-RAS output for discharge vs. velocity, and discharge vs. water depth are the required hydraulics input parameter.
- ❖ Geometry Input: For pier scour, the software needs the following information: the shape of the pier, number of piers perpendicular to the flow, center-to-center spacing of the piers, width and length of the piers, attack angle (angle between the direction of the water flow and the main axis of the pier) for the rectangular pier, and upstream channel width. For contraction scour, upstream uncontracted width, contracted channel width, contraction length, and the transition angle between the contracted and uncontracted sections are needed. For abutment and contraction scour (the SRICOS-EFA software cannot be used to calculate abutment scour alone), the shape of the abutment, bridge clearance, bridge deck thickness, skew angle, the slope of the abutment, length of the embankment, abutment top width, width, and Manning’s coefficient of the left floodplain, main channel and right floodplain, and slopes of the left and right floodplains are required.

Once all the input parameters are inserted at their defined tabs in the software, the model is run to determine the scour depth accumulated for the input daily discharges. The software output will provide the cumulative scour depth over a certain time period. This time period is the same span of time for which the daily discharges have been placed as input.

### 3.2.2 EIM

EIM stands for the Erodibility Index Method (Annandale 1995), which was originally developed for determining erosion resistance of any earth material. Later, this method was used to calculate pier scour for bridges founded on rocks (Annandale 1999; Annandale and Smith 2001; Annandale and Smith 1998; Annandale and Smith 1999). The erodibility index of any earth material can be calculated from the following equation (Eq. 3.4), where  $K$  stands for the erodibility index and all the parameters of the equation can be determined from the standard tables provided by Kirsten (1982) and/or using some equations (Annandale 1995; Arneson 2012):

$$K = M_s \cdot K_b \cdot K_d \cdot J_s \quad \text{Eq. 3.4}$$

where  $M_s$  is the mass strength number,  $K_b$  is the block/particle size number,  $K_d$  is the shear strength number and  $J_s$  is the relative orientation parameter or ground structure number. These numbers can be calculated/obtained in different ways for different materials, which will be introduced in the following.

#### For Rock

For rock,  $M_s$  can be obtained based on the UCS (Table 3.1).  $K_b$  and  $K_d$  can be calculated using the following equations (Eq. 3.5, Eq. 3.6):

$$K_b = \frac{RQD}{J_n} \quad \text{Eq. 3.5}$$

$$K_d = \frac{J_r}{J_a} \quad \text{Eq. 3.6}$$

where  $RQD$  is the Rock Quality Designation number,  $J_n$  for the number of joint sets (Table 3.2),  $J_r$  for joint roughness number based on the condition of the joint (Table 3.3),  $J_a$  is the joint alteration number based on the type of gouges and the joint separation (Table 3.4), and  $J_s$  is the relative orientation parameter or relative ground structure number based on the dip angle, dip direction, and joint spacing (Table 3.5). The values of  $M_s$ ,  $J_n$ ,  $J_r$ ,  $J_a$ , and  $J_s$  can be found from the

standard tables proposed by Kirsten (1982) based on field test/lab tests (Table 3.1 through Table 3.5).

Table 3.1 Mass strength number for rock ( $M_S$ ) based on Kirsten (1982) and Annandale (1995)

<b>Hardness</b>	<b>UCS (MPa)</b>	<b>Mass Strength Number (<math>M_S</math>)</b>
Very soft rock	< 1.7	0.87
	1.7 – 3.3	1.86
Soft rock	3.3 – 6.6	3.95
	6.6 - 13.2	8.39
Hard rock	13.2 - 26.4	17.70
Very hard rock	26.4 - 53.0	35.0
	53.0 - 106.0	70.0
Extremely hard rock	> 212	280.0

Table 3.2 Joint set number ( $J_n$ ) for rock based on Kirsten (1982) and Annandale (1995)

<b>Number of joint sets</b>	<b>Joint set number (<math>J_n</math>)</b>
Intact, no or few joints/fissures	1.00
One joint/fissure set	1.22
One joint/fissure set plus random	1.50
Two joint/fissure sets	1.83
Two joint/fissure sets plus random	2.24
Three joint/fissure sets	2.73
Three joint/fissure sets plus random	3.34
Four joint/fissure sets	4.09
Multiple joint/fissure sets	5.00

Table 3.3 Joint roughness number ( $J_r$ ) for rock based on Kirsten (1982) and Annandale (1995)

<b>Joint separation</b>	<b>Condition of joint</b>	<b>Joint roughness number (<math>J_r</math>)</b>
Joints/fissures tight or closing during excavation	Stepped joints/fissures	4.0
	Rough or irregular, undulating	3.0
	Smooth undulating	2.0
	Slickensided undulating	1.5
	Rough or irregular, planar	1.5
	Smooth planar	1.0

	Slickensided planar	0.5
Joints/fissures open and remain open during excavation	Joints/fissures either open or containing relatively soft gouge of sufficient thickness to prevent joint/fissure wall contact upon excavation	1.0
	Shattered or micro-shattered clays	1.0

Table 3.4 Joint alteration number ( $J_a$ ) for rock based on Kirsten (1982) and Annandale (1995)

Description of gouge	Joint alteration number ( $J_a$ ) for joint separation (mm)		
	1.0 <sup>1</sup>	1.0 – 5.0 <sup>2</sup>	5.0 <sup>3</sup>
Tightly healed, hard, non-softening impermeable filling	0.75	-	-
Unaltered joint walls, surface staining only	1.0	-	-
Slightly altered, non-softening, non-cohesive rock mineral or crushed rock filling	2.0	2.0	4.0
Non-softening, slightly clayey non-cohesive filling	3.0	6.0	10.0
Non-softening, strongly over-consolidated clay mineral filling, with or without crushed rock	3.0	6.0*	10.0
Softening or low friction clay mineral coatings and small quantities of swelling clays	4.0	8.0	13.0
Softening moderately over-consolidated clay mineral filling, with or without crushed rock	4.0	8.0*	13.0
Shattered or micro-shattered (swelling) clay gouge, with or without crushed rock	5.0	10.0*	18.0

Note:

<sup>1</sup>Joint walls effectively in contact

<sup>2</sup>Joint walls come into contact after approximately 100 mm shear

<sup>3</sup>Joint walls do not come into contact at all upon shear

\*Also applies when crushed rock occurs in clay gouge without rock wall contact

Table 3.5 Relative ground structure number ( $J_r$ ) for rock based on Kirsten (1982) and Annandale (1995)

Dip direction of closer spaced joint set (degrees)	Dip angle of closer spaced joint set (degrees)	Ratio of joint spacing, r			
		1:1	1:2	1:4	1:8
180/0	90	1.14	1.20	1.24	1.26
In direction of stream flow	89	0.78	0.71	0.65	0.61
	85	0.73	0.66	0.61	0.57
	80	0.67	0.60	0.55	0.52
	70	0.56	0.50	0.46	0.43

	60	0.50	0.46	0.42	0.40
	50	0.49	0.46	0.43	0.41
	40	0.53	0.49	0.46	0.45
	30	0.63	0.59	0.55	0.53
	20	0.84	0.77	0.71	0.67
	10	1.25	1.10	0.98	0.90
	5	1.39	1.23	1.09	1.01
	1	1.50	1.33	1.19	1.10
0/180	0	1.14	1.09	1.05	1.02
Against direction of stream flow	-1	0.78	0.85	0.90	0.94
	-5	0.73	0.79	0.84	0.88
	-10	0.67	0.72	0.78	0.81
	-20	0.56	0.62	0.66	0.69
	-30	0.50	0.55	0.58	0.60
	-40	0.49	0.52	0.55	0.57
	-50	0.53	0.56	0.59	0.61
	-60	0.63	0.68	0.71	0.73
	-70	1.84	0.91	0.97	1.01
	-80	1.26	1.41	1.53	1.61
	-85	1.39	1.55	1.69	1.77
	-89	1.50	1.68	1.82	1.91
180/0	-90	1.14	1.20	1.24	1.26

Note:

1. For intact material like massive rock or fine-grained massive clay  $J_s = 1$ .
2. For values of  $r$  greater than 8 take  $J_s$  as for  $r = 8$ .
3. If the flow direction FD is not in the direction of the true dip TD, the effective dip ED = AD + GS, where AD stands for the apparent dip and GS is the ground slope.

### For Granular Soil

The same equation (Eq. 3.4) can also be used for granular soil except that the parameters in the equation should be determined based on different parameters. For granular soil,  $M_s$  is determined based on SPT blow counts (Table 3.6),  $K_b$  is determined from  $D_{50}$  (Eq. 3.7),  $K_d$  from residual friction angle,  $\phi$  (Eq. 3.8), of the granular earth material, and  $J_s$  is 1 (Eq. 3.9).

$$K_b = 1000 D_{50}^3 \quad \text{Eq. 3.7}$$

$$K_d = \tan(\phi) \quad \text{Eq. 3.8}$$

$$J_s = 1 \quad \text{Eq. 3.9}$$

Table 3.6 Mass strength number for granular soil ( $M_s$ ) based on Kirsten (1982) and Annandale (1995)

Consistency	SPT Blow Count	Mass Strength Number ( $M_s$ )
Very loose	0 - 4	0.02
Loose	4 - 10	0.04
Medium dense	10 - 30	0.09
Dense	30 - 50	0.19
Very dense	50 - 80	0.41

Note: If SPT blow count exceeds 80 for a non-cohesive material, it must be taken as rock (Table 3.1)

### For Cohesive Soil

Eq. 3.4 can also be used for determining the erodibility of cohesive earth strata. Mass strength parameter,  $M_s$ , for cohesive soils should be determined based on vane shear strength (Table 3.7),  $K_b$  and  $J_s$  are taken as 1 (Eq. 3.10, Eq. 3.12) and  $K_d$  is obtained with residual friction angle,  $\phi$  (Eq. 3.11). The value of  $\phi$  is recommended to be  $8.1^\circ$  for very soft to soft clays and  $30^\circ$  for all other materials by Annandale and Smith (2001).

$$K_b = 1 \quad \text{Eq. 3.10}$$

$$K_d = \tan(\phi) \quad \text{Eq. 3.11}$$

$$J_s = 1 \quad \text{Eq. 3.12}$$

Table 3.7 Mass strength number for granular soil ( $M_s$ ) based on Kirsten (1982) and Annandale (1995)

Consistency	Vane shear strength (KPa)	Mass Strength Number ( $M_s$ )
Very soft	0 – 80	0.02
Soft	80 – 140	0.04
Firm	140 – 210	0.09
Stiff	210 – 350	0.19
Very stiff	350 - 750	0.41

Note: If vane shear strength for a cohesive soil exceeds 750 KPa, it must be taken as rock (Table 3.1)

Annandale (2006) proposed the following four equations (Eq. 3.13 to Eq. 3.16) for determining the scour depth. Erosion begins when water flows around bridge piers and the corresponding stream power increases to exceed the critical stream power. According to the research conducted by the Federal Highway Administration (FHWA) (Smith et al. 1999), the erosive power of water around bridge piers decreases as scour holes deepen. When the stream power at the bottom of the scour hole reaches the critical stream power of the channel bed, erosion ceases.

$$P_c = K^{0.75} \quad (\text{for } K > 0.1) \quad \text{Eq. 3.13}$$

$$P_c = 0.48K^{0.44} \quad (\text{for } K \leq 0.1) \quad \text{Eq. 3.14}$$

$$P_a = 7.853\rho \left(\frac{\tau}{\rho}\right)^{3/2} \quad \text{Eq. 3.15}$$

$$\frac{P}{P_a} = 8.42e^{-0.712(\frac{y_s}{b})} \quad \text{Eq. 3.16}$$

where  $P_c$  is the critical or required stream power below which there is no erosion,  $K$  is the erodibility index determined from Eq. 3.4,  $P_a$  is the stream power of the approaching flow,  $\tau$  is the shear stress,  $P$  stands for the stream power at the bottom of the scour hole- or in other words available stream power at the pier,  $y_s$  is the depth of the scour hole, and  $b$  is the pier width perpendicular to the flow direction.

The procedure of applying this method includes determining the erodibility of the earth material and available stream power at different depths and comparing the available stream power with the critical stream power. The first step is determining relative stream power using Eq. 3.16, and then obtaining approaching flow stream power using Eq. 3.15. Multiplying these two parameters will provide available stream power at the pier. At any depth, if available stream power is more than critical stream power, scour will take place. Here, available stream power is the erosive force of water discharging on the earth material and critical stream power is the required stream power to erode the earth material. Since, stream power decreases as the scour depth increases (Smith et al. 1999) , at one point available stream power will be equal to or less than the critical stream power where scour will cease to exist. That depth will be determined as the scour depth.

### 3.2.3 GSN

This method applies only to rock strata and is very specific to the site rock characteristics since one of the major input parameters comes from material testing. Especially, this method requires the use of the modified slake durability test on the samples to acquire needed input. This test is a modified version of the standard slake durability test, ASTM D4644 (ASTM 2016) where oven drying has been eliminated, the test-increment duration has been extended, and the number of test increments has been increased (Keaton and Mishra 2010).

Similar to the ASTM D4644 standard, the modified slake durability test requires a drum composed of 2 mm mesh (No. 10) with rigid end plates. The length and the diameter of the drum is 100 mm and 140 mm respectively, and the drum is partially submerged in distilled water. The test specimen is 10 equidimensional rock fragments with total mass between 450 - 550 gm. The specimen is placed in the drum and the drum is rotated in water at 20 rev/min. The test is run for 9 hours where each cycle extends to 60 mins. After each test cycle, Equivalent Scour Depth (*ESD*) and Equivalent Stream Power (*ESP*) are derived and plotted in a graph. The slope of the linear regression of the *ESD* vs *ESP* is determined as the Geotechnical Scour Number (*GSN*) and is multiplied with the stream power to get the scour depth for the design discharge. The initial data point/s can be neglected since the initial sample loss is dominated by rounding of sharp edges. To find the cumulative scour depth ( $y_s$ ), *GSN* must be multiplied with the varying stream power of the river for the given period (Keaton et al. 2012). The following equations (Eq. 3.17 through Eq. 3.20) can be used to predict the scour depth resulting from the abrasion mode of scour (Keaton and Mishra 2010; Keaton et al. 2010; Keaton et al. 2012).

$$ESD = \frac{\Delta W}{\gamma} \cdot \frac{1}{A_{unit}} \quad \text{Eq. 3.17}$$

$$ESP = W_{avg} \cdot \frac{d_{eq}}{\Delta t} \cdot \frac{1}{8} A_{test\ drum} \quad \text{Eq. 3.18}$$

$$GSN = \frac{ESD}{ESP} \quad (\text{slope of } ESD \text{ vs } ESP \text{ plot}) \quad \text{Eq. 3.19}$$

$$y_s = GSN \cdot \Omega \quad \text{Eq. 3.20}$$

where  $\Delta W$  is the weight loss of the sample during the test cycle,  $\gamma$  is the unit weight of the sample determined by ASTM procedure,  $A_{unit}$  is the unit area,  $W_{avg}$  is the average weight of the sample

during the test cycle,  $d_{eq}$  is the equivalent distance traveled by the test drum during the test cycle and can be obtained by multiplying the circumference of the drum with the rate of rotation and the duration of the test cycle,  $A_{test\ drum}$  is the area of the test drum,  $\Delta t$  is the test cycle duration, and  $\Omega$  is the cumulative stream power. Here, all the weight values should be normalized to the initial weight of the specimen.

Since the stream power varies with the discharge of the river, daily discharge data are important for this method. Discharge data can be easily obtained from the USGS gaging station whereas stream power cannot. However, stream power corresponding to multiple discharge values can be obtained from hydraulic modeling, e.g., HEC-RAS - which can be utilized to develop an equation (Eq. 3.21) for stream power in terms of discharge using the power law (Titi et al. 2017).

$$P = aQ^b \quad \text{Eq. 3.21}$$

here,  $P$  stands for Stream Power,  $Q$  stands for discharge and,  $a$  and  $b$  are constants.

## Chapter 4 Implementation of Selected Methods for Bridge Scour Analysis at Four Michigan Sites

### 4.1 Overview

The selected bridge scour analysis methods for cohesive soils and scour-susceptible rock, which were discussed in Chapter 3, were implemented to analyze the scour at four representative bridge sites in Michigan and to get a better understanding of the needed tests, input, processes, possible issues, and anticipated results. Two bridge sites founded on bedrock and two bridge sites founded on cohesive soil in Michigan were analyzed with geotechnical, structural, and hydraulic data from the design of the bridges and nearby USGS stations. M-43 EB over the Grand River and US-2 and US-41 over the Escanaba River are the two rock sites, and M-20 over the Tittabawassee River and M-64 over the Ontonagon River are the two clay sites. Pier scour analysis at these bridge sites will be described in the following sections.

While applying these methods to the selected bridge sites of Michigan, it was found that not all the required input parameters were directly available. Sometimes intermediate calculations were done to achieve the required data, while in some other cases, assumptions were made. The data preparation steps are summarized here.

- ❖ **Data preparation for SRICOS-EFA:** The first thing needed for this using method is the EFA test results of the sample, i.e., sample erodibility vs. erosion rate curve. This curve was available for only one earth layer at Pier #1 of M-20 over the Tittabawassee River. For all other cases, this curve was assumed based on other earth properties available in the geotechnical report.

In detail, when the earth layer was found to be a soil layer, the type of the soil and/or USCS soil classification were used to determine the erodibility range from the proposed erodibility curves of Briaud (2008). On the other hand, when a rock layer was found, joint spacing information was used (Figure 3.1). Unfortunately, this information is not always available in the geotechnical report. However, the rock RMR is common in such reports. Assigning an RMR value to any rock involves assigning a relative rating to the rock based on the rock strength, RQD, joint spacing, joint condition and groundwater condition, and finally summing them up (Table 4.1) (AASHTO 2010; Bieniawski 1988). RMR values for

the joint spacing of the rock layers were compared with the erosion category curves proposed by Briaud (2008) to assume the erosion curve for the rock layers. For instance, a joint spacing of 150 mm from the RMR implies the rock has very low erodibility (Figure 3.1).

- ❖ **Data preparation for EIM:** The EIM has a single procedure with different sets of equations based on the type of earth strata. Three sets of equations are there - one for cohesionless soils, one for cohesive soils, and another one for rock (Section 3.2.2). While applying this method, an appropriate set of equations was chosen for the different types of earth layers present at the selected sites. Input data required for applying the EIM in cohesionless soil and rock were easily found in the geotechnical report, though they may not always be available. In those cases, calculations could not be carried out. For cohesive soil, the vane shear strength ( $S_u$ ) is a required parameter, which may be absent in many geotechnical reports. This parameter was calculated from SPT  $N$  value using the following equation as per Hara et al. (1974) when needed.

$$S_u = 0.297N^{0.72} \text{ (kg/cm}^2\text{)} \quad \text{Eq. 4.1}$$

- ❖ **Data preparation for GSN:** This method was developed for bedrock. So, this method was applied only at the rock strata of the rock sites, i.e., M-43 over the Grand River and US -2 and US-41 over the Escanaba River.

Table 4.1 Table for assigning RMR to rocks after AASHTO (2010)

Parameter	Ranges of values							
1. Strength of Intact Rock Materials	Point load strength index	> 1,200 psi	600 - 1,200 psi	300 - 600 psi	150 - 300 psi	UCS is preferred for this low range		
	UCS	> 30,000 psi	15,000 - 30,000 psi	7,500 - 15,000 psi	3,600 - 7,500 psi	1,500 - 3,600 psi	500 - 1,500 psi	150 - 500 psi
Relative Rating		15	12	7	4	2	1	0
2. RQD	90% - 100%	75% - 90%	50% - 75%	75% - 90%	< 25%			
Relative Rating	20	17	13	8	3			
3. Joint Spacing	> 10 ft	3 - 10 ft	1 - 3 ft	2 in - 1 foot	< 2 in			
Relative Rating	30	25	20	10	5			
4. Joint Condition	Very rough surfaces Not continuous No separation Hard joint wall rock	Slightly rough surfaces, Separation < 0.05", Hard joint wall rock	Slightly rough surfaces, Separation < 0.05", Soft joint wall rock	Slickensided surfaces or Gouge < 0.2 in thick or Joints open 0.05-0.2 in, Continuous joint	Soft gouge > 0.2 in thick or Joints open > 0.2 in, Continuous joint			
Relative Rating	25	20	12	6	0			
5. Ground Water Condition	Inflow per 30 ft tunnel length	None	< 400 gal/hr	400 - 2,000 gal/hr	> 2,000 gal/hr			
	Ratio = Joint water pressure / major principal stress	0	0.0 - 0.2	0.2 - 0.5	> 0.5			
	General condition	Completely dry	Moist only	Water under moderate pressure	Severe water problem			
Relative Rating		10	7	4	0			

## **4.2 M-43 EB Over the Grand River**

### **4.2.1 General Information**

M-43 (EB) over the Grand River is located in the City of Lansing, Ingham County, Michigan (Figure 4.1). At this location, the river flows to the north, and the nearest USGS gaging station No. 04113000 is located downstream of the bridge. The area surrounding the site consists of glacial outwash consisting of primarily fine sands, although some materials are coarse sand and gravel. Overburden deposits consist of brown to gray silty sand and gravel. The subsurface of the bridge site consists of 4 strata with varying thickness. The top stratum is loose to medium dense sand and clay with various amounts of sand, and its thickness varies from 2 ft to 5.5 ft. Stratum 2 is approximately 4.5 ft thick and consists of brown to gray sand with gravel. Stratum 3 is extremely weathered sandstone with less weathered sandstone layers/lenses extending to about 6 ft. Below this stratum, there is gray sandstone which is slightly weathered to fresh with some fractures. This bedrock is documented as Parma or Marshall Sandstone (Milstein 1987).

The geotechnical report for this site recorded that the old bridge was replaced after 2011 with a 3-span, 286 ft long steel girder. Currently, drilled shafts support all the piers and abutments socketed into the sandstone bedrock. The bottom of the drilled shafts elevation varies from approximately 771 ft to 778 ft and the diameter varies from 57 inches to 48 inches for the piers, 60 inches to 54 inches for Abutment A, and 54 inches to 48 inches for Abutment B (Table 4.2) as per the geotechnical report and the proposed plan.



Figure 4.1 Location of M-43 EB over the Grand River (The image has been retrieved from Google Earth 2018 (Google))

Table 4.2 Summary of drilled shaft foundation of M-43 over the Grand River

Description	Abutment A	Pier 1	Pier 2	Abutment B
Bottom of Drilled Shaft Elevation (ft)	771.0	777.0	775.0	778.0

There are three earth strata/layers at Pier #1 of M-43 EB and four at Pier #2 (Figure 4.2). Table 4.3 represents the detailed attributes of each layer including the layer thickness and classification. Since the piers were founded on bedrock, scour analysis at this site has been done using all the available methods, i.e., SRICOS-EFA, EIM, and GSN. The SRICOS-EFA and GSN were applied to determine the cumulative scour depth over time since the bridge installation i.e. 2011, while the EIM was used to determine the scour depths for different design discharges.

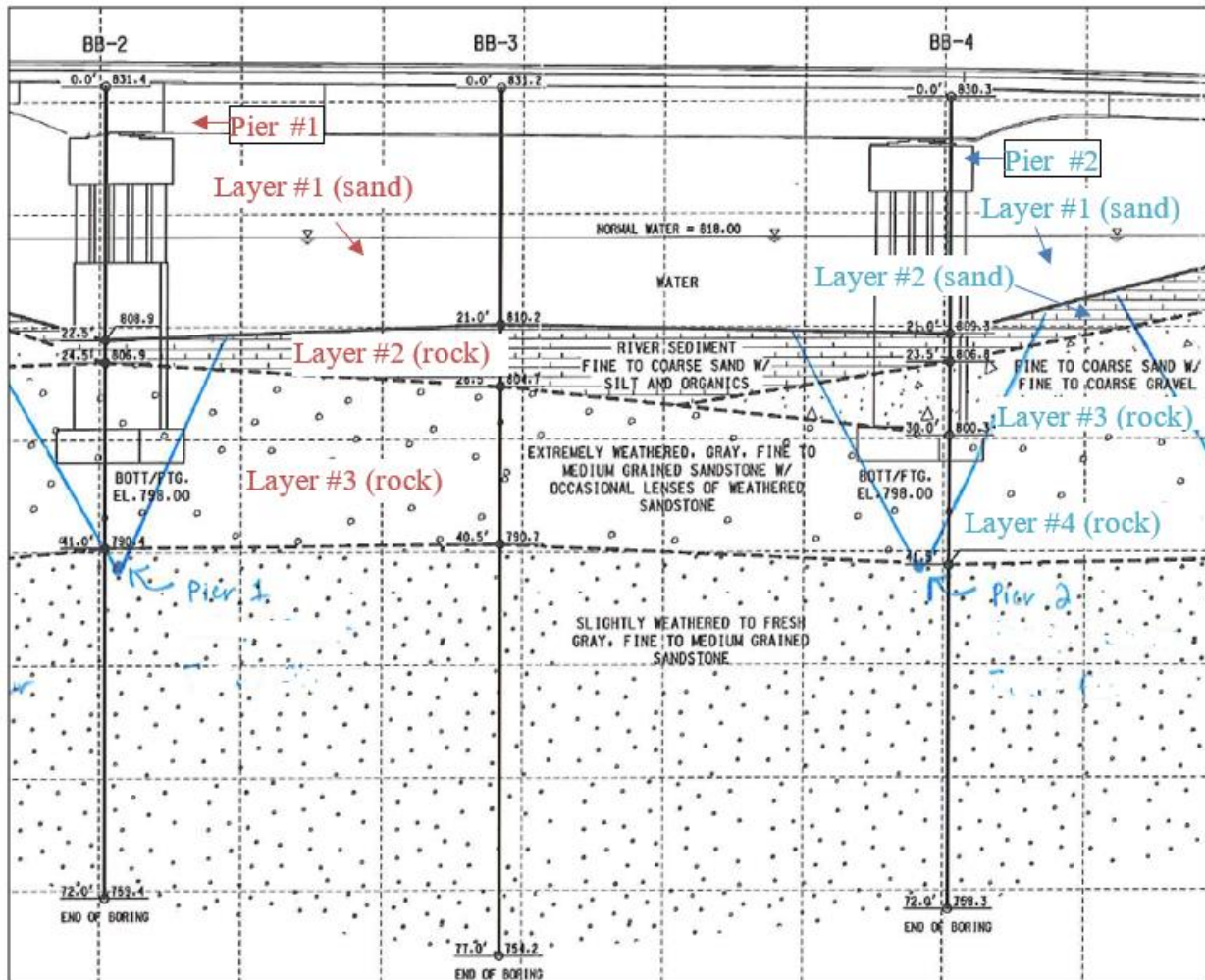


Figure 4.2 Earth cross-section at M-43 EB over the Grand River

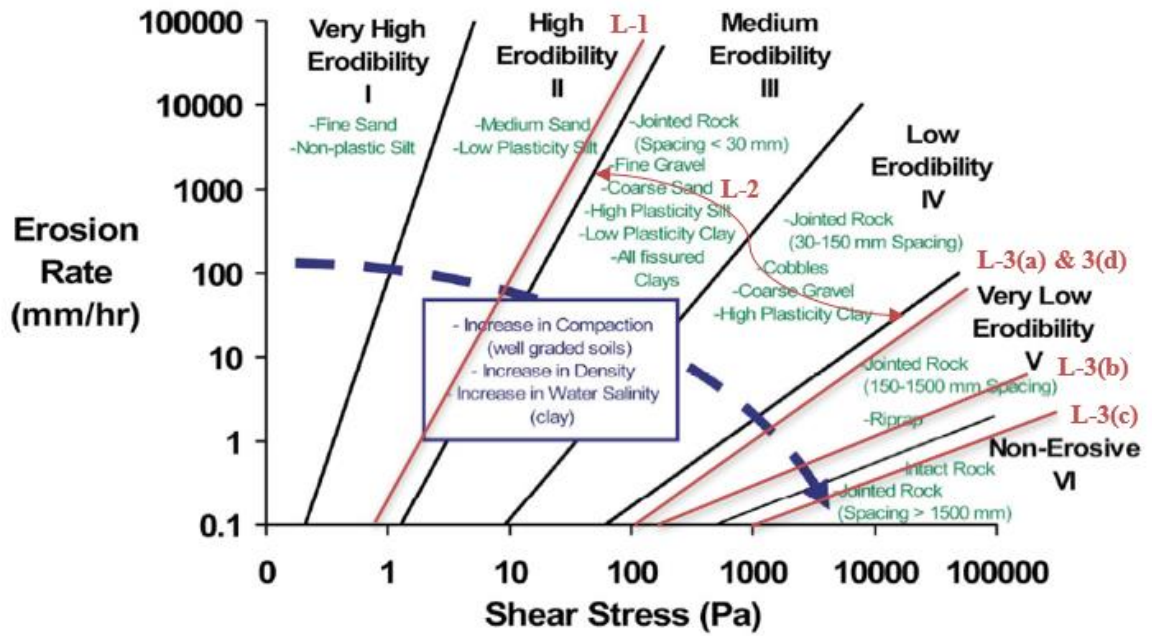
Table 4.3 Attributes of the earth layers at M-43 EB over the Grand River

Layer	Pier #1		Pier #2	
	Thickness (ft)	Classification	Thickness (ft)	Classification
1	2.0	Fine to Coarse Sand with Silt and Organics	2.5	Fine to Coarse Sand with Silt and Organics
2	16.5	Extremely Weathered, Gray, Fine to Medium Grained Sandstone	8.0	Fine to coarse sand with fine to coarse gravel
3	31.0	Slightly weathered to Fresh, Gray Fine to Medium Grained Sandstone	10.0	Extremely Weathered, Gray, Fine to Medium Grained Sandstone
4	-	-	30.5	Slightly weathered to Fresh, Gray Fine to Medium Grained Sandstone

#### 4.2.2 Scour Analysis Using SRICOS-EFA

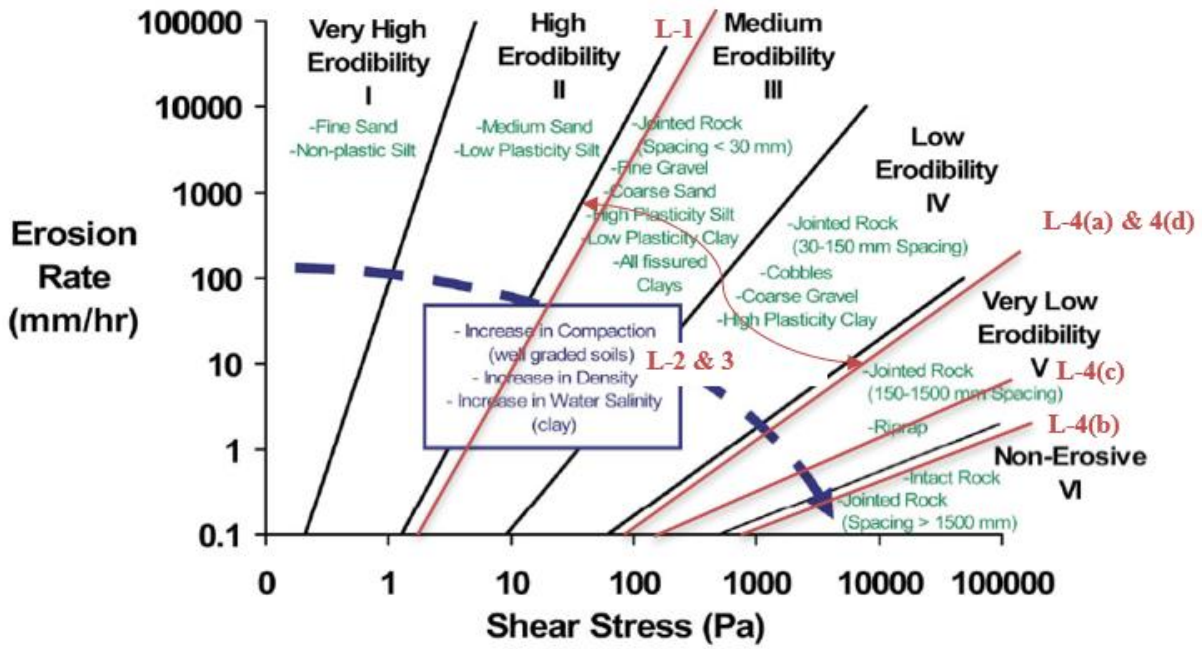
Itemized input categories used for the scour analysis of M-43 over the Grand River using SRICOS-EFA are described here followed by the simulation results.

Soil/Material Properties Input: Lab testing data for the earth layer erodibility at this site was not available in the geotechnical report. Therefore, the erosion category curves proposed by Briaud (2008) (Figure 3.1) were used for assuming the erosion characteristics of the material based on conventional material properties from the geotechnical report. The straight lines marked with “L #” in Figure 4.3 and Figure 4.4 show the assumed curves for the corresponding layer.



— Assumed erosion curve [Intersecting point of each curve & the x-axis is the critical shear stress]

Figure 4.3 Assumed/interpreted erosion curves on Briaud's erosion category plot (Briaud 2008; Briaud et al. 2019) for the earth layers at Pier #1 of M-43 EB over the Grand River



— Assumed erosion curve [Intersecting point of each curve & the x-axis is the critical shear stress]

Figure 4.4 Assumed/interpreted erosion curves on Briaud’s erosion category plot (Briaud 2008; Briaud et al. 2019) for the earth layers at Pier #2 of M-43 EB over the Grand River

Conventional soil properties found in the geotechnical report were classifications of all layers and  $D_{50}$  of some layers. The erodibility curve was determined based on  $D_{50}$  values when available, and in other cases, the earth layer classification from Table 4.3 was used. The  $D_{50}$  values of both the first layers of both the piers were found to be greater than 0.3 mm, which indicates the critical shear stresses of these layers are the same as the corresponding  $D_{50}$  values. This is because, according to Briaud et al. (2019), the critical shear stress equals the  $D_{50}$  if  $D_{50} > 0.3$  mm. When the critical shear stress was determined, the erodibility curve was assumed to be a straight line passing through the critical value and parallel to the nearest line available on Briaud’s (Briaud 2008) erosion category plot (Figure 3.1). Comparison of the earth classification (Table 4.3) of the 2<sup>nd</sup> layer at Pier #1, and the 2<sup>nd</sup> and 3<sup>rd</sup> layers at Pier #2 with the earth classification available in Briaud’s erosion category plot, it was shown that these layers have medium to low erodibility. So,

several curves within this range in Figure 4.3 and Figure 4.4 were adopted to observe the sensitivity of the scour analysis results to these assumed curves.

The 3<sup>rd</sup> layer at Pier #1 and the 4<sup>th</sup> layer at Pier #2 are rock layers with some sub-layers since the rock RMR test results from the geotechnical report indicate that these layers have different RMR values at different depths (Table 4.4). When the relative rating for the joint spacing of the rock layers was entered in the AASHTO (2010) RMR table (Table 4.1), it was found that both the 3<sup>rd</sup> layer of Pier #1 and 4<sup>th</sup> layer of Pier #2 have several ranges of rock joint spacing (Table 4.5). These ranges of joint spacing were compared with the erosion category plot of Briaud (2008) (Figure 3.1) to assume the erosion curves for the rock sub-layers (Figure 4.3, Figure 4.4).

Table 4.4 RMR of the 3<sup>rd</sup> layer at Pier #1 and the 4<sup>th</sup> layer at Pier #2 of M-43 EB over the Grand River

Depth within the layer (ft)	Relative Rating				Groundwater	RMR
	Rock Strength	RQD	Joint Spacing	Joint Condition		
3 <sup>rd</sup> layer at Pier #1						
1.0 – 2.3	2	10	10	6	7	35
2.3 – 4.0	0	3	10	6	7	26
4.0 – 6.0	2	15	13	6	7	43
6.0 – 11.0	2	13	15	10	7	47
11.0 – 16.0	2	13	15	12	7	49
16.0 – 21.0	2	17	20	15	7	61
21.0 – 26.0	2	20	18	12	7	59
26.0 – 31.0	2	17	10	10	7	46
4 <sup>th</sup> layer at Pier #2						
0.5 – 5.5	2	13	10	9	7	41
5.5 – 10.5	2	20	20	6	7	55
10.5 – 15.5	2	15	15	15	7	54
15.5 – 20.5	2	18	15	18	7	60
20.5 – 25.5	2	17	15	10	7	51
25.5 – 30.5	2	15	10	9	7	43

Table 4.5 Range of joint spacing for the 3<sup>rd</sup> layer at Pier #1 and the 4<sup>th</sup> layer at Pier #2 of M-43 EB over the Grand River

Depth within the layer (ft)	Relative Rating for Joint Spacing from Table 4.4	Range of Joint Spacing from Table 4.1
3 <sup>rd</sup> layer at Pier #1		
0.0 – 4.0	10	2 in – 1 ft (60 mm – 300 mm)
4.0 – 16.0	13-15	1 ft – 3 ft (300 mm – 900 mm)
16.0 – 260	18-20	> 10 ft (3000 mm)
26.0 – 31.0	10	2 in – 1 ft (60 mm – 300 mm)
4 <sup>th</sup> layer at Pier #2		
0.0 – 5.5	10	2 in – 1 ft (60 mm – 300 mm)
5.5 – 10.5	20	> 10 ft (3000 mm)
10.5 – 25.5	15	1 ft – 3 ft (300 mm – 900 mm)
25.5 – 30.5	10	2 in – 1 ft (60 mm – 300 mm)

Once all the erosion category curves were assumed, the critical shear stresses of each of the earth layers at both the piers were determined from Figure 4.3 and Figure 4.4, where, intersecting point of each curve and the x-axis is the critical shear stress (Briaud et al. 2019). Table 4.6 represents the critical shear stress of all the earth layers at Pier #1 and Pier #2 obtained from Figure 4.3 and Figure 4.4 respectively. Several data points from these curves and critical shear stress were entered in the SRICOS-EFA software as material input along with the thickness of each layer from Table 4.3.

Table 4.6 Critical shear stress of each earth layer at M-43 EB over the Grand River based on the erosion category curves

Pier #1		Pier #2	
Layer	Critical Shear Stress in lb/ft <sup>2</sup> (Pa) (From Figure 4.3)	Layer	Critical Shear Stress in lb/ft <sup>2</sup> (Pa) (From Figure 4.4)
1	0.02 (0.9)	1	0.07 (3.5)
2	0.04/0.2/ 0.9/1.67 (2.0/9.5/ 43.0/80.0)	2	0.02/ 0.10 (9.5/ 5.0)
3(a)	4.18 (200)	3	0.9/ 0.20 (43.0/ 9.5)
3(b)	6.27 (300)	4(a)	1.88 (90)
3(c)	20.89(1000)	4(b)	16.71 (800.1)
3(d)	4.18(200)	4(c)	4.18 (200)
-	-	4(d)	1.88 (90)

Hydraulic Parameter Input: Among the water parameters, Manning's coefficient of 0.035 was extracted from the HEC-RAS model. Other hydraulic parameters, i.e., corresponding water depth and velocity for different discharges were also extracted from the hydraulic model. The daily discharge of the river since 2011 was obtained from the gaging station data.

Geometry Input: The geotechnical report indicates that both of the piers at M-43 over the Grand River are circular with varying diameters. For analysis, a pier diameter of 4.5 ft (54 inches) was adopted. The other geometry input - the upstream channel width, was extracted from the HEC-RAS model, and it was 237.3 ft.

With all the input parameters, the SRICOS-EFA software was run to obtain the cumulative scour depth at Pier #1 and Pier #2 of M-43 EB over the Grand River. The cumulative scour depth is the scour accumulated due to the daily discharge of the river within the analyzed period of time. According to these simulation results, the cumulative scour depth at Pier #1 would be 5.3 ft since 2011 if the 2<sup>nd</sup> layer had a critical shear stress of 2 Pa (Figure 4.5). However, the cumulative scour depth would not exceed 2.1 ft if the 2<sup>nd</sup> layer had a critical shear stress higher than 9.5 Pa (Figure 4.6). On the other hand, simulation for Pier #2 resulted in similar outputs for the analyzed cases i.e. the cumulative scour depth at Pier #2 would be 2.3 ft since 2011 if all the assumptions were true (Figure 4.7). Since, the scour depth did not exceed the 1<sup>st</sup> layer thickness of 2.5 ft, different erosion category curves for the 2<sup>nd</sup> and 3<sup>rd</sup> layer of Pier #2 could not affect the output result. Here, the dramatic changes in the graphs were caused by higher discharges in high flow events.

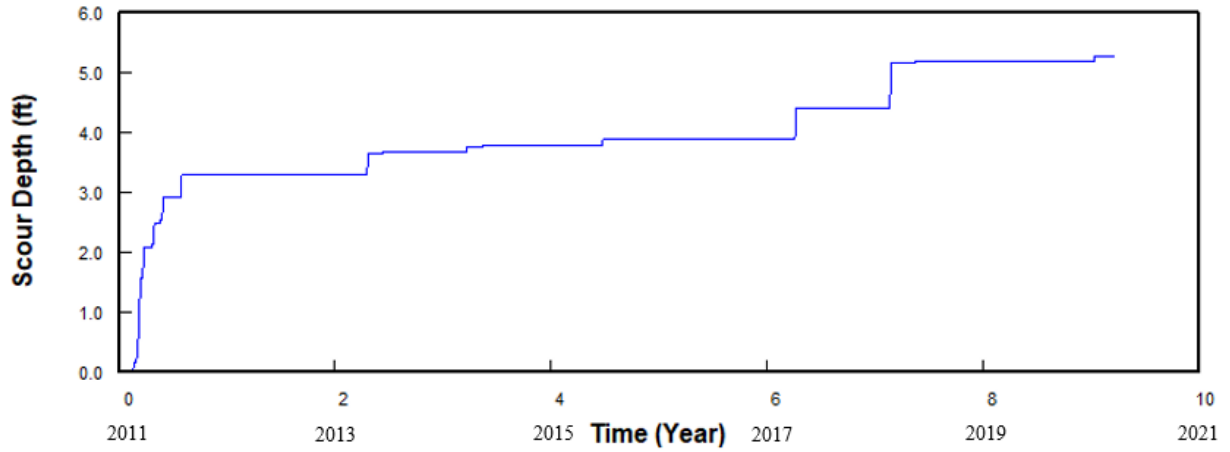


Figure 4.5 Scour depth at Pier #1 of M-43 EB when Layer # 2 has critical shear of 2 Pa

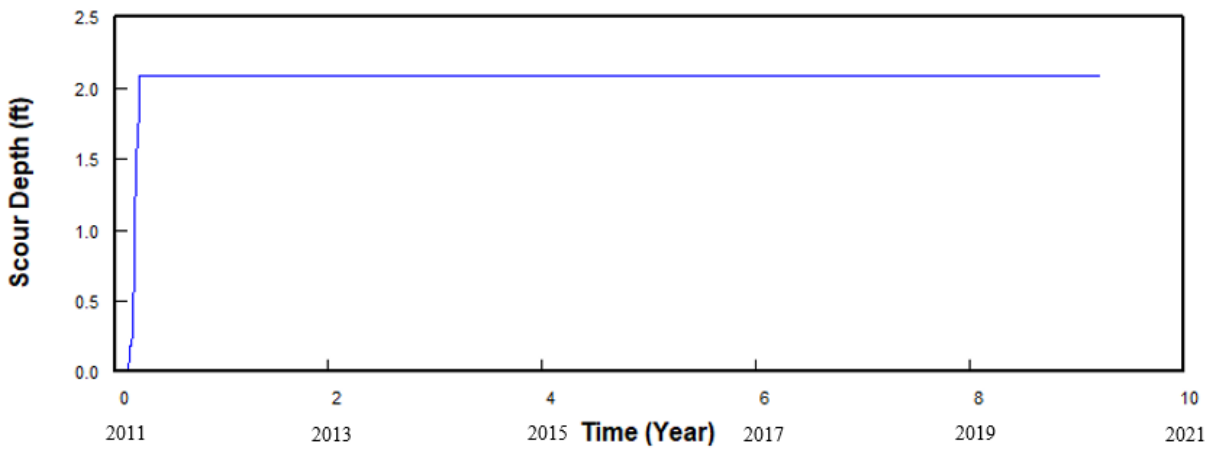


Figure 4.6 Scour depth at Pier #1 of M-43 EB when Layer # 2 has critical shear of 9.5 Pa or 43 Pa or 80 Pa

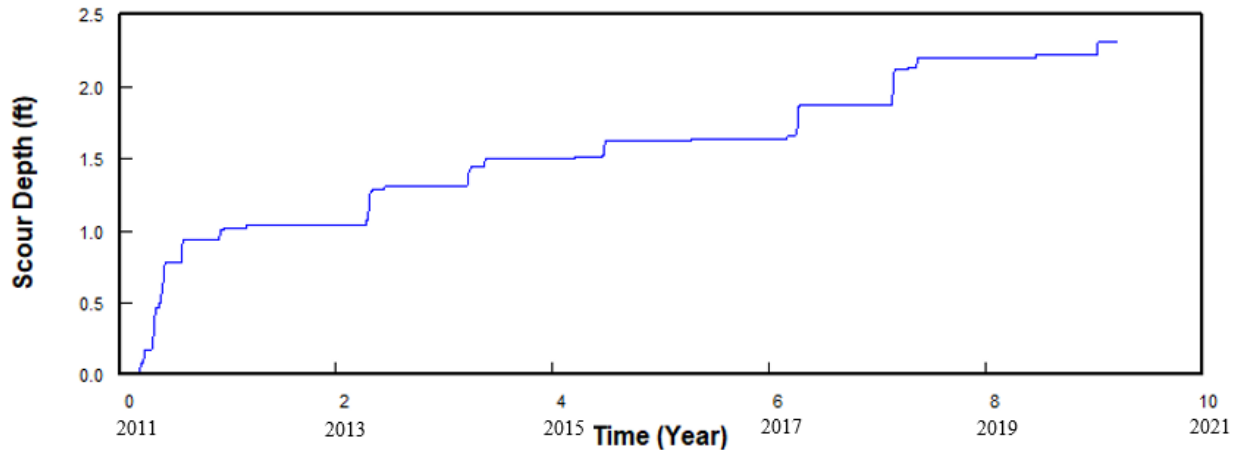


Figure 4.7 Scour depth at Pier #2 of M-43 EB when Layer # 2 has critical shear of 9.5 Pa & Layer #3 has 43 Pa or when Layer # 2 has critical shear of 5 Pa & Layer #3 has 9.5 Pa

#### 4.2.3 Scour Analysis Using EIM

Since neither the layer thickness nor the type of earth strata at Pier #1 and Pier #2 of M-43 EB is identical (Figure 4.2, Table 4.3), the scour calculations for these two piers were performed separately using the EIM (Table 4.7, Table 4.8). The first layer at Pier #1 is a sand layer followed by extremely weathered sandstone and slightly weathered sandstone, whereas the first two layers at Pier #2 are sand layers underlain by similar types of rock layers. The erodibility indices of the sand and rock layers were determined following the equations for the corresponding materials.

From the geotechnical report, it was found that the  $D_{50}$  of the sand layer at Pier #1 is 9 mm and the SPT N value is 8. At Pier #2, the  $D_{50}$  of the first sand layer is 3.5 mm and SPT N value is 5, and the second sand layer has an SPT N value of 85. Since the  $D_{50}$  of the second sand layer at Pier #2 was not available, it was assumed to be the same as the first sand layer at this location. The SPT N value was used to determine the mass strength number,  $M_s$ , from Table 3.6 and the  $D_{50}$  was used to determine the particle size number,  $K_b$ , using Eq. 3.7. The residual friction angle of all the sand layers was assumed to be 30 degrees and was used to determine the shear strength number,  $K_d$ , using Eq. 3.8. With the above parameters, Eq. 3.4 was used to determine the erodibility indices of the sand layers.

As per the geotechnical report, the extremely weathered sandstone layer is a highly fractured rock layer with a UCS value less than 1.7 MPa and an RQD within 0-25%. To determine the erodibility index of this rock layer, the following parameters were first determined to provide input for the analysis with the EIM. The rock was considered to be very soft according to the UCS value and the UCS value was used to determine the mass strength number,  $M_s$ , from Table 3.1. Since the RQD of this rock layer varied from 0-25%, 12% was used while doing the calculation. The number of the joint/fissure set was assumed to be “multiple” considering the highly fractured characteristics and was used to determine the joint set number,  $J_n$ , from Table 3.2. These RQD and  $J_n$  values were used to determine block size number,  $K_b$ , following Eq. 3.5. The joints were assumed to be tight smooth planer with a spacing of 1-5 mm and the gouge present in the joint was assumed to be clay and rock fragments – these specifications were used to determine joint roughness number,  $J_r$ , and joint alteration number,  $J_a$ , from Table 3.3 and Table 3.4 respectively. These values of  $J_r$  and  $J_a$  were used to obtain shear strength number,  $K_d$ , following Eq. 3.6. Also, a 5 degree dip angle was assumed in the direction of stream flow with a joint spacing of 1:1 to determine relative ground structure number,  $J_s$  from Table 3.5. With the above parameters, Eq. 3.4 was used to determine the erodibility index of the rock layer.

Finally, the obtained erodibility indices were used to determine the critical stream power,  $P_c$ , at different layers using Eq. 3.13 or Eq. 3.14 and consequently, the scour status at different depths from the riverbed was determined. Table 4.7 and Table 4.8 show the scour status of Pier #1 and Pier #2, respectively, for a design discharge values of 19,400 cfs and 26,800 cfs. Here, the dimensionless scour depth ( $y_s/b$ ) was obtained with the ratio of the depth and the pier width; the relative stream power ( $P/P_a$ ) was obtained using Eq. 3.16. For approaching flow stream power,  $P_a$  was determined using Eq. 3.15 and the available stream power at the pier,  $P$  was obtained by multiplying relative stream power and approaching flow stream power. The available stream power,  $P$ , at the pier was compared with the critical stream power,  $P_c$ , to obtain the scour status at different depths. At any depth, scour takes place if the available stream power at the pier is more than the critical stream power. It can be seen from Table 4.7 that at Pier #1, scour ceased at the depth of 2.1 ft for design discharge of 19,400 cfs, however, scour depth reached at 8.3 ft for design

discharge of 26,800 cfs. By contrast, at Pier #2, scour depth reached 10.5 ft for both the design discharges.

Table 4.7 Scour determination at Pier #1 of M-43 over the Grand River using EIM

Depth (ft)	Layer	Erodibility Index	$P_c$ (lb/ft-s)	Dimensionless scour depth ( $y_s/b$ )*	Relative Stream Power ( $P/P_a$ )	For 19,400 cfs			For 26,800 cfs		
						Approaching Flow Stream Power, $P_a$ (lb/ft-s)	Available Stream Power, $P$ (lb/ft-s)	Scour (Yes/No)	Approaching Flow Stream Power, $P_a$ (lb/ft-s)	Available Stream Power, $P$ (lb/ft-s)	Scour (Yes/No)
1	1	$1.6 \times 10^{-8}$	0.012	0.22	7.21	5.34	38.51	Yes	13.86	99.95	Yes
2				0.44	6.18		32.98	Yes		85.60	Yes
2.1				0.46	6.08		32.47	Yes		84.29	Yes
2.2				0.48	5.99		31.97	No		82.99	Yes
3				0.65	5.29		28.24	No		73.31	Yes
4	2	0.363	32.04	0.87	4.53	5.34	24.19	No	13.86	62.78	Yes
5				1.09	3.88		20.71	No		53.77	Yes
6				1.31	3.32		17.74	No		46.05	Yes
7				1.52	2.84		15.19	No		39.43	Yes
8				1.74	2.44		13.01	No		33.77	Yes
8.3				1.81	2.33		12.42	No		32.24	Yes
8.4				1.83	2.29		12.23	No		31.74	No

\*  $b$  is pier width perpendicular to the flow direction.

Table 4.8 Scour determination at Pier #2 of M-43 over the Grand River using EIM

						For 19,400 cfs			For 26,800 cfs		
--	--	--	--	--	--	----------------	--	--	----------------	--	--

Depth (ft)	Layer	Erodibility Index	$P_c$ (lb/ft-s)	Dimensionless scour depth ( $y_s/b$ )*	Relative Stream Power ( $P/P_a$ )	Approaching Flow Stream Power, $P_a$ (lb/ft-s)	Available Stream Power, $P$ (lb/ft-s)	Scour (Yes/No)	Approaching Flow Stream Power, $P_a$ (lb/ft-s)	Available Stream Power, $P$ (lb/ft-s)	Scour (Yes/No)
1				0.22	7.21		38.51	Yes		99.95	Yes
2	1	9.9x10 <sup>-7</sup>	0.08	0.44	6.18	5.34	32.98	Yes	13.86	85.60	Yes
2.5				0.54	5.71		30.52	Yes		79.22	Yes
3				0.65	5.29		28.24	Yes		73.31	Yes
4				0.87	4.53		24.19	Yes		62.78	Yes
5				1.09	3.88		20.71	Yes		53.77	Yes
6				1.31	3.32		17.74	Yes		46.05	Yes
7	2	2.1x10 <sup>-5</sup>	0.29	1.52	2.84	5.34	15.19	Yes	13.86	39.43	Yes
8				1.74	2.44		13.01	Yes		33.77	Yes
9				1.96	2.09		11.14	Yes		28.92	Yes
10				2.18	1.79		9.54	Yes		24.77	Yes
10.5				2.29	1.65		8.83	Yes		22.92	Yes
10.6	3	0.363	32.0 4	2.31	1.63	5.34	8.69	No	13.86	22.57	No

\*  $b$  is the pier width perpendicular to the flow direction.

To get accurate results, every parameter mentioned in the EIM is important. Parameters needed for cohesive soil strata are easily available in the geotechnical report. However, some parameters for rock strata are not available, e.g., dip angle, dip direction, and the ratio of joint spacing. As a result, these parameters had to be assumed in all the EIM scour calculations introduced in Chapter 4. To check the sensitivity of these parameters, multiple cases have been analyzed for the rock layer at Pier #1 of M-43 over the Grand River. Table 4.9 shows how the results might change if these parameters vary.

Table 4.9 Sensitivity study of selected parameters on erodibility index and scour depth for rock layer at Pier #1 of M-43 over the Grand River

Dip angle (degree)	Dip direction	Ratio of joint spacing	Erodibility index	Scour depth for 19,400 cfs (ft)	Scour depth for 26,800 cfs (ft)
5	In direction of stream flow	1:1	0.363	2	8
-70	Against direction of stream flow	1:8	0.264	3	9
-89	Against direction of stream flow	1:1	0.392	2	7
60	In direction of stream flow	1:4	0.110	7	14

#### 4.2.4 Scour Analysis Using GSN

The modified slake durability test, whose result is needed for using the GSN, was not available in the geotechnical report of M-43 EB over the Grand River. Thus, the GSN value of the bedrock at this site was obtained from the literature. Considering that the Grand River in Michigan has Pennsylvanian Sandstone (Milstein 1987), two values, i.e.,  $4.54 \times 10^{-6} \text{ ft} \left[ \frac{\text{ft} \cdot \text{lb}}{\text{sft}^2} \right]^{-1}$  and  $2.53 \times 10^{-5} \text{ ft} \left[ \frac{\text{ft} \cdot \text{lb}}{\text{sft}^2} \right]^{-1}$ , which were the only available data in the literature for sandstone, were adopted as the GSN values for this site. This range was obtained for the Cambrian Sandstone of Wisconsin in 2017 by Wisconsin DOT (Titi et al. 2017).

Stream power values corresponding to several discharge values were collected from the HEC-RAS model and were used to determine the constants of Eq. 3.21. Thus, Eq. 3.21 became ready to be used in determining stream power for daily discharges of this bridge site obtained from the USGS gaging station. After calculating corresponding stream power for daily discharge since 2011, Eq. 3.20 was used to determine the corresponding scour depth for the above mentioned GSN values. Finally, cumulative scour depth was determined. While using Eq. 3.20, the daily stream power value of the cumulative value was used instead, and the daily scour depth was determined to get cumulative scour depth. This has been done to represent the cumulative scour depth over time.

Figure 4.8 depicts the cumulative scour depth of the sandstone bedrock of the Grand River at M-43 EB since 2011 using the above-mentioned GSN values. Both of the two piers were founded on the same bedrock. Therefore, Figure 4.8 represents the scour condition at both piers. It is observed that both the GSN values have produced almost negligible scour depth even for a nine-year period.

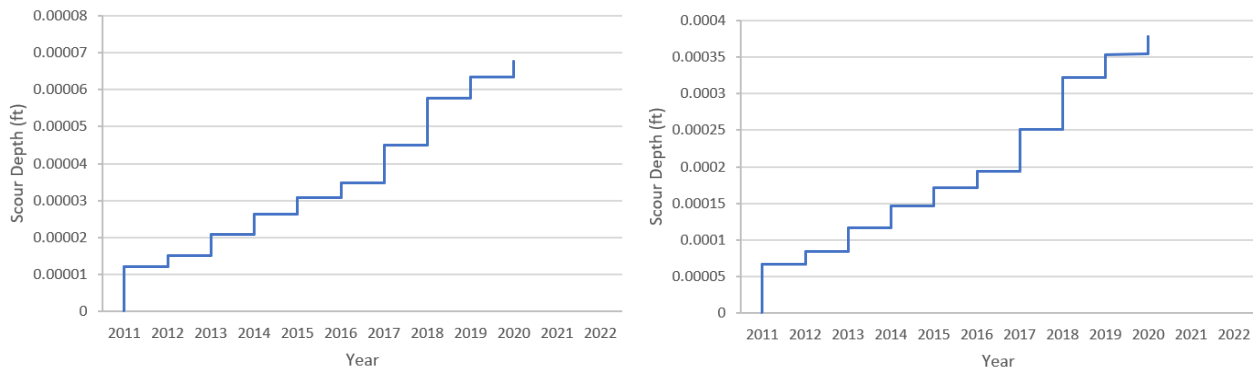


Figure 4.8 Cumulative scour depth of sandstone bedrock of Grand River at M-43 EB (a) using GSN as  $4.54 \times 10^{-6} \text{ ft} \left[ \frac{\text{ft-lb}}{\text{sft}^2} \right]^{-1}$  and (b) using GSN as  $2.53 \times 10^{-5} \text{ ft} \left[ \frac{\text{ft-lb}}{\text{sft}^2} \right]^{-1}$ .

#### 4.2.5 Comparison of Results

This section provides a comparison of the scour analysis results at the bridge site on M-43 EB over the Grand River. The scour analysis results for this site obtained from all the selected methods are summarized in Table 4.10.

The scour depth calculated using the SRICOS-EFA provided cumulative scour developed from 2011 to 2020. This SRICOS-EFA result is not very comparable with the scour depth calculated using the HEC-18 sand equation, because the HEC-18 sand equation can only provide the scour depth for the design discharge. Despite this fact, the scour depth calculated with the SRICOS-EFA method is much smaller than that with the HEC-18 sand equation. Also, to check the sensitivity of the erosion category curve, multiple curves within the range were assumed for Pier #1 and the resulting scour depth was 2.1 - 5.3 ft which is a difference of 60%.

The EIM made predictions that are comparable to those of the HEC-18 sand equation in three out of the four cases. The exception is for the discharge of the 19,400 cfs at Pier #1. The EIM prediction, i.e., 2.1 ft, is much smaller than the HEC-18 result, i.e., 8.5 ft. Overall, the scour depths at Pier #2 for both design discharges were higher than those at Pier #1. It is worthwhile to mention that Pier #1 has only a 2 ft sand layer above the rock layer, whereas, at Pier #2, a 10.5 ft sand layer is present before the rock layer begins to erode. This may imply that the EIM can yield a higher scour depth than the HEC-18 sand equation in non-cohesive strata.

The GSN was applied only at the bedrock for cumulative scour depth. At both piers, the predicted cumulative scour depth was found to be very small for the nine-year period. The predicted scour depths fall in the range of 0.000068 - 0.00038 ft, which can be viewed as negligible. The range was obtained with the two GSN values from the literature. As can be seen, the predictions with the assumed GSN values exhibited a variance of 81% in the result. The results may provide two implications for practice. First, the abrasion mode of scour may be very small and thus can be negligible for common Michigan rocks. Second, the use of the modified slake durability test may be necessary because assumed GSN values without conducting the test can lead to significant errors in the calculation results.

The SRICOS-EFA and GSN calculation results can be directly compared because both of them determine the cumulative scour depth over a certain period. Within them, the GSN method works with bedrock only, and it considers the rock in direct contact with water, which is the worst condition. By contrast, the EIM works on the concept of a decreasing stream power with depth, which makes the bedrock less susceptible to scour if it is present at a deeper depth. For example,

the calculation using the GSN predicted the same scour depth of the bedrock for both piers of M-43 over the Grand River, whereas the EIM estimated some scour in the bedrock at Pier #1 but none at the bedrock of Pier #2. The SRICOS-EFA result also indicated that the scour depth did not reach the bedrock at Pier #2, but there is some scour within the bedrock at Pier #1 (Table 4.10, Table 4.3).

Table 4.10 Comparison of scour analysis results of M-43 over the Grand River

Method	Scour Depth for 19,400 cfs	Scour Depth for 26,800 cfs	Scour Depth from 2011 – 2020*	Comment
<b>Pier #1</b>				
SRICOS-EFA	-	-	2.1 - 5.3 ft	Several erosion curves were assumed within the range of erosion categories which resulted in this range of scour depth. Some data were available for assuming the erosion category curves, others were assumed.
EIM	2.1 ft	8.3 ft	-	EIM for cohesionless soil + EIM for rock
GSN	-	-	0.000068 - 0.00038 ft scour depth of the <b>bedrock starting at 2.1ft</b>	Two values of GSN from the literature have been used.
HEC-18 Sand	8.5 ft	9.7 ft	-	-
<b>Pier #2</b>				
SRICOS-EFA	-	-	2.3 ft	Some data were available for assuming the erosion category curves, others were assumed.
EIM	10.5 ft	10.5 ft	-	EIM for cohesionless soil + EIM for rock
GSN	-	-	0.000068 - 0.00038 ft scour depth of the <b>bedrock starting at 10.6 ft</b>	Two values of GSN from the literature have been used.
HEC-18 Sand	8.5 ft	9.7 ft	-	-

\*This duration was taken since the bridge was installed in 2011.

## **4.3 US-2 and US-41 over the Escanaba River**

### **4.3.1 General Information**

US-2 and US-41 over the Escanaba River is in Wells Township, Delta County, Michigan (Figure 4.9) with the river flowing to the south. The nearest USGS gaging station No. 04059000 is located upstream of the bridge at Cornell, MI and the area around the site consists of dune sand, glaciofluvial sand, and gravel. Overburden deposits consist of brown to reddish-brown silty clay loam and sand and gravel. Some cobbles and boulders are also prevalent in these deposits. The subsurface of the bridge site consists of three strata where the top stratum is the embankment material, fill, peat and wood, and native soils with a thickness about 4 ft. Stratum 2 has a thickness of less than 5 ft and consists of brown to gray weathered limestone with cobbles and boulders. Stratum 3 is fresh, gray to dark gray, very fine-grained strong limestone, and dolomite layer and has a thickness of more than 20 ft. According to the geotechnical report, most of the rock layers are within the Trenton Limestone formation.

The old bridge was replaced after 2008 with a three-span bridge, which is about 375 ft long and consists of almost three equal spans of 125 ft. The geotechnical report for this site recorded that spread footings support both the abutments and drilled shafts support all the piers. Both of the foundation systems sit on the strong limestone and dolomite bedrock. The width of both the spread footing is 96 inches and the bottom is at an elevation of 574.5 ft. The diameter of both the drilled shaft is 48 inches and the bottom elevation varies from 562.5 ft to 563 ft (Table 4.11).

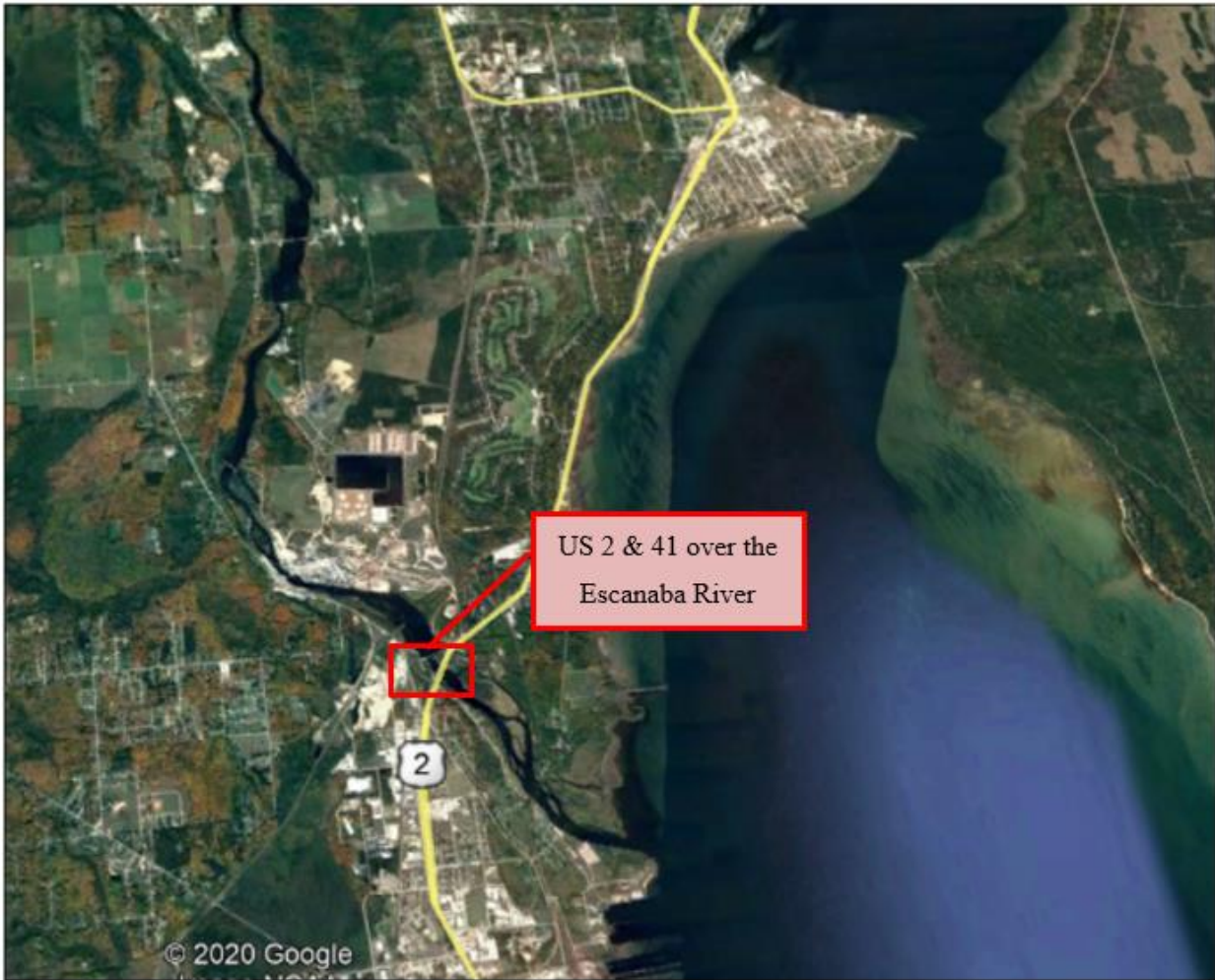


Figure 4.9 Location of US-2 and US-41 over the Escanaba River (The image has been retrieved from Google Earth, 2018 (Google))

Table 4.11 Summary of foundation system of US-2 and US-41 over the Escanaba River

Description*	Abutment A	Pier #1	Pier #2	Abutment B
Bottom of Spread Footing/Drilled Shaft Elevation	574.5	563.0	562.5	574.5
Spread Footing width/Drilled Shaft Diameter (in)	96.0	48.0	48.0	96.0

\*Spread footing for abutments and drilled shaft for piers

There are four types of earth strata at both the piers of US-2 and US-41. Pier scour analysis started from layer 2 considering that the first layer is primarily the embankment fill. Table 4.12 presents the detailed attributes of each layer including the sub-layers (if any), thickness, and classification. Since the piers are founded on bedrock, scour analysis at this site has been carried using all the selected methods, i.e., SRICOS-EFA, EIM, and GSN. SRICOS-EFA and GSN were applied to determine the cumulative scour depth at the bridge site since its installation, i.e., 2008, while the EIM was used to determine the scour depth for different design discharges.

Table 4.12 Attributes of the earth layers at US-2 and US-41 over the Escanaba River

Layer	Pier #1		Pier #2	
	Thickness (ft)	Classification	Thickness (ft)	Classification
1	3.0	Cobbles/Boulders	4.5	Weathered limestone, cobbles, boulders, and sand
2(a)	2.0	Weathered Limestone/Limestone Boulder	1.0	Weathered Limestone bedrock
2(b)	-		1.5	Weathered, grayish brown, very fine-grained, strong Limestone
3	7.3	Fresh, gray, very fine-grained, strong Dolomite, some calcite cavities/crystals	8.0	Fresh, light gray to dark gray, very fine-grained, strong Dolomite, some very thin shale seams and calcite cavities
4	22.7	Fresh, gray/ greenish-gray, very fine-grained, strong Limestone, some very thin shale seams/ pyrite inclusions	16.5	Fresh, gray/ greenish-gray, very fine-grained, strong Limestone, some very thin shale seams/ occasional pyrite inclusions

### 4.3.2 Scour Analysis Using SRICOS-EFA

How the input parameters were obtained from the geotechnical report and other available items e.g. proposed plan and hydraulic model for using SRICOS-EFA software in the scour analysis of US-2 and US-41 over the Escanaba River are described below followed by the simulation results:

Soil/Material Properties: Lab material testing data for the earth layers' erodibility at this site were not available, so the erosion category curves by Briaud (2008) was used for assuming erosion characteristics of the earth layers based on the available conventional material properties. The straight lines marked with "L #" in Figure 4.10 and Figure 4.11 show the assumed curves for the corresponding layer.

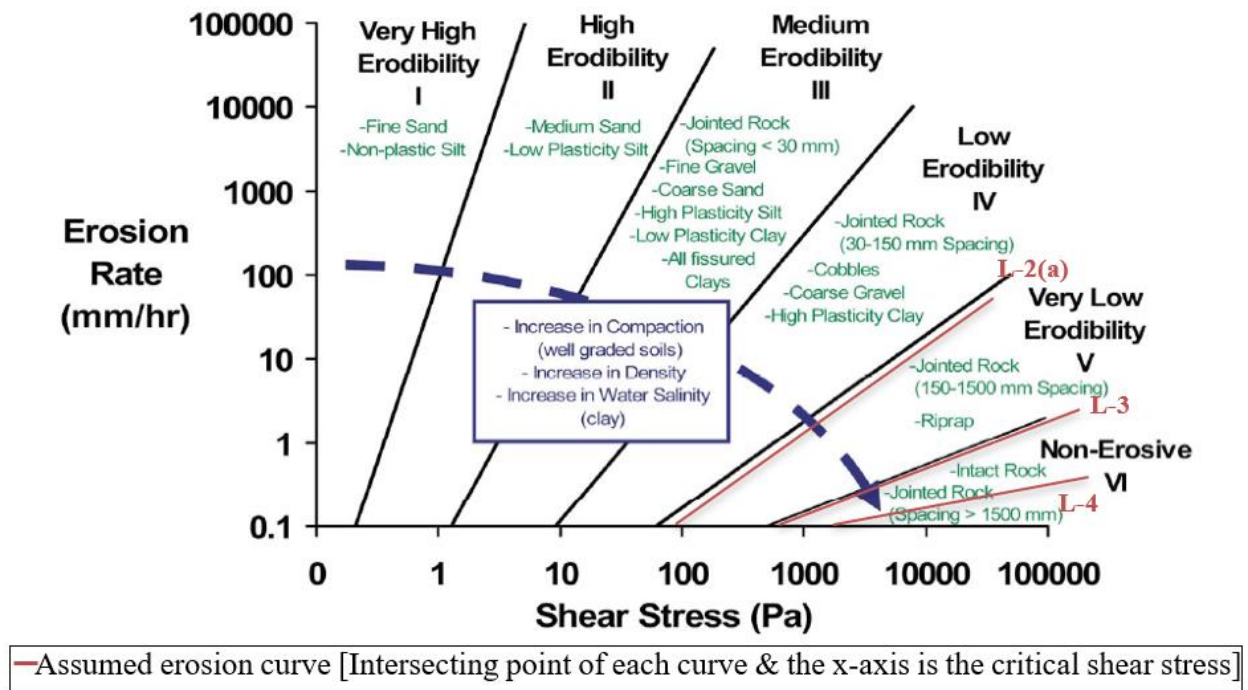


Figure 4.10 Assumed/interpreted erosion curves on Briaud's erosion category plot (Briaud 2008; Briaud et al. 2019) for the earth layers at Pier #1 of US-2 and US-41 over the Escanaba River

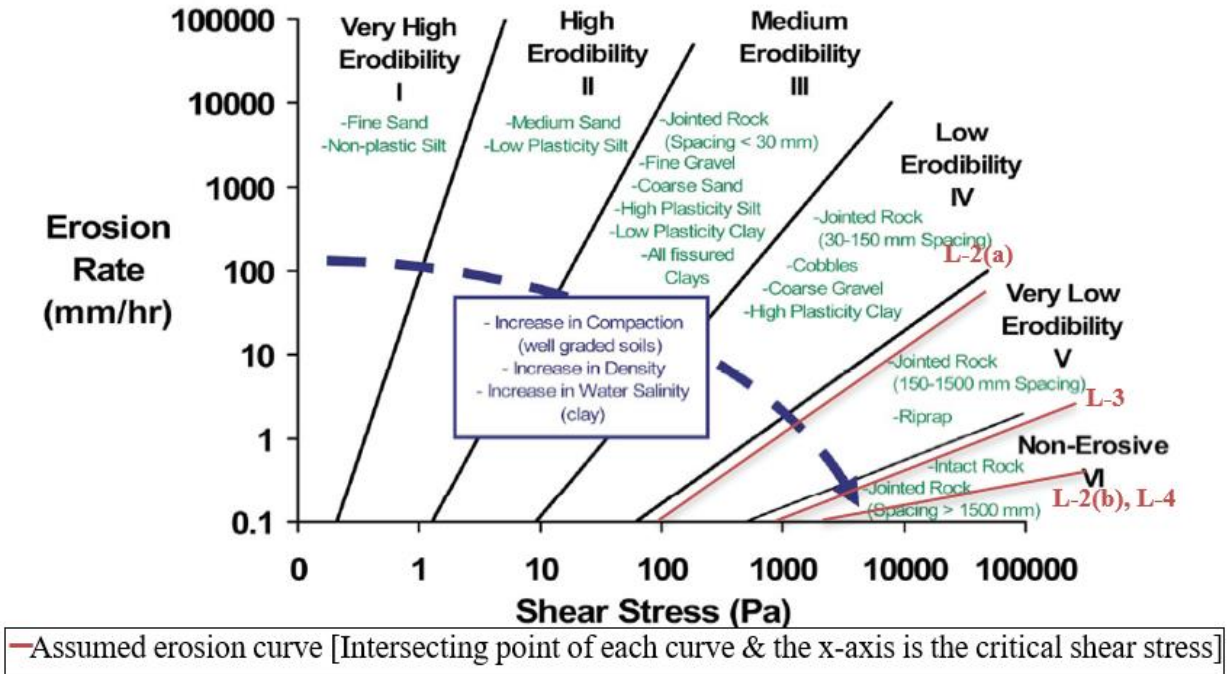


Figure 4.11 Assumed/interpreted erosion curves on Briaud’s erosion category plot (Briaud 2008; Briaud et al. 2019) for the earth layers at Pier #2 of US-2 and US-41 over the Escanaba River

Since, the 1<sup>st</sup> layer was not analyzed for scour calculation, no information of this layer has been included in this section. It is clear from Table 4.12 that all the earth layers except layer 1 are rock layers. So, the joint spacing of each of the rock layers documented in the geotechnical report (Table 4.13) was compared with the available joint spacing information in the erosion category plot of Briaud (2008) (Figure 3.1) to assume the erosion curves for these layers (Figure 4.10, Figure 4.11). When the erosion curves were assumed, the critical shear stress of each layer (Table 4.13) was determined as the intersection point of each curve with the x-axis as per Briaud et al. (2019).

Table 4.13 Joint spacing and critical shear stress of each earth layer at US-2 and US-41 over the Escanaba River

Layer	Pier #1	Pier #2
-------	---------	---------

	Joint Spacing from Geotechnical Report in ft (mm)	Critical Shear Stress from Figure 4.10 in lb/ft <sup>2</sup> (Pa)	Joint Spacing from Geotechnical Report in ft (mm)	Critical Shear Stress from Figure 4.11 in lb/ft <sup>2</sup> (Pa)
2(a)	1.5 (457)	2.09 (100)	1.5 (457)	2.09 (100)
2(b)	-	-	None	83.54 (4000)
3	>10 (3048)	20.88 (1000)	>10 (3048)	20.88 (1000)
4	None	83.54 (4000)	None	83.54 (4000)

Finally, the thickness of each layer from Table 4.12, critical shear stress from Table 4.13, and several data points from the assumed erosion curves from Figure 4.10 and Figure 4.11 were entered into the SRICOS-EFA software as the material input.

Hydraulic Parameters: Manning’s coefficient of 0.045 at this site was extracted from the HEC-RAS model. Other hydraulic parameters, i.e., water depths and velocities for different discharges were also extracted from the HEC-RAS model. The daily discharge of the river since 2008 was obtained from the gaging station data. All these parameters were entered in the SRICOS-EFA software as water input

Geometry Input: The geotechnical report recorded that both the piers of US-2 and US-41 over the Escanaba River are circular with the same diameter of 4 ft (48 inches). Upstream channel width of 352 ft was extracted from the HEC-RAS model.

With all the input parameters, the SRICOS-EFA software was run to determine the cumulative scour depth since 2008 at both the piers of US-2 and US-41 over the Escanaba River. Since the cumulative scour depth is the scour accumulated due to daily discharge over a period of time, the analysis was conducted to determine the accumulated scour taken place from the everyday discharge since 2008. Figure 4.12 and Figure 4.13 are the direct output from the SRICOS-EFA software for Pier #1 and Pier #2, respectively, and they indicate that no scour has taken place at any of the pier sites since 2008. Because scour analysis has only been conducted for the bedrock—we started from the second layer direction— ‘no evidence’ of scour is applicable only for the bedrock.

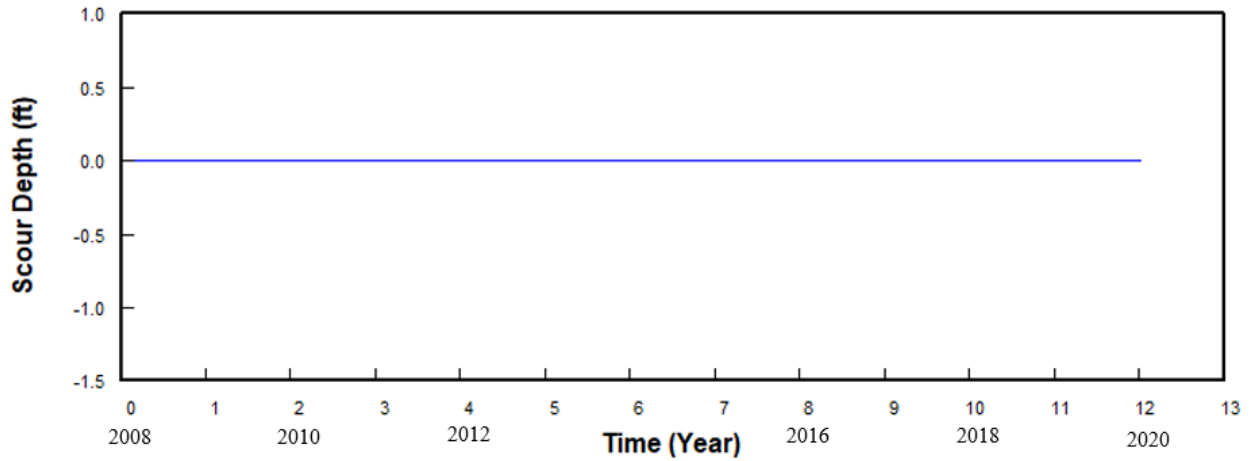


Figure 4.12 Scour depth at Pier #1 of US-2 and US-41 over the Escanaba River

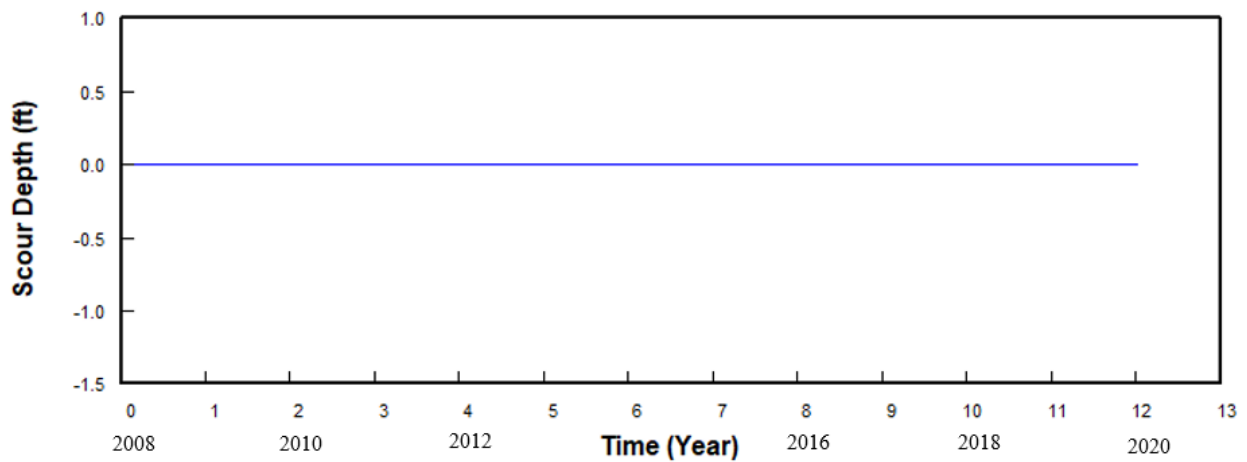


Figure 4.13 Scour depth at Pier #2 of US-2 and US-41 over the Escanaba River

### 4.3.3 Scour Analysis Using EIM

From the geotechnical report, it was found that both the second layers at Pier #1 and Pier #2 of US-2 and US-41 over the Escanaba River are slightly weathered limestone. However, joint information, which is a potential input category for the EIM, was available only at Pier #1. Thus,

similar characteristics were assumed for Pier #2. Erodibility indices were determined using the EIM equations for rock from Section 3.2.2.

The geotechnical report recorded that the upper limestone layer has a UCS of 16,525 psi (114 MPa), an RQD of 79, a varying number of the rough, planer joint set from none to one at different sample points of Pier #1 & Pier #2, and an RMR of 79.

To determine the erodibility index of this layer, the rock was considered as very hard according to the UCS value of 114 MPa and mass strength number,  $M_s$ , was determined from Table 3.1. The number of joint/fissures was assumed to be one from the reported 'none to one' and was used to determine the joint set number,  $J_n$ , from Table 3.2. This value of  $J_n$  along with the RQD value of 79 was used to determine the block size number,  $K_b$  using Eq. 3.5. The geotechnical report has documented the joint condition as rough planer. This information was used to determine joint roughness number,  $J_r$ , from Table 3.3. Since nothing was recorded in the geotechnical report about the gouge in the joints, the joint walls were assumed to be unaltered with surface staining only, and the joint separation was assumed to be 1 mm. These assumptions were used to determine the joint alteration number,  $J_a$ , from Table 3.4. These values of  $J_r$  and  $J_a$  were eventually used to determine the shear strength number,  $K_d$ , using Eq. 3.6. Also, a 90 degree dip angle was assumed in the direction of stream flow with joint spacing of 1:1 because no information about these parameters was available in the geotechnical report. These pieces of information were used to determine the relative ground structure number,  $J_r$ , from Table 3.5. With the above parameters, Eq. 3.4 was used to determine the erodibility index of the rock layer.

Finally, the erodibility index obtained from above was used to determine critical stream power,  $P_c$  of the rock layer using Eq. 3.13 or Eq. 3.14, and was compared with the available stream power at the pier,  $P$ , to determine the scour status at different depths from the river-bed. Table 4.14 and Table 4.15 represent the scour status at different depths of Pier #1 and Pier #2, respectively, for the design discharges of 13,000 cfs and 14,000 cfs. Since layer 1 was skipped for the scour calculation, no reasonable value/result is provided for this layer in the result tables. The dimensionless scour depth in the fifth column ( $y_s/b$ ) is the ratio of the depth and the pier width. The relative stream power ( $P/P_a$ ) in the sixth column was obtained using Eq. 3.16. The

approaching flow stream power,  $P_a$ , was obtained using Eq. 3.15 and the available stream power,  $P$ , at the pier was obtained by multiplying relative stream power and the approaching flow stream power. As we know, scour takes place when the available stream power at the pier is more than the critical stream power. Accordingly, the column for the ‘Available stream power at the pier,  $P$ ’ was compared with the column for the ‘Critical stream power,  $P_c$ ’ to obtain the scour status at different depths. It can be seen from the following result tables that no scour occurred at the second layer of both the piers. That confirmed that the scour depth did not extend beyond 3 ft for Pier #1 and 4.5 ft for Pier #2. Layer #2 was found to be hard enough to resist any scour. Therefore, no calculation was done for the succeeding layers.

Table 4.14 Scour determination at Pier #1 of US-2 and US-41 over the Escanaba River using EIM

Depth (ft)	Layer	Erodibility Index	$P_c$ (lb/ft-s)	Dimensionless scour depth ( $y_s/b$ )*	Relative Stream Power ( $P/P_a$ )	For 13,000 cfs			For 14,000 cfs		
						Approaching Flow Stream Power, $P_a$ (lb/ft-s)	Available Stream Power, $P$ (lb/ft-s)	Scour (Yes/No)	Approaching Flow Stream Power, $P_a$ (lb/ft-s)	Available Stream Power, $P$ (lb/ft-s)	Scour (Yes/No)
1	1	-	-	0.25	7.03		12.21	-		13.22	-
3	1	-	-	0.76	4.89	1.74	8.51	-	1.88	9.21	-
4	2(a)	16720.2	100,795	1.02	4.08		7.10	No		7.68	No

\*  $b$  is pier width perpendicular to the flow direction

Table 4.15 Scour determination at Pier #2 of US-2 and US-41 over the Escanaba River using EIM

Depth (ft)	Layer	Erodibility Index	$P_c$ (lb/ft-s)	Dimensionless scour depth ( $y_s/b$ )*	Relative Stream Power ( $P/P_a$ )	For 13,000 cfs			For 14,000 cfs		
						Approaching Flow Stream Power, $P_a$ (lb/ft-s)	Available Stream Power, $P$ (lb/ft-s)	Scour (Yes/No)	Approaching Flow Stream Power, $P_a$ (lb/ft-s)	Available Stream Power, $P$ (lb/ft-s)	Scour (Yes/No)
1	1	-	-	0.25	7.03		12.21	-		13.22	-
4.5	1	-	-	1.14	3.73	1.74	6.49	-	1.88	7.02	-
5	2(a)	16720.2	100,795	1.27	3.41		5.92	No		6.41	No

\*  $b$  is pier width perpendicular to the flow direction.

#### 4.3.4 Scour Analysis Using GSN

Since the modified slake durability testing was not available in the geotechnical report of US-2 and US-41 over the Escanaba River, the GSN value of the bedrock at this site has been obtained from the literature. Though the Escanaba River in Michigan has Trenton Limestone according to the geotechnical report, a GSN value of  $1.70 \times 10^{-4} \text{ ft} \left[ \frac{\text{ft} \cdot \text{lb}}{\text{sft}^2} \right]^{-1}$  was selected for this site, which was the only available data in the literature for limestone. This value was obtained for Oligocene Marianna Limestone at Chipola River, Florida by Keaton et al. (2012).

Daily discharge at this site was obtained from the USGS gaging station since 2008 and daily stream power was obtained from daily discharge using Eq. 3.21. The constants of Eq. 3.21 were pre-determined following the procedure mentioned in Section 3.2.3. Then the daily stream power was multiplied with the above-mentioned GSN value following Eq. 3.20 to get daily scour depth. Scour depth at the end of the analysis period is the accumulated scour depth over the same time. While using Eq. 3.20, daily stream power was used in place of cumulative stream power. This has been done to represent the cumulative scour depth over time which is more significant for this study.

Figure 4.14 represents the cumulative scour depth of the limestone bedrock of the Escanaba River at US-2 and US-41 since its installation, i.e., 2008 using the previously mentioned GSN value. Since both of the two piers were founded on the same bedrock, this condition led to identical predictions for both the sites as shown in Figure 4.14. It is clear that, if the assumed GSN value was true for this site, a scour depth of 0.036 ft would prevail in the bedrock since 2008.

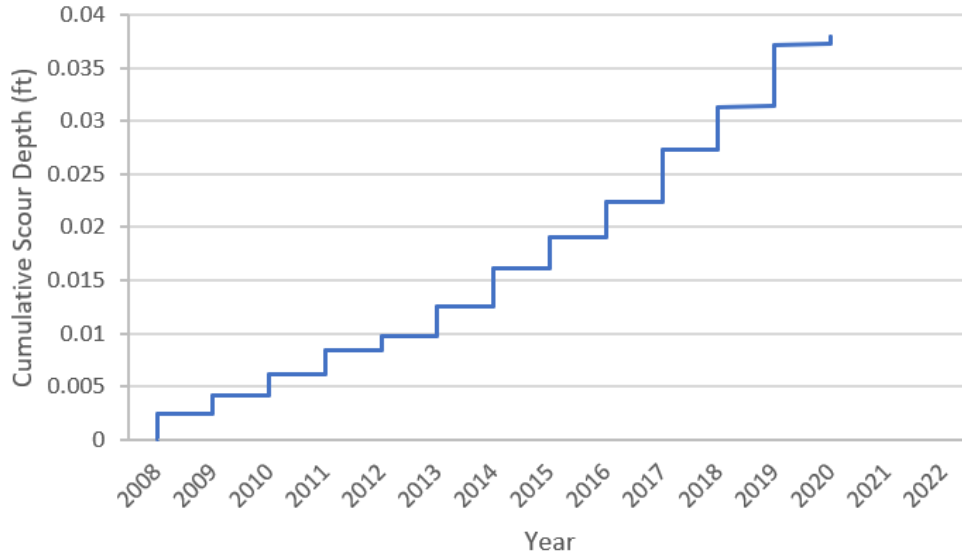


Figure 4.14 Cumulative scour depth of Limestone bedrock of Escanaba River at US-2 and US-41

#### 4.3.5 Comparison of Results

This site can be viewed as a pure rock site where the top-soil layers are embankment fill and, therefore, was not included in any of the scour analysis methods. The scour analysis results for US-2 and US-41 over the Escanaba River obtained from all the selected methods are summarized in Table 4.16. It is clear that the HEC-18 sand equation predicted very high scour depth for all the cases. A comparison of the results of EIM and GSN clearly shows that the bedrock at this site is susceptible to abrasion but shows no quarrying and plucking. This is because EIM was developed for determining the scour depth for a design discharge due to quarrying and plucking and the result shows ‘none’. As a result, the scour process should happen progressively here. This means scour does not develop within a big storm, but instead, takes place very slowly over a long period of time. By contrast, the cumulative scour depth calculated with the SRICOS-EFA indicates no scour in the bedrock in 12 years.

Table 4.16 Comparison of scour analysis results at the bedrock of US-2 and US-41 over the Escanaba River

Method	Scour Depth for 13,000 cfs	Scour Depth for 14,000 cfs	Scour Depth from 2008 – 2020*	Comment
Pier #1				
SRICOS-EFA	-	-	None	Joint spacing of the bedrock has been used to assume the erosion category curves
EIM	None	None	-	EIM for rock
GSN	-	-	0.036 ft	Value of GSN has been used from the literature.
HEC-18 Sand	6.5 ft	6.6 ft	-	-
Pier #2				
SRICOS-EFA	-	-	None	Joint spacing of the bedrock has been used to assume the erosion category curves
EIM	None	None	-	EIM for rock
GSN			0.036 ft	Value of GSN has been used from the literature.
HEC-18 Sand	6.5 ft	6.6 ft	-	-

\*This duration was taken since the bridge was installed in 2008.

#### 4.4 M-20 over the Tittabawassee River

##### 4.4.1 General Information

M-20 over the Tittabawassee River is situated within the City of Midland, Midland County, Michigan (Figure 4.15). The river flows to the southeast at this location. The nearest USGS gaging station, i.e., no. 04156000, is located in the same county and is situated downstream of the river. According to the geotechnical report, the bridge site has granular fill soils with a depth ranging from 3 ft to 32 ft and consists of sand, silty sand, clayey sand, and sometimes organic matter. In general, the native silty clay underlies the fill soil with occasional granular soil layers throughout the clay profile. The native silty clay is soft to very stiff in ‘consistency’ above an approximate elevation of 590 ft to 594 ft with natural moisture contents ranging from 13% to 29%, dry densities ranging from 89 to 141 pounds per cubic foot (pcf), and unconfined compressive strengths ranging

from 500 to 5,320 pounds per square foot (psf). Below these elevations, the silty clay is hard to very hard in consistency with natural moisture contents ranging from 7% to 14%, dry densities ranging from 118 pcf to 143 pcf, and unconfined compressive strengths ranging from 8,350 psf to 18,760 psf. The occasional granular soil layers generally consist of very compact silty sand or clayey sand with SPT N values over 50 blows per foot. Also, a layer of organic silt is present within some soil borings between the approximate depths of 3 ft and 8 ft. The organic silt is soft to medium in consistency with natural moisture contents ranging from 18% to 29% and has a UCS of 1,500 psf. A layer of organic peat is present within one soil boring between the approximate depths of 7 ft and 9 ft. The organic peat is very loose with a natural moisture content of 73% and organic matter content of 15%.

As per the geotechnical report, the old bridge was replaced after 2017 with an approximately 726-ft-long, four-span structure which has a steel girder superstructure, concrete deck, and cast-in-place concrete piers and abutments. All the piers and abutments are supported by concrete drilled shafts. The elevation of the bottom of the drilled shaft varies from 530.5 ft to 560.5 ft. The diameters of the piers vary from 72 inches to 78 inches and that of abutments is 42 inches (Table 4.17).

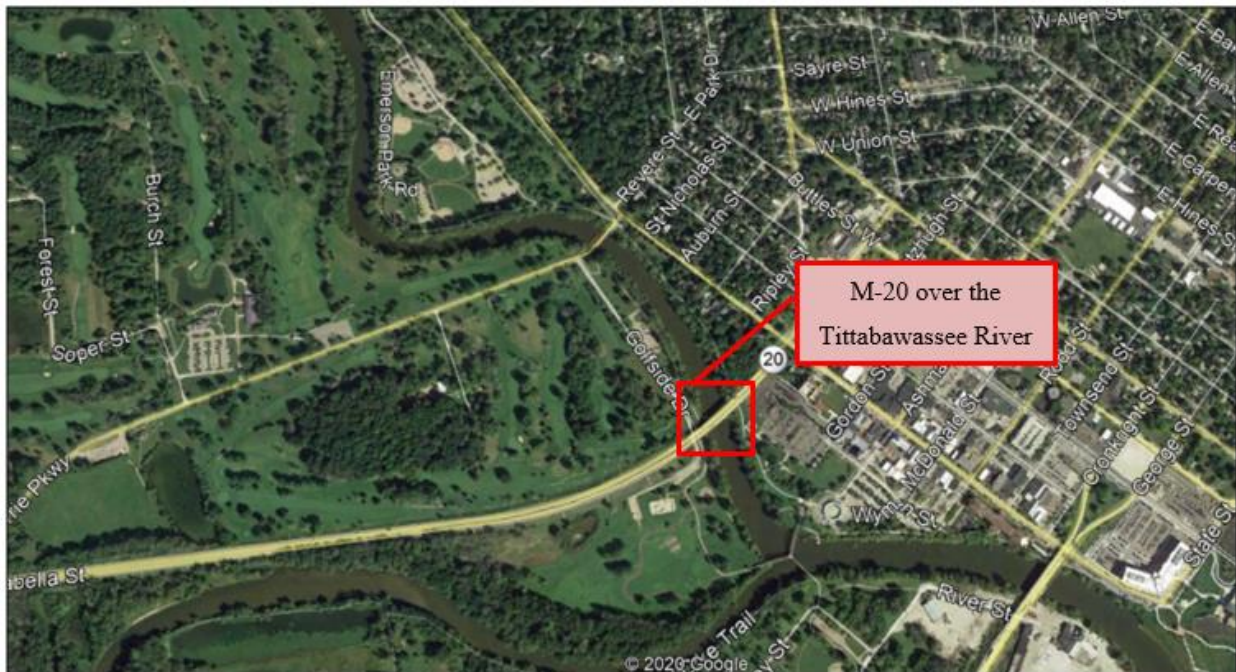


Figure 4.15 Location of M-20 over the Tittabawassee River (The image has been retrieved from Google Earth, 2018 (Google))

Table 4.17 Summary of drilled shaft foundation of M-20 over the Tittabawassee River

Description	Abutment A	Pier #1	Pier #2	Pier #3	Abutment B
Bottom of Drilled Shaft Elevation (ft)	544	530.5	539	545.5	560.5
Drilled Shaft Diameter (in)	42	78	78	72	42

The geotechnical report has recorded that, there are eight earth strata/layers at Pier #1 of M-20, while there are six layers at Pier #2 and 11 layers at Pier #3. Although there is fill soil all over the site, no scour analysis has been conducted in this study for the fill soil layer. Table 4.18 represents the detailed attributes of each layer (except the fill soil) including layer thickness and classification. Since the piers were founded on the clay layer, scour analysis at this site has been done using the SRICOS-EFA and EIM. The SRICOS-EFA has been applied to determine the cumulative scour depth at the bridge site since its installation, i.e., 2017, whereas the EIM was used to determine the scour depths for different design discharges.

Table 4.18 Attributes of the earth layers at M-20 over the Tittabawassee River

Layer	Pier #1		Pier #2		Pier #3	
	Thick-ness (ft)	Classification	Thick-ness (ft)	Classification	Thick-ness (ft)	Classification
1	4.0	Very Loose Gray Silty Sand with occasional clay seam (SM)	9.5	Medium to Stiff Gray Sandy Clay with trace gravel & occasional sand seams (CL)	3.0	Loose Brown Silty Sand with trace clay (SM)
2	5.5	Loose Brown Sand with trace silt & gravel (SP)	27.5	Very Compact Gray Clayey Sand with trace gravel & occasional cobbles (SC)	5.0	Very Loose Gray Silty Sand with trace gravel (SM)
3	2.5	Brown Gravel with occasional cobbles (GP)	5.0	Very Compact Gray Clayey Sand with trace gravel & occasional sand seams (SC)	5.0	Hard Gray Silty Clay with little sand & trace gravel (CL-ML)
4	51.0	Very Compact Gray Clayey Sand with trace gravel & occasional cobbles (SC)	25.0	Very Compact Gray Clayey Sand with trace gravel & occasional cobbles (SC)	32.3	Hard to very Hard Gray Silty Clay with little sand & trace gravel (CL-ML)
5	2.0	Very Compact Gray Sandy Gravel (GP)	5.0	Very Compact Gray Clayey Sand with trace gravel & occasional sand seams (SC)	2.7	Very Compact Gray Silty Sand with trace clay (SM)
6	10.5	Very Compact Gray Clayey Sand with trace gravel & occasional cobbles (SC)	12.0	Very Compact Gray Clayey Sand with trace gravel & occasional cobbles (SC)	5.0	Hard Gray Silty Clay with little sand & trace gravel (CL-ML)
7	16.5	Very Compact Gray Sand with trace silt & gravel & occasional clay seams (SP)	-	-	11.0	Very Compact Gray Silty Sand with trace clay (SM)

8	2.0	Very Compact Gray Clayey Sand with trace gravel (SC)	-	-	14.0	Hard Gray Silty Clay with little sand & trace gravel (CL-ML)
9	-	-	-	-	5.0	Very Compact Gray Silty Sand with some clay & trace gravel (SM)
10	-	-	-	-	5.0	Very Compact Gray Silty Sand (SM)
11	-	-	-	-	4.0	Hard Gray Silty Clay with little sand & trace gravel (CL-ML)

#### 4.4.2 Scour Analysis Using SRICOS-EFA

The strategies followed for this site to determine all the needed input parameters are described below followed by the SRICOS-EFA simulation results:

Soil/Material Properties Input: Lab testing data for the earth layer erodibility was available only at one place. Thus, the erosion category plot of Briaud (2008) (Figure 3.1) was compared with other available soil properties from the geotechnical report to select the erosion curves for most of the soil layers (Figure 4.16, Figure 4.17, Figure 4.18). The straight lines marked with “L #” in the figures show the assumed curves for the corresponding layer.

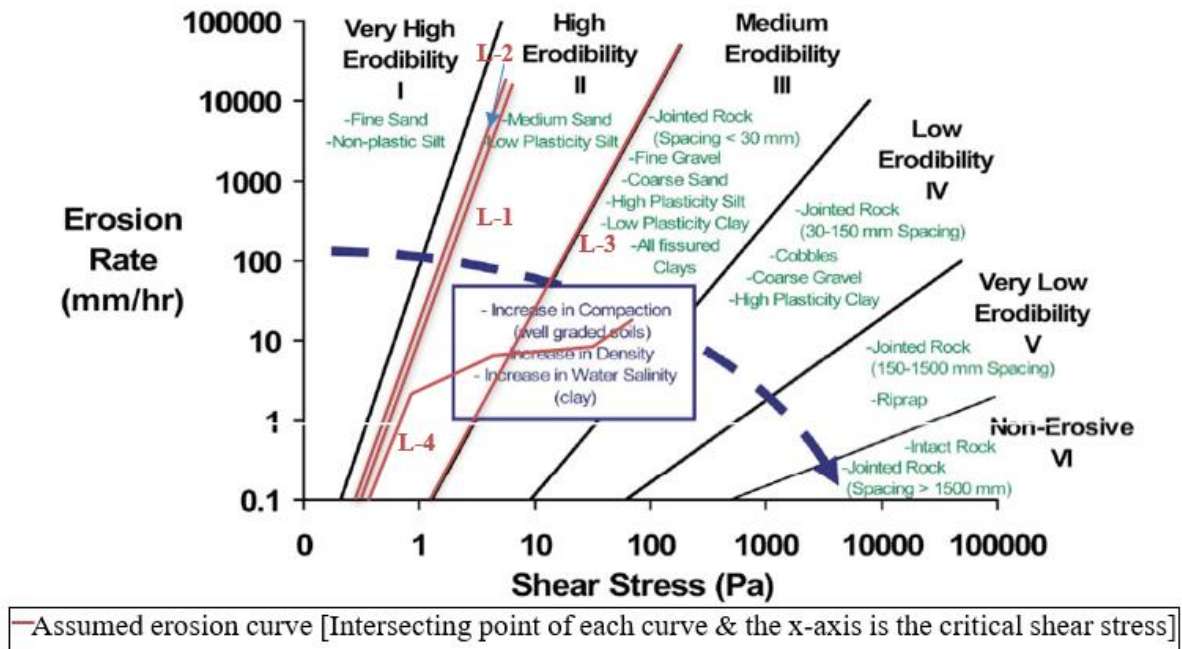
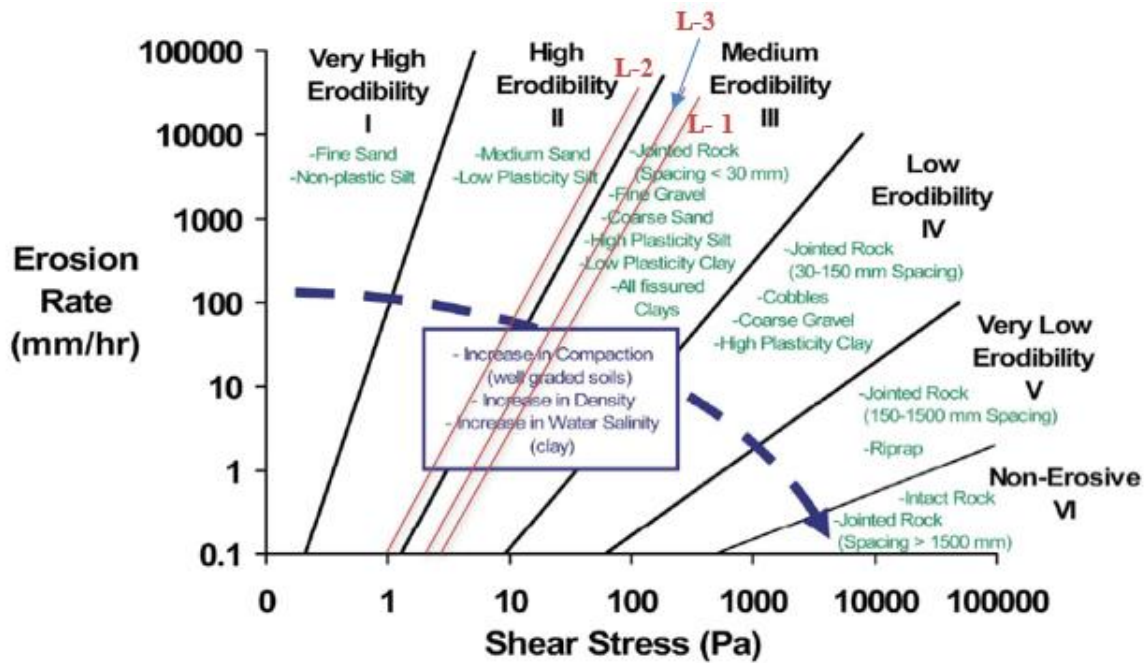


Figure 4.16 Assumed/interpreted erosion curves on Briaud’s erosion category plot (Briaud 2008; Briaud et al. 2019) for the earth layers at Pier #1 of M-20 over the Tittabawassee River



— Assumed erosion curve [Intersecting point of each curve & the x-axis is the critical shear stress]

Figure 4.17 Assumed/interpreted erosion curves on Briaud's erosion category plot (Briaud 2008; Briaud et al. 2019) for the earth layers at Pier #2 of M-20 over the Tittabawassee River

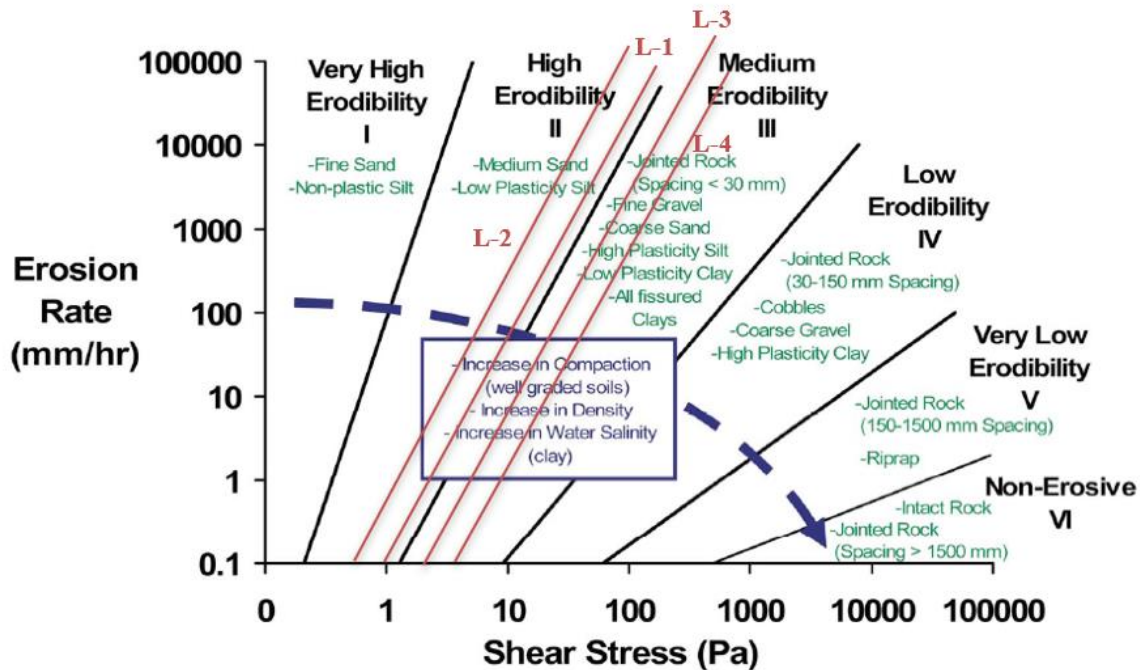


Figure 4.18 Assumed/interpreted erosion curves on Briaud’s erosion category plot (Briaud 2008; Briaud et al. 2019) for the earth layers at Pier #3 of M-20 over the Tittabawassee River

Available soil properties in the geotechnical report of this site include USCS soil classification,  $D_{50}$  of some layers, and an EFA erodibility curve of one layer. When  $D_{50}$  and erodibility curves were available, they were used to characterize the erosion properties of those layers and USCS soil classification was used for the rest of the cases. According to the geotechnical report, the  $D_{50}$  of the 1<sup>st</sup> layer at Pier #1 is less than 0.3 mm, however, the 2<sup>nd</sup> layer has a  $D_{50}$  greater than 0.3 mm (Table 4.19). So, the critical shear stress of the 2<sup>nd</sup> layer was determined to be the same as  $D_{50}$  noted in Briaud et al. (2019). When the critical shear stress was determined, the erosion curve was assumed to be parallel to the nearest erosion curve available in Briaud’s (Briaud 2008) erosion category plot represented in Figure 3.1 (Figure 4.17). On the other hand, the critical shear stress equation proposed by Briaud et al. (2019) for any earth layer having a  $D_{50}$  less than 0.3 mm requires more information, along with the  $D_{50}$  value, which was not recorded in the geotechnical report. So, the erosion curve of the 1<sup>st</sup> layer at Pier #1 was assumed as per the USCS soil classification.

The erosion curve for the 3<sup>rd</sup> layer at Pier #1 was also assumed according to its classification recorded in the geotechnical report. The USCS classification was compared with the information available in Briaud’s erosion category plot (Figure 3.1), and the erosion curve was chosen within the given range. An EFA test result was available for the 4<sup>th</sup> layer of Pier #1 which was directly used as the erosion curve of this layer. To select the erosion curves for all the earth layers at Pier #2 and Pier #3, the USCS soil classifications were used (Figure 4.17, Figure 4.18).

Once all the erosion curves were determined, the critical shear stress of each layer was obtained as the intersection point of each of the curves with the horizontal axis. Table 4.19, Table 4.20, and Table 4.21 contain all the information used for determining the erosion curves and the obtained critical shear stresses of the earth layers at Piers #1, #2, and #3 respectively.

Table 4.19 Attributes of earth layers at Pier #1 of M-20 over the Tittabawassee River

Layer	D <sub>50</sub> (mm) (from the geotechnical report)	Critical Shear Stress in lb/ft <sup>2</sup> (Pa) (From Figure 4.16)	Comment
1	0.202	0.01(0.5)	Critical shear stress equation proposed by Briaud et al. (2019) for any earth layer having D <sub>50</sub> < 0.3 mm requires more information along with D <sub>50</sub> , which was not available in the geotechnical report. So, the erosion curve of this layer was assumed from the USCS classification which is SM for this layer.
2	0.405	0.008(0.4)	$\tau_c = D_{50}$ (for D <sub>50</sub> > 0.3 mm) (Briaud et al. 2019)
3	-	0.0002(0.009)	Given data for this soil layer was not enough. So, it was assumed to have very high erodibility.
4	-	0.013(0.645)	EFA test result was available for this layer which was directly used as the erosion curve except the two smallest data points were extrapolated to determine the critical shear stress as per Briaud et al. (2019).

5 - 8	-			Since the SRICOS-EFA run showed cumulative scour depth within the previous layer, these layers were not included.
-------	---	--	--	---

Table 4.20 Attributes of earth layers at Pier #2 of M-20 over the Tittabawassee River

Layer	USCS Soil Classification	Erodibility*	Critical Shear Stress in lb/ft <sup>2</sup> (Pa) (From Figure 4.17)	Comment
1	CL	Medium	0.08(4.0)	Critical shear stress was assumed as per the erodibility so was the erosion category curve (Figure 4.17).
2	SC	High to Medium	0.019(0.9)	
3	SC	High to Medium	0.06(3.0)	
4 - 6	SC	High to Medium	-	SRICOS-EFA run showed cumulative scour depth did not cross 3 ft (Figure 4.20), thus these layers were not included.

\*As per Briaud et al. (2019) (Figure 3.1)

Table 4.21 Attributes of earth layers at Pier #3 of M-20 over the Tittabawassee River

Layer	USCS Soil Classification	Erodibility*	Critical Shear Stress in lb/ft <sup>2</sup> (Pa) (From Figure 4.18)	Comment
1	SM	High	0.02(1.0)	Critical shear stress was assumed as per the erodibility so was the erosion category curve (Figure 4.18).
2	SM	High	0.018(0.85)	
3	CL-ML	High to Medium	0.08(4.0)	
4	CL-ML	High to Medium	0.16(7.5)	
5	SM	-	-	SRICOS-EFA run showed cumulative scour depth did not cross 3 ft (Figure 4.21), thus these layers were not included.
6	CL-ML	-	-	
7	SM			
8	CL-ML			
9	SM			

10	SM
11	CL-ML

\*As per Briaud et al. (2019) (Figure 3.1)

Finally, thickness information from Table 4.18, critical shear stress from Table 4.19, Table 4.20 and Table 4.21, and several data points for each curve from Figure 4.16, Figure 4.17, and Figure 4.18 were entered in the SRICOS-EFA software as the material input parameter values.

Hydraulic Parameter Input: Hydraulic parameters include Manning’s coefficient, water depths, and velocities for different discharges. All these parameters were extracted from the HEC-RAS model. Manning’s coefficient of this bridge site was 0.03 which was the lowest among all the analyzed sites for this study. The daily discharge of this river was also obtained from the gaging station. The geotechnical report indicates that the bridge was replaced after 2017, hence the daily discharge was obtained since 2017.

Geometry Input: According to the geotechnical report, all the piers at M-20 over the Tittabawassee River are circular. Pier #1 and Pier #2 have the same diameter which is 6.5 ft (78 inches), except Pier #3, which has a diameter of 6 ft (72 inches). Along with the pier information, the SRICOS-EFA software also needs upstream channel width as a geometry input, which was extracted from the HEC-RAS model, having a value of 238.38 ft.

With all the input parameters entered in the SRICOS-EFA software, a simulation was run to get cumulative scour depth at the piers of M-20 over the Tittabawassee River. Figure 4.19, Figure 4.20, and Figure 4.21 show the predicted cumulative scour depths at Pier #1, Pier #2, and Pier #3, respectively, in the SRICOS-EFA analysis since 2017. It is observed that the scour depths at Pier #1 and Pier #3 of this bridge would exceed 9 ft since 2017 if all the assumptions were true. By contrast, the scour depth at Pier #2 would reach only about 2 ft.

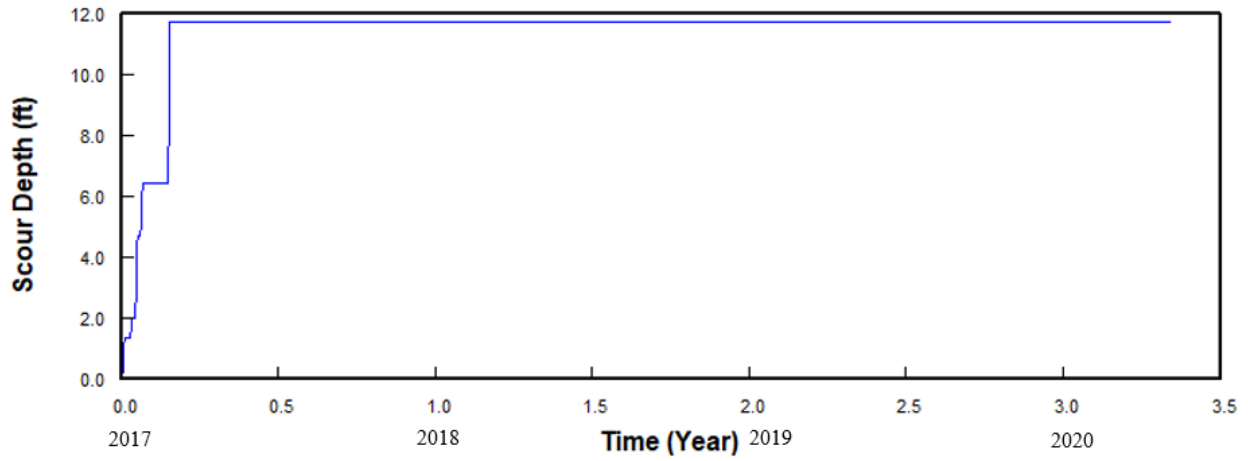


Figure 4.19 Scour depth of Pier #1 of M-20 over the Tittabawassee River

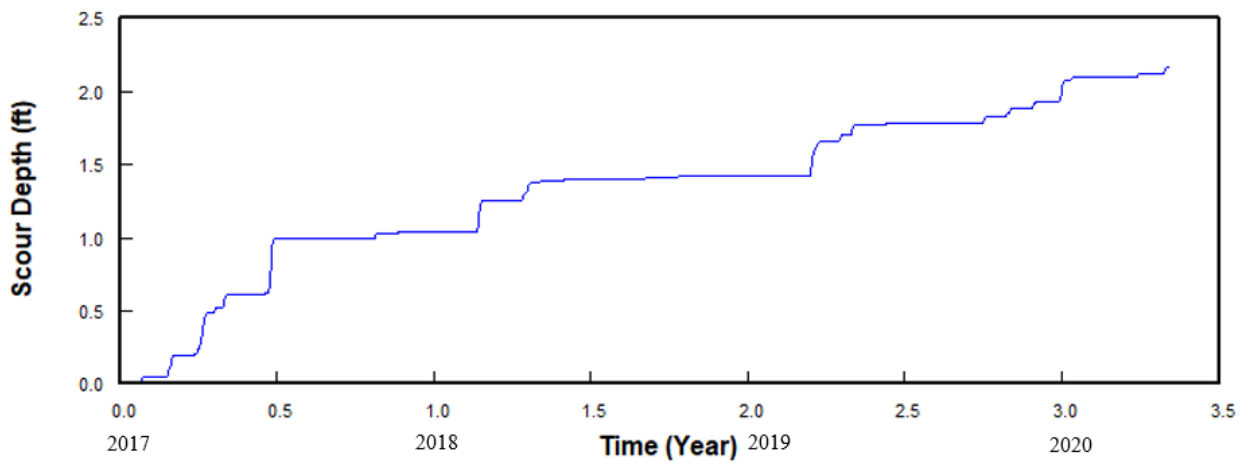


Figure 4.20 Scour depth of Pier #2 of M-20 over the Tittabawassee River

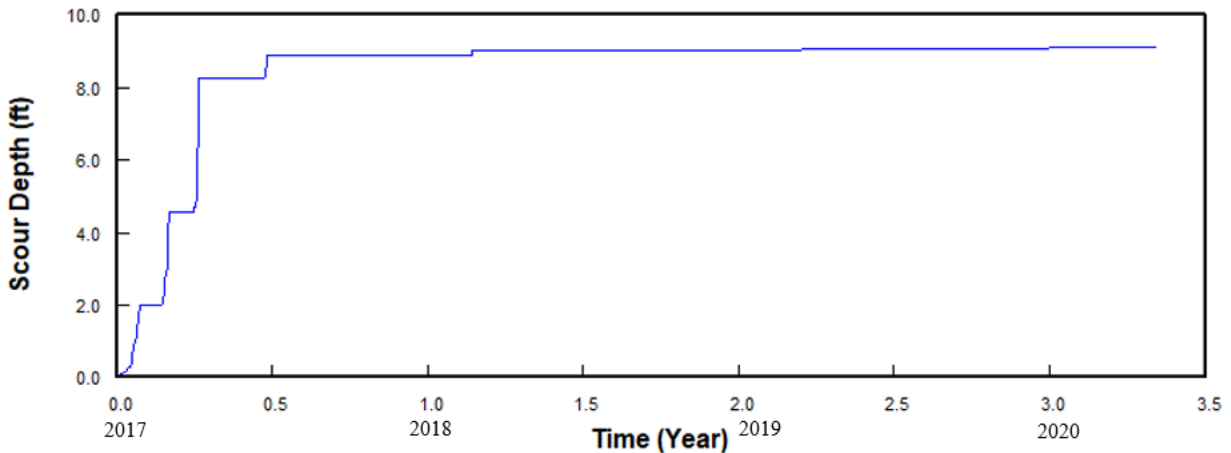


Figure 4.21 Scour depth at Pier #3 of M-20 over the Tittabawassee River

#### 4.4.3 Scour Analysis Using EIM

Soil layers at all the Piers of M-20 over the Tittabawassee River are either sand or clay layers. For the sand layers, the EIM for cohesionless soil is applied, and the EIM for cohesive soil was applied for the clay layers.

The first three layers at Pier #1 are sand layers followed by very compact gray clayey sand. From the geotechnical report, it was found that  $D_{50}$  values of the first two sand layers are 0.202 mm and 0.405 mm, and the SPT N has a value of 6 and 10, respectively. Inadequate information was available for the third sand layer to conduct the EIM calculation. Thus, this layer was assumed to be similar to the previous one. The fourth layer, which is a clayey sand layer, has a higher SPT N value about 60. No further information was needed since the scour ceased in the clay layer.

The first layer at Pier #2 is a clay layer, followed by a very compact gray clayey sand layer. The SPT N values are 5 to 9 and more than 50 for the two layers, respectively. Scour was contained within the second layer.

Not enough data was available for carrying out the scour depth calculation for the first two layers of Pier #3. Therefore, the scour depth was calculated for the 3<sup>rd</sup> layer which is a clay layer with an

SPT N of 26. It was found that scour will not proceed through this layer for the design discharges, therefore information of the succeeding layers is not included here.

For the sand layers, SPT N values were used to determine the mass strength number,  $M_s$  from Table 3.6,  $D_{50}$  was used to determine particle size number,  $K_b$  following Eq. 3.7, residual friction angle was assumed to be 30 deg as per Annandale and Smith (2001) and was used to determine the shear strength number,  $K_d$  following Eq. 3.8.

For the clay layers, the mass strength parameter,  $M_s$ , was determined from the vane shear strength based on Table 3.7. Because the vane shear strength of the clay layers was not recorded in the geotechnical report, this parameter was calculated from SPT  $N$  using Eq. 4.1. Shear strength number,  $K_d$ , was determined using Eq. 3.11, where the value of the residual angle was assumed to be 8.1 for very soft to soft clay material and 30 degrees for other materials.

With the above parameters, Eq. 3.4 was used to determine the erodibility indices of the earth layers at the piers. Consequently, the erodibility indices were used to determine the critical stream power,  $P_c$ , of each layer using Eq. 3.13 or Eq. 3.14. Then the critical stream power,  $P_c$ , was compared with the available stream power,  $P$ , to determine the scour status at different depths from the river bed around the piers. Table 4.22 through Table 4.24 show the scour status at different depths of Pier #1 through Pier #3, respectively, for design discharges of 26,400 cfs and 30,300 cfs. Here, dimensionless scour depths,  $(y_s/b)$  was obtained from the ratio of the depth and the pier width; the relative stream power,  $(P/P_a)$  was obtained using Eq. 3.16; the approaching flow stream power,  $P_a$ , was determined using Eq. 3.15; and the available stream power at the pier,  $P$ , was obtained by multiplying relative stream power and approaching flow stream power. Because scour takes place when  $P$  is greater than  $P_c$ , further calculation was not conducted when a value of  $P$  was found to be less than  $P_c$ .

It is seen from the result tables that Pier #1 has a scour depth of 12 ft and Pier #2 has a scour depth of 9.5 ft. On the other hand, since calculations could not be performed for the 1<sup>st</sup> and 2<sup>nd</sup> layers of Pier #3 due to lack of enough information, calculation was only carried out for the 3<sup>rd</sup> layer, which was a clay layer, showing that the clay layer is scour resistant for these design discharges. When a

scour resistant layer was obtained from the calculation, no further calculation would be conducted for the succeeding layers.

Table 4.22 Scour determination at Pier #1 of M-20 over the Tittabawassee River using EIM

Depth (ft)	Layer	Erodibility Index	$P_c$ (lb/ft-s)	Dimensionless scour depth ( $y_s/b$ )	Relative Stream Power ( $P/P_a$ )	For 26,400 cfs			For 30,300 cfs		
						Approaching Flow Stream Power, $P_a$ (lb/ft-s)	Available Stream Power, $P$ (lb/ft-s)	Scour (Yes/No)	Approaching Flow Stream Power, $P_a$ (lb/ft-s)	Available Stream Power, $P$ (lb/ft-s)	Scour (Yes/No)
1	1	$1.9 \times 10^{-10}$	0.002	0.15	7.55	1.410	10.65	Yes	1.408	10.63	Yes
2				0.30	6.78		9.56	Yes		9.54	Yes
3				0.46	6.08		8.57	Yes		8.56	Yes
4				0.61	5.46		7.69	Yes		7.68	Yes
5				0.76	4.89		6.90	Yes		6.89	Yes
6				0.91	4.39		6.19	Yes		6.18	Yes
7	2	$1.53 \times 10^{-9}$	0.004	1.07	3.94	1.410	5.56	Yes	1.408	5.55	Yes
8				1.22	3.53		4.98	Yes		4.98	Yes
9				1.37	3.17		4.47	Yes		4.46	Yes
10				1.52	2.84		4.01	Yes		4.00	Yes
11	3	$1.53 \times 10^{-9}$	0.004	1.68	2.55	1.410	3.60	Yes	1.408	3.59	Yes
12				1.83	2.29		3.23	Yes		3.22	Yes
12.1	4	0.237	23.264	1.84	2.27		3.19	No		3.19	No

\*b is the pier width perpendicular to the flow direction.

Table 4.23 Scour determination at Pier #2 of M-20 over the Tittabawassee River using EIM

Layer	For 26,400 cfs	For 30,300 cfs
-------	----------------	----------------

Depth (ft)	Erodibility Index	$P_c$ (lb/ft-s)	Dimensionless scour depth ( $y_s/b$ )	Relative Stream Power ( $P/P_a$ )	Approach			Approach		
					ing Flow Stream Power, $P_a$ (lb/ft-s)	Available Stream Power, $P$ (lb/ft-s)	Scour (Yes/No)	ing Flow Stream Power, $P_a$ (lb/ft-s)	Available Stream Power, $P$ (lb/ft-s)	Scour (Yes/No)
1			0.15	7.55		10.65	Yes		10.63	Yes
2			0.30	6.78		9.56	Yes		9.54	Yes
3			0.46	6.08		8.57	Yes		8.56	Yes
4			0.61	5.46		7.69	Yes		7.68	Yes
5	1	0.003	2.50	0.76	4.89	1.410	Yes	1.408	6.89	Yes
6				0.91	4.39		Yes		6.18	Yes
7				1.07	3.94		Yes		5.55	Yes
8				1.22	3.53		Yes		4.98	Yes
9				1.37	3.17		Yes		4.46	Yes
9.5				1.45	3.00		Yes		4.23	Yes
9.6	2	0.237	23.26	1.46	2.97	1.410	No	1.408	4.18	No

\*b is the pier width perpendicular to the flow direction.

Table 4.24 Scour determination at Pier #3 of M-20 over the Tittabawassee River using EIM

Depth (ft)	Layer	Erodibility Index	$P_c$ (lb/ft-s)	Dimensionless scour depth ( $y_s/b$ )	Relative Stream Power ( $P/P_a$ )	For 26,400 cfs			For 30,300 cfs		
						Approach ing Flow Stream Power, $P_a$ (lb/ft-s)	Available Stream Power, $P$ (lb/ft-s)	Scour (Yes/No)	Approach ing Flow Stream Power, $P_a$ (lb/ft-s)	Available Stream Power, $P$ (lb/ft-s)	Scour (Yes/No)

						$P_a$ (lb/ft-s)					
1	1	-	-	0.17	7.46		10.52	-		10.51	-
3	1	-	-	0.51	5.86		8.27	-		8.26	-
4	2	-	-	0.68	5.20	1.410	7.33	-	1.408	7.32	-
8	2	-	-	1.35	3.21		4.53	-		4.52	-
8.1	3	0.110	13.07	1.37	3.17		4.47	No		4.46	No

\*b is the pier width perpendicular to the flow direction.

#### **4.4.4 Comparison of Results**

Among all the piers of M-20 over the Tittabawassee River, only Pier #2 can be considered as a pure clay site, other piers have non-cohesive layers above the clay layer (Table 4.18). A comparison of the scour analysis results of Pier #2 shows that the SRICOS-EFA could determine reasonable scour depth compared to other methods (Table 4.25). The scour depth calculated using the EIM is similar to that with the HEC-18 sand equation. If we accept that the HEC-18 sand equation tends to overestimate scour depths in cohesive soils, then we may conclude that the EIM might not be suitable for cohesive beds, either. By contrast, the SRICOS-EFA gives much different results for the three piers. The predictions for Pier #1 and Pier #3 are even higher than those obtained by the HEC-18 sand equation even for only 3 years. The predicted scour depth for Pier #2 is much lower for the three years. Therefore, the above comparisons do not lead to very clear conclusions. However, such comparisons emphasize the importance of soil erosion properties obtained from lab tests in the applications of these methods. Without accurate measurements, the methods may lead to much different predictions with different assumed erosion characteristics.

Table 4.25 Comparison of scour analysis results at M-20 over the Tittabawassee River

Method	Scour Depth for 26,400 cfs	Scour Depth for 30,300 cfs	Scour Depth from 2017 to 2020*	Comment
Pier #1				
SRICOS-EFA	-	-	11.7 ft	Erosion category curve/required data were available for some of the layers. Others were assumed.
EIM	12 ft	12 ft	-	EIM for cohesionless soil + EIM for cohesive soil
HEC-18 Sand	10.9 ft	11 ft	-	-
Pier #2				
SRICOS-EFA			2.1 ft	USCS soil classification was available based on which erodibility was determined as per Briaud et al. (2019). Erosion category curves were assumed as per the erodibility of the soil layers.
EIM	9.5 ft	9.5 ft		EIM for cohesive soil
HEC-18 Sand	10.9 ft	11 ft	-	-
Pier #3				
SRICOS-EFA			9.1 ft	USCS soil classification was available based on which erodibility was determined as per Briaud et al. (2019). Erosion category curves were assumed as per the erodibility of the soil layers.
EIM	None at the clay layer	None at the clay layer		Due to lack of data, scour calculation was not possible to conduct before 8.1 ft of depth and the soil layer at 8.1 ft will have no erosion for the design scenario. (EIM for cohesive soil at 8.1ft)

HEC-18 Sand	10.3 ft	10.4 ft		-
----------------	---------	---------	--	---

\*This duration was taken since the bridge was installed in 2017.

## 4.5 M-64 over the Ontonagon River

### 4.5.1 General Information

M-64 over the Ontonagon River is in the village of Ontonagon, Ontonagon County, Michigan (Figure 4.22), where the river flows north-eastward. The nearest USGS gaging station is No. 04040000 located at Rockland, MI. The geotechnical report documented that the site is underlain primarily by fine to medium sand, sandy silty clay, and hard clay.

The old bridge was replaced in 2006 with a thirteen-span, nearly 1,700 ft long one. Currently, the bridge is supported by 12 piers and 2 abutments at both ends. Abutment A and Piers #1 through #6 are situated at the left bank, Piers #7 through #10 are situated within the channel, and Piers #11, #12, and Abutment B are at the right bank.



Figure 4.22 Location of M-64 over the Ontonagon River (The image has been retrieved from Google Earth, 2018 (Google))

All the piers of M-64 over the Ontonagon River have the same diameter of 3.5 ft. Since Piers #7 through #10 are situated in the riverbed, scour analysis has been conducted for these piers only. Piers #7 and #8 have six soil layers while Piers #9 and #10 have five soil layers at their location. All the piers have fine to medium/coarse sand as the first layer, then there is a soft to hard clay layer. Below the clay layer, there is again a silt/sand layer (Table 4.26). Since the piers are founded on a clay layer, scour analysis at this site was conducted using SRICOS-EFA and EIM. The SRICOS-EFA was applied to determine the cumulative scour depth at the bridge site starting from its installation in 2006; the EIM was used to determine scour depths corresponding to different design discharges.

Table 4.26 Attributes of the earth layers at M-64 over the Ontonagon River

Layer	Pier #7		Pier #8		Pier #9		Pier #10	
	Thick- ness (ft)	Classification	Thick- ness (ft)	Classification	Thick- ness (ft)	Classification	Thick- ness (ft)	Classification
1	15.0	Very Loose, Brown Fine & Medium Sand. Trace of Fine Gravel.	13.5	Very Loose Fine & Medium Sand	15.5	Loose Brown Fine to Coarse Sand. Trace of Fine Gravel	13.0	Very Loose Brown Fine and Medium Sand. Trace of Rotted Wood
2	10.0	Soft Red Sandy Silty Clay	7.0	Soft Red Silty Sandy Clay	2.0	Plastic Red Sandy Silty Clay	5.0	Plastic Red Very Sandy Silty Clay
3	11.0	Hard Red Very Sandy Silty Clay. Sand & silt lenses & layers. Trace of Fine Gravel.	6.0	Hard Red Very Silty Sandy Clay. Silt partings & lenses	8.0	Hard Red Very Silty Sandy Clay. Silt & Sand lenses	3.0	Stiff Red Very Sandy Silty Clay.
4	9.0	Very Compact Red Clayey Sandy Silt	20.0	Very Compact Red Sandy Silt. Trace of Fine Gravel	10.0	Very Compact Red Sandy Clayey Silt.	13.0	Hard Very Silty Sandy Clay. Silt & Sand lenses & layers
5	29.0	Very Compact Red Fine Silty Sand with Silt layers	20.0	Very Compact Red Fine Very Silty Sand with Fine Gravel	43.0	Very Compact Red Fine & Medium Silty Sand with Silt lenses	47.0	Very Compact Red Fine Silty Sand with Silt layers

---

6	3.0	Very Compact Red Fine Sand	12.0	Very Compact Red Fine Sand	-	-	-	-
---	-----	-------------------------------	------	-------------------------------	---	---	---	---

---

## 4.5.2 Scour Analysis Using SRICOS-EFA

In this section, information about all the input parameters is described first, which is followed by the SRICOS-EFA simulation results.

Soil/Material Properties Input: Lab test data for the earth layers erodibility at this site was not available, so the erosion category plot by Briaud (2008) (Figure 3.1) was used for obtaining the soil properties to be used as model input. Also, due to the lack of enough data to obtain the erosion curve for each layer, the erosion curves were selected by comparing the soil classification obtained in the plan (Table 4.26) with the information available in Briaud’s plot (Figure 4.23, Figure 4.24, Figure 4.25, Figure 4.26, Table 4.27). The straight lines marked with “L #” in the figures show the assumed curves for the corresponding layer.

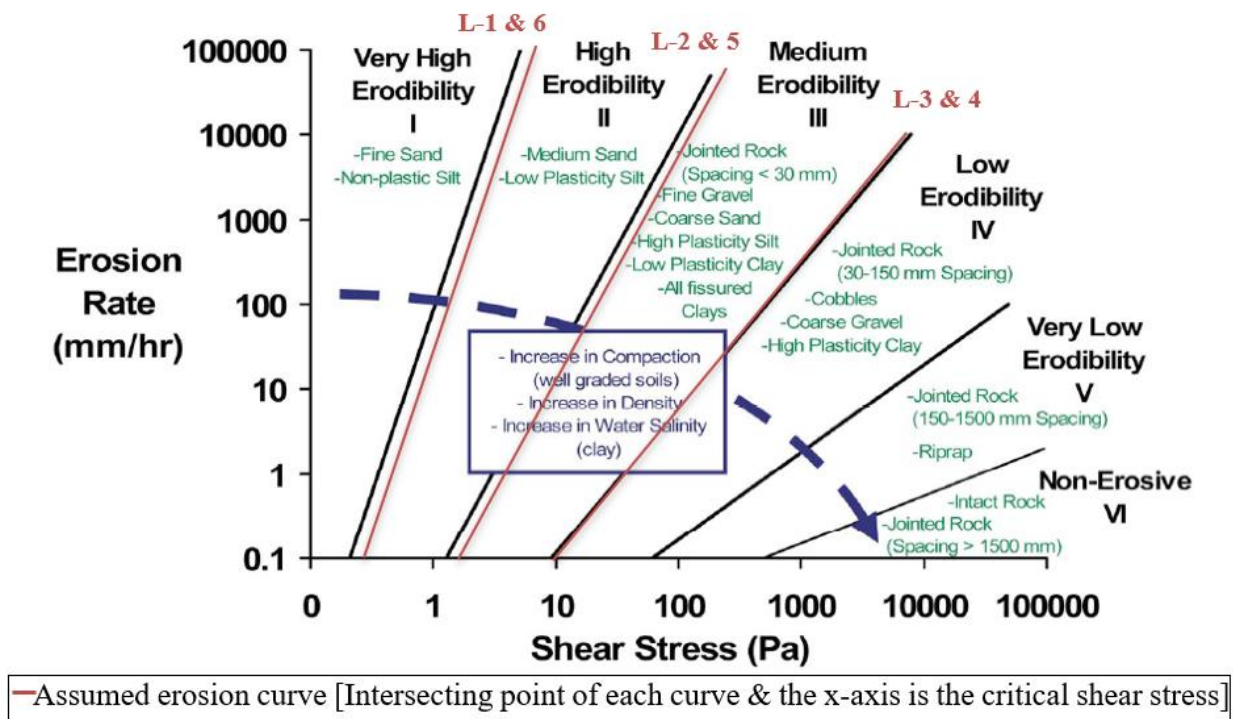
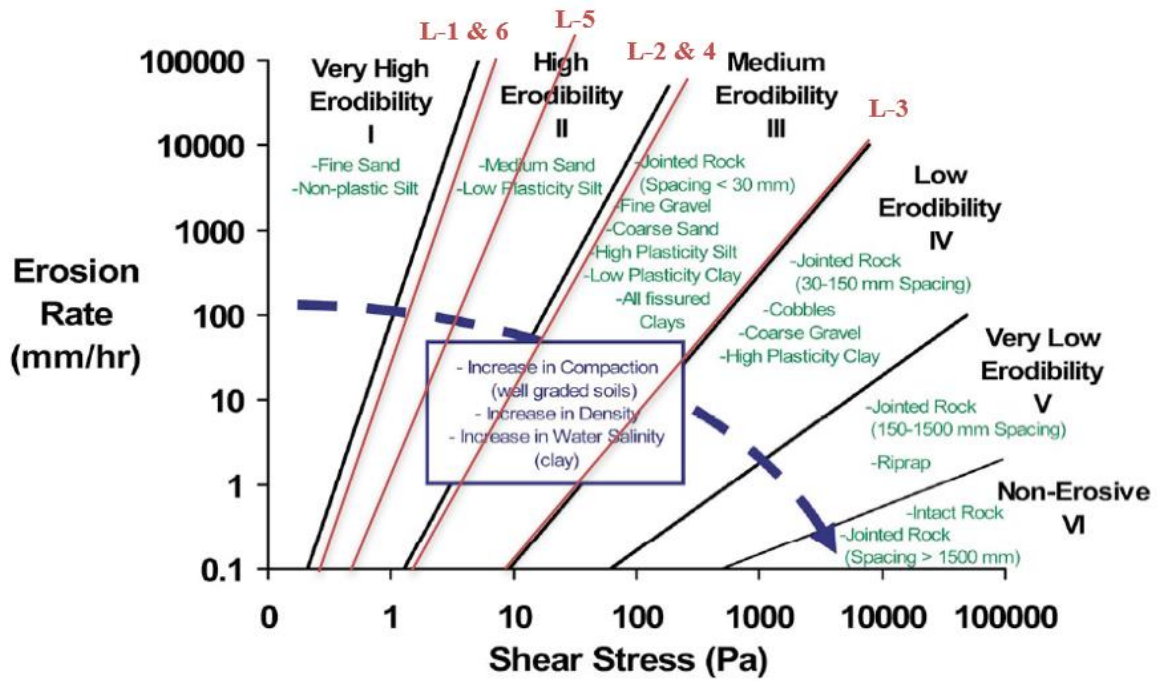


Figure 4.23 Assumed erosion curves on Briaud’s erosion category plot (Briaud 2008; Briaud et al. 2019) for the earth layers at Pier #7 of M-64 over the Ontonagon River



— Assumed erosion curve [Intersecting point of each curve & the x-axis is the critical shear stress]

Figure 4.24 Assumed erosion curves on Briaud's erosion category plot (Briaud 2008; Briaud et al. 2019) for the earth layers at Pier #8 of M-64 over the Ontonagon River

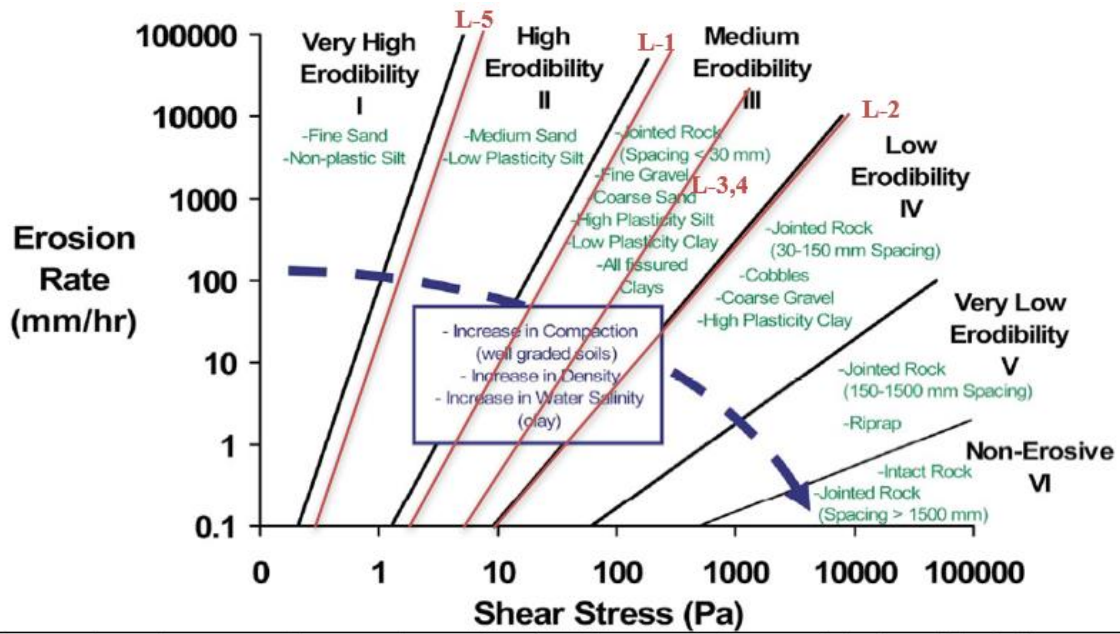
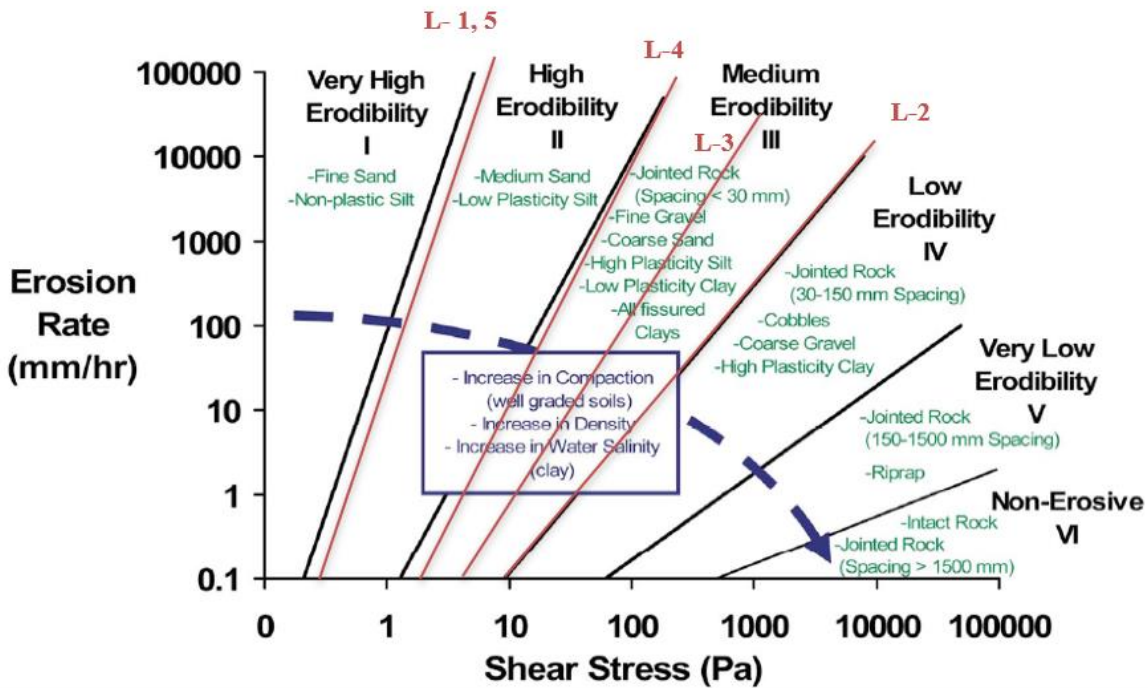


Figure 4.25 Assumed erosion curves on Briaud’s erosion category plot (Briaud 2008; Briaud et al. 2019) for the earth layers at Pier #9 of M-64 over the Ontonagon River



—Assumed erosion curve [Intersecting point of each curve & the x-axis is the critical shear stress]

Figure 4.26 Assumed erosion curves on Briaud’s erosion category plot (Briaud 2008; Briaud et al. 2019) for the earth layers at Pier #10 of M-64 over the Ontonagon River

Thickness information from Table 4.26, critical shear stress from Table 4.27 and several data points from each of the assumed curves from Figure 4.23 through Figure 4.26 were entered in the SRICOS-EFA software as material properties. Critical shear stress of each layer was obtained from the respective erosion category curve where the critical shear stress is the intersecting point of the curve with the horizontal x-axis.

Table 4.27 Critical Shear Stress [lb/ft<sup>2</sup> (Pa)] of different earth layers at the Piers #7 through #10 of M-64 over the Ontonagon River

Layer	Pier #7 (from Figure 4.23)	Pier #8 (from Figure 4.24)	Pier #9 (from Figure 4.25)	Pier #10 (from Figure 4.26)	Comment
1	0.005(0.3)	0.005(0.3)	0.04(2.0)	0.005(0.3)	

2	0.04(2.0)	0.04(2.0)	0.20(9.5)	0.20(9.5)	Since enough data was not available, all the erosion category curves are assumed based on the soil classification.
3	0.20(9.5)	0.20(9.5)	0.14(6.5)	0.14(6.5)	
4	0.2(9.5)	0.04(2.0)	0.14(6.5)	0.04(2.0)	
5	0.04(2.0)	0.02(0.7)	0.005(0.3)	0.005(0.3)	
6	0.005(0.3)	0.005(0.3)	-	-	

Hydraulic Parameter Input: Water depths and velocities for different discharges were extracted from the HEC-RAS model. Manning’s coefficient equivalent to 0.035, was also extracted from the HEC-RAS model. The daily discharge of the river since 2006 was obtained from the gaging station.

Geometry Input: All the piers of M-64 over the Ontonagon River are circular with the same diameter of 4 ft (42 inches). Besides pier information, the other geometry input, i.e., the upstream channel width equivalent to 297 ft, was obtained from the HEC-RAS model.

With all the input parameters entered in the SRICOS-EFA software, a simulation was run to estimate the cumulative scour depth over time. Figure 4.27, Figure 4.28, Figure 4.29, and Figure 4.30 are the output from the software for Piers #7, #8, #9, and #10 of M-64, respectively. It is observed that Piers #7, #8, and #10 have a cumulative scour depth of about 15 ft since its installation in 2006, while Pier #9 has a cumulative scour depth of about 4.5 ft.

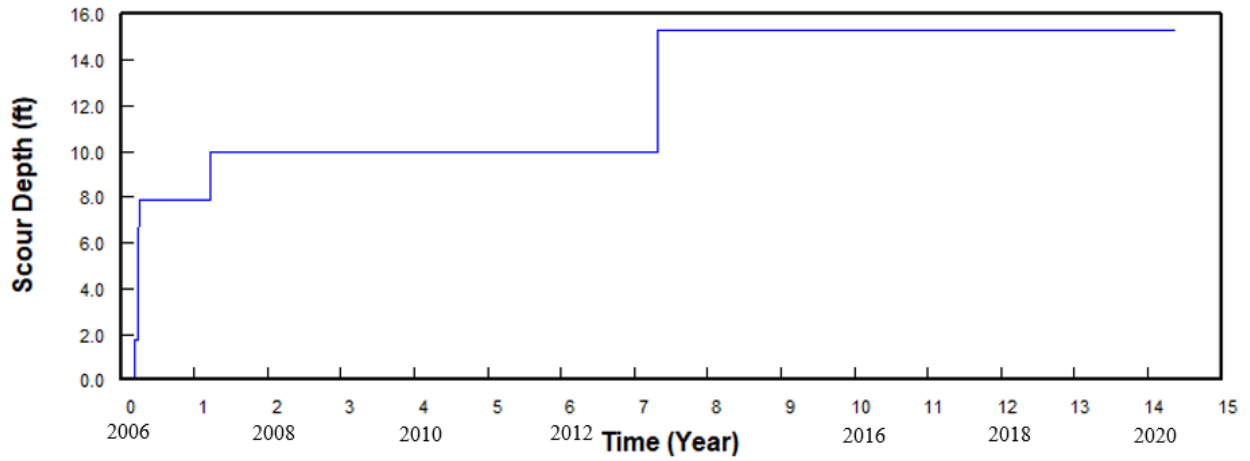


Figure 4.27 Scour depth at Pier #7 of M-64 over the Ontonagon River

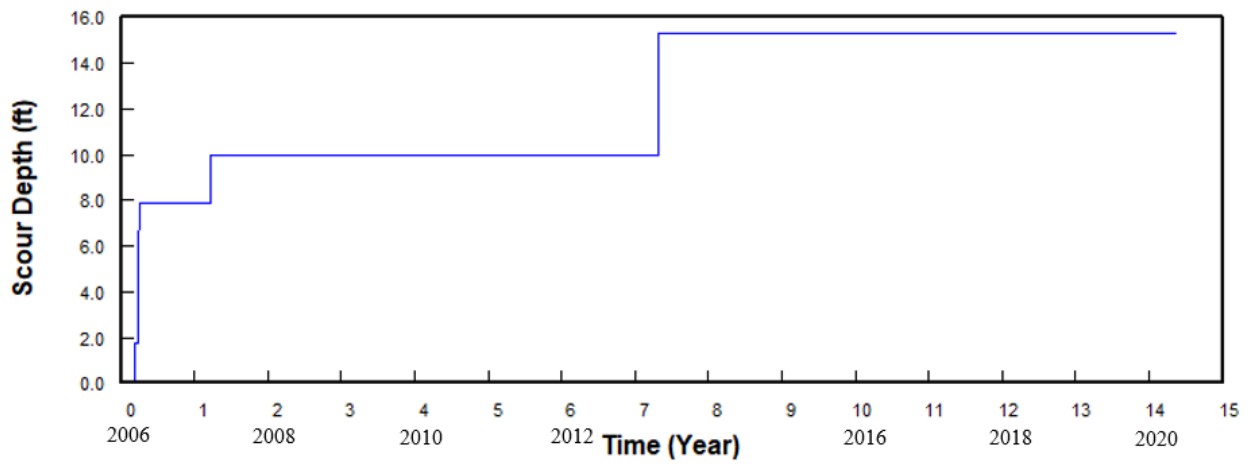


Figure 4.28 Scour depth at Pier #8 of M-64 over the Ontonagon River

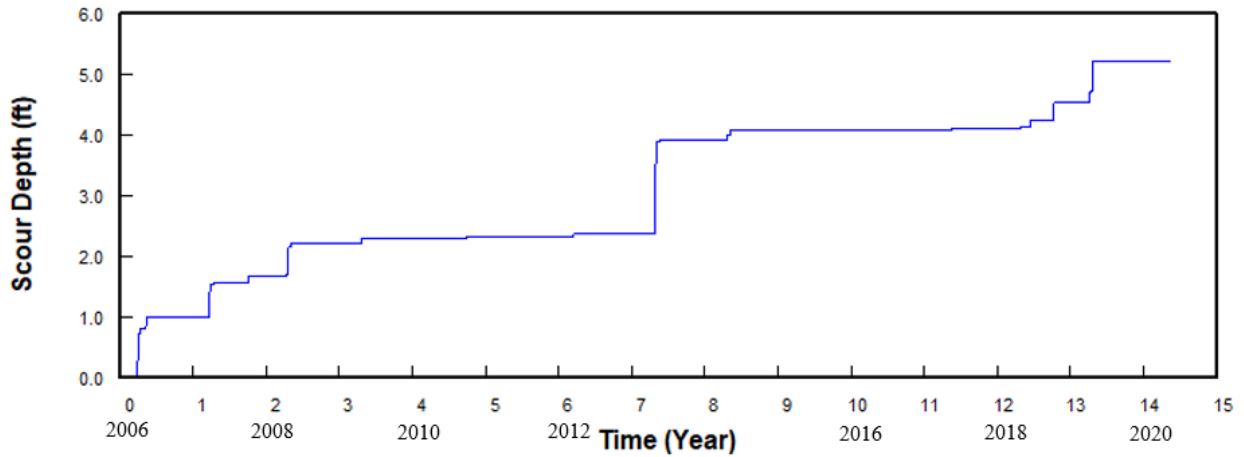


Figure 4.29 Scour depth at Pier #9 of M-64 over the Ontonagon River

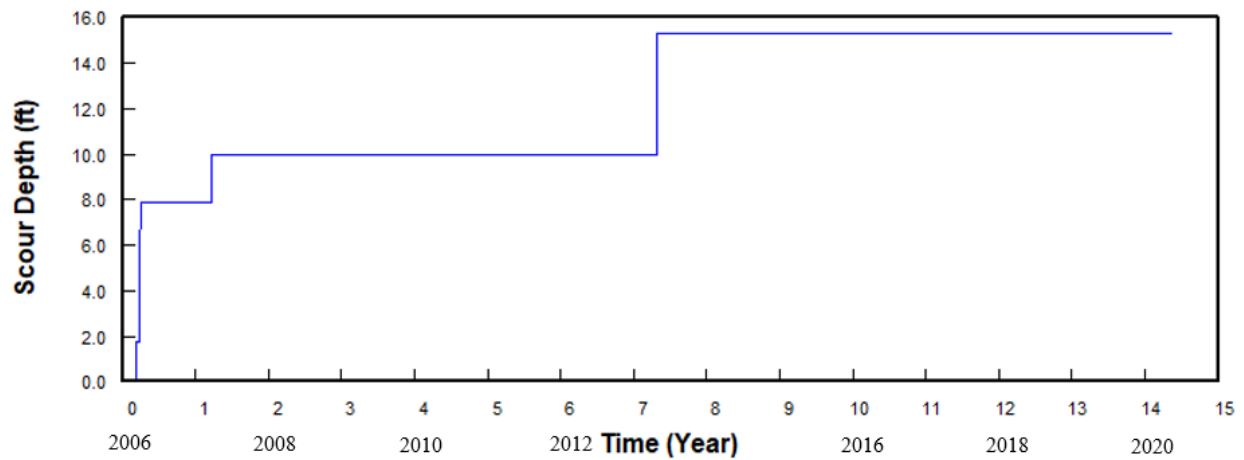


Figure 4.30 Scour depth at Pier #10 of M-64 over the Ontonagon River

### 4.5.3 Scour Analysis Using EIM

The first layer at Piers #7, #8, #9, and #10 of M-64 over the Ontonagon River is cohesionless. However, there is not enough data for conducting the EIM scour analysis for these layers. Hence, scour calculation started with the 2<sup>nd</sup> layer at each pier, which is a clay layer.

The plan of the bridge site marked that the SPT  $N$  of Layer #2 is 2 to 4 at Pier #7, 2 at Pier #8, 34 at Pier #9, and 5 at Pier #10. This SPT  $N$  value was used to determine the vane shear strength of the clay layer at each pier using Eq. 4.1 which was eventually used to determine the mass strength parameter,  $M_s$ , from Table 3.7. In addition, the shear strength number,  $K_d$ , was determined using Eq. 3.11 where, the value of the residual angle was assumed to be 8.1 for very soft to soft clay material and 30 degrees for other materials.

Once all the above parameters were obtained, erodibility indices were determined using Eq. 3.4 which were eventually used to determine the critical stream power,  $P_c$ , of each of the layers with the help of Eq. 3.13 or Eq. 3.14. Next, the scour status at different depths from the river bed at the pier sites were determined (Table 4.28 through Table 4.31) for design discharge values of 43,000 cfs and 51,000 cfs. Here, dimensionless scour depths, ( $y_s/b$ ) were obtained from the ratio of the depth and the pier width; the relative stream power, ( $P/P_a$ ) was obtained using Eq. 3.16; the approaching flow stream power,  $P_a$ , was determined using Eq. 3.15; and the available stream power at the pier,  $P$ , was obtained by multiplying relative stream power and approaching flow stream power. The available stream power,  $P$ , at the pier was compared with the critical stream power,  $P_c$ , to obtain the scour status at different depths. The results summarized in the tables indicate that the second layer at every pier is strong enough to resist scour for the design discharges.

Table 4.28 Scour determination at Pier #7 of M-64 over the Ontonagon River using EIM

Depth (ft)	Layer	Erodibility Index	$P_c$ (lb/ft-s)	Dimensionless scour depth ( $y_s/b$ )*	Relative Stream Power ( $P/P_a$ )	For 43,000 cfs			For 51,000 cfs		
						Approaching Flow Stream Power, $P_a$ (lb/ft-s)	Available Stream Power, $P$ (lb/ft-s)	Scour (Yes/No)	Approaching Flow Stream Power, $P_a$ (lb/ft-s)	Available Stream Power, $P$ (lb/ft-s)	Scour (Yes/No)
1	1	-	-	0.28	6.91		19.02	-		22.59	-
15	1	-	-	4.16	0.44	2.75	1.20	-	3.27	1.43	-
16	2	0.003	2.495	4.43	0.36		0.99	No		1.17	No

\* $b$  is the pier width perpendicular to the flow direction

Table 4.29 Scour determination at Pier #8 of M-64 over the Ontonagon River using EIM

Depth (ft)	Layer	Erodibility Index	$P_c$ (lb/ft-s)	Dimensionless scour depth ( $y_s/b$ )*	Relative Stream Power ( $P/P_a$ )	For 43,000 cfs			For 51,000 cfs		
						Approaching Flow Stream Power, $P_a$ (lb/ft-s)	Available Stream Power, $P$ (lb/ft-s)	Scour (Yes/No)	Approaching Flow Stream Power, $P_a$ (lb/ft-s)	Available Stream Power, $P$ (lb/ft-s)	Scour (Yes/No)
1	1	-	-	0.28	6.91		19.02	-		22.59	-
13.5	1	-	-			2.75	1.61		3.27	1.92	
14	2	0.003	2.495	0.44	6.18		1.46	No		1.74	No

\*  $b$  is the pier width perpendicular to the flow direction

Table 4.30 Scour determination at Pier #9 of M-64 over the Ontonagon River using EIM

Depth (ft)	Layer	Erodibility Index	$P_c$ (lb/ft-s)	Dimensionless scour depth ( $y_s/b$ )*	Relative Stream Power ( $P/P_a$ )	For 43,000 cfs			For 51,000 cfs		
						Approaching Flow Stream Power, $P_a$ (lb/ft-s)	Available Stream Power, $P$ (lb/ft-s)	Scour (Yes/No)	Approaching Flow Stream Power, $P_a$ (lb/ft-s)	Available Stream Power, $P$ (lb/ft-s)	Scour (Yes/No)
1	1	-	-	0.28	6.91		19.02	-		22.59	-
15.5	1	-	-	4.29	0.40	2.75	1.09	-	3.27	1.29	-
16	2	0.237	23.264	4.43	0.36		0.99	No		1.17	No

\*  $b$  is the pier width perpendicular to the flow direction

Table 4.31 Scour determination at Pier #10 of M-64 over the Ontonagon River using EIM

Depth (ft)	Layer	Erodibility Index	$P_c$ (lb/ft-s)	Dimensionless scour depth ( $y_s/b$ )*	Relative Stream Power ( $P/P_a$ )	For 43,000 cfs			For 51,000 cfs		
						Approaching Flow Stream Power, $P_a$ (lb/ft-s)	Available Stream Power, $P$ (lb/ft-s)	Scour (Yes/No)	Approaching Flow Stream Power, $P_a$ (lb/ft-s)	Available Stream Power, $P$ (lb/ft-s)	Scour (Yes/No)
1	1	-	-	0.28	6.91		19.02	-		22.59	-
13	1	-	-	3.60	0.65	2.75	1.78	-	3.27	2.12	-
14	2	0.023	6.269	3.88	0.53		1.46	No		1.74	No

\*  $b$  is the pier width perpendicular to the flow direction

#### **4.5.4 Comparison of Results**

The scour analysis results obtained with the three selected methods for M-64 over the Ontonagon River were compared in Table 4.32. It is interesting to notice that the cumulative scour depths calculated with the SRICOS-EFA are twice those obtained with HEC-RAS non-cohesive equations at three piers while much smaller at the remaining one. From a different angle, the SRICOS-EFA is more sensitive to the field conditions of sites on cohesive soils than the HEC-18 sand equation. When assessing the error source of the SRICOS-EFA analysis, the primary source was attributed to the fact that no data was available to determine the erosion category curve needed for the SRICOS-EFA input. In the analysis, this curve was always assumed at the border of the erosion category, which could be a major source of error. This again indicates the importance of lab test data. Besides, the EIM was applied only at the clay layers and no scour depth was determined at any of the piers. This may indicate that EIM may underestimate the scour depth in cohesive soils.

Table 4.32 Comparison of scour analysis results at M-64 over the Ontonagon River

Method	Scour Depth for 43,000 cfs	Scour Depth for 51,000 cfs	Scour Depth from 2006 to 2020*	Comment
Pier #7				
SRICOS-EFA	-	-	15.3 ft	Erosion category curves were always assumed at the outer range, which have presumably resulted in this great scour depth.
EIM	None at the clay layer	None at the clay layer	-	Due to lack of data, scour calculation was not possible to conduct before 15.1 ft of depth and the soil layer at 15.1 ft will have no erosion for the design scenario. (EIM for cohesive soil at 15.1ft)
HEC-18 Sand	7 ft	7.3 ft	-	-
Pier #8				
SRICOS-EFA			15.3 ft	Erosion category curves were always assumed at the outer range, which have presumably resulted in this great scour depth.
EIM	None at the clay layer	None at the clay layer		Due to lack of data, scour calculation was not possible to conduct before 13.6 ft of depth and the soil layer at 13.6 ft will have no erosion for the design scenario. (EIM for cohesive soil at 13.6 ft)
HEC-18 Sand	7 ft	7.3 ft	-	-
Pier #9				
SRICOS-EFA			5.2 ft	Erosion category curves were always assumed at the outer range, which have presumably resulted in this great scour depth.
EIM	None at the clay layer	None at the clay layer		Due to lack of data, scour calculation was not possible to conduct before 15.6 ft of depth and the soil layer at 15.6 ft will have no erosion for the design scenario. (EIM for cohesive soil at 15.6 ft)
HEC-18 Sand	7 ft	7.3 ft		-
Pier #10				

SRICOS-EFA			15.3 ft	Erosion category curves were always assumed at the outer range, which have presumably resulted in this huge scour depth.
EIM	None at the clay layer	None at the clay layer		Due to lack of data, scour calculation was not possible to conduct before 13.1 ft of depth and the soil layer at 13.1 ft will have no erosion for the design scenario. (EIM for cohesive soil at 13.1 ft)
HEC-18 Sand	7 ft	7.3 ft		-

\*This duration was taken since the bridge was installed in 2006.

## 4.6 Summary of the Implementation

The bedrock present in Michigan could be susceptible to the abrasion mode of scour, which takes place progressively rather than happening just after a big storm. The results of the selected pure rock site, US-2 and US-41 over the Escanaba River, showed that the GSN could determine this progressive scour depth at this site. However, the SRICOS-EFA failed to show any, perhaps because of the very little value of the scour depth. The EIM also proved the progressive nature of the scour at this site for the quarrying and plucking mode of scour. At the other rock site, i.e., M-43 over the Grand River, both the SRICOS-EFA and GSN could successfully show the relationship between the scour depth and the rock type. However, the EIM predicted no scour possibly because the rock has negligible fractures and weathering and thus is not susceptible to the quarrying and plucking mode of scour.

None of the bridge pier sites were pure clay except for Pier #2 at M-20 over the Tittabawassee River. Perhaps because of this reason, the scour depth obtained with the SRICOS-EFA was similar or even sometimes higher than the scour depth calculated by the HEC-18 sand equation. On the other hand, the EIM predicted no scour at the clay layer in most of the cases. Analysis of the results of Pier #2 at M-20 over the Tittabawassee River indicated that the SRICOS-EFA predicted comparatively low scour depth, which is supposed to be the case in cohesive soils. Even though it was a pure clay site, the EIM estimated a great scour depth, which contradicts the concept of cohesive soil scouring slowly.

Finally, attention will need to be paid to factors that may lead to errors in the analyses. Especially, assumptions were made for the input parameters, e.g., soil/rock erosion rates for the SRICOS-EFA, GSN value for the GSN method, and geotechnical information of rock/soil for the EIM.

From the above discussion, the following can be concluded:

- ❖ The SRICOS-EFA method exhibited consistent performance in predicting the scour conditions in the cohesive soil sites. However, it is sensitive to the input parameters. It is recommended that the EFA test is conducted to conduct accurate scour analysis with the SRICOS-EFA.

- ❖ The EIM was developed for the quarrying and plucking mode of rock scour. The case studies showed that the EIM predicts high scour depths for rocks that are heavily fractured or/and weathered. Therefore, this mode of scour in rock can be considered when heavy fractures or/and weathering is observed in any layers under the bridge. Also, it is recommended to obtain adequate input parameters, especially observations of the geological conditions, for accurate implementation of this method.
- ❖ The EIM is not recommended for cohesive beds due to its inconsistency of results in the analyzed cases. The performance of the SRICOS-EFA was thought to be somewhat “questionable” in rocks based on these case studies. This is especially an issue considering that the rocks exposed on the ground surface usually have relatively good engineering properties due to the heavy glaciation history of Michigan (glaciers remove soft and weak surface rocks).
- ❖ The GSN can be used for scour analysis of bridges founded on the bedrock of Michigan. While hard igneous and metamorphic rock, which did not show up at the four sites but are common in Upper Michigan, may exhibit the negligible abrasion mode of scour. Therefore, GSN can be only considered for the sedimentary rocks. When using the GSN, the use of a slake durability test is highly recommended. This is because it is very hard to find documented testing results for this test in the literature, and assumptions could lead to much different predictions (e.g., 81%)

## **Chapter 5 Michigan-Specific Considerations for Scour Analysis in Erodible Rock and Cohesive Soil**

### **5.1 Surface Geology of Michigan**

The geologic time scale is used by most geologists and earth scientists to categorize rocks based on their age. This time scale is divided into several periods starting with the Precambrian period which existed since the origin of the earth about 4.6 billion years ago with three eons- Hadean, Archean, and Proterozoic. The Paleozoic era in the Phanerozoic eon began 541 mya (Million years ago) with the Cambrian period and ended 251.9 mya with the Permian period. In between this time, there are several periods. Among them, the Ordovician period started 485.4 mya just after the Cambrian period and extended until 443.8 mya, after that the Silurian period started and ended at 419.2 mya. Then came the Devonian period and ended at 358.9 mya followed by the Carboniferous period with two subperiods – Mississippian and Pennsylvanian which advanced till 298.9 mya. Finally, the Permian period began and ended at 251.9 mya. After the Paleozoic era, the Mesozoic era spanned over three eras: Triassic, Jurassic, and Cretaceous, which ended 66 mya and are followed by the Cenozoic era which is considered as the present era (Crick and Robinson 2019; Ogg et al. 2016; Windley 2020).

The geologic formations of Michigan span more than 3.5 billion years, from some of the oldest Precambrian rocks to loose, unconsolidated drift left behind by the continental ice sheets of the Pleistocene period. The geology is mainly dominated by two rock formations: the Paleozoic sedimentary Michigan Basin and Pre-Cambrian. Michigan Basin covers the entire Lower Peninsula and the eastern half of the Upper Peninsula. And the Pre-Cambrian old crystalline igneous and metamorphic with some sedimentary and metasedimentary rocks are present in the western Upper Peninsula (Figure 5.1). The Basin occupies approximately 80,000 square miles (180,000 square kilometers), and the sedimentary rocks in the Basin, which are predominantly Paleozoic in age, reach a maximum thickness of 16,000 feet (4,848 meters) (Sommers 2019).

The underlying bedrock of Michigan is primarily hidden from view by unconsolidated material, predominantly Pleistocene Glacial deposits and landforms. However, there are several places in

the Lower Peninsula where the bedrock can be seen such as in rock quarries and outcrops along rivers and lakes. The rest of the surface is characterized by ridges of sand, gravel, and clay known as moraines, which were deposited as the ice advanced and retreated in the state. In the western Upper Peninsula, a considerable amount of bedrock is visible (Harrison 2016; Sommers 2019).

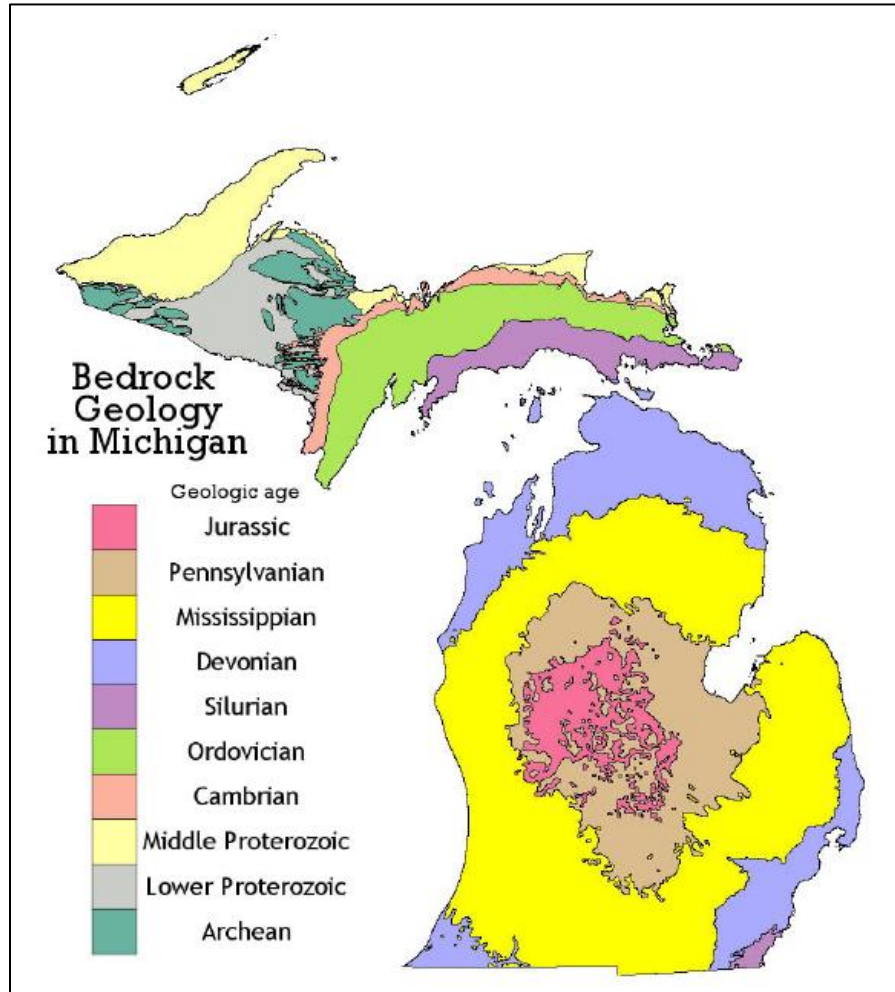


Figure 5.1 Generalized bedrock geology of Michigan (DEQ 2020)

Detail of the bedrock geology of the State of Michigan is summarized in Figure 5.2. The following subsections sequentially present the geologic information of the Lower Peninsula, the Eastern Upper Peninsula, and the Western Upper Peninsula.

### 5.1.1 Bedrock Geology of the Lower Peninsula

The rock geology in the Lower Peninsula is primarily attributed to the Michigan Basin. As we move from the rim to the center, the sedimentary rocks will become younger, which are also softer and more susceptible to scour, as a general trend. The youngest rocks can be found in a small area near the center of the Michigan Basin named 'Red Beds'. This area consists of rocks as young as Jurassic age, e.g., shale, sandstone, and minor limestone and gypsum. This area is entirely covered by glacial outwash and has no outcrop of these rocks. Pennsylvanian rock occurs surrounding the Jurassic rock containing Grand River Formation and Saginaw Formation. Lithological constituents of Grand River Formation are sandstone and shale, and that of Saginaw Formation are sandstone, shale, limestone, and coal. These formations have outcrops at multiple counties- Arenac, Branch, Calhoun, Clinton, Eaton, Huron, Ingham, Ionia, Jackson, Ottawa Saginaw, and Shiawassee.

Around the Pennsylvanian rock, there lies rocks of Mississippian age – the Bayport Limestone, Michigan Formation, Marshall Formation, and Coldwater Shale. A thin layer of the Sunbury Shale of the Mississippian-Devonian age overlies the Coldwater Shale at most places. The Bayport Limestone occurs with a minor portion of dolostone, sandstone, shale, chert, and evaporites. The lithological constituents of the Michigan Formation are shale, black-shale, gypsum, limestone, sandstone, and anhydrite, whereas the Marshall Formation is composed of sandstone and siltstone. Besides, Coldwater Shale occurs with dolostone, sandstone, limestone, and siltstone. These Mississippian rocks have outcrops at Antrim, Arenac, Branch, Calhoun, Charlevoix, Clinton, Eaton, Hillsdale, Huron, Iosco, Ingham, Jackson, Kent, Ogemaw, Sanilac, Saginaw, Shiawassee, and Tuscola counties.

Devonian rock occurs primarily in the northern part of the Lower Peninsula; however, a significant amount is also present in the southeastern and southwestern zone of the Lower Peninsula. The Berea Sandstone & Bedford, Bedford Shale, Ellsworth Shale, and Antrim Shale are old as late Devonian. On the other hand, the Traverse Group, Bell Shale, Dundee Limestone, and Detroit River Group are middle Devonian. Sylvania Sandstone, Mackinac Breccia, Bois Blanc Formation, and Garden Island Formation are early Devonian. The Berea Sandstone occurs with incidental siltstone, and the Bedford Shale occurs with incidental sandstone. None of these rocks are exposed

at any place in Michigan. Among the shales, the Ellsworth Shale occurs with a minor amount of siltstone and sandstone, the Antrim Shale is Black-Shale with a small percentage of limestone, and the Bell Shale has both limestone and black-shale as the major components but occurs as a very thin layer. On the other hand, the Traverse Group is mainly limestone with shale. The Dundee Limestone is present at both the northern and southeastern parts of the Lower Peninsula with a minor portion of dolostone and overlies the Detroit River Group. This Detroit River Group is mainly dolostone with a minor amount of limestone and incidental sandstone.

Among the early Devonian rocks, the Sylvania Sandstone occurs with incidental dolostone and the Mackinac Breccia has both limestone and sedimentary-breccia as major components. Apart from this, the Bois Blanc Formation is mainly limestone with a minor percentage of dolostone, and the Garden Island Formation is composed of dolostone and limestone. The Devonian group has isolated outcrops at Alcona, Alpena, Antrim, Charlevoix, Cheboygan, Emmet, Leelanau, Monroe, Presque Isle, St. Clair, Washtenaw, and Wayne counties. Only two types of rocks as old as late the Silurian age are present in the Lower Peninsula and exist mainly at the southeastern corner. The Bass Island Group is mainly dolomite and occurs with a minor amount of sandstone, shale, and limestone, and the Salina Group is composed of shale, evaporites, and dolostone. The Silurian rock at the Lower Peninsula exists at Monroe county, also is exposed in some of the places there (Cannon et al. 1997; Cannon 1986; Cannon et al. 2008; DEQ 2020; MDEQ 2003; Milstein 1987; Ojakangas 1994; Reed and Daniels 1987; Schmidt 1980; Sims 1992; USGS 2020a; USGS 2020b; Vickers 1956).

### **5.1.2 Bedrock Geology of the Eastern Upper Peninsula**

The Eastern Upper Peninsula has rocks as old as early Devonian, late Silurian, early Silurian, late Ordovician, early Ordovician, and late Cambrian. The Mackinac Breccia and Bois Blanc Formation of early Devonian are present here. The Mackinac Breccia has both limestone and sedimentary-breccia as major components, and the Bois Blanc Formation is mainly limestone with a minor amount of dolostone. No part of these rocks is exposed in the Eastern Upper Peninsula.

Compared to the Lower Peninsula, a larger proportion of Silurian rock is present in the Eastern Upper Peninsula in the form of the Bass Island Group, Salina Group, Saint Ignace Dolomite, Point Aux Chenes Shale, Engadine Group, Manistique Group, Burnt Bluff Group, Cabot Head Shale, and Manitoulin Dolomite. The Bass Island Group, Salina Group, Saint Ignace Dolomite, and Point Aux Chenes Shale are as old as late Silurian and the rest are early Silurian. The lithological formation of Bass Island Group and Salina group are the same as those found in the Lower Peninsula, i.e., dolomite with a minor amount of sandstone, shale, and limestone, and shale, evaporites, and dolostone, respectively. The Saint Ignace Dolomite, Point Aux Chenes Shale, Engadine Group, and Burnt Bluff Group do not have any other lithological constituents other than their major ones. The major constituents are dolostone, shale, dolostone, and limestone respectively. Contrarily, the Manistique Group has two major constituents: limestone and dolostone. The Cabot Head Shale and Manitoulin Dolomite are the members of the Cataract formation where the lithological constituents are shale, limestone, sandstone, and dolostone. Some parts of the Silurian rocks are exposed in Delta, Luce, Mackinac, Schoolcraft, and Chippewa counties.

Quite a good number of Ordovician aged rocks can be seen in the Western Upper Peninsula including the Queenston Shale, Big Hill Dolomite, Stonington Formation, Utica Shale Member, Collingwood Shale Member, Trenton Group, and Black River Group. Where the Queenston Shale is silty red shale, the Utica Shale Member is black shale and the Collingwood Shale Member is composed of black shale and limestone. On the other hand, both the Big Hill Dolomite the Trenton Group is composed of dolostone and limestone. The only difference is that limestone is present as a minor constituent in the Big Hill Dolomite and shale is the minor one in the Trenton Group. Apart from this, the Stonington Formation has limestone and shale as major constituents, and the Black River Group is mainly limestone. Among the Ordovician rocks, only the Prairie Du Chien Group is as old as early Ordovician and is composed of dolostone as the major constituent, sandstone as minor, and shale as incidental. Ordovician rocks are exposed in several counties including Alger, Chippewa, Delta, Marquette, and Menominee.

Besides the Trempealeau Formation, only the Munising Formation of the Eastern Upper Peninsula is as old as late Cambrian. The Munising Formation is sandstone with a minor portion of dolostone

and incidental shale, and the Munising Formation is sandstone with incidental conglomerate and shale. The Late Cambrian of Eastern Upper Peninsula has isolated outcrops at Menominee, Dickinson, Marquette, Alger, Luce, and Chippewa counties (Cannon et al. 1997; Cannon 1986; Cannon et al. 2008; DEQ 2020; MDEQ 2003; Milstein 1987; Ojakangas 1994; Reed and Daniels 1987; Schmidt 1980; Sims 1992; USGS 2020a; USGS 2020b; Vickers 1956).

### **5.1.3 Bedrock Geology of the Western Upper Peninsula**

Only the Bois Blanc Formation as old as the Early Devonian is present in the Western Upper Peninsula with limestone as the major constituent and dolostone as the minor one. Though this rock is present here as a very small volume, it has some outcrops in Houghton and Baraga counties.

A subdivision of the Precambrian geologic time scale, Proterozoic and Archean aged rocks, are also present in the Western Upper Peninsula. The Jacobsville Sandstone, Freda Sandstone, Nonesuch Formation, Copper Harbor Conglomerate, Oak Bluff Formation, Portage Lake Volcanics, and Siemens Creek Formation are Middle Proterozoic aged rocks. First, the Jacobsville Sandstone occurs with siltstone, shale, and conglomerate as minor constituents. Second, the Freda Sandstone occurs as siltstone, arkose, and shale. Third, the Nonesuch Formation has siltstone, shale, and sandstone. Fourth, the Copper Harbor Conglomerate occurs with conglomerate and sandstone as major constituents and mafic-volcanic as the minor one. Fifth, the Oak Bluff Formation has andesite and felsite as dominant lithology. Sixth, the Portage Lake Volcanics occurs as rhyolite. Finally, the Siemens Creek Formation has basalt as a major constituent and andesite as a minor constituent.

Early Proterozoic rock of the Western Upper Peninsula includes the Intrusive, Quinnesec Formation, Paint River Group, Riverton Iron Formation, Bijiki Iron Formation, Negaunee Iron Formation, Ironwood Iron Formation, Michigamme Formation, Goodrich Quartzite, Amasa Formation, Hemlock Formation, Menominee & Chocolay Groups, Emperor Volcanic Complex, Siamo Slate and Ajibik Quartzite, Palms Formation, Chocolay Group, and Randville Dolomite. The Intrusive and Quinnesec Formation is a similar type of rock and occurs as basalt and basaltic-

andesite with ultramafic and metagabbro as the minor constituents. The Paint River Group includes the Riverton Iron Formation and Dunn Creek Formation, and occurs with slate, banded-iron-formation, and graywacke as major constituents. On the other hand, the Bijiki Iron Formation contains black slate, argillite-siltstone, iron carbonate and locally iron oxides or grunerite, the Negaunee Iron-formation is banded-iron-formation with a minor portion of metadiabase, and the Ironwood Iron Formation contains banded-iron-formation and slate. In addition, the Badwater Greenstone occurs with greenstone and basalt, the Michigamme Formation is metagraywacke and mixed-clastic with a minor portion of volcanic rocks and the Goodrich Quartzite is composed of granite and schist. Again, the Amasa Formation is from both the Menominee Group and Baraga Group, the Hemlock Formation is mafic-volcanic with incidental slate, the Menominee & Chocolay Groups have metavolcanic and metasedimentary as the major constituents. Likewise, the Emperor Volcanic Complex is metavolcanic, the Siamo Slate & Ajibik Quartzite is under Menominee Group and contains slate, quartzite, and banded-iron-formation, and the Palms Formation contains thinly bedded argillite, fine siltstone, and quartzite near the top. On the other hand, the Chocolay Group includes the Randville Dolomite and has dolostone and quartzite as major constituents and slate as the minor constituent.

A significant portion of Archean Ultramafic, Archean Granite & Gneissic, and Archean Volcanic & Sedimentary are present in Gogebic, Baraga, Marquette, Dickinson, and Iron counties. Precambrian rocks have several outcrops at all the counties of Western Upper Peninsula (Cannon et al. 1997; Cannon 1986; Cannon et al. 2008; DEQ 2020; MDEQ 2003; Milstein 1987; Ojakangas 1994; Reed and Daniels 1987; Schmidt 1980; Sims 1992; USGS 2020a; USGS 2020b; Vickers 1956).

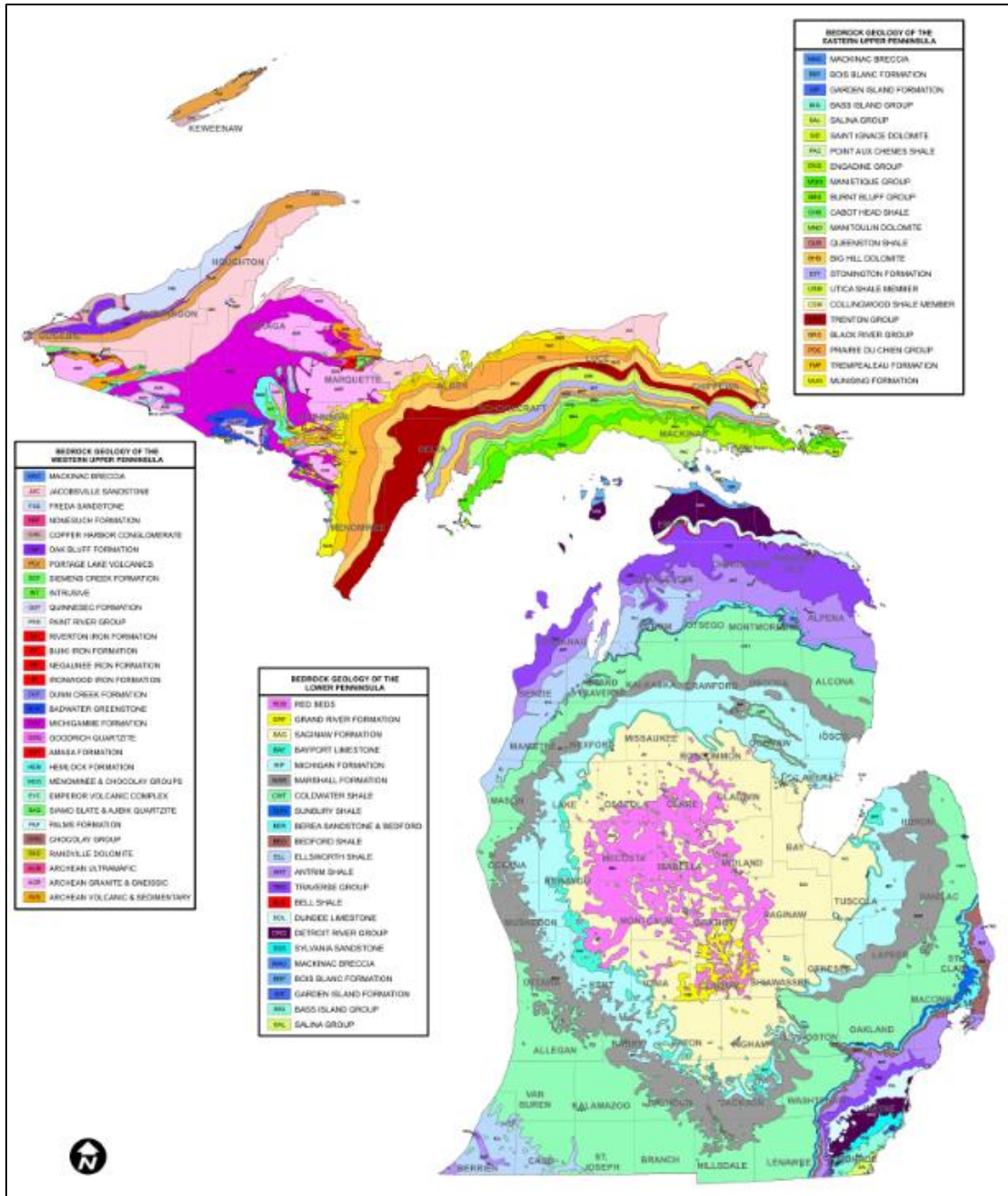


Figure 5.2 Bedrock geology of Michigan in detail (DEQ 2020)

## 5.2 Material (Rock) Classification for Scour Considerations

The Michigan rocks, which were discussed in the previous section, were assessed for their scour susceptibility. As can be seen in Table 5.1, a three-tier classification system was used to classify the rocks. It is noted that this classification of the rocks with the system was carried out based on information from the literature and the research team's experience. It is recommended that this table is used as the starting point before testing or/and field observations or a reference when no tests or field data are available. The assessment method used for the Michigan Bedrock Classification assessment is based on NCHRP Report 717 - Scour at Bridge Foundations on Rock by Keaton et al. (2012) and modified by Niemann et al. (2017) in a paper "A Proposed Risk-Based Screening Strategy for Bridges Potentially Affected by Rock Scour" that applied the NCHRP recommendations in a West Virginia DOT study.

For the three-tier system, test or site evaluation recommendations are:

Tier I – No testing required

Tier II – Recommend guidance in the 1988 paper "Rock weathering in engineering time" by Fookes, Gourley and Ohikere, Quarterly Journal of Engineering Geology, London, 1988, Vol. 21, pp. 33-57 (Fookes et al. 1988).

Tier III – Determination of the rock's erodibility index for the EIM in addition to the tests for Tier II will be needed for Tier III. Details for the EIM including the input and testing for obtaining the input have been described in Chapter 2 and Chapter 3. An alternative is the Geological Strength Index (GSI), modified for erosion (eGSI) as prescribed in Pells (2016), Erosion of Rock in Spillways, Volume 1. The eGSI takes into account the orientation and inclination of rock fractures. The eGSI is then assigned a maximum stream power, identified as  $\Pi_{UD}$ , and plotted on a graph as shown below (Figure 5.3) to indicated negligible, minor, moderate, large, or extensive erosion.

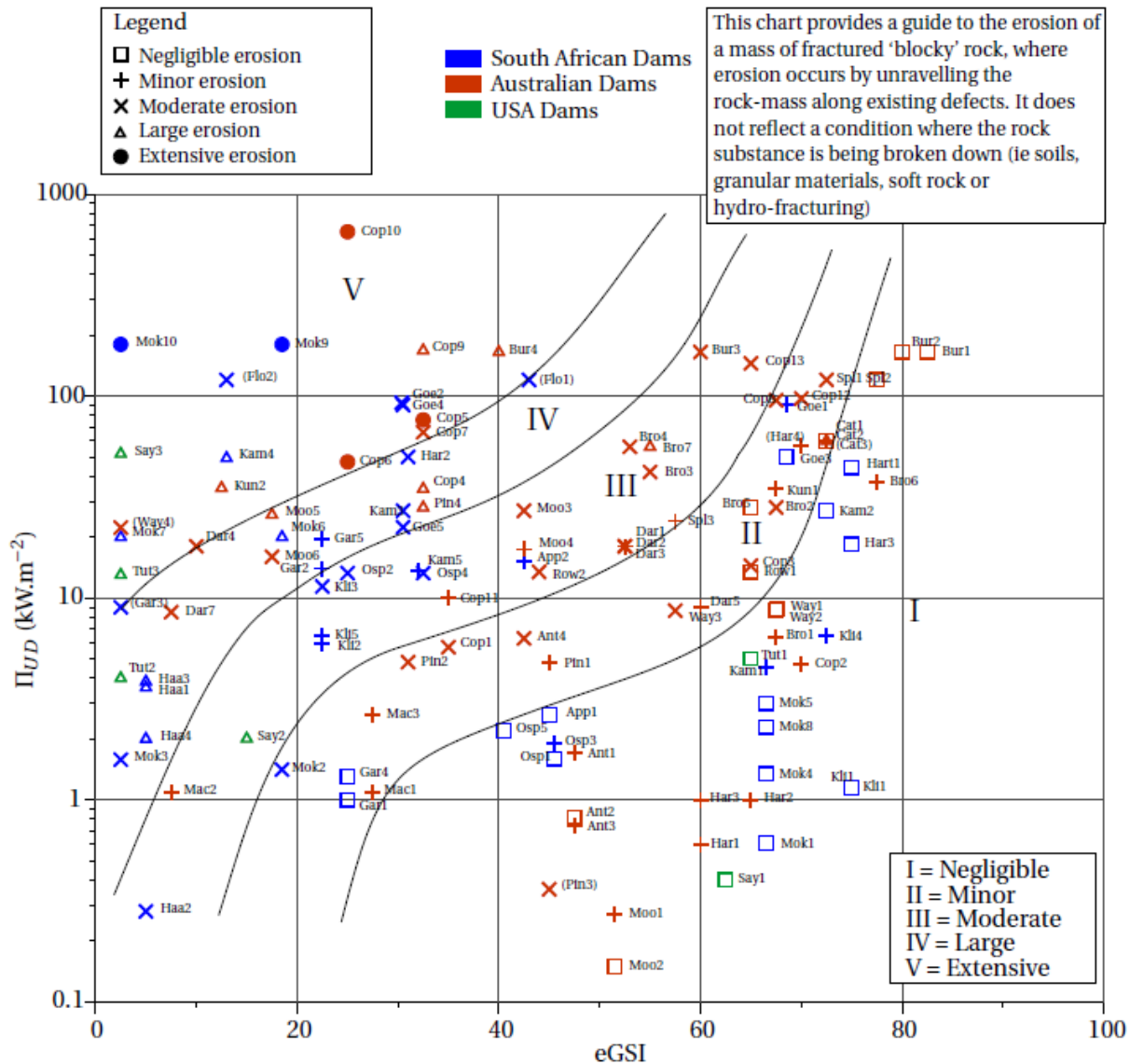


Figure 5.3 Interpreted erosion categories – unit stream power dissipation vs eGSI (datapoints in brackets have high uncertainty in one or more parameters, and are not contoured) (based on Pells (2016))

The classification results in Table 5.1 indicate that the major types of rocks in Michigan have no scour concerns. Besides, it is not surprising that most of the rocks in the Lower Peninsula can possibly be susceptible to at least one mode of scour, which were assessed in a conservative way. While in the Upper Peninsula, there is only a small portion of the rocks may need to be considered

for one or both modes of scour. For some rocks, the actual modes of scour and the classifications with regard to the three tiers may vary with the actual field conditions.

Table 5.1 Classification of Michigan Bedrock for Scour Considerations

<b>Outcrop Bedrock (Based on the State of Michigan GeoWebFace GIS System)</b>	<b>Classification of the bedrock Igneous (IGN) Metamorphic (MET) Sedimentary (SED)</b>	<b>Dominant scour mode: 1.Abrasion (ABR) 2. Quarrying and Plucking (Q&amp;P) Both (1) and (2) None</b>	<b>Tier I Shows evidence of long-term channel stability and requires no further action in assessing rock scour.</b>	<b>Tier II requires consideration of abrasion and/or weathering as the primary mode of scour.</b>	<b>Tier III requires consideration of quarrying/plucking as the primary or significant mode with some abrasion and/or weathering scour.</b>
Eastern Upper Peninsula					
Mackinac Breccia	SED	BOTH	NO	NO	YES
Bois Blanc Formation	SED	BOTH	NO	NO	YES
Garden Island Formation	SED	BOTH	NO	NO	YES
Salina Group					
Dolomudstones	SED	ABR	NO	YES	NO
Dolomitic Shale	SED	BOTH	NO	NO	YES
Anhydrites and Salts	SED	Most likely not exposed at the surface			
Saint Ignace Dolomite	SED	NONE	YES	NO	NO
Point Aux Chenes Formation (Shale)	SED	Q&P	NO	NO	YES
Engadine Group	SED	NONE	YES	NO	NO
Manistique Group	SED	NONE	YES	NO	NO
Burnt Bluff Group	SED	NONE	YES	NO	NO
Cabot Head Shale	SED	NONE	YES	NO	NO
Manitoulin Dolomite	SED	NONE	YES	NO	NO
Queenston Shale	SED	Both	NO	NO	YES
Big Hill Dolomite	SED	NONE	YES	NO	NO

<b>Outcrop Bedrock (Based on the State of Michigan GeoWebFace GIS System)</b>	<b>Classification of the bedrock Igneous (IGN) Metamorphic (MET) Sedimentary (SED)</b>	<b>Dominant scour mode: 1.Abrasion (ABR) 2. Quarrying and Plucking (Q&amp;P) Both (1) and (2) None</b>	<b>Tier I Shows evidence of long-term channel stability and requires no further action in assessing rock scour.</b>	<b>Tier II requires consideration of abrasion and/or weathering as the primary mode of scour.</b>	<b>Tier III requires consideration of quarrying/plucking as the primary or significant mode with some abrasion and/or weathering scour.</b>
Stonington Formation	SED	NONE	YES	NO	NO
Utica Shale Member	SED	NONE	YES	NO	NO
Collingwood Shale Member	SED	NONE	YES	NO	NO
Trenton Group	SED	NONE	YES	NO	NO
Black River Group	SED	NONE	YES	NO	NO
Prairie Du Chien Group	SED	NONE	YES	NO	NO
Trempealeau Formation	SED	NONE	YES	NO	NO
Munising Formation	SED	NONE	YES	NO	NO
<b>Western Upper Peninsula</b>					
Jacobsville Sandstone	SED	BOTH	NO	NO	YES
Freda Sandstone	SED	BOTH	NO	NO	YES
Nonesuch Formation	SED	NONE	YES	NO	NO
Copper Harbor Conglomerate	SED	NONE	YES	NO	NO
Oak Bluff Formation	IGN	NONE	YES	NO	NO
Portage Lake Volcanics	IGN	NONE	YES	NO	NO

<b>Outcrop Bedrock (Based on the State of Michigan GeoWebFace GIS System)</b>	<b>Classification of the bedrock Igneous (IGN) Metamorphic (MET) Sedimentary (SED)</b>	<b>Dominant scour mode: 1.Abrasion (ABR) 2. Quarrying and Plucking (Q&amp;P) Both (1) and (2) None</b>	<b>Tier I Shows evidence of long-term channel stability and requires no further action in assessing rock scour.</b>	<b>Tier II requires consideration of abrasion and/or weathering as the primary mode of scour.</b>	<b>Tier III requires consideration of quarrying/plucking as the primary or significant mode with some abrasion and/or weathering scour.</b>
Siemens Creek Formation	IGN	NONE	YES	NO	NO
Quinnesec Formation	MET	NONE	YES	NO	NO
Paint River Group	MET	NONE	YES	NO	NO
Riverton Iron Formation	MET	NONE	YES	NO	NO
Bijiki Iron Formation	MET	NONE	YES	NO	NO
Negaunee Iron Formation	MET	NONE	YES	NO	NO
Ironwood Iron Formation	MET	NONE	YES	NO	NO
Dunn Creek Formation	MET	NONE	YES	NO	NO
Badwater Greenstone	MET	NONE	YES	NO	NO
Michigamme Formation	MET	Q&P	NO	NO	YES
Goodrich Quartzite	MET	NONE	YES	NO	NO
Amasa Formation	MET	NONE	YES	NO	NO
Hemlock Formation	MET	NONE	YES	NO	NO
Menominee & Chocolay Groups	MET	NONE	YES	NO	NO
Emperor Vulcanic Complex	MET	NONE	YES	NO	NO

<b>Outcrop Bedrock (Based on the State of Michigan GeoWebFace GIS System)</b>	<b>Classification of the bedrock Igneous (IGN) Metamorphic (MET) Sedimentary (SED)</b>	<b>Dominant scour mode: 1.Abrasion (ABR) 2. Quarrying and Plucking (Q&amp;P) Both (1) and (2) None</b>	<b>Tier I Shows evidence of long-term channel stability and requires no further action in assessing rock scour.</b>	<b>Tier II requires consideration of abrasion and/or weathering as the primary mode of scour.</b>	<b>Tier III requires consideration of quarrying/plucking as the primary or significant mode with some abrasion and/or weathering scour.</b>
Siamo Slate & Ajibik Quartzite	MET	Q&P	NO	NO	YES
Palms Formation	MET	NONE	YES	NO	NO
Chocolay Group	MET	NONE	YES	NO	NO
Randville Dolomite	MET	NONE	YES	NO	NO
Archean Ultramafic	MET/IGN	NONE	YES	NO	NO
Archean Granite & Gneissic	MET/IGN	NONE	YES	NO	NO
Archean Volcanic & Sedimentary	MET/IGN/SED	NONE	YES	NO	NO
<b>Lower Peninsula</b>					
Grand River Formation	SED	Q&P	NO	NO	YES
<b>Saginaw Formation</b>					
Sandstone Unit	SED	Q&P	NO	NO	YES
Lower Shale Unit	SED	ABR	NO	YES	NO
Main Coal Unit	SED	Q&P	NO	NO	YES
Upper Shale Unit	SED	ABR	NO	YES	NO
<b>Bayport Formation</b>					
Limestone	SED	Q&P	NO	NO	YES
Sandstone	SED	Q&P	NO	NO	YES
Siltstone	SED	ABR	NO	YES	NO
<b>Michigan Formation</b>					

<b>Outcrop Bedrock (Based on the State of Michigan GeoWebFace GIS System)</b>	<b>Classification of the bedrock Igneous (IGN) Metamorphic (MET) Sedimentary (SED)</b>	<b>Dominant scour mode: 1.Abrasion (ABR) 2. Quarrying and Plucking (Q&amp;P) Both (1) and (2) None</b>	<b>Tier I Shows evidence of long-term channel stability and requires no further action in assessing rock scour.</b>	<b>Tier II requires consideration of abrasion and/or weathering as the primary mode of scour.</b>	<b>Tier III requires consideration of quarrying/plucking as the primary or significant mode with some abrasion and/or weathering scour.</b>
Anhydrite and Gypsum	SED	ABR/Dissolution	NO	YES	NO
Shale	SED	ABR	NO	YES	NO
Limestone/Dolomite	SED	Q&P	NO	NO	YES
Sandstone	SED	Q&P	NO	NO	YES
<b>Marshall/Napoleon Formation</b>					
Sandstone	SED	NONE	YES	NO	NO
Siltstone	SED	ABR	NO	YES	NO
<b>Coldwater Shale</b>					
Shale	SED	ABR	NO	YES	NO
Red argillaceous limestone/dolomite	SED	Q&P	NO	NO	YES
Sandstone	SED	Q&P	NO	NO	YES
Ellsworth Shale	SED	Q&P	NO	NO	YES
Antrim Shale	SED	Q&P	NO	NO	YES
<b>Traverse Group</b>					
Traverse Shale/Limestone	SED	Q&P	NO	NO	YES
Traverse Limestone	SED	None	Yes	NO	NO
Bell Shale	SED	ABR	NO	YES	NO
Dundee Limestone	SED	NONE	YES	NO	NO
Detroit River Group	SED	NONE	YES	NO	NO
Sylvania Sandstone	SED	NONE	YES	NO	NO
Mackinac Breccia	SED	BOTH	NO	NO	YES

<b>Outcrop Bedrock (Based on the State of Michigan GeoWebFace GIS System)</b>	<b>Classification of the bedrock Igneous (IGN) Metamorphic (MET) Sedimentary (SED)</b>	<b>Dominant scour mode: 1.Abrasion (ABR) 2. Quarrying and Plucking (Q&amp;P) Both (1) and (2) None</b>	<b>Tier I Shows evidence of long-term channel stability and requires no further action in assessing rock scour.</b>	<b>Tier II requires consideration of abrasion and/or weathering as the primary mode of scour.</b>	<b>Tier III requires consideration of quarrying/plucking as the primary or significant mode with some abrasion and/or weathering scour.</b>
Bois Blanc Formation	SED	BOTH	NO	NO	YES
Garden Island Formation	SED	BOTH	NO	NO	YES
Bass Island Group	SED	BOTH	NO	NO	YES
<b>Salina Group</b>					
Dolomudstones	SED	ABR	NO	YES	NO
Dolomitic Shale	SED	Q&P	NO	NO	YES
Anhydrites and Salts	SED	Unlikely to occur at the surface			

### 5.3 Scour Analysis without Gage Data

A good number of gaging stations have been installed at various sections of different rivers in the USA by USGS to monitor river flow. Despite this fact, there are numerous bridge sites that do not have a gaging station near them. Two of the selected scour analysis methods for cohesive bed (i.e., SRICOS-EFA) and rock strata (i.e., GSN) use daily river flow as an important input parameter. This raises the question of how to use these methods in the absence of a nearby gaging station. One solution can be using these methods (if possible) with a design discharge value. Though design discharge is calculated from the peak annual flows of the river collected at the gaging station, methods are available for determining design flow for an ungaged site (Jennings et al. 1994).

For pier founded on bedrock, scour depth can be calculated using the SRICOS-EFA, EIM, or GSN. For piers in cohesive soils, scour depth can be calculated using either the SRICOS-EFA or EIM method. The EIM always calculates scour depth for design discharge. By contrast, the SRICOS-EFA and GSN are well recognized for calculating cumulative scour depth over time. However, the SRICOS-EFA has equations available for determining the scour depth for any design flow. Though the GSN has never been used to calculate scour depth for a design discharge, a method has been developed as a part of this research to use the GSN in such a scenario.

#### 5.3.1 Use of SRICOS-EFA at Ungaged Sites

The summary report of SRICOS-EFA (Briaud et al. 2011) has included both the procedures for using this method for cumulative scour depth over time and for design discharge. This provides a way to conduct scour analysis for an ungaged cohesive site. In fact, the same equations, along with the daily flow effect and multi-layer concept, were used in these early versions of the SRICOS-EFA software (Briaud et al. 2011). The scour depth after any design event can be expressed by Eq. 5.1.

$$y_s(t) = \frac{t}{z_i \gamma_s} \quad \text{Eq. 5.1}$$

where,  $y_s(t)$  is the scour after the design event of duration  $t$ ,  $z_i$  is the initial rate of scour,  $y_s$  is the maximum scour depth, and  $t$  is the duration of the event. The initial rate of scour is the erosion rate corresponding to the maximum shear stress developed at the pier and can be obtained from the erosion category plot of Briaud (2008) (Figure 3.1). The maximum shear at the pier ( $\tau_{pier}$ ) and the maximum pier scour depth ( $y_s$ ) can be calculated using Eq. 5.2 and Eq. 5.8, respectively. Multiple correction factors are incorporated in the equations based on different pier parameters effects which are shown in Figure 5.4 based on Briaud et al. (2011).

$$\tau_{pier} = K_w K_{sh} K_{sp} K_{\theta} \cdot 0.094 \rho V_1^2 \left( \frac{1}{\log R_e} - \frac{1}{10} \right) \quad \text{Eq. 5.2}$$

where  $K_w$  is the water depth correction factor (Eq. 5.3),  $K_{sh}$  is the pier shape correction factor (Eq. 5.4),  $K_{sp}$  is the pier spacing correction factor (Eq. 5.5),  $K_{\theta}$  is the attack angle correction factor (Eq. 5.6),  $\rho$  is the density of water (62.4 lb/ft<sup>3</sup> or 1000 kg/m<sup>3</sup>),  $V_1$  is the approach flow velocity, and  $R_e$  is the Reynold's number (Eq. 5.7).

$$K_w = 1 + 16 \exp\left(-\frac{4y}{a}\right) \quad \text{Eq. 5.3}$$

$$K_{sh} = 1.15 + 7 \exp\left(-\frac{4L}{a}\right) \quad \text{Eq. 5.4}$$

$$K_{sp} = 1 + 5 \exp\left(-\frac{1.1S}{a}\right) \quad \text{Eq. 5.5}$$

$$K_{\theta} = 1 + 1.5 \left(\frac{\theta}{90}\right)^{0.57} \quad \text{Eq. 5.6}$$

$$R_e = \frac{V_1 a}{\nu} \quad \text{Eq. 5.7}$$

here,  $y$  is the flow depth,  $a$  is the pier width,  $L$  is the pier length,  $S$  is the spacing between piers,  $\theta$  is the attack angle, and  $\nu$  is the kinematic viscosity of water (10<sup>-6</sup>m<sup>2</sup>/s at 20<sup>0</sup>c).

$$y_s = 2.2 K_w K_1 K_L K_{sp} (a')^{0.65} \left(\frac{2.6V_1 - V_c}{\sqrt{g}}\right)^{0.7} \quad \text{Eq. 5.8}$$

where,  $K_w$  is the water depth correction factor (Eq. 5.9, Eq. 5.10),  $K_1$  pier nose correction factor (Table 5.2),  $K_L$  is the aspect ratio correction factor for a rectangular pier (Eq. 5.11),  $K_{sp}$  is the pier

spacing correction factor (Eq. 5.12, Eq. 5.13),  $a'$  is the projected pier width,  $V_1$  is the approach flow velocity,  $V_c$  is the critical velocity obtained from material testing, and  $g$  is the gravity.

$$K_w = 0.89 \left( \frac{y}{a'} \right)^{0.33} \quad \text{for } \frac{y}{a'} < 1.43 \quad \text{Eq. 5.9}$$

$$K_w = 1 \quad \text{Eq. 5.10}$$

$$K_L = 1 \quad \text{for the whole range of } \frac{L}{a} \quad \text{Eq. 5.11}$$

$$K_{sp} = 2.9 \left( \frac{S}{a'} \right)^{-0.91} \quad \text{for } \frac{S}{a'} < 3.42 \quad \text{Eq. 5.12}$$

$$K_{sp} = 1 \quad \text{Eq. 5.13}$$

Table 5.2 Correction factor,  $K_1$  for pier nose shape (Richardson et al. 2001)

Shape of Pier Nose	$K_1$
Square Nose	1.1
Round Nose	1.0
Circular Cylinder	1.0
Sharp Nose	0.9

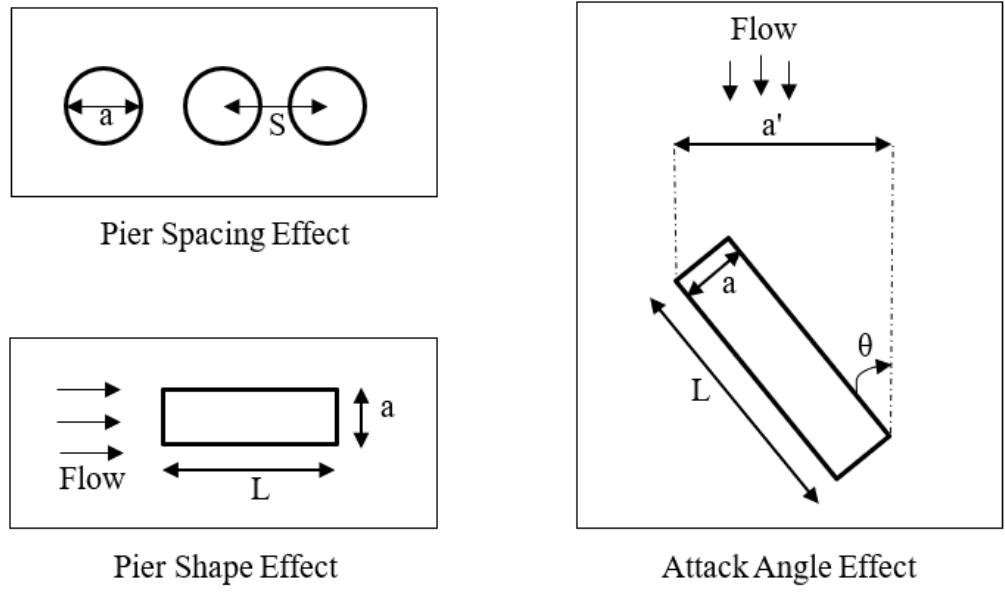


Figure 5.4 Effects of different pier parameters [based on Briaud et al. (2011)]

Scour analysis has been conducted using the SRICOS-EFA design discharge procedure for Pier #2 of M-20 over the Tittabawassee River and the results are shown in Table 5.3.

Table 5.3 Scour depth at Pier #2 of M-20 over the Tittabawassee River over the for different discharges

<b>Q (cfs)</b>	<b>Velocity, ft/s</b>	<b>y (ft)</b>	<b>Scour depth for t=24 hr (ft)</b>	<b>Scour depth for t=48 hr (ft)</b>
17,700	3.92	22.90	0.07	0.14
34,000	5.56	27.86	0.68	1.30

**5.3.2 Use of GSN at Ungaged Sites**

Attempts at the use of the GSN at ungaged sites were made in two different approaches. The first approach was assumed that the GSN can be used with the design discharge as the input, which is similar to the use of the SRICOS-EFA and EIM at ungaged sites as discussed above. The other direction was thought to be possible because the GSN depends more on the long-term effect of the

average flow instead of extreme events. These two will be discussed in detail in the following. Some relevant information and discussions were presented in this sub-section.

In the first approach, it seems that the GSN can be used to determine the scour depth if the associated stream power of a design discharge is known, since the GSN determines scour depth by multiplying the GSN of the sample with the stream power (Eq. 3.20). To check this possibility, the scour depth for some design discharge has been calculated for the Limestone bedrock of US-2 and US-41 over the Escanaba River (Table 5.4) using the GSN. The stream power values were obtained from HEC-RAS for the design discharges of 13,000 cfs and 14,000 cfs, and the GSN was taken as  $0.00017 \text{ ft}[\frac{\text{ft-lb}}{\text{sft}^2}]^{-1}$  following Section 4.3.4. Table 5.4 shows the design discharge and the corresponding stream power for two assumed extreme events. However, the predicted scour depth is negligible even compared with the results reported in Chapter 4 for the same site, which were obtained for a period without extreme events instead of a single event. This confirms that rock erosion, which usually takes a long time to occur, does not primarily result from a single event, but instead, it takes place due to hydraulic loading over time. This hydraulic loading is the cumulative stream power (Keaton et al. 2012).

Table 5.4 Scour depth of US-2 and US-41 over the Escanaba River for different discharges

<b>Return Period</b>	<b>Q (cfs)</b>	<b>Stream Power (from HEC-RAS) (lb/ft-s)</b>	<b>GSN (ft/unit of stream power)</b>	<b>Scour depth (ft)</b>
50 years	13,000	1.34	0.00017	$0.23 \times 10^{-3}$
100 years	14,000	1.46		$0.25 \times 10^{-3}$

The second approach was explored based on the above viewpoint. Now we confirmed that the GSN will not provide any effective value for scour depth if used for design discharge directly and daily flow data will be unavailable in an ungagged site. For this condition, a new way was proposed in this project to roughly estimate the scour depth of a bridge pier founded in bedrock. For this purpose, we assumed the abrasion of scour in rock is primarily affected by the long-term average

flow, which is usually not difficult to obtain or assume based on limited data. For the same example, the following assumptions were made: 1. the Escanaba River has a constant flow of 5,900 cfs, 2. the bridge has a life span of 75 years, and that the bedrock has a GSN value of  $1.70 \times 10^{-4} \text{ ft} \left[ \frac{\text{ft} \cdot \text{lb}}{\text{sft}^2} \right]^{-1}$ , and 3. cumulative scour depth has been calculated using Eq. 3.20. Calculation results with the above assumptions showed that the piers of US-2 and US-41 over the Escanaba River at the end of the lifetime of 75 years will have a scour depth of about 1.7 ft at the bedrock (Figure 5.5).

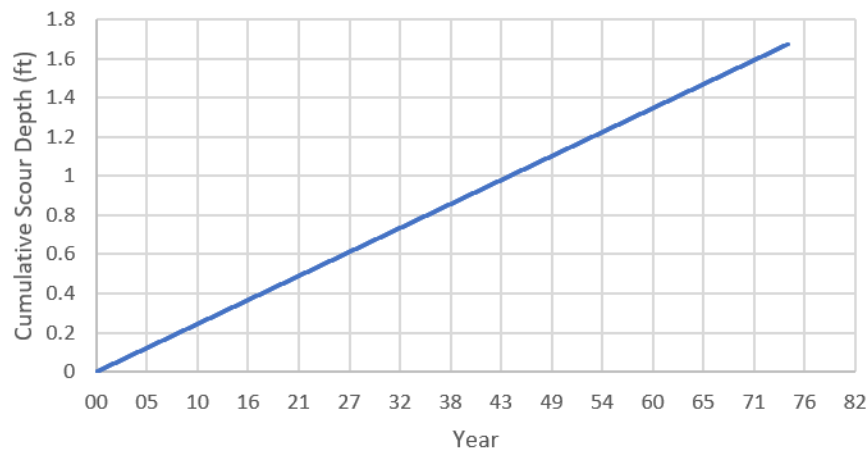


Figure 5.5 Cumulative Scour depth of US-2 and US-41 over the Escanaba River assuming a constant flow for 75 years

#### 5.4 Scour Analysis in Layered Earth Strata

One difficulty that was encountered when applying the selected three methods to Michigan bridges is regarding how to apply the methods at sites with layered earth strata. Bridges founded on earth strata with different erodibility values are a more common situation than an exception. Also, the literature for the three methods has not been specifically developed for this difficulty. Therefore, one advantage of using the SRICOS-EFA is that the software can be used to directly calculate the scour depth for multi-layer earth strata. The software has an input window where soil information can be entered layer by layer with the thickness and critical shear stress of each layer and shear

stress vs. erosion rate data (Figure 5.6). The output of the software package is the predicted scour depth vs. time (Figure 5.7).

Soil Data (Pier and Contraction Scour) ×

Number of Layers:

Current Layer: Layer 1  
Layer 2  
Layer 3

Erodibility Properties (Layer 2)

Layer Thickness:  feet

Critical Shear Stress:  lb/feet<sup>2</sup>

Points on EFA Curve:

Point No	Shear Stress (lb/ft <sup>2</sup> )	Scour Rate (mm/hr)
1	0.04	0.1
2	0.09	1
3	0.2	10
4	0.44	100
5	0.96	1000
6	2.09	10000

Figure 5.6 SRICOS-EFA Software Soil Input Window

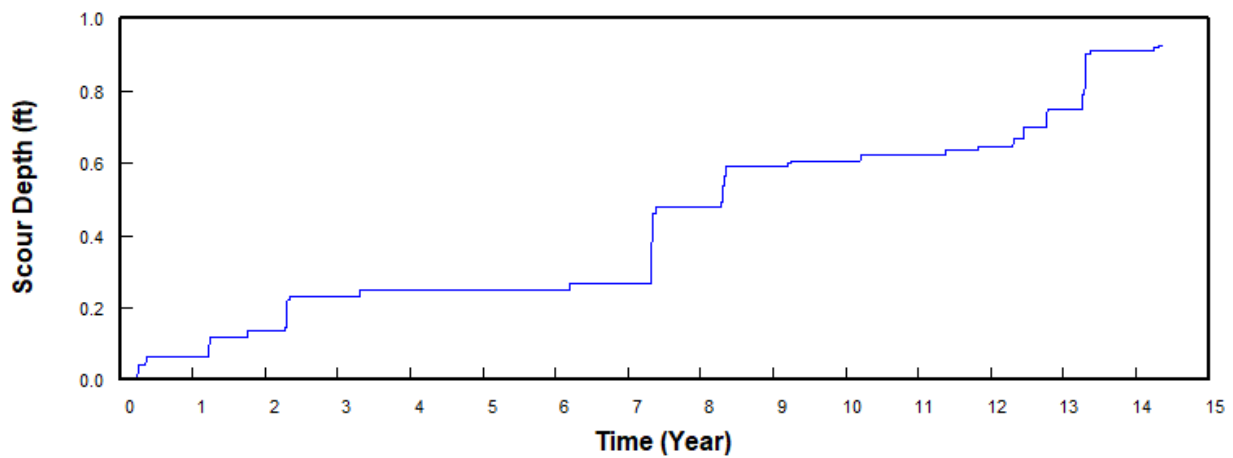


Figure 5.7 An example of SRICOS-EFA software output for scour depth over time

The EIM works in a different way. This method can be used to calculate the erodibility and scour susceptibility of a soil layer at any depth for any design discharge. The first type of input needed for this method is the approach-flow stream power at the location of the bridge pier, which can be obtained using Eq. 3.15, as per Annandale (2006). As scour occurs, the stream power,  $P$ , at the bottom of the scour hole decreases as the scour hole becomes deeper. Stream power at the bottom of the scour hole can be calculated using Eq. 3.16 provided by Annandale (2006), which relates the relative depth of the scour hole to the stream power at the bottom of the scour hole for a variety of pier shapes (round, square, and rectangular). When the stream power at the scour hole bottom reaches the critical stream power,  $P_c$ , scour development ceases (Annandale and Smith 2001). Therefore, the above process can be iteratively implemented in layered strata until the condition for the cessation of the scour development is met. What requires extra attention is the use of correct depths and material properties for the corresponding layers.

In Chapter 4, the Erodibility and scour susceptibility of the earth layers at Pier #1 of M-43 EB over the Grand River has been calculated with the EIM (Table 5.5) for the design discharge of 26,800 cfs. The soil has different values for the erodibility and critical stream power at depths beyond 2 ft. It is clear from the table that, after the 8.3 ft depth, the stream power at the scour hole bottom becomes less than the critical stream power, which means the scour depth will cease at the depth of 8.3 ft for this design discharge. In other words, it can be concluded that the scour depth at Pier #1 of M-43 over the Grand River is 8.3 ft for the design discharge of 26,800 cfs.

The GSN method does not cover anything regarding multi-layered earth strata. However, the GSN method was developed for erodible rock exposed to the abrasion mode of scour (Keaton et al. 2012). Generally, this type of rock is sufficiently thick to avoid scour within the life span of the bridge.

Table 5.5 Calculations of available and required stream power for scour depth determination at  
M-43 EB Pier #1

Depth (ft)	Layer	Erodibility	P <sub>c</sub> (lb/ft-s)	Dimensionless scour depth (y <sub>s</sub> /b)*	Relative Stream Power (P/P <sub>a</sub> )	For 26,800 cfs		
						Approach Flow Stream Power, P <sub>a</sub> (lb/ft-s)	Available Stream Power, P (lb/ft-s)	Scour (Yes/No)
1	1	1.6x10 <sup>-8</sup>	0.01	0.22	7.21	13.86	99.95	Yes
2				0.44	6.18		85.60	Yes
2.1				0.46	6.08		84.29	Yes
2.2				0.48	5.99		82.99	Yes
3				0.65	5.29		73.31	Yes
4	2	0.363	32.0	0.87	4.53	13.86	62.78	Yes
5				1.09	3.88		53.77	Yes
6				1.31	3.32		46.05	Yes
7				1.52	2.84		39.43	Yes
8				1.74	2.44		33.77	Yes
8.3				1.81	2.33		32.24	Yes
8.4				1.83	2.29		31.74	No

\*b is the pier width perpendicular to the flow direction.

## 5.5 Material Testing Methods

This section is intended to provide more information regarding the material testing needed for applying the three selected methods for scour analysis. Some information was provided in the literature review in Chapter 2. However, more insights were gained in the process of applying the three selected methods at the four Michigan bridge sites. Some extra information and discussions will be shared in the following sub-sections.

### 5.5.1 SRICOS-EFA

The SRICOS-EFA requires the following types of soil data:

1. Critical shear stress of each layer
2. Relationship between the erosion rate and shear stress for each layer

The SRICOS-EFA method recommends EFA testing for obtaining the above data. With the EFA apparatus, the above data can be measured directly. However, it is worthwhile to mention that RETA and JET can also produce such data with some limitations.

**RETA:** This is a rotating type of device, where the sample is inserted into a cylinder with a large diameter. The cylinder is usually filled with water and is rotated with a set amount of torque for a specified time period. The mass of the eroded material is measured after each test run. The following equation is used to determine the shear stress developed during each run.

$$\tau = \frac{T}{2\pi R^2 L} \quad \text{Eq. 5.14}$$

where  $\tau$  is the average shear stress during a test,  $T$  is the torque set for the test,  $R$  is the radius of the test sample, and  $L$  is the length of the test sample. The erosion rate,  $E$  at each test run can be computed using the following equation,

$$E = \frac{\Delta m}{2\pi \rho R L D} \quad \text{Eq. 5.15}$$

where  $\Delta m$  is the mass removed during the test,  $\rho$  is the dry density of the sample,  $R$  and  $L$  are the radius and length of the sample, respectively, and  $D$  is the test duration (Bloomquist et al. 2012).

To use the RETA results in the place of EFA, an  $E$  vs.  $\tau$  plot in the logarithmic scale will need to be developed at least with three data points. Such a plot will be comparable with Briaud's erosion category curves (Briaud 2008). Finally, the intersecting point of the curve and the x-axis will be the critical shear stress according to Briaud et al. (2019).

A disadvantage of using RETA is that the test is applicable only for stiff clay and erodible rock such as limestone, sandstone, and samples that can be self-supporting (Briaud et al. 2019).

**JET:** This device is suitable for both field tests and laboratory tests. It has an adjustable head tank, a point gauge, one jet tube, one nozzle, and a submergence tank. In this test procedure, water is allowed to pass through the jet to hit the soil sample in submerged conditions. The head tank is for setting the pressure head and the point gauge is for recording the scour depth. Subtracting the point

gauge reading at any time from the initial reading will represent the scour depth for that time interval, i.e., erosion rate,  $E$ . Changing the jet height will allow us to apply various velocities and shear stresses. The following equations presented by Hanson and Cook (2004) can be used to determine the shear stress.

$$\tau_0 = C_f \rho U_0^2 \quad \text{Eq. 5.16}$$

$$U_0 = \sqrt{2gh} \quad \text{Eq. 5.17}$$

where,  $\tau_0$  is the maximum stress due to the jet velocity at the nozzle,  $C_f$  is the coefficient of friction with a value of 0.00416,  $\rho$  is the density of water,  $U_0$  is the velocity at the jet nozzle,  $g$  is the gravity acceleration constant, and  $h$  is the head set prior to the test.

To use the JET to replace EFA, the  $E$  vs.  $\tau$  plot in the logarithmic scale will be developed at least with three data points. Such a plot will be comparable with Briaud's erosion category curves (Briaud 2008). Finally, the intersecting point of the curve and the x-axis will be the critical shear stress according to Briaud et al. (2019).

A limitation of JET is that the test is applicable only for cohesive soil and is used in agriculture and levee erosion (Briaud et al. 2019). Since no bridge scour study has used the JET erodibility test, careful measures should be taken while using this test in this field.

### 5.5.2 EIM

This method needs both field observations and lab/field test results. The tests required for this method are the UCS and RQD for rocks and the UCS/Vane Shear test for cohesive soil. Bridge construction projects in Michigan require these tests. However, the field observations required for this method are usually not included in conventional design or construction materials. What is more, these observations cannot be replaced with any other types of information.

Some of these observations can be assumed or predicted if the RMR test results are available. The RMR results include the following information in addition to the UCS and RQD:

1. Spacing of discontinuities
2. Condition of discontinuities.
3. Groundwater conditions
4. Orientation of discontinuities

Scour calculation with the EIM will need the UCS and RQD (part of the RMR) as well as other geological characteristics of the rock including the number of joint sets, joint roughness, joint alteration, and block dimensions (ratio between length and thickness). As can be seen, these extra input parameters partially overlap with the above information from the RMR results. The RMR results will lend support for assuming or predicting the input for the EIM. This may be attempted when the above field observations of the geological conditions are unavailable.

However, close attention needs to be paid to the above use of the RMR results, including the UCS and RQD, for scour analysis with the EIM. The RMR was proposed for construction in rock such as tunneling, therefore, it is by nature not a perfect fit for scour considerations. Rock coring for obtaining samples to measure the UCS and RQD may produce rock samples with engineering properties that are significantly different from those of the original rock. For example, coring in hard rock in the U.P., highly resistant to bridge scour, can generate highly fractured rock due to stresses in drilling, which could be determined as scour-susceptible. In addition, observations such as the number of joint sets and block dimensions should be for the natural samples. RMR results obtained with cores, which may be significantly different from the natural rock, are not suitable for inferring these properties of natural rock.

### **5.5.3 GSN**

The implementation of the GSN requires the modified slake durability test. There is no other test available that can produce the input needed for this method at this time. However, this modified slake durability test is a modified version of the standard slake durability test. So, no new apparatus or lab equipment will be necessary if the test equipment is available. This test can be performed with the lab apparatus of the standard slake durability test following the same test method. The

same steps can be following except for the following changes: the elimination of the oven drying step, an extension of the test-increment duration, and an increase in the number of test increments. Details of this test procedure have already been explained in Section 3.2.3. It is also worthwhile to mention that the major testing device can be self-fabricated without significant costs and effort.

## **5.6 Comparison of Scour Analysis Methods**

Since the EIM showed some inconsistency in all the analyzed cases, this method has not been included in this section. Comparisons between the SRICOS-EFA and GSN with the HEC-18 sand equation, which is used in the current MDOT scour analysis, will be presented and discussed in the next sub-sections.

### **5.6.1 SRICOS-EFA and HEC-18 Sand Equation**

Pier #2 at M-20 over the Tittabawassee River, which is a pure clay site, was chosen to compare the results from the HEC-18 sand equation and those obtained with the SRICOS-EFA for scour analysis in cohesive soils. It is critical to compare the results directly since these methods do not consider a similar type of input data. The HEC-18 sand equation directly calculates scour depth for a design discharge and thus does not consider the flow duration. So, the HEC-18 sand equation always gives out the same scour depth irrespective of the flow duration. By contrast, the SRICOS-EFA can calculate the scour depth considering the duration in addition to the monitored or design discharge. This is important because a clay site might not reach the maximum scour depth within a single event.

For this comparison, a 50 year flow event for the Tittabawassee River at M-20 was calculated using the Log Pearson type III (Council 1981). Peak stream flow data of the river at USGS gaging station No. 04156000 from 1969 to 2019 was used for the calculation. 32,678 cfs was determined to be the 50-year flow discharge. The comparison of HEC-18 sand equation analysis and the SRICOS-EFA was carried out in two cases. First, scour depth was calculated for the 50-year flow (Table 5.6). Since the SRICOS-EFA needs flow duration as an input, it was assumed to be 24 hrs,

which is usual. It was found that the HEC-18 sand equation yielded a scour depth of 11.3 ft for the 50-year flow and the SRICOS-EFA only obtained 0.7 ft for the same discharge. This may indicate that the HEC-18 sand equation used by MDOT predicts scour depth that is much higher than that obtained with the SRICOS-EFA when talking about a single event. Second, to further understand the above comparison, the flow duration for the SRICOS-EFA was changed several times to find how long it would take to reach the scour depth calculated by the HEC-18 sand equation. The time was found to be 300 days as shown in Table 5.7. Therefore, according to the SRICOS-EFA calculation, if the 50-year flow event continues for 300 days, a scour depth of 11.3 ft will be reached at Pier #2 of M-20 over the Tittabawassee River. That is, if such a 50-year event occurs once every year and lasts 3 days each time, it will still take 100 years to reach the maximum scour depth. This further confirmed that the HEC-18 sand bed equation will overestimate scour if we accept that the SRICOS-EFA is a better prediction approach for scour in cohesive soils.

The SRICOS-EFA method emphasizes scour development for everyday flow. Though this value is not significant for a one-day flow event, adding them up for a certain period of time may help us gain some insights. For example, cumulative scour depth at Pier #2 of M-20 over the Tittabawassee River has been calculated using the SRICOS-EFA software for the time from 1969 to 2019 assuming the bridge was installed there in 1969 (Figure 5.8). It was found that Pier #2 of the bridge would reach a scour depth of 7.6 ft if all the assumptions were true.

Table 5.6 Scour depth in the event of 50-year flow equivalent to 32,678 cfs at Pier #2 of M-20 over the Tittabawassee River

<b>Method</b>	<b>HEC-18 sand</b>	<b>SRICOS-EFA</b>
Scour Depth (ft)	11.3	0.7

Table 5.7 Comparison between HEC-18 sand method and SRICOS-EFA for different flow duration at Pier #2 of M-20 over the Tittabawassee River

<b>HEC-18 sand</b>	<b>SRICOS-EFA</b>
--------------------	-------------------

Return Period	Flow (cfs)	Duration (days)	Scour Depth(ft)	Duration (days)	Scour Depth(ft)
50 year	32,678	HEC-18 sand equation does not consider flow duration. So, it will always give the same scour depth irrespective of the flow duration.	11.3	1	0.7
				2	1.3
				3	1.8
				4	2.3
				5	2.7
				6	3.1
				7	3.5
				8	3.8
				9	4.2
				10	4.4
				300	11.3

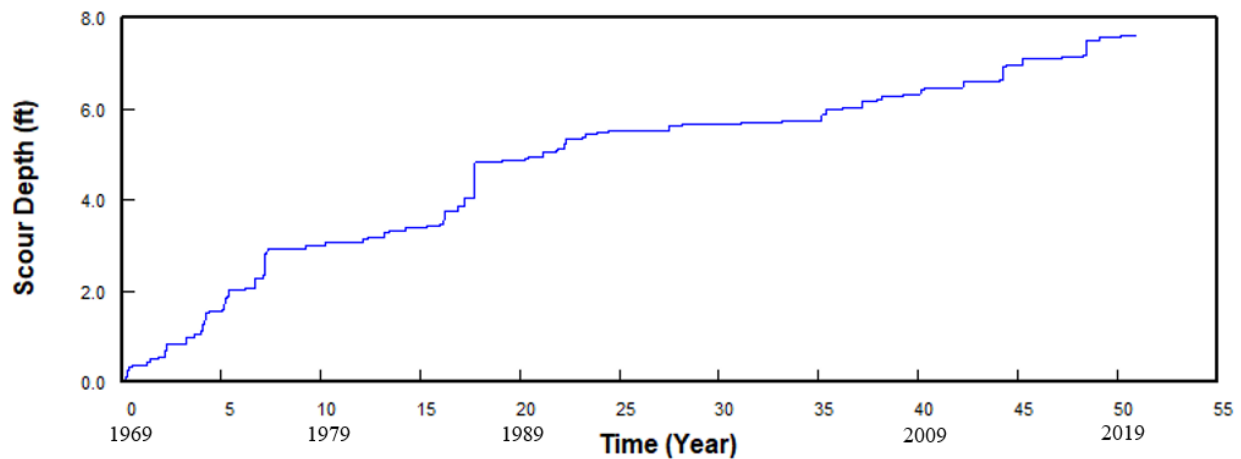


Figure 5.8 Cumulative scour depth at Pier #2 of M-20 over the Tittabawassee River using SRICOS-EFA software

The SRICOS-EFA software also provides an option for risk analysis, where a hydrograph, i.e., daily discharge of the river for past years, can be inserted as a category of input along with the other input parameters. Also, the software can develop synthetic hydrographs from the input parameters and can produce the exceedance probability of certain scour depths along with their

frequency of occurrence. These extra features are not available with the simple HEC-18 sand bed equation, though they can be obtained with extra effort.

### 5.6.2 GSN and HEC-18 Sand Equation

Originally, the GSN provides cumulative stream power and cumulative scour depth over time. However, when the cumulative stream power over a certain time is plotted and linear regression is applied, the slope of the linear regression represents the average stream power for that period of time (Titi et al. 2017). Now, if the average daily stream power at any bridge site is known, cumulative stream power at the end of the bridge life span can be estimated by multiplying the slope, i.e., average daily stream power, by the life-span. Then the estimated cumulative stream power can be multiplied with the GSN to determine the scour depth at the end of the bridge life. For example, when the daily stream power for US-2 and US-41 over the Escanaba River obtained in Section 4.3.4. was plotted against time and linear regression was applied, the slope of the curve was found to be 0.0469. That is, the average daily stream power at the bridge was  $0.0469 \left[ \frac{ft-lb}{sft^2} \right]$ . For a simple analysis, we assume the GSN is 0.00017 ft/unit of stream power as that used in the case study in Chapter 4 and assume the bridge has a 75-year design life. According to Eq. 3.20, the scour depth at the end of the bridge life span will be

$$y_s = 0.00017 * 0.0469 * 75 * 365 = 0.22 \text{ ft}$$

For the same example, if we adopt the HEC-18 sand equation to calculate the scour depth, a scour depth of 6.6 ft for the design discharge of 14,000 cfs will be obtained. This also indicates that the use of the HEC-10 sand bed equation will possibly overestimate scour depth if the GSN is accepted as a better option for analyzing the bridge scour in rock (abrasion mode).

## **Chapter 6 Recommended Procedure for Bridge Scour Analysis in Erodible Rock and Cohesive Soil in Michigan**

### **6.1 Overview**

This chapter summarizes the procedures for implementing the selected bridge analysis methods, including sampling and testing (introduced in Chapter 2), analysis (Chapter 3), and knowledge for application to Michigan sites (Chapter 4) as well as Michigan-specific considerations (Chapter 5). To obtain products that can directly guide engineering practice, flowcharts will be provided and explained in the following sections to illustrate everything that is needed for analyzing the bridge scour in cohesive soils and erodible rock with the selected methods. For pier founded on bedrock, scour depth can be calculated using the SRICOS-EFA, EIM, or GSN. For piers in cohesive soils, scour depth can be calculated using either the SRICOS-EFA or EIM. Despite the capabilities of the methods, the SRICOS-EFA is recommended for cohesive soils, while the EIM and GSN are recommended for the quarrying and plucking mode of scour and the abrasion mode of scour in scour-susceptible rock. All three methods can be used to calculate the scour depth for a design discharge. The SRICOS-EFA and GSN methods are well recognized for calculating cumulative scour depth over time. Since structures founded on cohesive soil or rock may not experience the maximum scour depth within single events or even their lifetime, scour depth over time is more important for these soil strata (Chaulagai et al. 2016; Keaton et al. 2012). Detailed procedures for the application of these methods are described next.

### **6.2 Selection of New Methods**

The improved calculation of bridge scour studied in this project can serve as an extension to the bridge scour analysis method currently adopted by MDOT, i.e., the HEC-18 equation proposed based on cohesionless materials. The SRICOS-EFA is proposed for calculating the scour depth in cohesive soils, the EIM is recommended for predicting the quarrying and plucking mode of scour in scour-susceptible rock, and the GSN is recommended for analyzing the abrasion mode of scour in scour-susceptible rock. Figure 6.1 presents a flowchart for a comprehensive consideration of

scour in differential types of bed materials including both sand, clay, and rock with an improved scour analysis framework discussed in this study. The flowchart shows how to select the correct method. Detailed procedures for using individual methods will be provided in the following sub-sections.

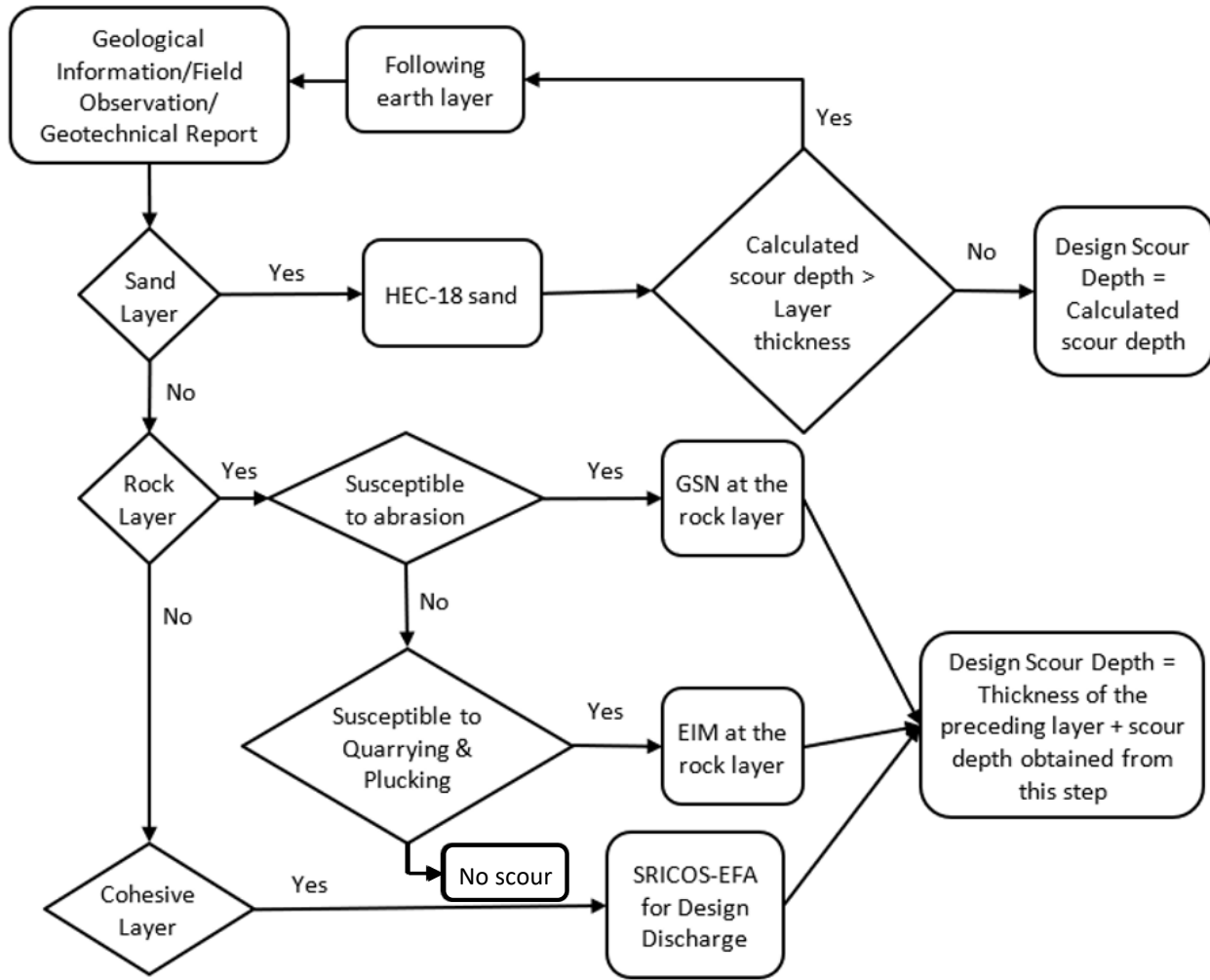


Figure 6.1 Flow-chart showing the steps for selecting scour analysis method.

As illustrated in Figure 6.1, the scour analysis starts with the assessment of existing geological information, field observations, and existing geotechnical reports. The analysis needs to be carried out layer by layer because different types of materials may be present in multi-layer strata where a bridge is founded on. For each layer, we first test whether it is a sand layer, or cohesionless soil

in a broader sense. If yes, we can resort to the HEC-18 sand equation or the spreadsheet developed for it to calculate the scour depth. If the calculated depth is smaller than the thickness of the layer, then the scour does not reach the underlying layers and the analysis can end here; otherwise, we will start from the first estimation (i.e., sand layer or not) for the next layer. If no, we will move to the next step to see whether this layer is a rock layer. If no, then this layer is thought to be cohesive soil, and accordingly, the SRICOS-EFA can be adopted for the scour analysis. If this layer is a rock layer, we will need to tell whether the abrasion model or/and quarrying and plucking mode exists. In theory, the abrasion mode of scour exists in all types of rocks. However, this type of scour in the hard, igneous rocks, metamorphic rocks, as well as hard sedimentary rocks will be very small and thus can be overlooked. However, the abrasion mode of scour needs to be considered in soft sedimentary rocks such as soft shale and mudstone, especially those with high clay content. The GSN method needs to be employed to analyze this type of scour. The quarrying and plucking mode of scour needs to be considered in highly fractured or/and heavily weathered rocks. However, as discussed in Chapter 5, such characteristics need to be that of natural rock instead of samples significantly disturbed in the sampling process, e.g., heavily fractured by inappropriate coring techniques. The EIM will be adopted for calculating the scour depth in the quarrying and plucking mode. The above procedure will be continued until scour cannot touch the underlying layer. All the scour depths obtained in the process will be added up to obtain the total scour. This procedure is laid down to consider a complicated condition. In many cases, the top layer could be a thick layer consisting of one type of material. In this condition, we will just need to go with one method for the corresponding bed material.

### **6.3 SRICOS-EFA**

If the earth layer is cohesive soil or soft rock, the SRICOS-EFA can be used to analyze the scour depth. Notwithstanding, SRICOS-EFA is recommended for cohesive soil only, considering that the rocks in Michigan are in general scour resistant. All the input data needed for this method can be obtained from field observations, geotechnical reports, hydraulic reports, and hydraulic modeling, the USGS website, and project proposal, except the EFA testing results. The input

information is categorized into three categories: soil input, geometry input, and water input. If the pier is founded on the rock layer, rock core samples will be required for lab tests, and standard Shelby tube samples will work for cohesive soil strata. In the EFA, two types of data will be obtained from lab tests: the critical shear stress of each earth layer and the relationship between the scour rate and shear stresses. Though the SRICOS-EFA recommends doing an EFA test for determining these parameters, JET or RETA can also be used, depending on the type of the earth strata (see Chapter 5 for discussions). When EFA test results are not available, rough estimates of the scour depth can be made by assuming the EFA results based on basic soil properties as performed in the case studies in Chapter 4. However, according to the sensitivity analysis, the error in such predictions could be high (e.g., 60%). Different types of structure-related information are also needed as geometry input depending on the type of scour, i.e., pier scour, abutment scour, or contraction scour, or a combined mode of scour. Daily flow data is a major piece of information for representing the hydraulic conditions.

The steps for implementing the SRICOS-EFA are shown in a flowchart in Figure 6.2. The method starts from the geologic information of the site from the geotechnical report or field observations, which lead to some information regarding the earth layer, e.g., the number of different earth layers and their thickness, which are directly used as the soil input. The geologic information also leads to a decision box for each layer of the site, and the decision box depends on the type of the earth layer, i.e., cohesive soil or rock. If the earth layer is a rock layer then a rock core sample is needed for the lab test; if the earth layer is a cohesive soil, a Standard Shelby Tube sample will be required for performing the lab test. Whatever the lab test is, EFA, JET, or RETA, the critical shear stress of each layer and the scour rate (depth/time) vs. shear stress for each layer need to be collected as the soil input parameters for the SRICOS-EFA.

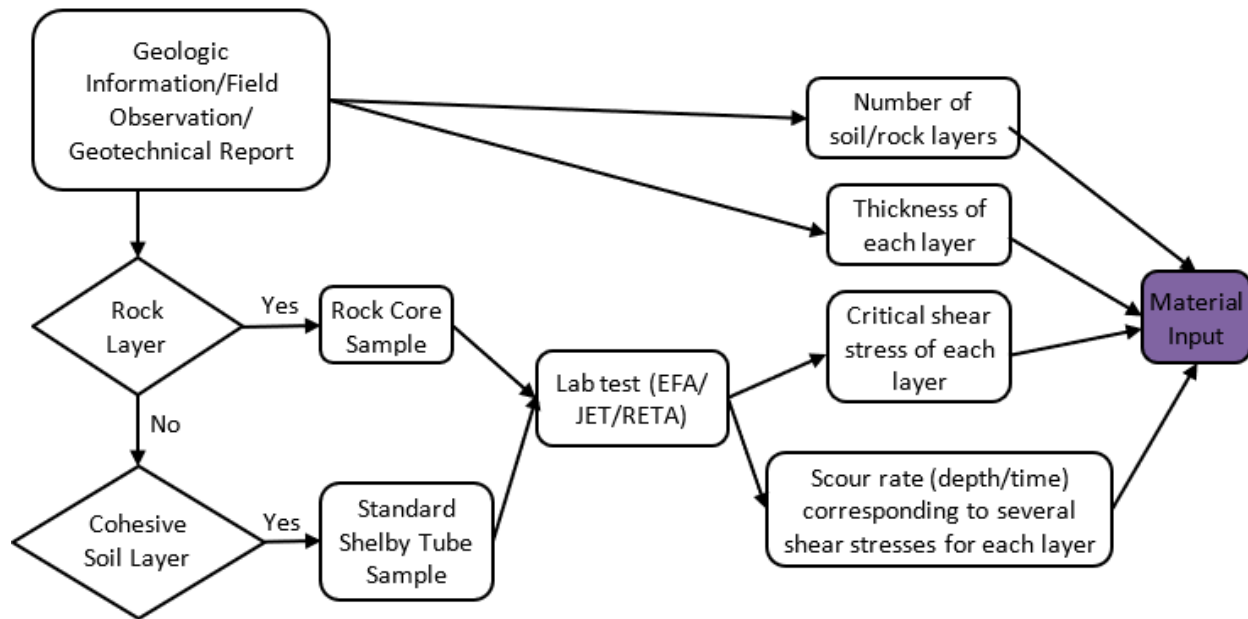


Figure 6.2 Flow-chart showing the steps for obtaining the soil input categories for SRICOS-EFA

The flow chart of Figure 6.3 shows that the geometry input of the SRICOS-EFA, which starts from the judgment of the scour type, i.e., pier scour, contraction scour, abutment scour, or any scour combination. This information can be obtained with guidelines from HEC-18. Depending on the type of scour, different types of information will be needed for the geometry input. If the concerned type of scour is pier scour, then the shape of the pier, the number of the piers perpendicular to the flow, center-to-center spacing of the piers when multiple piers are present, width and length or diameter of the pier, the angle between the direction of the water flow, and the main axis of the pier if the pier is rectangular and upstream channel width are required. For the contraction type of scour, upstream uncontracted width, contracted channel width, contraction length, transition angle, i.e., the angle between the contracted and uncontracted section, are required. If the scour type is abutment scour, the shape, slope and top width of the abutment, bridge clearance and deck thickness, skew angle and length of embankment, width and Manning's coefficient of the left floodplain, main channel and right floodplain, and slope of the left floodplain and right floodplain are needed. If the project demands any scour combination, e.g., pier and contraction scour or abutment and contraction scour, input information for the individual scour types should be

combined. Input information for all types of scour can be retrieved from the geotechnical reports and hydraulic modeling.

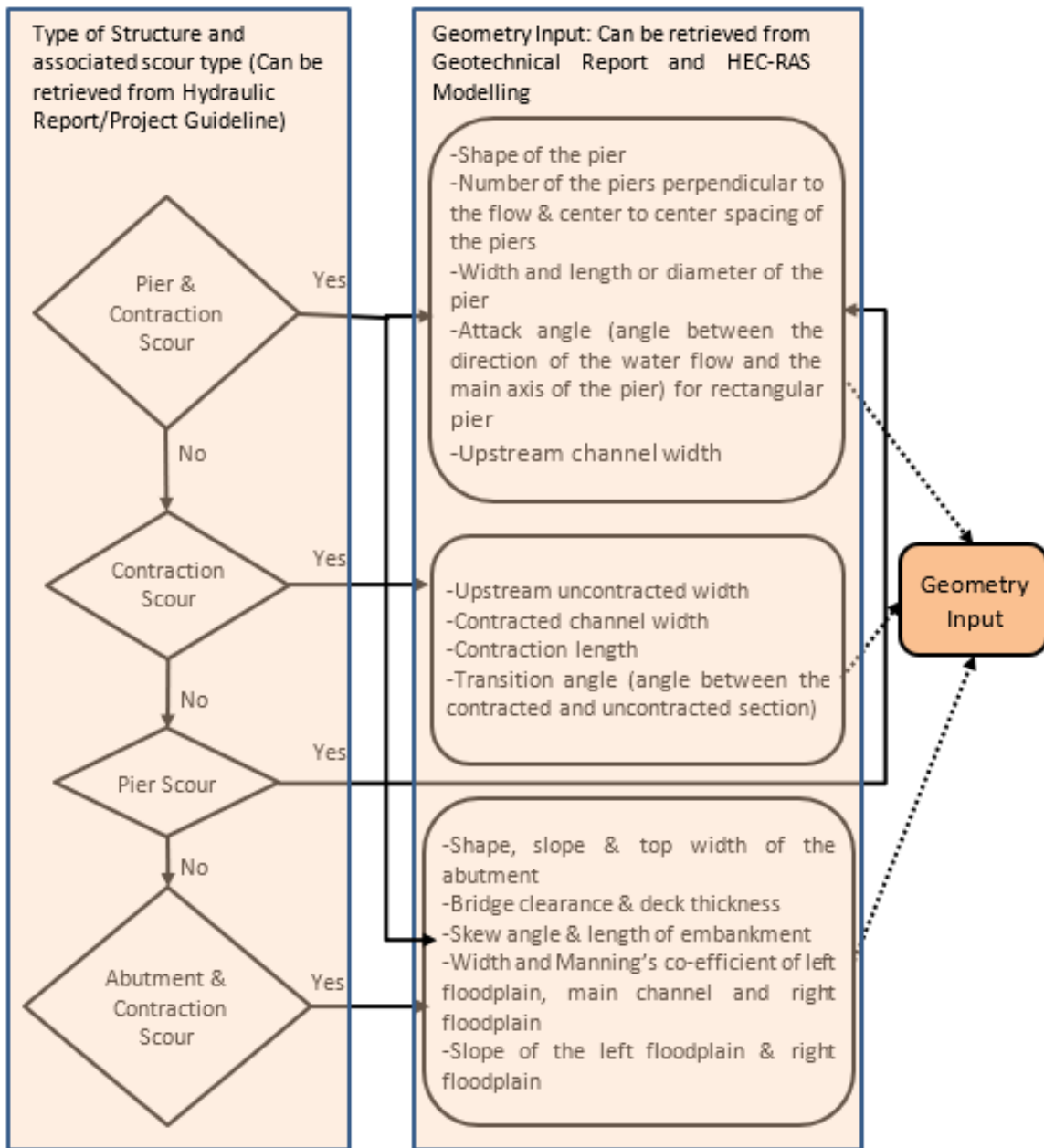


Figure 6.3 Flow-chart showing the steps for obtaining the geometry inputs for SRICOS-EFA

The water input flow chart (Fig. 6.4) illustrates the idea that the information needed for the SRICOS-EFA software comes from four different paths (sources). All the paths reach the final node in two steps. The first path starts with the field observation, hydraulic report, and/or hydraulic modeling, which imparts Manning’s ‘n’. Both the second and the third path start with the hydraulic model, which provides information regarding water depth corresponding to several discharges and velocity depth corresponding to several discharges. The fourth path starts with the USGS website, which can provide daily discharge values recorded at the nearest gaging station since the establishment of the structure. All this information obtained in the second step of each path is the data required for the water input category.

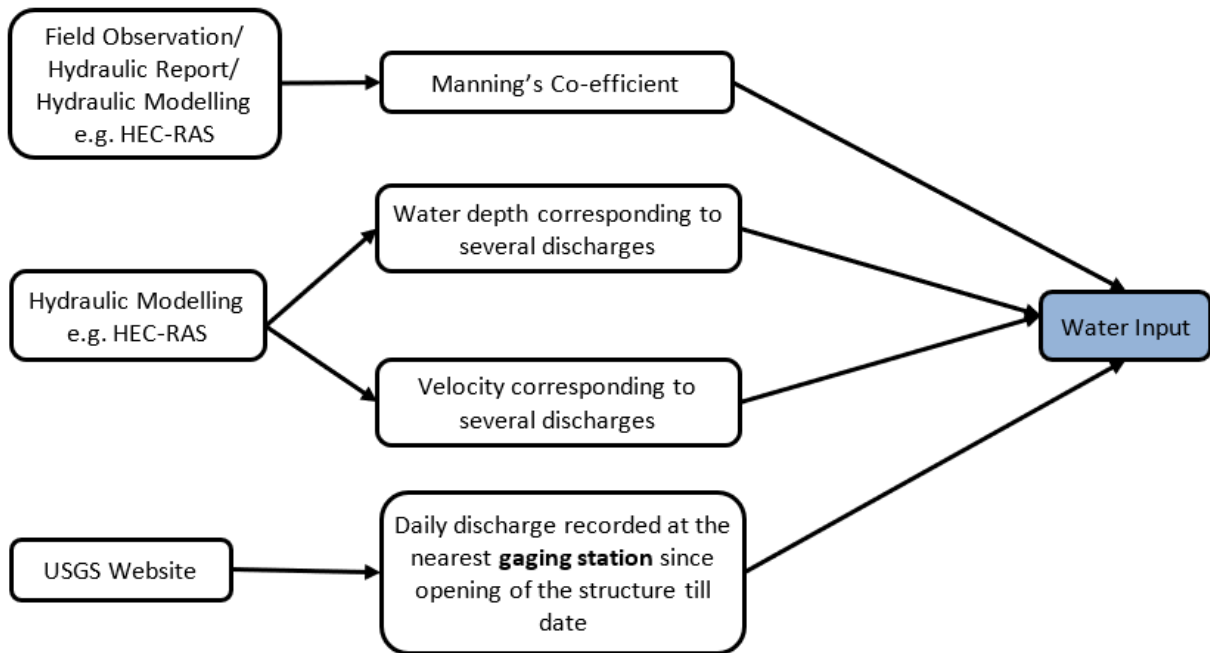


Figure 6.4 Steps for obtaining the water input categories for SRICOS-EFA

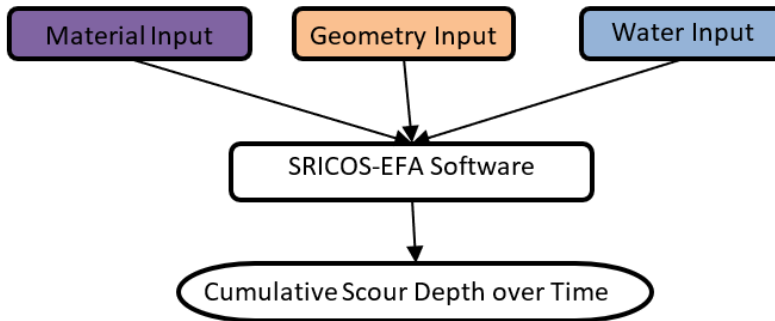


Figure 6.5 Conceptual flow chart of SRICOS-EFA

When all the input categories, i.e., material input, geometry input, and water input are obtained, they are finally fed to the SRICOS-EFA software (<https://ceprofs.civil.tamu.edu/briaud/sricos-efa.htm>) to get the cumulative scour depth over time (Figure 6.5).

#### 6.4 EIM

Though the EIM was developed for soft rock, this method can also be used for cohesive soil strata. Water and geometry categories of input are the same for both types of earth strata: the depth and slope of the design discharge obtained from the hydraulic model and pier width perpendicular to the flow direction. If the earth stratum is a rock layer, information like the rock joint frequency and their condition set, joint infilling and their condition, and dip angle and direction are needed. Such information can be obtained either from the field observations or geotechnical report. If the earth stratum is a cohesive soil layer, borehole samples are needed for lab testing for obtaining the UCS, or vane shear strength and the consistency of the soil layer.

Figure 6.6 illustrates how the EIM works for a rock layer. This method starts from multiple initial points where the first starting point is either the geologic information obtained from the field observations or geotechnical report to extract information like the number of joint/fissure set, joint spacing, joint condition, the ratio of joint spacing, condition of joint gouge/infilling, dip direction, and dip angle.

The second starting point is the rock core collection for later lab tests. The RQD and UCS are obtained from the tests and finally used together with the information obtained from the first starting point to get the erodibility index and the critical stream power of the rock layer. The third point is the hydraulic model for getting the depth of the approaching flow and the slope of the energy grade line for the design discharge, which are used together in the scour depth equation (Eq. 3.15) to get the stream power of the approaching flow for the design discharge. The fourth and the fifth initial starting points lead to a ratio of any depth and width of the pier perpendicular to the flow direction, which eventually provides relative stream power using Eq. 3.16. Results obtained from the first two points and those from the last three points then enter a decision box, which ultimately decides whether there will be scour at the depth of interest. This method recommends starting the calculation at a smaller depth and continuing the calculation until a scour resistant earth layer is reached.

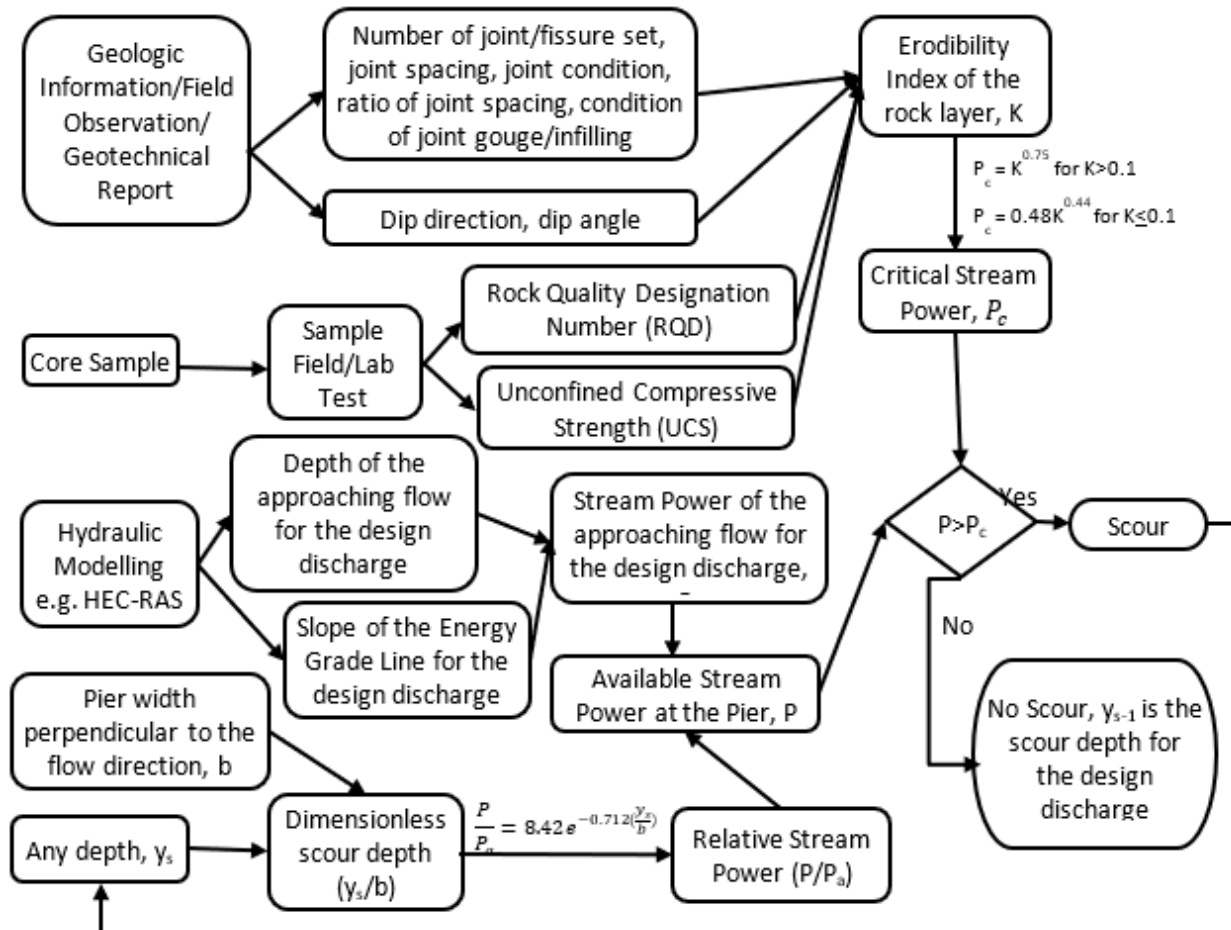


Figure 6.6 Flow-chart showing the steps for scour analysis using the EIM for rock

The use of EIM for cohesive soils is like the EIM for rock, except for the erodibility-determining step. Here, the erodibility index determination starts from the collection of borehole samples for later lab tests or field tests for the sample consistency and USC or Vane Shear Strength. These parameters are used to find the erodibility index and critical stream power of the soil layer. Figure 6.7 represents the steps of the EIM for cohesive soil layers.

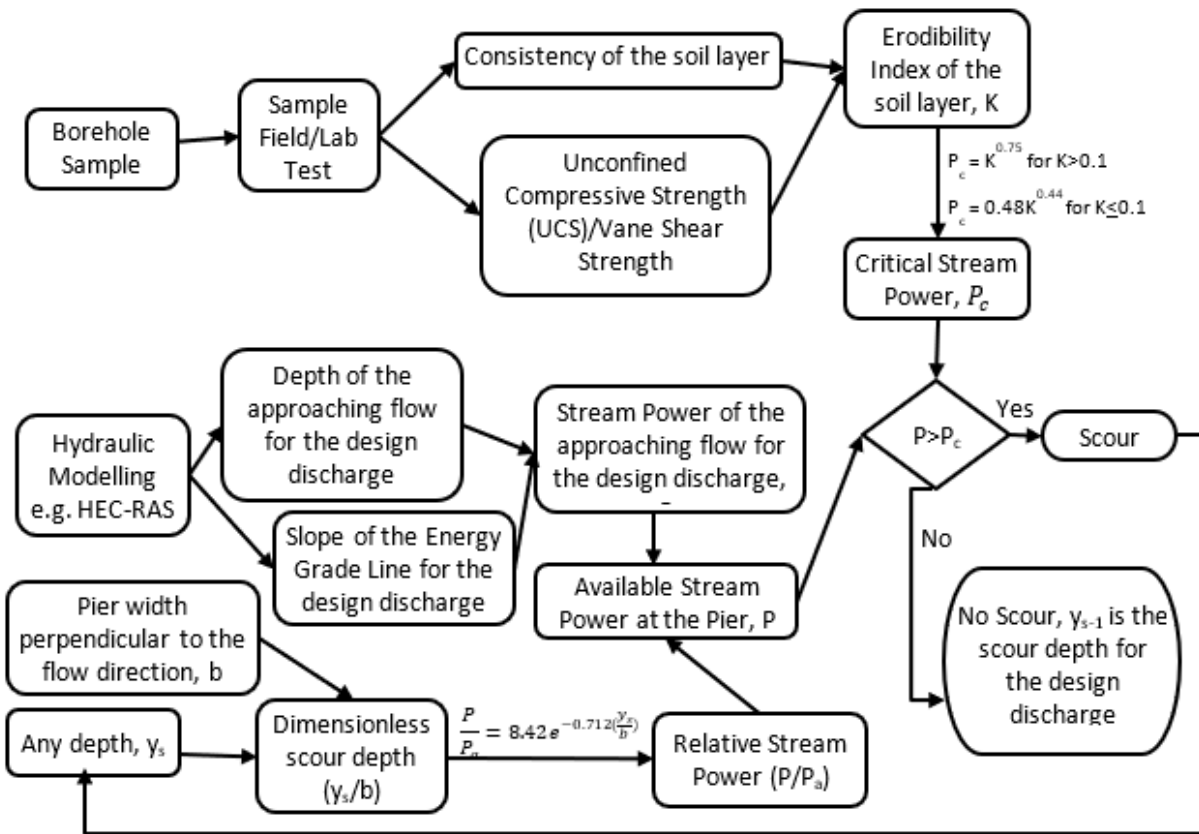


Figure 6.7 Flow-chart showing the steps for scour analysis using the EIM for cohesive soil layers

## 6.5 GSN

If the earth layer is hard rock, the GSN can be used to analyze the scour depth. The first input needed by this method is the Geotechnical Scour Number (GSN), which can be obtained from a modified slake durability test performed on any hand sample or core sample from the site. Another two input types are the stream power corresponding to multiple discharges and daily stream flow since the installation of the structure. The daily stream flow data can be obtained from hydraulic modeling, e.g., HEC-RAS modeling with gage data from nearby USGS stations.

The steps involved in the GSN method are shown in the flowchart of Figure 6.8. As can be seen, the method has three paths that eventually meet at one point to provide the final output. The first path starts with the sample collection to the lab test, i.e., modified slake durability test on the sample. The GSN is directly obtained from the lab test and later used in scour depth calculation. The second path starts with hydraulic modeling which provides the stream power corresponding to several discharge values. Since the GSN method needs cumulative stream power over time, stream powers corresponding to several discharge values are used to formulate an equation for the stream power ( $P$ ) in terms of discharge ( $Q$ ) using the power law. The daily discharge values obtained from the element of the third path, USGS website, are combined with the stream power equation from the second path to finally get the cumulative stream power. This cumulative stream power works with the GSN from the first path to provide the cumulative scour depth over time.

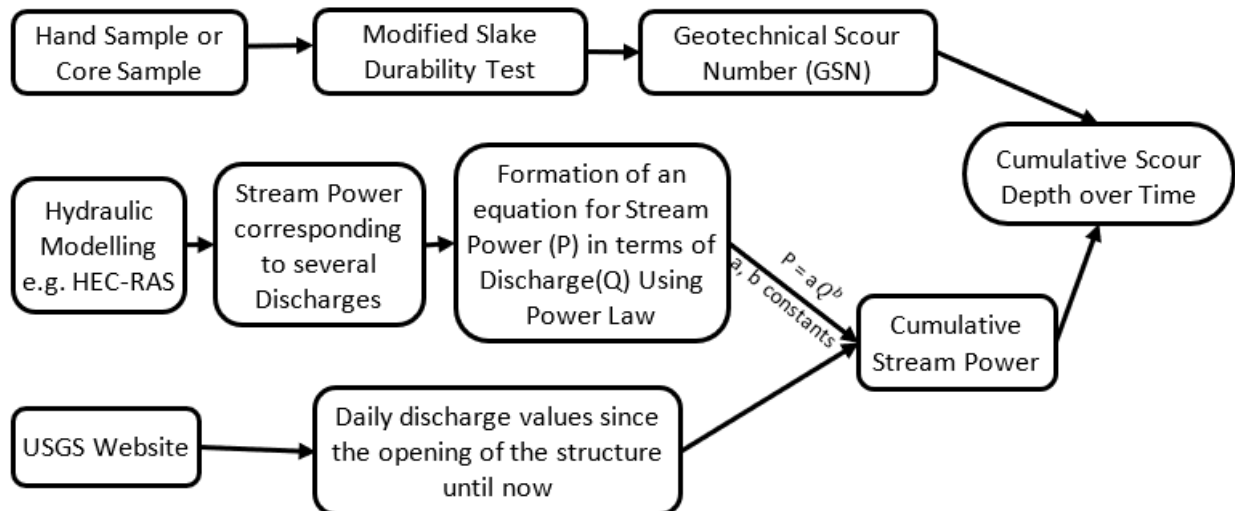


Figure 6.8 Flow-chart showing the steps for scour analysis using the GSN method

## Chapter 7 Conclusions

### 7.1 Summary of Major Findings

This project primarily consists of surveys via both a literature review, interviews and questionnaires for understanding the current state of practice for scour analysis in cohesive soils and scour-susceptible rock, and the selection, implementation, and adjustments of suitable analysis methods for applications in Michigan. The research team evaluated the existing scour analysis methods including sampling, testing, and bridge scour calculations for cohesive soils and scour-susceptible rock. Implementation of three selected bridge scour calculation methods were performed at four bridge sites in Michigan to understand the applications of these methods in Michigan, as well as sampling and testing methods that are needed for their applications. The sites were selected to comprehensively consider both earth material types, i.e., two bridges founded on cohesive soil and two bridges founded on bedrock, and geological conditions, i.e., two sites in Upper Michigan and two in Lower Michigan.

The research started with a state-of-the-practice survey including the scour susceptibility of bridges on these earth strata, sampling, and erodibility testing techniques, scour depth calculation procedures, and practices of the other state DOTs. Emphasis was placed on three major scour analysis methods: the SRICOS-EFA and EIM, which can be used for both cohesive soils and rock, and the GSN, which can be used for rock. Implementations of these methods were carried out for the four selected bridge sites to understand their input and testing required to obtain such input, detailed procedures for their applications in Michigan, with information from typical plans and geotechnical reports, and factors and issues that can significantly affect the analysis results. Based on the implementation, Michigan's bedrock geology and a rock classification for bridge scour were presented.

Aiming at improved scour calculation in clay and rock, calculation methods were paid primary attention in this study, though sampling and testing methods that are needed for supporting the implementation of such methods, i.e., for acquiring the model input parameters, such as material properties, were also reviewed and discussed. Overall, the development and application of scour analysis methods in cohesive soils and scour-susceptible rock are still in a preliminary stage in the

U.S., according to the state-of-the-practice survey. This project was focused on the selection, testing, and adjustments of existing methods for use in Michigan. The three selected methods, i.e., SRICOS-EFA, EIM, and GSN, were concluded to be the best.

Among the three methods, the SRICOS-EFA is recommended for cohesive soils, whereas its application in rock is questionable. The SRICOS can be used in two different ways. In a simple way, the method can be applied with information that is easily available for most existing and new bridge projects, e.g., conventional soil properties from geotechnical reports, structural information from plans, hydraulics information from HEC-RAS simulation with flow data from nearby USGS gaging stations. This method can also be employed at bridge sites without hydraulic data. However, in that case, we can only obtain an equilibrium scour depth corresponding to the selected design discharge event instead of a variation of the scour depth with time, which can be obtained when hydraulics information is available. In this simple way, assumptions need to be made to correlate conventional material properties/classifications with scour characteristics of the material as input for the scour calculation. The sensitivity analysis in this study indicated that such assumptions may lead to a high variance in the calculated scour depths, e.g., 60% at Pier #1 of M-43 over the Grand River. In a more detailed analysis, testing of soil samples with the EFA is carried out for obtaining the erosion characteristics of the material to replace the assumptions. Unfortunately, only EFA testing results are available in this study, and no field scour depth measurements are available. Thus, a quantitative evaluation of the detailed analysis with the simple analysis results could not be obtained. However, the validity of the SRICOS-EFA method has been confirmed in the literature. Therefore, it is recommended that the SRICOS is used with the EFA whenever possible for high-accuracy scour analysis. The use of other tests such as the RETA and JET to replace the EFA is also possible, but extra effort may be needed to calibrate/convert the test results. When EFA test results are absent, scour analysis can still be conducted, but such analysis needs to be carried out very carefully, and users of the scour analysis results, e.g., geotechnical engineers for foundation design, need to be aware of the risk. The research team suggests using sensitivity analysis with different assumptions to better demonstrate possible scour depths.

The EIM is recommended for analyzing the quarrying and plucking mode of scour in rock. However, close attention needs to be paid to the use of this method in Michigan. First, the use of

this method in Michigan may be limited due to the relatively rare existence of highly weathered and highly fractured rocks. Due to Michigan's history of glaciation, primarily "weak rocks" on the ground surface, e.g., with lots of fractures and heavy weathering situations, have been removed. In addition, some literature and field observations also indicated that the stream power at normal bridge sites rarely predicts severe scour in the quarrying and plucking mode in common rocks in Michigan. As a result, unless highly fractured or highly weathered rock is observed in situ, the quarrying and plucking mode of scour may not be a major concern. Second, it is hard to identify appropriate sampling methods to obtain samples needed for the EIM. The EIM requires input such as the UCS and RQD (part of the RMR) as well as other geological characteristics of the rock, such as the number of joint sets, joint roughness, joint alteration, and block dimensions (ratio between length and thickness). These properties as well as appropriate samples for measuring these properties are not easy to obtain. The RMR was proposed for construction in rock such as tunneling and mining, therefore, it is not a perfect fit for scour considerations. Rock coring for obtaining samples to measure the UCS and RQD may produce rock samples with engineering properties that are significantly different from those of the natural rock. For example, coring in hard rocks in the U.P., which are highly resistant to bridge scour, can generate highly fractured rock due to the stresses induced by drilling. Use of such rock samples can lead to false testing results, indicating the rock as scour-susceptible. In addition, the geological characteristics of rock mentioned above are usually absent in geotechnical reports. Therefore, it is recommended to include such information when developing future geotechnical reports for bridges. Finally, the EIM is not recommended for cohesive bed conditions, due to its inconsistency of results in the cases analyzed.

The GSN can be used for analyzing the abrasion mode of scour at bridges founded on rock, which may be very common in Michigan. Scour caused by grain-scale wearing of rocks is a primary concern in sedimentary rocks in the Lower Michigan, especially those with a considerable content of clay-like minerals. However, the use of the GSN requires results from the modified slake durability test. Unfortunately, no testing data is available at the four selected sites. Due to this reason, the GSN values from existing studies for rocks that are similar to those at the selected site were used in this study. Further sensitivity analysis with different assumed slake durability index values resulted in a variance of 81% in the scour depth predictions for the bedrock of M-43 over the Grand River. The analysis results also indicated that the abrasion mode of scour may not be a

concern unless very highly erodible sedimentary rocks such as soft shale are present. But for design purposes, it is recommended to perform a modified slake durability test to get accurate material properties for calculating the scour depth attributed to the abrasion mode of scour in rock.

Compared with MDOT's current calculation method of bridge scour, i.e., an equation based on cohesionless materials (sand) from HEC-18 Edition 4, the use of the SRICOS-EFA can possibly estimate scour depths that are smaller and better reflect the field conditions. The EIM usually yielded predictions that are much smaller than those obtained with the MDOT's current method. Calculations with the GSN obtained negligible scour depths in all cases. Therefore, while it is hard to tell whether the three methods are more accurate than the current method due to the absence of field measurements of scour depth, we can confirm that the current method will yield scour depth predictions in cohesive soils and erodible rock that are possibly much higher or even much higher than the three newly-tested methods, especially in rock. Considering the consensus that the current method tends to overpredict the scour depth and has led to over-conservative bridge foundation designs in Michigan, it is reasonable to conclude that the three new methods are better options for cohesive soils and erodible rock.

In addition to the above concluding remarks on the three methods, the application of the three methods to Michigan geological and hydraulic conditions also yielded the following conclusions.

The SRICOS-EFA and GSN methods were originally proposed for obtaining cumulative scour depth over time, for which daily gage data is a required parameter. However, the absence of (USGS) gaging stations near the study site is not rare. This study presented a way of applying the selected methods in such cases.

Both the SRICOS-EFA and EIM are applicable for multi-layer earth strata. By contrast, the GSN method cannot be directly used for considering multi-layer strata. However, the GSN method was developed for abraded erodible rock (Keaton et al. 2012). Generally, this type of rock is very thick and the scour depth in such strata rarely exceeds the layer thickness within the life span of the bridge.

A direct comparison of the output results from different methods of the same site was not possible since the SRICOS-EFA and GSN have been applied for obtaining the cumulative scour depth and

the EIM has been applied for attaining the scour depth for design discharges. Also, the GSN can only be applied for the rock strata, whereas both the EIM and SRICOS-EFA can be applied to both cohesive soils and rock.

The geological information and rock classification for scour considerations in Chapter 5 can be used to obtain a rough estimate of rock conditions, possible scour mode(s), and the need for further testing. The classification indicates that most of the rocks in the Lower Peninsula can possibly be susceptible to at least one mode of scour when being assessed conservatively. While in the Upper Peninsula, only a small portion of the rocks may need to be considered for one or both modes of scour.

## **7.2 Recommendations for Future Work**

The project provided an opportunity to assess the scour evaluation of bridge scour in cohesive soils and scour-susceptible rocks, considering Michigan geological and geological conditions and existing MDOT implementation. Despite the valuable knowledge and deliverables that have been gained, we also identify several areas that will need future investigations.

- ❖ Further studies are especially needed to validate the results obtained in this research study. Especially, field measurements of bridge scour depths are needed to evaluate the accuracy of the selected methods. These measurements can be obtained manually via field trips or continuously via scour monitoring techniques. Adaptation, modification, and calibration may be needed based on such evaluations.
- ❖ In the implementation of the selected scour analysis methods for the bridge sites in Michigan, many input parameters were assumed because these parameters were not generally documented in the geotechnical reports. This is one major cause of the uncertainty in the scour analysis as tested in this study. It is recommended that future geotechnical reports for bridges founded on erodible rock or cohesive soil include all the parameters needed to conduct the scour analysis calculation using the SRICOS-EFA, EIM, and/or GSN. For the SRICOS-EFA, EFA test results are highly desired. For the EIM, accurate analysis will need the UCS and RQD (part of the RMR) as well as other geological

characteristics of the rock including the number of joint sets, joint roughness, joint alteration, and block dimensions (ratio between length and thickness). In addition, for soft rocks (e.g., sedimentary rocks in the Lower Michigan), it is extremely important to ensure that drilling and coring will not significantly affect the mechanical properties of the collected sample, while for hard rocks (e.g., igneous and metamorphic rocks in the Upper Michigan), scour may not be a concern unless heavy fractures or/and weathering are observed.

- ❖ Case studies that involve the construction of new bridge sites, especially one including cost-benefit analysis, will help MDOT understand the value of adopting the improved evaluation of bridge scour in cohesive soils and scour-susceptible rocks studied in this project. It is better to apply these methods to a real project starting from the site investigation. A comparison between the costs and benefits associated with the designs obtained with the traditional and improved scour evaluation procedures is especially valuable.
- ❖ The erodibility testing procedures recommended for the SRICOS-EFA and GSN methods, i.e., EFA testing and modified slake durability tests, respectively, are still rare in practice and absent in most geotechnical reports. It is recommended to perform these tests for typical clays and rocks that are highly susceptible to the abrasion mode of scour in Michigan. Such tests will help us locate scour-susceptible materials and obtain data and experience with them in Michigan to facilitate future bridge scour design and analysis. FHWA has recently launched a pooled fund program where the EFA along with some other erodibility testing devices will be used to determine the erodibility of the samples from different states. This program is hoped to provide more insights about the EFA performance in this field (TPF 2020).
- ❖ Michigan is a state of unique and diversified geology. However, bridge scour may only be a concern in a few rocks. Future studies are needed to identify a more detailed list of such rock types, especially based on solid lab testing and field projects. This will save significant costs in constructing unnecessary expensive bridge foundations.
- ❖ There is limited information about the scour at abutments on cohesive soil and scour-susceptible rock. It may be necessary to investigate this type of scour if noticeable scour

issues are observed at abutments on cohesive soils and scour-susceptible rocks in Michigan.

## Appendix

The information provided below was collected based on phone calls or a review of the DOTs website. The information, in general, pertains to rock scour. Some information dealing with cohesive soils is also included. The geotechnical section at each DOT was the first contact and their contact information is generally provided.

### Illinois

Website: <http://dot.state.il.us/default.asp>

Contact: William M. Kramer

State Foundations and Geotechnical Engineer (217) 782-7773

[William.Kramer@illinois.gov](mailto:William.Kramer@illinois.gov)

Matt O'Connor

Bridge Hydraulic Engineer [matthew.oconnor@illinois.gov](mailto:matthew.oconnor@illinois.gov)

Manuals: Illinois Drainage Manual, HEC-18, HEC-20 and HEC-23 Highways and River Environment (HIRE).

Scour Calculation Method: Utilizes methods from HEC-18 outlined within Illinois Drainage Manual.

Description: Three manuals are currently available to provide guidance for bridge scour and stream stability analyses. They are part of a set of Hydraulic Engineering Circulars (HEC) issued by FHWA. HEC-18, Evaluating Scour at Bridges Fourth Edition, contains equations for computing scour depths and designing countermeasures. HEC-20, Stream Stability at Highway Structures Third Edition, provides a guide for identifying stream instability problems. HEC 23, Bridge Scour and Stream Instability Countermeasures Second Edition, provides guidelines for the selection and design of appropriate countermeasures to mitigate potential damage to bridges and other highway

components at stream crossings. HEC-18 forms the primary basis of the text in this chapter and is an excellent reference for more in-depth information.

**Current Research:** Illinois DOT has a study under way on the SRICOS-EFA. The Erosion Function Apparatus (EFA) is used in conjunction with the Scour Rate in Cohesive soils (SRICOS) method of scour prediction. The SRICOS method is a site-specific method that involves collecting soil samples and testing them in the EFA. This research includes field verification of the SRICOS-EFA and Synthetic Hydrograph generation for Illinois Streams. The Scour rate in cohesive soils Erosion function apparatus methodology provides a potentially useful methodology for assessing scour in cohesive soils. The overall objective of this study is to test the SRICOS-EFA method for estimating scour depth of cohesive soils in Illinois Streams.

**Past Research:** None

## **Indiana**

Website <http://www.in.gov/dot/>

Contact: Bill Dittrich

Hydraulics Engineer Supervisor 317-232-5474

[bdittrich@indot.in.gov](mailto:bdittrich@indot.in.gov)

**Manuals:** The Indiana Design Manual: Hydrology and Hydraulics, HEC-18 and HEC-20, AASHTO Model Drainage Manual.

**Scour Calculation Method:** Utilizes methods from HEC-18 and AASHTO Model Drainage Manual.

**Description:** Before the various scour forecasting methods for contraction and local scour can be applied, it is necessary to obtain the fixed-bed channel hydraulics, estimate the profile and planform scour or aggradation, adjust the fixed bed hydraulics to reflect these changes, and compute the bridge hydraulics. Refer to Ch. 10 AASHTO Model Drainage Manual, Chapter 10

for combining the contraction and local scour components to obtain a total scour. There are two methods described within this manual, Indiana DOT typically uses method one. In Method 1, armoring is not a concern or precise scour estimates are not necessary and in Method 2, armoring is of concern and more precise scour estimates are pertinent. INDOT typically utilizes method one. Method 1 is

- ❖ Estimate the natural channel's hydraulics for a fixed bed condition based on existing conditions.
- ❖ Assess the expected profile and plan-form changes.
- ❖ Adjust the fixed bed hydraulics to reflect any expected profile or plan-form changes.
- ❖ Estimate contraction scour using the empirical contraction formula and the adjusted fixed bed hydraulics, assuming no bed armoring.
- ❖ Estimate local scour using the adjusted fixed-bed channel and bridge hydraulics, assuming no bed armoring.
- ❖ Add the local scour to the contraction scour to obtain the total scour. If contraction scour is negative, then use zero for contraction scour.

General Description of Scour Analysis and Computations: Decide which analysis method is applicable. Method 1 shall be used to evaluate existing bridges to identify significant potential scour hazards or, where armoring is obviously not of concern, on a proposed bridge. Method 2 should be used to evaluate bridges where significant armoring may occur. Step 2. Determine the magnitude of the 100-year flood and the 500-year super flood. Step 3. Develop a water surface profile through the site's reach for fixed bed conditions using WSPRO or HEC-2. Step 4. Obtain the variables necessary to perform contraction and local scour. Step 5. Compute the predicted scour depths using the equations in HEC-18 for contraction and pier scour for the 100-year and 500-year floods or an overtopping flood of a lesser recurrence interval.

Current Research: None Past Research: None

Additional Sources: Through a conversation with Bill Dittrich, many printed sources not updated and limited financial resources therefore no research is being conducted.

## **Iowa**

Website: <http://www.dot.state.ia.us/>

Contact: Dave Claman, P.E.

Preliminary Bridge Engineer

Office of Bridges and Structures, Iowa DOT [david.claman@dot.iowa.gov](mailto:david.claman@dot.iowa.gov)

(515) 239 - 1487

Manuals: Use Appendix C from Office of Bridges and Structures HEC-18

Scour Calculation Method: At this time, IDOT recommends not using FHWA's abutment scour equations or, at most, use them with caution. However, be aware that abutment scour can occur. Concerning pier scour, the equation in HEC-18 generally gives reliable results. However, a much simpler method that gives very similar results is found in Iowa Highway Research Board's Bulletin No. 4, "Scour Around Bridge Piers and Abutments," by Emmett M. Laursen and Arthur Toch, May 1956. This method for estimating pier scour can be used in most cases instead of the methods in HEC-18.

Description: The Federal Highway Administration has attempted to find the best equations and published them in HEC-18. HEC-18 contains equations for contraction scour, abutment scour, and pier scour. The contraction scour equations are the best available equations of their type and sometimes provide reliable estimates, although these estimates still need to be evaluated considering soil types, site scour history, etc. The abutment scour equations frequently give questionable estimates. Because of comments similar to this from various states, FHWA is conducting additional research to develop new methods. For contraction scour, use HEC-18. Most Iowa stream channels will be live-bed. In other words, the velocities in the channel will be high enough to cause movement of the soil particles in the streambed. In order to be sure if the channel is live-bed, Chapter 2 in HEC-18 gives a simple equation to calculate the velocity needed to cause

movement of the soil, Live-bed scour from HEC-1 and, clear-water scour from HEC-18 do not calculate abutment scour at this time due to this questionable equation.

Current Research: Research is being performed at the University of Iowa's Hydraulic Institute, NCHRP 24-20 which is reviewing abutment scour in compound channels.

Past Research: The Center for Transportation Research and Education at Iowa State University has released a report that examines the first integral abutment bridge in the state of Iowa that utilized precast, prestressed concrete piles in the abutment. Use "Scour Around Bridge Piers and Abutments", Emmett M. Laursen Highway Research Board, Bulletin No. 4, 1956. This report outlines procedures both field and laboratory for the investigation of scour around piers and abutments. The material used was sand. ("Scour at Bridge Crossings," Emmett M. Laursen Iowa Institute of Hydraulic Research)

## **Kansas**

Website: <http://www.ksdot.org/>

Contact: Tom Allen

Publications Writer [thallen@ksdot.org](mailto:thallen@ksdot.org)

Manuals: KU-HR Bridge Scour Program User's Manual First Edition

Description: This study was performed to develop a computer program for analyzing bridge scour. The program is referred to as KU-BSP. The visual basic program used the methods presented in HEC-18 and the hydraulic modeling results of HEC-RAS Version.

The program allows users to compute contraction, abutment, and pier scour at bridges using hydraulic and geometry parameters from HEC-RAS output. The complex pier scour calculations presented in HEC-18 can be used with this program. This option is not available in scour module of HEC-RAS 3.1.2. This document outlines the functions of KU-BSP, the compatibility with HEC-RAS, and is an overall step-by-step user- friendly manual for the KU-BSP program.

There are three types of scour incorporated into KU-BSP, Contraction Scour, Pier Scour, and Abutment Scour. Contraction Scour is based off of HEC-18 and incorporates either Live Bed Scour or Clear Water Scour. The Pier Scour is based off of HEC-18 and incorporates the CSU equation. In addition, complex pier scour analysis is included, where either the footing (pile cap) or the footing and the pile group are exposed to flow. Each of these factors can be contributors to pier scour. Therefore, utilizing superposition, total pier scour may be determined by adding the three components (pile cap, pier stem, and pile group). Abutment Scour is based on HEC-18 Foehlich's live-bed abutment scour equation and the HIRE live bed abutment scour equation. The KU-BSP may be used to account for the hydraulic effect of contraction scour before computing pier scour and/or abutment scour.

Current Research: None

Past Research: None

## **Kentucky**

Website: <http://www.transportation.ky.gov/default2.html>

Contact: David Moses

Chief Drainage Engineer [david.moses@ky.gov](mailto:david.moses@ky.gov)

Manuals: Drainage Guidance Manual Ch.8 Bridges, Correlation of Rock Quality and Rock Scour Around Bridge Piers and Abutments Founded on Rock, HEC-18, and HEC- 20.

Scour Calculation Method: Refer to HEC-18 and HEC-20 for bridge scour evaluation.

Description: Calculate the 100-year and 500-year storm and design bridge according to larger scour potential.

Additional Sources: Kentucky Transportation Center, <http://www.ktc.uky.edu/>

Current Research: An investigation on three-sided bottomless culvert scour countermeasures research.

Past Research: Correlation of Rock Quality and Rock Scour Around Bridge Piers and Abutments Founded on Rock. There is significant information on local scour for unconsolidated alluvial material, however, there is a lack of information pertaining to scour on abutments and piers located on rock. The purpose is to study is to evaluate scour around bridge piers and abutments founded on rock. [http://www.ktc.uky.edu/Reports/KTC\\_99\\_57\\_SPR\\_94\\_157.pdf](http://www.ktc.uky.edu/Reports/KTC_99_57_SPR_94_157.pdf)

## **Maryland**

Website: <http://www.mdt.state.md.us/mdta/servlet/dispatchServlet?url=/Home/main.jsp>

Contact: Stan Davis

410-545-8362

[SDavis6@sha.state.md.us](mailto:SDavis6@sha.state.md.us)

Andrzej Kosicki

Assistant Division Chief - Bridge Design Division [akosicki@sha.state.md.us](mailto:akosicki@sha.state.md.us)

Manuals: Manual of Hydrologic and Hydraulic Design Ch. 11, HEC-18, HEC-20, HEC- 23, HIRE, AASHTO Model Drainage Manual, 1998, AASHTO Standard Specifications for Highway Bridges, Sixteenth Edition, 1996 and including all Interim Revisions through 2002, Corps of Engineers Hydraulic Engineering Center, UNET—One Dimensional Unsteady Flow Through a Full Network of Open Channels, User's Manual, CPD-66, Version 3.1, 1996.

Scour Calculation Method: Reference Manual of Hydrologic and Hydraulic Design Ch. 11 which refers to HEC-18.

Description: This chapter incorporates the recommendations and policy guidance of various FHWA, AASHTO, and ASCE manuals and guidelines. The FHWA Manuals have served as basic

guidelines in the preparation of Chapter 11. The FHWA guidance has been expanded on or modified where necessary in keeping with the experience and practices of the Office of Bridge Development (OBD) as set forth in this Manual for Hydrologic and Hydraulic Design.

One-dimensional hydraulic models such as the Corps of Engineers HEC-RAS model is commonly used for this purpose. However, sites with complex flood flow patterns may warrant the use of a two-dimensional model, such as the FESWMS model, to establish the hydraulic flow conditions. The ABSCOUR Program is to be used to estimate scour at bridges and bottomless arch culverts.

Current Research: None to date

Past Research: Estimation of long-term bridge pier scour in cohesive soils at Maryland bridges using the EFA/SRICOS. This study consisted of three stages, using the erosion function apparatus (EFA) to characterize cohesive soils at selected bridge crossing sites in Maryland, developing a method to generate synthetic discharge hydrographs for ungaged sites in Maryland to provide the required inputs to the SRICOS; and based on inputs from the first two stages, using the SRICOS method to predict bridge pier scour at the selected sites. This thesis comprises stages 1 and 3. Stage 2 was performed at the University of Maryland by other personnel and is briefly described in this thesis as relevant to stages 1 and 3.

## **Minnesota**

Website: <http://www.dot.state.mn.us/>

Contact: Andrea Hendrickson

State Hydraulic Engineer 651-366-4466

[andrea.hendrickson@dot.state.mn.us](mailto:andrea.hendrickson@dot.state.mn.us)

Manuals: Minnesota Department of Transportation Bridge Scour Evaluation Procedure for Minnesota Bridges. General guidelines for monitoring bridges are included in the

Mn/DOT Flood Response Plan for state bridges and the Bridge Scour Monitoring Plan for Local Roads. Bridge Inspection Manual contains the FHWA National Bridge Inventory Rating System and Sufficiency Rating, MNDOT Smart Flag Coding.

Scour Calculation Method: HEC-18 and HEC-20. Additional considerations provided in Practical Methods for Calculating Scour Practical Method for Calculating Scour by E.V. Richardson and J. R. Richardson, located within the appendix of Bridge Scour Evaluation Procedure for Minnesota Bridges, and utilizes the same equations as HEC-18 but gives detailed instructions and examples.

Description: MnDOT has a primary screening process. This process leads to determining whether the bridge is low risk, scour-susceptible, or unknown. Next, a secondary screening process determines whether the bridge should be monitored or move to a Level 1 evaluation. The secondary screening process evaluates seven key parameters, such as historical scour performance, scour resistant foundations, debris and blockage, geomorphic conditions, hydraulic conditions, structural conditions, and special low risk conditions.

The Level 1 evaluation then determines the MnDOT Scour Codes or determines if a Level 2 evaluation is necessary. Within the Level 2 evaluation, the MnDOT scour codes can be determined.

Current Research: None

Past Research: Analysis of Real Time Data by FHWA in response to flooding in 1997. USGS bridge scour data collection team to collect real-time scour (contraction and local) measurements at contracted bridge openings. An analysis of two sites that were surveyed during the April 1997 flooding. Research for Bridge Scour Evaluation Procedure for Minnesota Bridges March 1995. Effects of Footing Location on Bridge Pier Scour by J. Sterling Jones, Roger T. Kilgore, and Mark P. Mistichelli. This was a laboratory study conducted to investigate the effects of placement of footing versus pier scour.

## **Missouri**

Website: <http://www.modot.mo.gov/>

Contact: Keith Ferrell

Structural Hydraulics Engineer [keith.ferrell@modot.mo.gov](mailto:keith.ferrell@modot.mo.gov)

Manuals: HEC-18, Bridge Design Manual Section 8.2 Missouri Department of Transportation. (2004), HEC-20.

Scour Calculation Method: Utilize HEC-18 and are presented in section 8.2 of Missouri DOT Bridge Design Manual.

Description: The methods used to calculate those depths are based on the FHWA HEC-18 publication (13), Abutment scour calculated using FHWA publication Highways in the River Environment (HIRE), which is consistent with the required location of the approaching cross-section in both HEC-RAS and WSPRO. If the threshold is exceeded for any one of the categories, the second stage of the risk analysis process, the Least Total Economic Cost (LTEC) design, should be employed. The FHWA publication HEC-17 provides detailed procedures for performing an LTEC design.

Current Research: None Past Research: None

## **Nebraska**

Website: <http://www.nebraskatransportation.org/>

Contact: Don Jisa

Hydraulics Engineer [djisa@dor.state.ne.us](mailto:djisa@dor.state.ne.us)

Manuals: Nebraska Department of Roads. Bridge Operations and Procedures. (2005). Scour

Calculation Method: Currently use HEC-18 and HEC-20.

Description: In process of updating Bridge scour documents. Current Research: None

Conducted Research: None

## **New Jersey**

Website: <http://www.nj.gov/transportation/eng/>

Contact: Jose A. Lopez

Supervising Engineer Dot.state.nj.us

Manuals: Current (2002) AASHTO Manual for Condition Evaluation of Bridges, Current (2002) AASHTO Standard Specification for Highway Bridges, Current FHWA Bridge Inspector Reference Manual, 1987 AASHTO Manual for Bridge Maintenance, 1994 NJDOT Underwater Inspection and Evaluation Guidelines Manual, 2003 FHWA Recording and Coding Guide for the Structure Inventory & Appraisal (SI&A) of the Nation's Bridges, 2003 NJDOT Recording and Coding Guide, 2003 NJDOT Pointis/Seismic manual, 1998 AASHTO Movable Bridge Inspection Maintenance Evaluation Manual and Standard Specifications for Movable Highway Bridges, 2006 Pointis Lite User's Manual. HEC-18 and HEC-23, Bridge Scour Evaluation Program Plan of Action Report.

Scour Calculation Method: Refer to Plan of Action Report which refers to HEC-18 Description: Bridge Scour Evaluation Program Plan of Action Report

The scour evaluation program started with the selection of a technical and management consultant to assist the department in the development and implementation of the program.

Divided into 4 stages, Stage 1 screening and prioritization process was developed to establish a logical sequence and focus on most critical needs. This process included the use of standard data forms and criteria for coding appraisal factors related to each bridge's potential susceptibility to scour damage. These key scour factors were, Type of Foundation, Bridge Characteristics, Collapse Vulnerability, Waterway Characteristics, and History of Scour Problems. The tasks for the Stage 1 program included, the collection of readily available data and field visits by an interdisciplinary team of experienced hydraulic, structural, and geotechnical engineers. Based upon these efforts numerical appraisal ratings were coded for the previously defined key scour factors. The ratings

for the key scour factors were used to determine an overall numerical scour sufficiency rating from 0 to 100, which was used to assess the structure's potential sufficiency to resist scour damage. In addition, the scour evaluation consultants coded each bridge with a prioritization category rating of 1 to 4, which assessed the necessity for in-depth scour evaluations. These ratings were then used to identify the bridges that were most susceptible to scour and required an in-depth evaluation to determine whether they were scour-critical.

Stage 2, In-depth scour evaluation. The procedure recommended by HEC-18 for conducting a scour evaluation study includes a determination of waterway characteristics for flood flow conditions and the calculation of potential scour depths at the substructure units, followed by an assessment of the stability. Use Bridge Scour Evaluation Program Guidelines Manual for Stage 2 in-depth scour evaluation (1994) for procedures and scope of work for scour analysis. The scope of work included within Stage 2 includes data collection and review, field investigation, determination of scour analysis variables, scour analysis and evaluation, evaluation of countermeasures, and bridge scour evaluation report.

Current Research: None.

Past Research: None.

## **New York**

Website: <https://www.nysdot.gov/portal/page/portal/index>

Contact: Scott Lagace

Bridge Safety Assurance Unit

[slagace@dot.state.ny.us](mailto:slagace@dot.state.ny.us)

Wayne Gannett Hydraulic Engineer [wgannett@dot.state.ny.us](mailto:wgannett@dot.state.ny.us)

Manuals: Bridge Manual NYDOT Structures Design and Construction Division River Engineering for Highway Encroachments. FHWA. HEC18, 20 23 Highways in the River Environment. FHWA.

Scour Calculation Method: Utilize methods outlined in HEC-18, Nordin (1971) Straub (1940), Colorado State University's (CSU) equation, Jain and Fisher's equation, Graded and/or armored streambeds equations, Froehlich's equations.

Description: All bridges over water in New York State are assessed for scour vulnerability using the procedures outlined in the NYSDOT Hydraulic Vulnerability Manual. New bridges are evaluated for scour according to FHWA Hydraulic Engineering Circular No. 18 (HEC-18). HEC-23 is used for countermeasure design. The NYSDOT Hydraulic Vulnerability Assessment (HVA), Scour Analysis (if available), Countermeasure Installed (if present), and Bridge Inspection Erosion ratings are all considered when assigning a code for FHWA Item 113 - Scour Critical Bridges. In accordance with FHWA Technical Advisory T 5140.23, a Plan of Action will be developed for each bridge in New York State which is coded '0'-3' (Scour Critical), '7' (Countermeasures Installed), or 'U' (Unknown Foundation) for Item 113. Part of the Plan of Action for NYSDOT bridges includes placing the bridge on the Flood Watch list, which would then be monitored during a flood event. In addition, some bridges have a post-flood inspection performed after a flood event.

Current Research: None Past Research: None

## **Ohio**

Website:

<http://www.dot.state.oh.us/Divisions/HighwayOps/Structures/Pages/default.aspx>

Contact: Bill Krouse, P.E.

Bridge Hydraulic Engineer (614) 466-2398

[Bill.Krouse@dot.state.oh.us](mailto:Bill.Krouse@dot.state.oh.us)

David Riley, P.E.

State Hydraulic Engineer [david.riley@dot.state.oh.us](mailto:david.riley@dot.state.oh.us)

Manuals and Papers: Bridge Design Manual (BDM) in section 203.3 Scour and FHWA publication NHI 01-001 Evaluation Scour at Bridges fourth edition. ODOT Manual of Bridge Inspection, HEC-18.

Scour Calculation Method: Utilizes methods from HEC-18 referred to in Ohio Bridge Design Manual.

Description: The Department developed an alternative method of scour assessment based upon the observance of geomorphic, hydrologic, and hydraulic features at the bridge site. This assessment is seen as a cost-effective approach meeting the NBIS requirements for evaluating existing bridges without analytical scour computations.

A scour assessment of a bridge using the theoretical scour calculations is a method based on hydrologic and hydraulic analyses of the stream and bridge opening. The method is described in the Bridge Design Manual in section 203.3 Scour and FHWA publication NHI 01-001 Evaluation Scour at Bridges fourth edition (HEC-18).

Current Research: None

Past Research: Time Domain Reflectometry (TDR) scour monitoring.

## **Pennsylvania**

Website: <http://www.dot.state.pa.us/>

Contact: Lance Savant

PENNDOT – BQAD 717-783-7498

[lsavant@state.pa.us](mailto:lsavant@state.pa.us)

Scour Calculation Method: Use DM4 Chapter 7 and FHWA Technical Advisory. Evaluating Scour at Bridges. (T 5140.23 October 1991) for guidance on the methodology.

Manuals: Procedures for Bridge Scour Assessments. Peter J. Cinotto and Kirk E. White. Bridge Safety Inspection Manual 238, AASHTO Manual for the Condition Evaluation of Bridges, DM4 Chapter 7, and FHWA Technical Advisory, Evaluating Scour at Bridges. (T 5140.23 October 1991), Scour Calculator Manual.

Description: Pennsylvania, with the assistance of USGS, has developed Procedures for Bridge Scour Assessments at Bridges in Pennsylvania: This document outlines procedures for assessing bridge scour. Focusing on two methods, field reviewed bridge sites and office reviewed field sites. The field reviewed procedures identify appropriate methodologies and data to collect to analyze bridges' susceptibility to bridge scour. Both these methods then enable the evaluator to identify an appropriate Scour-Critical Bridge Indicator Code (Code) and a Scour Assessment Rating (Rating). This then enables a decision to be made on the appropriate scour countermeasures that are applicable, if any.

In addition, Publication 238 was developed and includes inspection methods, scour assessments, recommendations, and calculations. To combat this loss of structures from the transportation system and protect our valued infrastructure, PA uses a threefold approach:

Underwater inspection of bridge substructure units is used to verify the structural condition of the underwater elements, to verify the integrity of their foundations, and to identify critical anti-scour maintenance needs.

An assessment of the bridges' vulnerability to scour is made so that critical bridges can be identified for closer monitoring and scour countermeasures.

During high water events, bridges whose safety is very susceptible to scour are required to be monitored.

The two acceptable methods of performing scour assessments in PA are:

Theoretical Scour Calculations Use DM4 Chapter 7 and FHWA Technical Advisory. Evaluating Scour at Bridges. (T 5140.23 October 1991) for guidance on the methodology.

PA's Observed Scour Assessment for Bridges methodology. (Procedures for Bridge Scour Assessments at Bridges Pennsylvania outlines this methodology).

The PA OSAB uses an algorithm in a Department software program named SCBI/SAR Calculator to determine the value for BMS Item W06 Scour Critical Bridge Indicator. If the W06 SCBI value from the PA OSAB is based on conditions valid at the time of inspection, it should be used in the inspection as the value for BMS. In addition, a new data item called Scour Assessment Rating (SAR) was developed for the PA OSAB to assist bridge owners with another measure of threat for hydraulic failure of the bridge. The SCBI/SAR Calculator also computes the SAR that ranges from 0 to 100, extremely vulnerable to scour resistant. The SAR analysis also provides a list of potential scour- related deficiencies at the bridge.

Software User's Guide for Determining the Pennsylvania Scour Critical Indicator Code and Streambed Scour Assessment Rating for Roadway Bridges. The Scour Critical Bridge Indicator (SCBI) Code and Scour Assessment Rating (SAR) use algorithms to rate bridge sites for observed and potential streambed scour on the basis of USGS field observations and/or existing PennDOT data. SCBI Code indicates the vulnerability of the bridge to future scour. The SCBI is based on the FHWA code (NBI Item 113) and PennDOT's interpretation of the FHWA Code. The SCBI Code contains a whole number between 9 and 2. Each code number has one or more cases. Codes and cases are not a straightforward numeric sequence; they describe a specific type of site condition only; for example, a Code 6 isn't necessarily better or worse than a Code 5. The SCBI Code and SAR calculator uses various factors from the field or office scour evaluations to determine the SCBI Code for individual subunits of the bridge. The data fields must be complete to determine the SCBI Code for each substructure unit.

The SAR is composed of component values for each bridge subunit and selected site conditions that are combined to provide an overall bridge rating from 0 to 100. It was designed by PennDOT and USGS to incorporate all factors that could lead to hydraulic failure at a bridge site. The SAR indicates the observed scour condition of a bridge site and generally can be interpreted as 100 to 80 =good, 79 to 51, average, 50 to 20= potential problems, and 19 to 0= poor; however, all bridge-site data must be reviewed before making this interpretation.

Current Research: None

Past Research: Scour Calculator Code presents the instructions required to use the Scour Critical Bridge Indicator (SCBI) Code and Scour Assessment Rating (SAR) calculator developed by the Pennsylvania Department of Transportation (PennDOT) and the U.S. Geological Survey to identify Pennsylvania bridges with excessive scour conditions or a high potential for scour. Procedures for Scour Assessments at Bridges in Pennsylvania describes procedures for the assessment of scour at all bridges that are 20 feet or greater in length that span water in Pennsylvania. There are two basic types of assessment: field-viewed bridge site assessments, for which USGS personnel visit the bridge site and office-reviewed bridge site assessments

## **Virginia**

Website: <http://www.virginiadot.org/>

Contact: Mr. Kendal Walus

State Structure and Bridge Engineer [Kendal.Walus@VDOT.Virginia.gov](mailto:Kendal.Walus@VDOT.Virginia.gov)

Mr. John Matthews, P.E.

Assistant State Hydraulic Engineer [John.Matthews@VDOT.Virginia.gov](mailto:John.Matthews@VDOT.Virginia.gov)

Mr. Stephen Kindy, P.E. State Hydraulic Engineer

[Stephen.Kindy@VOT.Virginia.gov](mailto:Stephen.Kindy@VOT.Virginia.gov)

Manuals: HEC-18 Evaluating Scour at Bridges and Hec-20 Stream Stability at Highway Structures, and HEC-23 Bridge Scour and Stream Instability Countermeasures Experience, Selection, and Design Guidance

Scour Calculation Method: Reference Virginia DOT Drainage Manual which references HEC-18 methods.

Description: The VDOT Drainage manual refers to procedures and criteria presented in the FHWA's "Evaluating Scour at Bridges" (HEC-18) and "Stream Stability at Highway Structures" (HEC-20) to determine and counteract the impact of scour and long-term aggradation/degradation at bridges.

Current Research: None Past Research: None

## **West Virginia**

Website: <http://www.transportation.wv.gov/>

Contact: Douglas Kirk

State Hydraulics Engineer [douglas.w.kirk@wv.gov](mailto:douglas.w.kirk@wv.gov)

Manuals: Bridge Design Manual Federal Highway Administration Technical Advisory T5140.23, "Evaluating Scour at Bridges, Design of Riprap Revetment, Hydraulic Engineering Circular No.11," (HEC11), Evaluating Scour at Bridges, Fourth Edition, Hydraulic Engineering Circular No. 18, (HEC-18), Stream Stability at Highway Structures, Third Edition, Hydraulic Engineering Circular No. 20, (HEC-20), Bridge Scour and Stream Instability Countermeasures Experience, Selection, and Design Guidance, Second Edition, Hydraulic Engineering Circular No. 23, (HEC 23)

The WVDOH Drainage Manual, 3rd Edition, 2007 is online at <http://www.transportation.wv.gov/highways/engineering/Pages/publications.aspx>. Relevant chapters are 7 and 10.

Scour Calculation Method: References HEC-18 for Scour computations, no drainage manual available on the website.

Description: All designs will be performed in accordance with the Federal Highway Administration Technical Advisory T5140.23, "Evaluating Scour at Bridges". A DS-34 form will be completed during the design phase of the project. Refer to WVDOH Bridge Maintenance

Directive (BMD) S-102-2 for additional information regarding the DS-34 form. Stated in the WV DOT Bridge Design Manual, scour calculations are based upon the discharge created by the flood of 1% annual incidence of return (Q100) and the “super flood” defined as 0.2% annual incidence of return (Q500). Scour depth, average stone size ( $D_{50}$ ), and any necessary designs shall be based upon the provisions of the following FHWA publications:

Design of Riprap Revetment, Hydraulic Engineering Circular No.11, (HEC11)

Evaluating Scour at Bridges, Fourth Edition, Hydraulic Engineering Circular No. 18, (HEC-18)

Stream Stability at Highway Structures, Third Edition, Hydraulic Engineering Circular No. 20, (HEC-20)

Bridge Scour and Stream Instability Countermeasures Experience, Selection, and Design Guidance, Second Edition, Hydraulic Engineering Circular No 23, (HEC 23)

Current Research: None

Past Research: None

## **Wisconsin**

Website: <http://www.dot.wisconsin.gov/>

Contact: Najoua Ksontini

Bridge Hydraulic Engineer [najoua.ksontini@dot.state.wi.us](mailto:najoua.ksontini@dot.state.wi.us)

Manuals: Bridge Manual, HEC-18 and HEC-20

Scour Calculation Method: Utilizes methods from HEC-18, outlined within Wisconsin Bridge Manual.

Description: Evaluating scour potential at bridges is based on recommendations and background from FHWA Technical Advisory “Evaluating Scour at Bridges” dated October 28, 1991 and

procedures from the FHWA Hydraulic Engineering Circular No. 18, Evaluating Scour at Bridges revised April 1993 (English), November 1995 (Metric), and Hydraulic Engineering Circular No. 20 Stream Stability at Highway Structures, February 1991 (English), November 1995 (Metric).

The bridge design manual contains all formulas used to calculate the three primary forms of scour, aggradation and degradation, and local and contraction scour. Local scour is computed utilizing the Colorado State University equation. Abutment scour is calculated utilizing Froelich's Live-Bed Scour at Abutments and Highways and River Environment (HIRE) equation.

Current Research: None

Past Research: Bridge Scour Monitoring Methods at Three Sites in Wisconsin USGS Report. Two monitoring approaches were employed: (1) manual monitoring using moderately simple equipment, and (2) automated monitoring, using moderately sophisticated electronic equipment.

## **Others**

The research team also contacted the following state DOTs and got feedback: Alabama, Arkansas, California, Florida, Idaho, Louisiana, Nevada, Oklahoma, Oregon, South Dakota, Texas. However, the feedback was not as detailed as the those listed above, and were, therefore, not compiled and listed in this report.

## References

- AASHTO (2010). "AASHTO LRFD Bridge Design Specifications." *American Association of State Highway and Transportation Officials, Washington, D.C.*, Customary U.S. Units, 5th Edition, with 2010 Interim Revisions.
- Abou-Seida, M. M., Elsaheed, G. H., Mostafa, T. M., and Elzahry, E. F. (2012). "Local scour at bridge abutments in cohesive soil." *Journal of hydraulic research*, 50(2), 171-180.
- Annandale, G. (1995). "Erodibility." *Journal of hydraulic research*, 33(4), 471-494.
- Annandale, G. (1999). "Erosion of rock by hydraulic forces." *Proc., Vail Rocks 1999, The 37th US Symposium on Rock Mechanics (USRMS)*, American Rock Mechanics Association.
- Annandale, G., and Smith, S. (2001). "Calculation of Bridge Pier Scour Using the Erodibility Index Method." Golden Associates.
- Annandale, G. W. (2000). "Prediction of scour at bridge pier foundations founded on rock and other earth materials." *Transportation research record*, 1696(1), 67-70.
- Annandale, G. W. (2006). *Scour technology*, McGraw-Hill.
- Annandale, G. W. (2009). "Processes and Proxies Defining Maximum and Time Rate of Scour of Rock around Bridge Piers." *Contemporary Topics in In Situ Testing, Analysis, and Reliability of Foundations*, 514-521.
- Annandale, G. W., and Kirsten, H. A. (1994). "On the erodibility of rock and other earth materials." *Proc., Hydraulic Engineering*, ASCE, 68-72.
- Annandale, G. W., and Smith, S. P. (1998). "Proposed Pier Scour Procedure for Rock Formations." *Proc., Stream Stability and Scour at Highway Bridges: Compendium of Stream Stability and Scour Papers Presented at Conferences Sponsored by the Water Resources Engineering (Hydraulics) Division of the American Society of Civil Engineers*, ASCE, 180-180.

- Annandale, G. W., and Smith, S. P. (1999). "Scour in Erodible Rock I: The Erodibility Index." *Proc., Stream Stability and Scour at Highway Bridges: Compendium of Stream Stability and Scour Papers Presented at Conferences Sponsored by the Water Resources Engineering (Hydraulics) Division of the American Society of Civil Engineers, ASCE*, 77-77.
- Ansari, S., Kothyari, U., and Ranga Raju, K. (2002). "Influence of cohesion on scour around bridge piers." *Journal of Hydraulic Research*, 40(6), 717-729.
- Arneson, L. (2012). "Evaluating scour at bridges." United States. Federal Highway Administration.
- ASTM (2016). "Standard Test Method for Slake Durability of Shales and Other Similar Weak Rocks." *ASTM D4644-16*.
- Bagnold, R. A. (1966). *An approach to the sediment transport problem from general physics*, US government printing office.
- Benedict, S. T. (2014). "Assessment of the NCHRP Abutment Scour Prediction Equations with Laboratory and Field Data."
- Benedict, S. T., and Caldwell, A. (2016). "Development and evaluation of clear-water pier and contraction scour envelope curves in the Coastal Plain and Piedmont provinces of South Carolina." Geological Survey (US).
- Benedict, S. T., Feaster, T. D., and Caldwell, A. (2016). "The South Carolina bridge-scour envelope curves." Geological Survey (US).
- Bieniawski, Z. (1988). "The rock mass rating (RMR) system (geomechanics classification) in engineering practice." *Rock Classification Systems for Engineering Purposes*, ASTM International.
- Bloomquist, D., Sheppard, D. M., Schofield, S., and Crowley, R. W. (2012). "The rotating erosion testing apparatus (RETA): A laboratory device for measuring erosion rates versus shear stresses of rock and cohesive materials." *Geotechnical Testing Journal*, 35(4), 641-648.

- Bloomquist, D. G., and Sheppard, D. M. (2010). "Apparatus for estimating the rate of erosion and methods using the same." Google Patents.
- Bolduc, L. C., Gardoni, P., and Briaud, J.-L. (2008). "Probability of exceedance estimates for scour depth around bridge piers." *Journal of geotechnical and geoenvironmental engineering*, 134(2), 175-184.
- Bollaert, E. (2004). "A comprehensive model to evaluate scour formation in plunge pools." *International Journal on Hydropower & Dams*, 11(1), 94-101.
- Bollaert, E., and Schleiss, A. (2002). "Transient water pressures in joints and formation of rock scour due to high-velocity jet impact." EPFL-LCH.
- Bollaert, E. F. (2010). "Numerical modeling of scour at bridge foundations on rock." *Scour and Erosion*, 767-776.
- Bollaert, E. F., and Schleiss, A. J. (2005). "Physically based model for evaluation of rock scour due to high-velocity jet impact." *Journal of Hydraulic Engineering*, 131(3), 153-165.
- Brandimarte, L., Montanari, A., Briaud, J.-L., and D'Odorico, P. (2006). "Stochastic flow analysis for predicting river scour of cohesive soils." *Journal of hydraulic engineering*, 132(5), 493-500.
- Briaud, J.-L. (2004). *Pier and contraction scour in cohesive soils*, Transportation Research Board.
- Briaud, J.-L. (2008). "Case histories in soil and rock erosion: woodrow wilson bridge, Brazos River Meander, Normandy Cliffs, and New Orleans Levees." *Journal of Geotechnical and Geoenvironmental Engineering*, 134(10), 1425-1447.
- Briaud, J.-L. (2015). "Scour depth at bridges: Method including soil properties. I: Maximum scour depth prediction." *Journal of Geotechnical and Geoenvironmental Engineering*, 141(2), 04014104.
- Briaud, J.-L., Bernhardt, M., and Leclair, M. (2012). "The pocket erodometer test: Development

and preliminary results." *Geotechnical Testing Journal*, 35(2), 342-352.

Briaud, J.-L., Chedid, M., Chen, H.-C., and Shidlovskaya, A. (2017). "Borehole Erosion Test." *Journal of Geotechnical and Geoenvironmental Engineering*, 143(8), 04017037.

Briaud, J.-L., Chen, H.-C., Li, Y., and Nurtjahyo, P. (2004). "SRICOS-EFA method for complex piers in fine-grained soils." *Journal of geotechnical and geoenvironmental engineering*, 130(11), 1180-1191.

Briaud, J.-L., Chen, H.-C., Li, Y., Nurtjahyo, P., and Wang, J. (2005). "SRICOS-EFA method for contraction scour in fine-grained soils." *Journal of geotechnical and geoenvironmental engineering*, 131(10), 1283-1294.

Briaud, J.-L., and Oh, S. J. (2010). "Bridge foundation scour." *Geotechnical Engineering Journal of the SEAGS & AGSSEA*, 41(2), 1-16.

Briaud, J.-L., Ting, F., Chen, H., Cao, Y., Han, S., and Kwak, K. (2001a). "Erosion function apparatus for scour rate predictions." *Journal of geotechnical and geoenvironmental engineering*, 127(2), 105-113.

Briaud, J.-L., Ting, F. C., Chen, H., Gudavalli, R., Perugu, S., and Wei, G. (1999). "SRICOS: Prediction of scour rate in cohesive soils at bridge piers." *Journal of Geotechnical and Geoenvironmental Engineering*, 125(4), 237-246.

Briaud, J., Chen, H., Chang, K., Oh, S., Chen, S., Wang, J., Li, Y., Kwak, K., Nartjaho, P., and Gudaralli, R. (2011). "The SRICOS-EFA Method, Summary Report." *Texas A&M University*.

Briaud, J., Chen, H., Chang, K., Oh, X., and Chen, X. (2009). "Abutment scour in cohesive materials." *NCHRP Report*, 24-15.

Briaud, J., Chen, H., Kwak, K., Han, S., and Ting, F. (2001b). "Multiflood and multilayer method for scour rate prediction at bridge piers." *Journal of Geotechnical and Geoenvironmental Engineering*, 127(2), 114-125.

- Briaud, J., Shafii, I., Chen, H.-C., and Medina-Cetina, Z. (2019). *Relationship Between Erodibility and Properties of Soils*, Transportation Research Board.
- Calappi, T., Miller, C. J., and Carpenter, D. (2010). "Revisiting the HEC-18 scour equation." *Scour and erosion*, 1102-1109.
- Cannon, W., Kress, T., Sutphin, D., Morey, G., and Meints, J. (1997). "Digital geologic map and mineral deposits of the Lake Superior region; Minnesota, Wisconsin, Michigan."
- Cannon, W. F. (1986). *Bedrock Geologic Map of the Iron River 1° X 2° Quadrangle, Michigan and Wisconsin*, The Survey.
- Cannon, W. F., LaBerge, G. L., Klasner, J. S., and Schulz, K. J. (2008). *The Gogebic Iron Range—a sample of the northern margin of the Penokean fold and thrust belt*, US Geological Survey.
- Carpenter, D. D., and Miller, C. (2011). "A critical evaluation of bridge scour for Michigan specific conditions." Lawrence Technological University. Dept. of Civil Engineering.
- Chapuis, R. P., and Gatien, T. (1986). "An improved rotating cylinder technique for quantitative measurements of the scour resistance of clays." *Canadian geotechnical journal*, 23(1), 83-87.
- Chaudhuri, S., and Debnath, K. (2013). "Observations on initiation of pier scour and equilibrium scour hole profiles in cohesive Sediments." *ISH Journal of Hydraulic Engineering*, 19(1), 27-37.
- Chaudhuri, S., Debnath, K., Roy, S., and Manik, M. K. (2019). "Flume study on contraction scour in clay–sand mixed cohesive bed." *ISH Journal of Hydraulic Engineering*, 25(1), 79-86.
- Chaulagai, R., Safarian Bahri, P., and Osouli, A. (2016). "Estimation of scour for bridges in Illinois." *Proc., 8th International Conference on Scour and Erosion*.
- Coleman, S. E., Melville, B. W., and Gore, L. (2003). "Fluvial entrainment of protruding fractured rock." *Journal of Hydraulic Engineering*, 129(11), 872-884.
- Coleman, S. E., Melville, B. W., and Gore, L. (2005). "Closure to “Fluvial Entrainment of

- Protruding Fractured Rock” by Stephen E. Coleman, Bruce W. Melville, and Lance Gore." *Journal of Hydraulic Engineering*, 131(2), 143-144.
- Council, W. R. (1981). *Guidelines for determining flood flow frequency*, Hydrology Committee, US Water Resources Council.
- Crick, R. E., and Robinson, R. A. (2019). "Paleozoic Era." <<https://www.britannica.com/science/Paleozoic-Era>>.
- Crowley, R. W., Bloomquist, D. B., Shah, F. D., and Holst, C. M. (2012). "The sediment erosion rate flume (SERF): A new testing device for measuring soil erosion rate and shear stress." *Geotechnical Testing Journal*, 35(4), 649-659.
- Daly, E. R., Fox, G. A., Miller, R. B., and Al-Madhhachi, A.-S. T. (2013). "A scour depth approach for deriving erodibility parameters from jet erosion tests." *Transactions of the ASABE*, 56(6), 1343-1351.
- Danish, M. (2014). "Prediction of scour depth at bridge abutments in cohesive bed using gene expression programming." *International Journal of Civil Engineering and technology (IJCIET)*, 5(11), 25-32.
- Debnath, K., and Chaudhuri, S. (2010). "Laboratory experiments on local scour around cylinder for clay and clay–sand mixed beds." *Engineering Geology*, 111(1-4), 51-61.
- Debnath, K., Chaudhuri, S., and Manik, M. K. (2014). "Local scour around abutment in clay/sand-mixed cohesive sediment bed." *ISH Journal of Hydraulic Engineering*, 20(1), 46-64.
- Deere, D. (1988). "The rock quality designation (RQD) index in practice." *Rock classification systems for engineering purposes*, ASTM International.
- Deere, D., Hendron, A., Patton, F., and Cording, E. (1966). "Design of surface and near-surface construction in rock." *Proc., The 8th US symposium on rock mechanics (USRMS)*, American Rock Mechanics Association.

- DEQ (2020). "GeoWebFace." <<http://www.deq.state.mi.us/geowebface/>>.
- Devi, Y. S., and Barbhuiya, A. (2017). "Bridge pier scour in cohesive soil: a review." *Sādhanā*, 42(10), 1803-1819.
- Dickenson, S. E., and Bailie, M. W. (1999). "Predicting scour in weak rock of the Oregon Coast Range." Oregon State University. Dept. of Civil, Construction, and Environmental Engineering.
- Ettema, R., Melville, B. W., and Constantinescu, G. (2011). *Evaluation of bridge scour research: Pier scour processes and predictions*, Citeseer.
- FDOT (2005). "Bridge Scour Manual." Florida Department of Transportation, Tallahassee, FL.
- FDOT (2019). "Bridge Scour Policy Guidance." <<https://www.fdot.gov/roadway/drainage/bridge-scour-policy-guidance.shtm>>.
- FHWA (2002). "Geotechnical Engineering Circular No. 5 Evaluation of Soil and Rock Properties." Federal Highway Administration. Office of Bridge Technology, United States.
- Fiorotto, V., and Rinaldo, A. (1992). "Turbulent pressure fluctuations under hydraulic jumps." *Journal of Hydraulic Research*, 30(4), 499-520.
- Fookes, P., Gourley, C., and Ohikere, C. (1988). "Rock weathering in engineering time." *Quarterly Journal of Engineering Geology and Hydrogeology*, 21(1), 33-57.
- Gabr, M., Caruso, C., Key, A., and Kayser, M. (2013). "Assessment of in situ scour profile in sand using a jet probe." *Geotechnical testing journal*, 36(2), 264-274.
- Gazi, A. H., Afzal, M. S., and Dey, S. (2019). "Scour around piers under waves: Current status of research and its future prospect." *Water*, 11(11), 2212.
- Ghelardi, V. M. (2004). "Estimation of long term bridge pier scour in cohesive soils at Maryland bridges using EFA/SRICOS."
- Google (n.d.). "Google Earth." <[earth.google.com/web/](http://earth.google.com/web/)>. (2018).

- Gudavalli, S. R. (1998). "Prediction model for scour rate around bridge piers in cohesive soil on the basis of flume tests."
- Güven, O., Melville, J. G., Curry, J. E., and Crim, J., Samuel H (2005). "Observations and Evaluations of Scour at Two Bridge Sites with Cohesive Soils." *Erosion of Soils and Scour of Foundations*, 1-13.
- Hancock, G. S., Anderson, R. S., and Whipple, K. X. (1998). "Beyond power: Bedrock river incision process and form." *Geophysical Monograph-American Geophysical Union*, 107, 35-60.
- Hanson, G. (1990a). "Surface erodibility of earthen channels at high stresses part I-open channel testing." *Transactions of the ASAE*, 33(1), 127-0131.
- Hanson, G. (1990b). "Surface erodibility of earthen channels at high stresses part ii-developing an in situ testing device." *Transactions of the ASAE*, 33(1), 132-0137.
- Hanson, G., and Cook, K. (1997). "Development of excess shear stress parameters for circular jet testing." *ASAE Paper*, 972227.
- Hanson, G., and Cook, K. (2004). "Apparatus, test procedures, and analytical methods to measure soil erodibility in situ." *Applied engineering in agriculture*, 20(4), 455.
- Hanson, G. J., and Hunt, S. L. (2007). "Lessons learned using laboratory JET method to measure soil erodibility of compacted soils." *Applied engineering in agriculture*, 23(3), 305-312.
- Hanson, G. J., and Simon, A. (2001). "Erodibility of cohesive streambeds in the loess area of the midwestern USA." *Hydrological processes*, 15(1), 23-38.
- Hara, A., Ohta, T., Niwa, M., Tanaka, S., and Banno, T. (1974). "Shear modulus and shear strength of cohesive soils." *Soils and Foundations*, 14(3), 1-12.
- Harris, J. M., and Whitehouse, R. J. (2017). "Scour development around large-diameter monopiles in cohesive soils: Evidence from the field." *Journal of Waterway, Port, Coastal, and Ocean*

*Engineering*, 143(5), 04017022.

Harrison, W. B. I. (2016). "Geology of Michigan." <<https://scholarworks.wmich.edu/michigangeologicalrepository/2>>.

Henderson, M. R. (1999). "laboratory method to evaluate the rates of water erosion of natural rock materials."

Hopkins, T. C., and Beckham, T. L. (1999). "Correlation of rock quality designation and rock scour around bridge piers and abutments founded on rock." University of Kentucky Transportation Center.

Hosny, M. M. (1996). "Experimental study of local scour around circular bridge piers in cohesive soils." Ph.D. thesis, Colorado State University, Fort Collins, CO.

Huang, M., Liao, J.-J., Pan, Y.-W., and Cheng, M. (2013). "Modifications of the erodibility index method for the evaluation of the soft bedrock erosion." *Proc., 47th US Rock Mechanics/Geomechanics Symposium*, American Rock Mechanics Association.

ISRM (1981). "ISRM Report on Teaching of Rock Mechanics." International Society for Rock Mechanics, ISRM Secretariat, Lisbon, Portugal.

Jennings, M. E., Thomas, W. O., and Riggs, H. (1994). *Nationwide summary of US Geological Survey regional regression equations for estimating magnitude and frequency of floods for ungaged sites, 1993*, US Geological Survey.

Jones, S. J., and Richardson, E. V. (2004). "A Decade of High Priority Bridge Scour Research in the US." *Proc., Proceedings 2nd International Conference on Scour and Erosion (ICSE-2). November 14.–17., 2004, Singapore.*

Kamphuis, J. W., and Hall, K. R. (1983). "Cohesive material erosion by unidirectional current." *Journal of Hydraulic Engineering*, 109(1), 49-61.

Kassem, A., Salaheldin, T. M., Imran, J., and Chaudhry, M. H. (2003). "Numerical modeling of

scour in cohesive soils around artificial rock island of Cooper River Bridge." *Transportation research record*, 1851(1), 45-50.

Keaton, J. (2015). "Reassessing a 1997 bridge failure in a semiarid region of the United States with geotechnical scour number."

Keaton, J. R. (2011). "Modified Slake Durability Test Applicability for Soil." *Proc., International Symposium on Erosion and Landscape Evolution (ISELE), 18-21 September 2011, Anchorage, Alaska*, American Society of Agricultural and Biological Engineers, 7.

Keaton, J. R. (2013). "Estimating erodible rock durability and geotechnical parameters for scour analysis." *Environmental & Engineering Geoscience*, 19(4), 319-343.

Keaton, J. R., and Mishra, S. K. (2010). "Modified slake durability test for erodible rock material." *Scour and Erosion*, 743-748.

Keaton, J. R., Mishra, S. K., and Clopper, P. E. (2009). "Evaluating Scour at Bridge Foundations on Rock: Status of NCHRP Project." *Contemporary Topics in In Situ Testing, Analysis, and Reliability of Foundations*, 498-505.

Keaton, J. R., Mishra, S. K., and Clopper, P. E. (2010). "Scour at bridge foundations on rock: Overview of NCHRP Project No. 24-29." *Scour and Erosion*, 749-756.

Keaton, J. R., Mishra, S. K., and Clopper, P. E. (2012). *Scour at bridge foundations on rock*, Transportation Research Board.

Kerr, K. R. (2001). "A Laboratory Apparatus and Methodology for Testing Water Erosion in Rock Materials." *ME Thesis, University of Florida, Gainesville, Florida*.

Kho, K. T., Valentine, E., and Glendinning, S. (2004). "An experimental study of local scour around circular bridge piers in cohesive soils." *Proc., Proceedings 2nd International Conference on Scour and Erosion (ICSE-2). November 14.-17., 2004, Singapore*.

Kirsten, H. (1982). "A classification system for excavating in natural materials." *Civil*

*Engineering= Siviele Ingenieurswese*, 24(7), 293-308.

Kothyari, U. C., and Jain, R. K. (2008). "Influence of cohesion on the incipient motion condition of sediment mixtures." *Water resources research*, 44(4).

Kothyari, U. C., and Jain, R. K. (2010). "Experimental and numerical investigations on degradation of channel bed of cohesive sediment mixtures." *Water Resources Research*, 46(12).

Kothyari, U. C., Kumar, A., and Jain, R. K. (2014). "Influence of cohesion on river bed scour in the wake region of piers." *Journal of Hydraulic Engineering*, 140(1), 1-13.

Kwak, K., Lee, J., Park, J., and Chung, M. (2004). "Pier scour and erosion characteristics at Choji bridge." *Proc., Proceedings of International Conference on Scour and Erosion*, 292-300.

KYTC (2019). "Scour Considerations, Geotechnical Guidance Manual on Scour." Kentucky Department of Transportation.

Lagasse, P., Clopper, P., Pagan-Ortiz, J., Zevenbergen, L., Arneson, L., Schall, J., and Girard, L. (2009). "Bridge Scour and Stream Stability Countermeasures (Vols. 1 and 2), HEC-23." FHWA-NHI-09-111, Federal Highway Administration, US Department of Transportation, Washington, DC.

Lagasse, P., Zevenbergen, L., Spitz, W., and Arneson, L. (2012). "Stream Stability at Highway Structures, US Department of Transportation, Report No. HIF 12-004, HEC-20, Federal Highway Administration, Arlington, VA."

Lagasse, P. F. (2007). *Countermeasures to protect bridge piers from scour*, Transportation Research Board.

Lagasse, P. F., and Richardson, E. V. (2001). "ASCE compendium of stream stability and bridge scour papers." *Journal of Hydraulic Engineering*, 127(7), 531-533.

Lee, K., and Hedgecock, T. (2008). "Clear-water contraction scour at selected bridge sites in the Black Prairie Belt of the Coastal Plain in Alabama, 2006." Geological Survey (US).

- Li, Y. (2003). "Bridge pier scour and contraction scour in cohesive soils on the basis of flume tests."
- Liang, F., Bennett, C. R., Parsons, R. L., Han, J., and Lin, C. (2009). "A literature review on behavior of scoured piles under bridges." *Contemporary topics in in situ testing, analysis, and reliability of foundations*, 482-489.
- Little, R. G. (2003). "Toward more robust infrastructure: observations on improving the resilience and reliability of critical systems." *Proc., 36th Annual Hawaii International Conference on System Sciences, 2003. Proceedings of the*, IEEE, 9 pp.
- Location (2018). "Google Earth." <earth.google.com/web/>.
- MDEQ (2003). "General Geology of Michigan." <[https://www.michigan.gov/documents/deq/GIMDL-GGGM\\_307771\\_7.pdf](https://www.michigan.gov/documents/deq/GIMDL-GGGM_307771_7.pdf)>.
- Melville, B. W., and Coleman, S. E. (2000). *Bridge scour*, Water Resources Publication.
- Milstein, R. L. (1987). *Bedrock geology of southern Michigan*, Michigan. Department of Natural Resources.
- Mishra, S. K., Keaton, J. R., Clopper, P. E., and Lagasse, P. F. (2010). "Hydraulic Loading for Bridges Founded on Rock." *Scour and Erosion*, 734-742.
- Molinas, A., and Hosny, M. (1999). "Experimental study on scour around circular piers in cohesive soil." *Publication No. FHWA-RD-99-186, Federal Highway Administration, US Department of Transportation, McLean, VA*.
- Monnet, J. (2015). *In situ tests in geotechnical engineering*, John Wiley & Sons.
- Moore, A. (2012). "Determination of scour susceptibility through rapid assessment." University of Missouri--Kansas City.
- Moore, J. S. (1997). "Field procedures for the headcut erodibility index." *Transactions of the ASAE*, 40(2), 325-336.

- Moore, J. S., Temple, D. M., and Kirsten, H. (1994). "Headcut advance threshold in earth spillways." *Bulletin of the Association of Engineering Geologists;(United States)*, 31(2).
- Moore, W. L., and Masch Jr, F. D. (1962). "Experiments on the scour resistance of cohesive sediments." *Journal of Geophysical Research*, 67(4), 1437-1446.
- Mueller, D. S., and Wagner, C. R. (2005). "Field observations and evaluations of streambed scour at bridges." United States. Federal Highway Administration. Office of Research ....
- Najafzadeh, M. (2009). "Experimental and numerical study of local scour around a vertical pier in cohesive soils." Ms. Thesis, Shahid Bahonar University, Kerman, Iran.
- Najafzadeh, M., and Barani, G.-A. (2014). "Experimental study of local scour around a vertical pier in cohesive soils." *scientiairanica*, 21(2), 241-250.
- Najafzadeh, M., Barani, G.-A., and Azamathulla, H. M. (2013). "GMDH to predict scour depth around a pier in cohesive soils." *Applied ocean research*, 40, 35-41.
- Niemann, W. L., Wait, I. W., and Keaton, J. R. (2017). "A Proposed Risk-Based Screening Strategy for Bridges Potentially Affected by Rock Scour." *Environmental and Engineering Geoscience*, 23(3), 221-241.
- NRCS (2001). "Field Procedures Guide for the Headcut Erodibility Index." U.S. Department of Agriculture Natural Resources Conservation, National Engineering Handbook, Chapter 52, Part 628.
- Ogg, J. G., Ogg, G. M., and Gradstein, F. M. (2016). *A concise geologic time scale: 2016*, Elsevier.
- Oh, S. J. (2009). *Experimental study of bridge scour in cohesive soil*, Zachry Dept. of Civil Engineering, Texas A&M Univ., College Station, TX.
- Ojakangas, R. W. (1994). *Sedimentology and provenance of the Early Proterozoic Michigamme Formation and Goodrich Quartzite, northern Michigan: Regional stratigraphic implications and suggested correlations*, US Government Printing Office.

- Palmstrom, A. (2005). "Measurements of and correlations between block size and rock quality designation (RQD)." *Tunnelling and Underground Space Technology*, 20(4), 362-377.
- Pells, S. (2016). "Erosion of rock in spillways." *University of New South Wales*, PhD Thesis.
- Rahimnejad, R., and Ooi, P. S. (2016). "Factors affecting critical shear stress of scour of cohesive soil beds." *Transportation Research Record*, 2578(1), 72-80.
- Rahimnejad, R., and Ooi, P. S. (2017). "Model for the erosion rate curve of cohesive soils." *Transportation Research Record*, 2657(1), 19-28.
- Rambabu, M., Rao, S. N., and Sundar, V. (2003). "Current-induced scour around a vertical pile in cohesive soil." *Ocean Engineering*, 30(7), 893-920.
- Reed, R., and Daniels, J. (1987). "Bedrock geology of Northern Michigan: Michigan Department of Natural Resources." *Geological Survey Division, scale, 1(500,000)*.
- Richardson, E. V., and Davis, S. R. (2001). "Evaluating scour at bridges." United States. Federal Highway Administration. Office of Bridge Technology.
- Richardson, E. V., Simons, D. B., and Lagasse, P. F. (2001). "River engineering for highway encroachments: Highways in the river environment." United States. Federal Highway Administration.
- Robinson, K., and Hanson, G. (1995). "Large-scale headcut erosion testing." *Transactions of the ASAE*, 38(2), 429-434.
- Salaheldin, T., Imran, J., Kassem, A., and Chaudhry, H. (2003). "Scale physical modeling of local scour in cohesive soil." *Proc., TRB Annual Meeting. Washington, DC, January*, 12-16.
- Schmidt, G. (1980). "The Marquette range supergroup in the Gogebic Iron district, Michigan and Wisconsin."
- Schuring, J. R., Dresnack, R., Golub, E., Khan, M. A., Young, M. R., Dunne, R., and Aboobaker, N. (2010). "Review of bridge scour practice in the US." *Scour and Erosion*, 1110-1119.

- Sheppard, D. M., and Bloomquist, D. (2005). "Water erosion of Florida rock materials."
- Sidorchuk, A. (2005). "Stochastic modelling of erosion and deposition in cohesive soils." *Hydrological Processes: An International Journal*, 19(7), 1399-1417.
- Sims, P. (1992). "Geologic map of Precambrian rocks, southern Lake Superior region, Wisconsin and northern Michigan."
- Smith, S., Annandale, G., Johnson, P., Jones, J., and Umbrell, E. (1999). "Pier Scour in Resistant Material: Current Research on Erosive Power." *Proc., Stream Stability and Scour at Highway Bridges: Compendium of Stream Stability and Scour Papers Presented at Conferences Sponsored by the Water Resources Engineering (Hydraulics) Division of the American Society of Civil Engineers*, ASCE, 78-78.
- Smith, S. P. (1994). *Preliminary Procedure to Predict Bridge Scour in Bedrock*, Colorado Department of Transportation [Division of Transportation Development].
- Sommers, L. M. (2019). *Michigan: A geography*, Routledge.
- Song, Y., Liu, L., Yan, P., and Cao, T. (2005). "A review of soil erodibility in water and wind erosion research." *Journal of Geographical Sciences*, 15(2), 167-176.
- Teisson, C., Ockenden, M., Le Hir, P., Kranenburg, C., and Hamm, L. (1993). "Cohesive sediment transport processes." *Coastal Engineering*, 21(1-3), 129-162.
- Ting, F. C., Briaud, J.-L., Chen, H., Gudavalli, R., Perugu, S., and Wei, G. (2001). "Flume tests for scour in clay at circular piers." *Journal of hydraulic engineering*, 127(11), 969-978.
- Ting, F. C., Larsen, R. J., and Jones, A. L. (2011). "Hydrographs and Estimates of Scour Depth Excess for Pier Scour Prediction: Use for Ungauged Streams with Scour Rate in Cohesive Soils Method." *Transportation research record*, 2262(1), 193-199.
- Titi, H. H., Liao, Q., Laflin, A., Keaton, J. R., Kean, W., and Wheeler, A. F. (2017). "Predicting Scour of Bedrock in Wisconsin." Wisconsin. Dept. of Transportation. Research and Library

Unit.

TPF (2020). "Soil and Erosion Testing Services for Bridge Scour Evaluations." <<https://www.pooledfund.org/Details/Study/688>>.

TxDOT (2018). "Geotechnical Manual." *Texas Department of Transportation*.

USGS (2020a). "Geologic units in Michigan (state in United States)." <<https://mrdata.usgs.gov/geology/state/fips-unit.php?code=fUS26>>.

USGS (2020b). "National Geologic Map Database, Geolex Search." <<https://ngmdb.usgs.gov/Geolex/search>>.

Utley, B., and Wynn, T. (2008). "Cohesive soil erosion: Theory and practice." *Proc., World Environmental and Water Resources Congress 2008: Ahupua'A*, 1-10.

Vickers, R. C. (1956). "Geology and monazite content of the Goodrich quartzite, Palmer area, Marquette County, Michigan." *US Geol. Survey Bull.*, 1030.

Wei, G., Chen, H., Ting, F., Briaud, J., Gudavalli, S., and Perugu, S. (1997). "Numerical simulation to study scour rate in cohesive soils." *Res. Rep. to the Texas Dep. of Trans., Dep. of Civil Engineering, Texas A&M University, College Station, TX*.

Whipple, K. X., Hancock, G. S., and Anderson, R. S. (2000). "River incision into bedrock: Mechanics and relative efficacy of plucking, abrasion, and cavitation." *Geological Society of America Bulletin*, 112(3), 490-503.

Williams-Sether, T. (1999). *Estimated and measured bridge scour at selected sites in North Dakota, 1990-97*, US Department of the Interior, US Geological Survey.

Windley, B. F. (2020). "Precambrian." <<https://www.britannica.com/science/Precambrian>>.

Zatar, W., Wait, I., Niemann, W., and Rahall, N. J. (2013). "Criteria for Predicting Scour of Erodible Rock in West Virginia." West Virginia. Dept. of Transportation.

Zhang, G., Hsu, S. A., Guo, T., Zhao, X., Augustine, A. D., and Zhang, L. (2013). "Evaluation of design methods to determine scour depths for bridge structures." Louisiana. Dept. of Transportation and Development.

Zinner, M., Meyer, T., Shan, H., Shen, J., Bergendahl, B., and Kerenyi, K. (2016). "A field erodibility testing device for scour evaluation of bridges."